

Developing sustainable methods in polar main group chemistry

Michael Fairley

A thesis submitted to the Department of Pure and Applied Chemistry, University of Strathclyde, in part fulfilment of the requirements for the degree of *Doctor of Philosophy*.

Oct 2019

This thesis is the result of the author's original research. It has been composed by the author and has not been previously submitted for examination which has led to the award of a degree.

The copyright of this thesis belongs to the author under the terms of the United Kingdom Copyright Acts as qualified by University of Strathclyde Regulation 3.50. Due acknowledgement must always be made of the use of any material contained in, or derived from, this thesis.

Signed:

Date:

Acknowledgments

I would like to thank my supervisors Prof. Eva Hevia and Dr Charlie O'Hara for allowing me to do the PhD with them and for everything during the last four years. I would also like to thank Prof. Robert Mulvey and Dr Stuart Robertson.

I have enjoyed my time in the lab and am glad to have met everyone who has been present during my time there. I would like to especially acknowledge Laia for introducing me to the lab and training me in inert atmosphere chemistry. Alberto showing me how to carry out kinetic studies. And of course Vicky who began the journey with me at the same time.

Further to this I would like to thank Craig Irving for help with NMR, Patricia Keating for help with GCMS, and Janie-Anne Pickrell for help in all aspects of lab affairs.

As three months of this PhD was spent in the University of Oviedo, I am also very grateful to Dr Joaquín García-Álvarez and Marichu for being very friendly and welcoming during my time there, and Isabel Scott for helping with the procedural aspects of the visit. I should also thank Marichu and Marina for help in the lab.

Abstract

Sustainability in polar main group organometallic chemistry was investigated in two approaches: the investigation of alternative, more sustainable, solvents rather the traditional VOCs for use in selected addition reactions of pyrophoric organolithium reagents in air and the use of *s*-block bimetallic cooperative catalysis in isomerisation reactions in which homometallic compounds struggle, as an alternative to less abundant and more expensive transition metal catalysts.

The ultrafast addition of a range of aryllithium reagents to nitriles has been accomplished using glycerol and water as solvent in the presence of air. These occurred heterogeneously, being 'on glycerol' and 'on water', with the addition being faster than the competitive hydrolysis of the aryllithium species, therefore providing a convenient route to produce imines and onward to ketones for a range of nitriles and aryllithium reagents.

2-MeTHF was used as a solvent in the amidation of esters under air. These reactions involved the homogeneous addition of lithium amide solutions to esters to form the product the carboxamides. The reactions occurred in 20 s, with the amidation occurring quicker than the competing hydrolysis. The lifetime of the lithium amide in air was also examined.

Mixed *s*-block metal organometallic reagents have been successfully utilised in the catalytic intramolecular hydroalkoxylation of alkynols. This success has been attributed to the unique manner in which the two metals can work cooperatively to overcome the challenges of the reaction: namely OH activation and coordination to and then addition across a C≡C bond. Of a series of alkali metal magnesiates tested a combination of $K_2Mg(CH_2SiMe_3)_4(PMDETA)_2/18\text{-crown-6}$ was found to be the best catalyst. After optimising the reaction substrate scope was examined to probe the range and robustness of the system. A series of alkynols, including terminal and internal alkynes which contain a variety of potentially reactive functional groups, were cyclised. In comparison to previously reported monometallic systems, bimetallic $K_2Mg(CH_2SiMe_3)_4(PMDETA)_2/18\text{-crown-6}$ displays enhanced reactivity towards internal alkynol-cyclisation. Kinetic studies revealed an inhibition effect of substrate on the catalysts via adduct formation and requiring dissociation prior to the rate limiting cyclisation step. Following from this success the possibility of performing the isomerisation of terminal alkynes to internal alkynes was examined. Despite some successfully catalysed reactions the optimal conditions remained elusive.

Peer reviewed academic journal articles

“Introducing Glycerol as a Sustainable Solvent to Organolithium Chemistry: Ultrafast Chemoselective Addition of Aryllithium Reagents to Nitriles under Air and at Ambient Temperature” - María J. Rodríguez-Álvarez, Joaquín García-Álvarez, Marina Uzelac, Michael Fairley, Charles T. O’Hara and Eva Hevia, *Chem Eur. J.*, 2018, **24**, 1720-1725.

- Basis for Part 1, Chapter 1

“s-Block cooperative catalysis: alkali metal magnesiate-mediated cyclisation of alkynols” – Michael Fairley, Laia Davín, Alberto Hernán-Gómez, Joaquín García-Álvarez, Charles T. O’Hara and Eva Hevia, *Chem. Sci.*, 2019, **10**, 5821-5831.

- Basis for Part 2, Chapter 1

Conference presentations

“Alkali-metal magnesiate mediated catalytic hydroalkoxylation/cyclisation of alkynyl alcohols” M. Fairley, C.T. O’Hara, E. Hevia [Poster] - *Universities of Scotland Inorganic Conference (USIC 50)*, University of Strathclyde, Aug 2016

“Alkali-metal magnesiate mediated catalytic hydroalkoxylation/cyclisation of alkynyl alcohols” M. Fairley, C.T. O’Hara, E. Hevia [Poster] - *RSC Dalton Scottish Regional Meeting*, University of Edinburgh, Jun 2017

“Alkali-metal magnesiate mediated catalytic hydroalkoxylation/cyclisation of alkynyl alcohols” [Oral] - *Universities of Scotland Inorganic Conference (USIC 51)*, University of St Andrews, Aug 2017

“Cooperative catalysis: alkali metal mediated catalytic alkynol cyclisation” M. Fairley, C.T. O’Hara, E. Hevia [Poster] - *International Conference on Organometallic Chemistry (ICOMC 28)*, Florence, Jul 2018

“Cooperative catalysis: alkali metal mediated mediate catalytic alkynol cyclisation” M. Fairley, C.T. O’Hara, E. Hevia [Poster] - *Universities of Scotland Inorganic Conference (USIC 52)*, University of Edinburgh, Sep 2018

Nomenclature & abbreviations

(R,R)-TMEDA	(1R,2R)- <i>N,N,N',N'</i> -tetramethyl-1,2-cyclohexanediamine
12-c-4	12-crown-4 / 1,4,7,10-tetraoxacyclododecane
15-c-5	15-crown-5 / 1,4,7,10,13-pentaoxacyclopentadecane
18-c-6	18-crown-6 / 1,4,7,10,13,16-hexaoxacyclooctadecane
2-MeTHF	2-methyltetrahydrofuran
ChCl	choline chloride / (2-hydroxyethyl)trimethylammonium chloride
DES	Deep eutectic solvent
DFT	Density functional theory
EG	ethylene glycol / ethane-1,2-diol
Gly	glycerol / propane-1,2,3-triol
HBA	Hydrogen bond acceptor
HBD	Hydrogen bond donor
HMDS	1,1,1,3,3,3-hexamethyldisilazide / 1,1,1-trimethyl- <i>N</i> -(trimethylsilyl)silanamide
IL	Ionic liquid
LiNMA	lithium <i>N</i> -methylanilide
Me ₆ TREN	<i>N,N,N',N',N'',N''</i> -hexamethyltris(2-aminoethyl)amine / <i>N,N</i> -Bis[2-(dimethylamino)ethyl]- <i>N',N'</i> -dimethyl-1,2-ethanediamine
PMDETA	<i>N,N,N',N'',N''</i> -pentamethyldiethylenetriamine
THF	tetrahydrofuran
TMEDA	<i>N,N,N',N'</i> -tetramethylethane-1, 2-diamine
TMEEA	tris[2-(2-methoxyethoxy)ethyl]amine / 2-(2-methoxyethoxy)- <i>N,N</i> -bis[2-(2-methoxyethoxy)ethyl]ethanamine
TMP	2,2,6,6-tetramethylpiperidide
VOCs	Volatile organic compounds

Acknowledgments	i
Abstract	ii
Publications & conferences	iii
Nomenclature & abbreviations	iv
Contents	v
I – Sustainability in synthetic chemistry	1
I.I – A perspective on the use of solvents	7
I.II – An introduction to deep eutectic solvents	10
I.III – Deep eutectic solvents, glycerol, and sustainability	16
I.IV – 2-Methyltetrahydrofuran	18
I.V – s-Block metals: abundance and provenance	21
I.VI – Polar main group organometallic reagents: reactivity, limitations and incompatibility	25
I.VII – Cooperativity in polar main group organometallic chemistry	28
Part 1 – Organolithium reagents in alternative solvents	34
1.1 Addition of organolithium reagents to nitriles under air	37
1.1.1 Initial reactions and solvent assessment	38
1.1.2 “On glycerol” reactions and surface phenomena	42
1.1.3 Assessing nitrile and aryllithium substrate scope	44
1.1.4 Aryllithium lifetime study	49
1.2 Amidation of esters using lithium amides under air	50
1.2.1 Initial reactions and solvent assessment	51
1.2.2 Assessing ester substrate scope	61
1.2.3 Lithium amide assessment and synthesis of target products	63

1.3	Solvent directed reactivity using DESs	68
1.3.1	α,β -unsaturated ketones	68
1.3.2	Transition metal catalysed cross-couplings	83
	Alternative solvents - Conclusions & Further work	88
	Part 2 – s-Block cooperative catalysis	91
2.1	Hydroalkoxylation/cyclisation of alkynols	102
2.1.1	Assessing alkali metal and stoichiometric effects	107
2.1.2	Assessing the role of Lewis donors as co-catalysts	110
2.1.3	Optimisation of reaction conditions and substrate compatibility	116
2.1.4	Exploration of alkynol substrate scope & functional group tolerance	120
2.1.5	Mechanistic studies	133
2.1.6	Mechanistic interpretation	140
2.2	Isomerisation of terminal alkynes	146
	2.2.1 – Optimisation & Substrate scope	147
	s-Block cooperative catalysis - Conclusions & Further work	151
	II – Global conclusions and further work	153
	III - Experimental	155
III.I	Addition of organolithium reagents to nitriles	156
III.II	Amidation of esters using lithium amides	161
III.III	Solvent directed reactivity	168
III.IV	Hydroalkoxylation/cyclisation of alkynols	169
III.V	Isomerisation of terminal alkynes	176
	IV – References	177

I – Sustainability in synthetic chemistry

As advances in science and technology progress at an ever-increasing rate we take increasing large steps to change the world around us to better suit our needs and our continual growth. These advances have allowed the human population to sustain an immense population, over 7 billion in 2019.¹ Amidst all this progress and expansion we are beginning to realise that the resources required to provide for such a burgeoning population are putting a strain on the sources of our resources. The rate of consumption of resources increases year upon year, with the estimated renewable resources available for this year, 2019, being depleted in July, the earliest ever ‘overshoot day’.² It is with this realisation of the finite nature and destructibility of our environment that in recent years we have looked for ways to allow for advancement and growth, but minimise or eliminate any effects to our environment.

This idea of valuing safe and sustainable methods in the area of chemistry is known as ‘green chemistry’.³ Despite appearing a somewhat nebulous concept, in the last 20 years guidelines and indicators have been developed to guide the design or assessment of the sustainability of a chemical process,^{4, 5} although these guidelines also apply to smaller scale syntheses and are therefore discussed in this thesis.

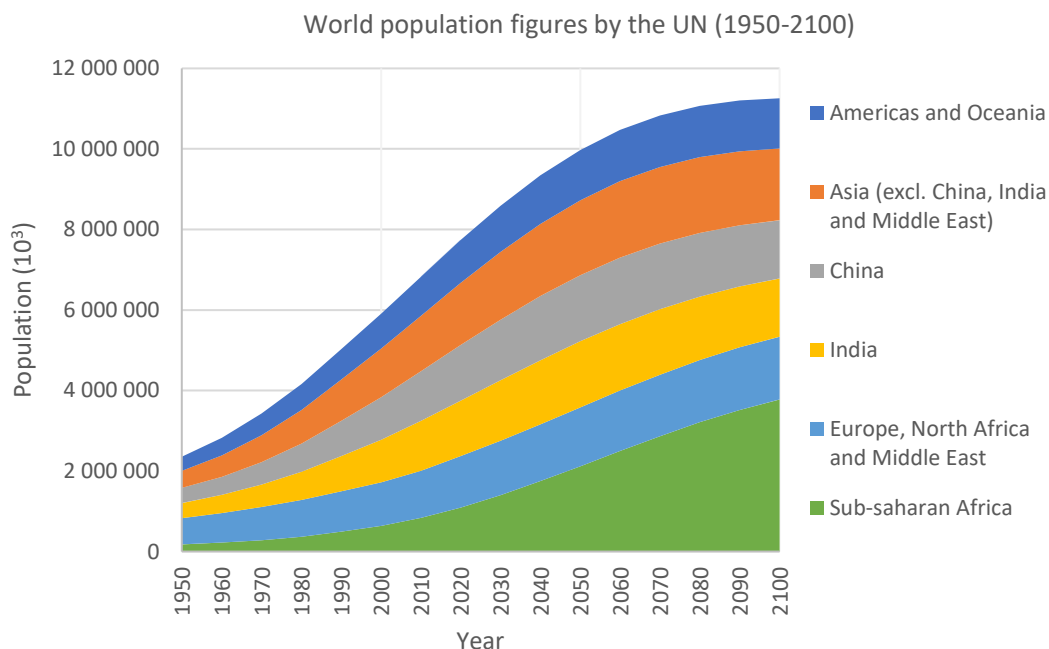


Figure 1 – Historic and estimated population figures by the UN ‘World Population Prospectus 2019’.¹

One tool that can be used when assessing or planning chemical processes with sustainability in mind is to follow the '12 principles of green chemistry'. These principles, developed by Anastas and Warner⁶ have been used and refined over the last 20 years since their inception, and serve as a guide to the aspects of chemical processes that can be implemented in a more sustainable way. The 12 principles are closely related, with a good deal of overlap. However, each is briefly outlined in turn below: ⁷

- **1 Prevent waste**

– *'it is better to prevent waste than to treat it or clean it up after it has been created'*

The production of waste should be considered along the full journey of the materials involved, from acquisition of raw materials to the end of the substance's useful lifecycle. An example of how this can be achieved is through the use of a one-pot syntheses: avoiding the need for separations and isolation of intermediates and the additional solvents or components required to carry out these steps. Additionally, any waste/by-products that can be efficiently recycled as feedstocks more economically and environmentally than the species can be obtained from a new source should be reused.

One such measurement for the efficiency of a process is its *E-factor*,⁸⁻¹⁰ which is the ratio of the mass of waste to product and is a helpful metric to compare both lab scale production and industrial scale processes. Whilst being a simple metric *E-factor* does not give a rounded picture of the efficiency of a process as it does not give any consideration to the type of waste produced or the energy and water quantities required.

- **2 Atom economy**

– *'design methods for the incorporation of all materials used into the final product'*

Atom economy involves the concept of the incorporation of as many of the atoms of which the starting materials consist into the desired product. It is one of the simplest 'green' indicators and is simply the ratio of the molecular weight of the product and those of the starting materials, with highly atom efficient synthetic routes being considered more 'elegant'. Atom economy together with product yield can be used as a simple metric for the efficiency of the process and synthetic route.

- **3 Less hazardous synthesis**

– *‘design for the use and generation of species non-harmful to people and the environment’*

Principles 3 and 4 are closely related, with principle 3 being concerned with avoiding and monitoring the use of compounds which are known to be harmful to people, animals or the environment, or generate harmful intermediates. Harmful in this case refers to being hazardous in any capacity fitting the common hazard categories for which substances are commonly classified (e.g. the Globally Harmonised System of Classification and Labelling of Chemicals). The most challenging aspect of minimising the use of harmful species is that many substances, especially intermediates, have often not been hazard tested. This aspect leads into principle 4.

- **4 Design benign chemicals**

– *‘minimise product toxicity without diminishing its efficacy’*

Following on from principle 3, principle 4 concerns itself with the exploration of chemical space for non-hazardous but equally efficient alternatives to desirable compounds. The development of effective non-hazardous alternatives can often be a complicated and multidisciplinary task, involving steps such as: modelling and predictions; synthetic route exploration; compound screening; and testing of chemical, biological and physical properties.

- **5 Benign solvents and auxiliaries**

– *‘altogether avoid or only use innocuous auxiliaries’*

In a similar vein to principles 3 and 4, principle 5 is concerned with avoiding the use of hazardous solvents, separating agents and other substances involved in the undertaking of or processing of reactions and unit operations such as separations amongst others. As solvents contribute a major part of the mass of all substances involved in chemical processes their nature, including inherent hazards and ability to be renewable sourced so be carefully considered. Additionally, informed solvent choice can reduce the need for resource intense separation steps.

- **6 Design for energy efficiency**

– *‘minimise environmental and economic impact of processes by reducing energy use through selection of routes able to operate at ambient pressure and temperature’*

Principle 6 distances itself from concerns about the properties of the chemical species involved in a chemical process, and instead focusses on the energy intensity of performing each unit operation, and being aware of the environmental and economic cost of these steps. Steps involving heating or separations can require large quantities of energy to carry out. Alternative heating methods such as microwave irradiation or non-thermal reaction pathways such as electro-, sono-, or photochemistry can be more efficient due to shorter reaction times. Use of a catalyst (see principle 9) can also reduce energy expenditure.

- **7 Use renewable feedstocks**

- *‘use renewable feedstocks wherever technically and economically possible’*

The source of the primary materials is of concern of principle 7, which underlines the need for resources to come from renewable sources where reasonable. Renewable sources often start from biomass which is then processed in a range of ways, including by chemical, biochemical, or biological means to yield suitable primary materials.

- **8 Reduce derivatives**

- *‘avoid derivatisation (e.g. protecting groups and temporary modification of reaction conditions) to minimise waste and auxiliaries’*

This principle states that the use of modifying chemicals such as protecting groups or temporary chirality scaffold should be minimised to reduce waste. Furthermore, temporary changes of pH by addition of acids/bases or temporary changes in reaction conditions such as temperature changes should also be minimised to prevent additional neutralisation or energy costs.

- **9 Catalysis**

- *‘selective catalytic reagents are superior to stoichiometric’*

The use of catalytic regimes is the prime focus of principle 9, where the energy savings through the facilitation of a reaction by a catalyst and the saving in materials are key. The nature of the catalyst must however be considered in cases requiring expensive, rare metal catalysts more consideration may be required. Homogenous, heterogenous, and enzymatic catalysts should all be considered, with each bringing its own share of benefits and challenges.

- **10 Design for degradation**

- *‘design products for innocuous degradation and timely degradation at the end of their lifetime’*

All products and by-products should be degradable of a reasonable timescale for the compound in question. Importantly the decomposition products, along with the parent compound, should pose no risk to humans, animals, or the environment. Ideally this degradation should occur under ambient conditions.

- **11 Real-time analysis and pollution prevention**

- *‘use real-time in-process monitoring and control when producing hazardous substances’*

Principle 11 is concerned with the continuous monitoring of a chemical process, with the mindset that ‘in-line’ or ‘on-line’ analysis can spot deviations or problems soon enough that undesirable or hazardous changes can be noticed early enough to correct or mitigate for effects further downstream.

- **12 Inherently benign chemistry for accident prevention**

- *‘inherently safer, or safer forms, of substances should be used to help reduce the risk and mitigate the hazard of accidental process deviations’*

Finally, principle 12 is one of the most commonly acted upon due to being as much a safety principle as green chemistry. It concerns itself with the inherently safer design of chemical processes, where a route, which in the case of an accident would lead to the least damage, e.g., fire, explosion, toxicity. Consideration for the consequences of a process deviation are already commonly considered, such as hazard and operability studies (HAZOP) being commonly carried out in the UK.

Building from these 12 principles of green chemistry this thesis intends to outline the investigation of two different approaches to sustainability in polar main group organometallic chemistry:

1. In line with principle 5; the investigation of alternative, more sustainable, solvents rather than the traditional VOCs for use in selected addition reactions of pyrophoric organolithium reagents in air.
2. In line with principle 9; the investigation of *s*-block bimetallic cooperative catalysis in isomerisation reactions in which homometallic compounds struggle, as an alternative to less abundant and more expensive transition metal catalysts.

Throughout the investigation of these topics, where appropriate, any reasonable changes should be implemented to adhere more closely to the principles not directly addressed.

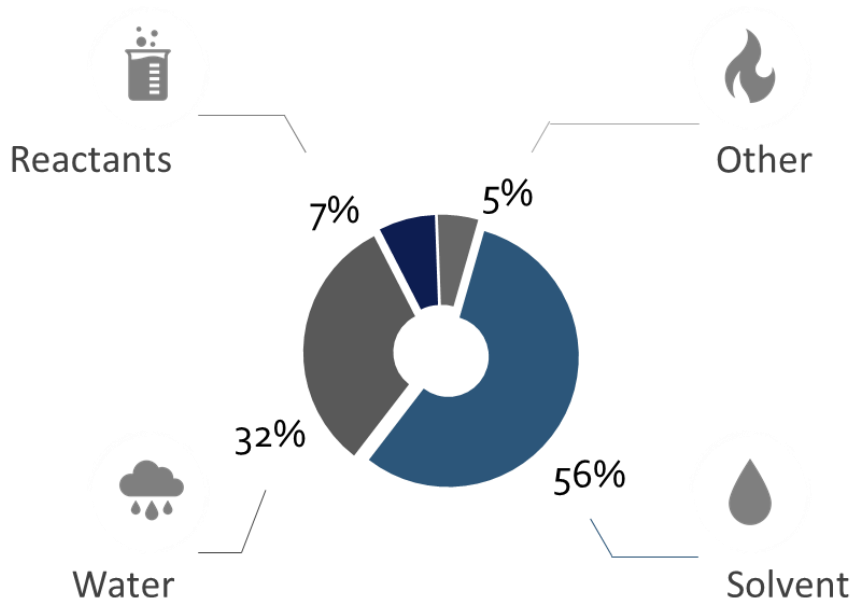


Figure 2 – The process mass intensity (PMI) of materials in the manufacture of APIs.¹¹

Solvents are the biggest source of waste in chemical processes¹² having been said to comprise between 56¹¹ - 80%^{4,13} of the materials used in chemical processes. The variation in this figure appears due to a difference in measurement (percentage mass used per gram of product, or volume of substances involved in the process), additionally figures vary slightly between those applying to all chemical processes or only the pharmaceutical industry. One thing that all sources agree upon is that traditional solvents are inherently hazardous and do not comply with the principles of green chemistry.^{13, 14} Due to the large volumes of solvent used in industrial processes, lifecycle studies have estimated that they account for 60% of the total energy used, and up to 50% of post-treatment greenhouse gasses emissions produced in pharmaceutical processes.^{4, 15} A simple solution to this would seem to be the elimination of solvents all together, an area which has seen some focus,¹⁶ although generally solvents are very useful in synthesis: both influential in the nature of chemical reaction itself in terms of reaction rates, equilibria, selectivity and speciation; also physical processes such as ensuring reaction homogeneity (in terms of composition and heat), controlling any heat production or requirement, allowing for easy and measured transportation of components in and out of vessels (specially in flow systems), and are often prerequisite for purification steps.^{4, 17}

Due to the prevalence of solvents, it is therefore clearly necessary to research viable alternatives across all areas of chemistry, especially in synthesis. At a conference on green solvents held in Germany in 2010 attendees were asked their opinion on which types of solvents would likely lead the way in environmentally-friendly synthesis [a, Figure 3]. A range of solvents were suggested, with water and carbon dioxide making up a large part of the suggestions due to their ubiquity and obvious driving factors for their use. Some of the less common categories of solvents included ionic liquids, bio-derived and solventless. When this is compared to the number articles published in 'Green Chemistry' in 2010 regarding each of these solvent types [b, Figure 3] a disparity is observed, with ionic liquids being the largest category of solvents on which research was published in that year, and the other categories of bio-derived, switchable, and organic much less prevalent.

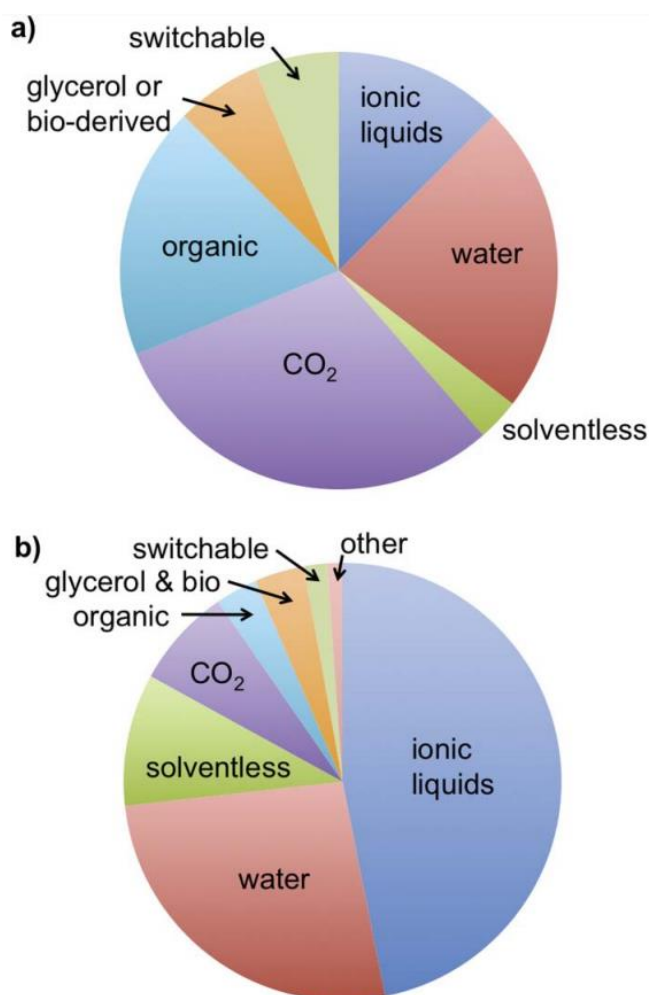


Figure 3 –a) a survey of “...what class of solvents will be responsible for the greatest reduction in environmental damage?” at ‘Green Solvents for Synthesis’, 2010, Berchtesgaden, Germany. b) Articles published in the journal *Green Chemistry* in 2010 – Figure from “Searching for Green Solvents”.¹²

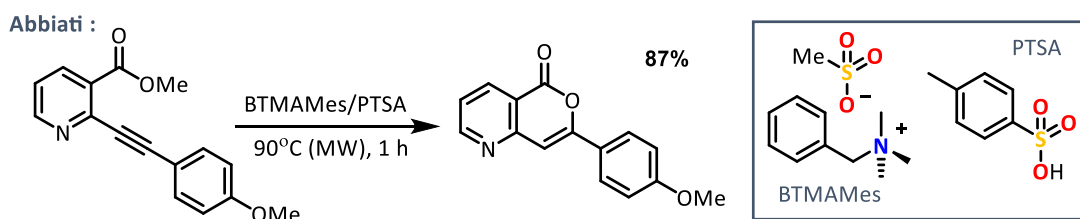
The solvents involved in this thesis regarding the exploration of the feasibility of using *s*-block organometallic reagents in alternative solvents will focus on solvents from this less represented 'bio-derived' category,¹⁸ namely glycerol and 2-methyltetrahydrofuran (2-MeTHF), but also deep eutectic solvents (DESs) which sit in an overlap of ionic liquids and bio-derived, as they are generally considered a sub-category of ionic liquids but can often comprise of glycerol and bio-derived components.

I.II – An introduction to deep eutectic solvents

Normally considered a sub-category of ionic liquids, deep eutectic solvents have of recent become a highly investigated due to their useful physical and chemical properties. They differ from ionic liquids in that they are composed of a hydrogen bond acceptor and hydrogen bond donor in place of an anion and cation,¹⁹ as will be explained in greater detail later in this section. Therefore, despite appearing similar to ionic liquids and sharing many properties (such as: negligible vapour pressure, high thermal stability, non-flammability, and an ability to solvate both organic and inorganic compounds) they are fundamentally different on a molecular level.¹⁹ In general DESs are also formed from the combination of cheaper, less toxic, and more biodegradable components than ionic liquids²⁰ which combines with their ability to tailored to a particular application to make them useful in both organic and inorganic synthesis.²¹

Due to desirable physical properties DESs have been used in many applications ranging from electrochromic applications¹³ and electrodeposition, to nanoparticle and MOF synthesis,²² with other applications such as CO₂ capture, lubricants and heat absorbers also having been investigated.¹⁹ Apart from these, the use of DESs in extractions has also been explored, including the extraction of chitin from prawn shells²³ and the fractionation of ligno-cellulose.²⁴

Aside from their desirable physical properties they have also been used for their chemical properties, such as in asymmetric²⁵ and acid catalysed²⁰ organocatalysis.²⁶ The sustainability of DESs has even been maximised in ‘natural’ deep eutectic solvents comprised of exclusively plant-based compounds. These natural DESs have already found applications in extractions,²⁷ as reagents,²⁷ and in the capture of CO₂.^{28, 29}



Scheme 1 – ‘Active green solvents’: the acidic DES catalysed cyclisation of alkyne esters.²⁰

Deep eutectic solvents are mixtures formed of two (or three) components where the mixture has a greatly reduced melting point compared to the individual components. The molar ratio at which the melting point of the mixture is at its minimum is known as the eutectic point, 'deep' simply refers to the scale of depression in melting point compared to the individual components being significantly large [Figure 4]. The reduction in melting point stems from the strong H-bonding interactions formed between the components of the DES, of which one is a hydrogen bond acceptor (HBA) and the other a hydrogen bond donor (HBD).³⁰

DESs are classified into four types based on their components:

- I - A hydrogen bond acceptor and an anhydrous metal salt
- II - A hydrogen bond acceptor and a hydrated metal salt
- III - A hydrogen bond acceptor and donor
- IV - A metal salt and a hydrogen bond donor

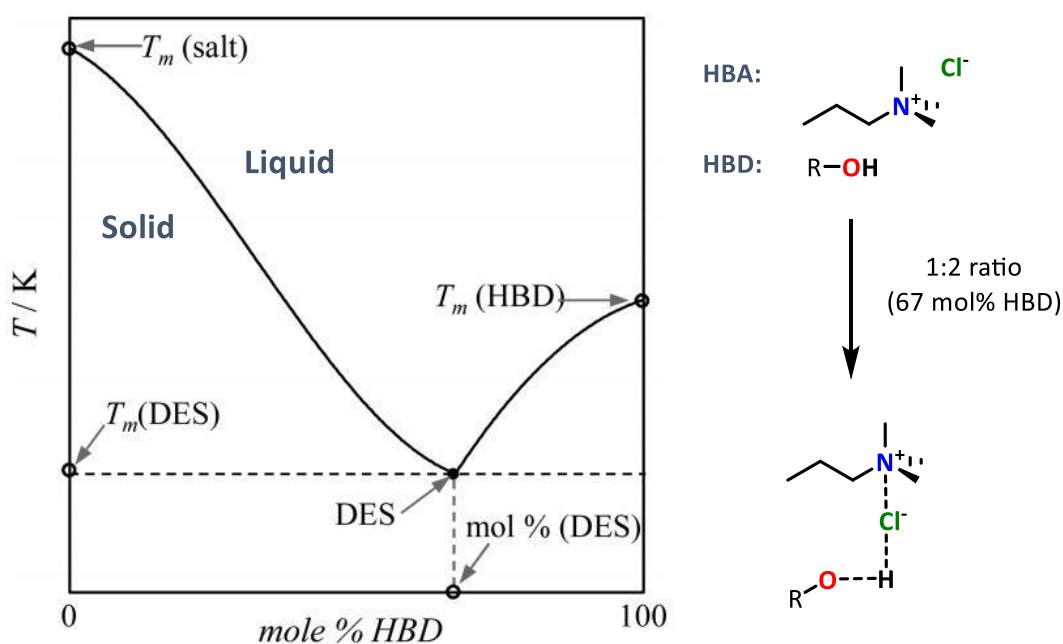


Figure 4 – Scheme of a phase diagram of a eutectic mixture with a eutectic point at a 1:2 ratio of HBA:HBD.³¹

Type I - A hydrogen bond acceptor and an anhydrous metal salt.

This category of DESs is small and uncommonly found, due to the inherent difficulty in handling anhydrous metal salts. Additionally, they are highly viscous and often have higher than ambient melting points, although there are examples of lower melting point type I DESs such as ChCl/2ZnCl₂ (24°C) and ChCl/2FeCl₃ (65°C). Some example components of type I DESs are shown below.³²⁻³⁴

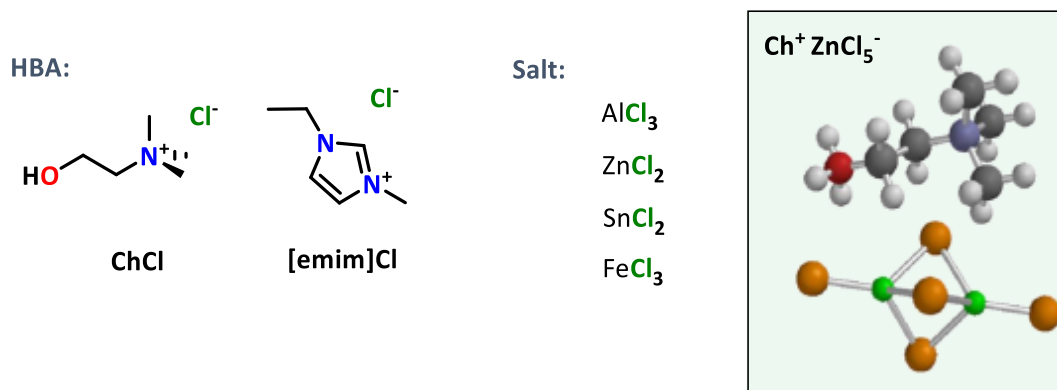


Figure 5 – Example constituents of a type I DES.³⁴

Type II – A hydrogen bond acceptor and a hydrated metal salt.

Type II DESs involving cheaper, more easily handled hydrated metal salts are more prevalent than their type I counterparts. They also have the added benefit of generally lower melting points and reduced viscosity, and so can be found consisting of a wider range of metals. Their more favourable properties make them suitable for use in industry.^{33, 35-37}

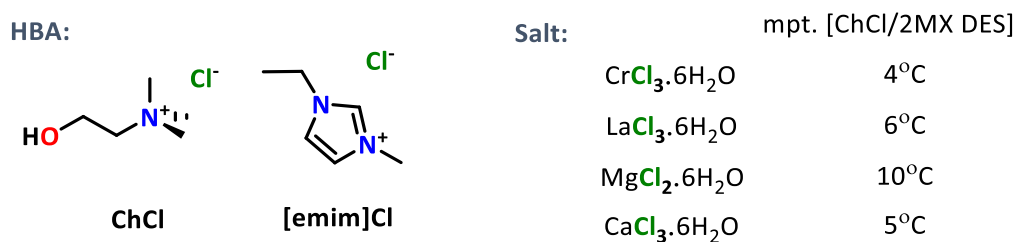


Figure 6 – Example constituents of a type II DES.

Type III - A hydrogen bond acceptor and donor.

In type III DESs both H-bond donor and acceptors are often organic compounds such as the small selection shown in **Figure 7**, these even include amino acids, amides, sugars and fatty acids. Because of the large catalogue of components which can form type III DESs they are some of the most tailorable, for example pH can be tuned by use of urea for a more basic DES vs. an organic acid for a more acid mixture. A large number of type III DESs have been developed focusing on their physical properties due to their prowess in metal oxide and metal chloride solvation.

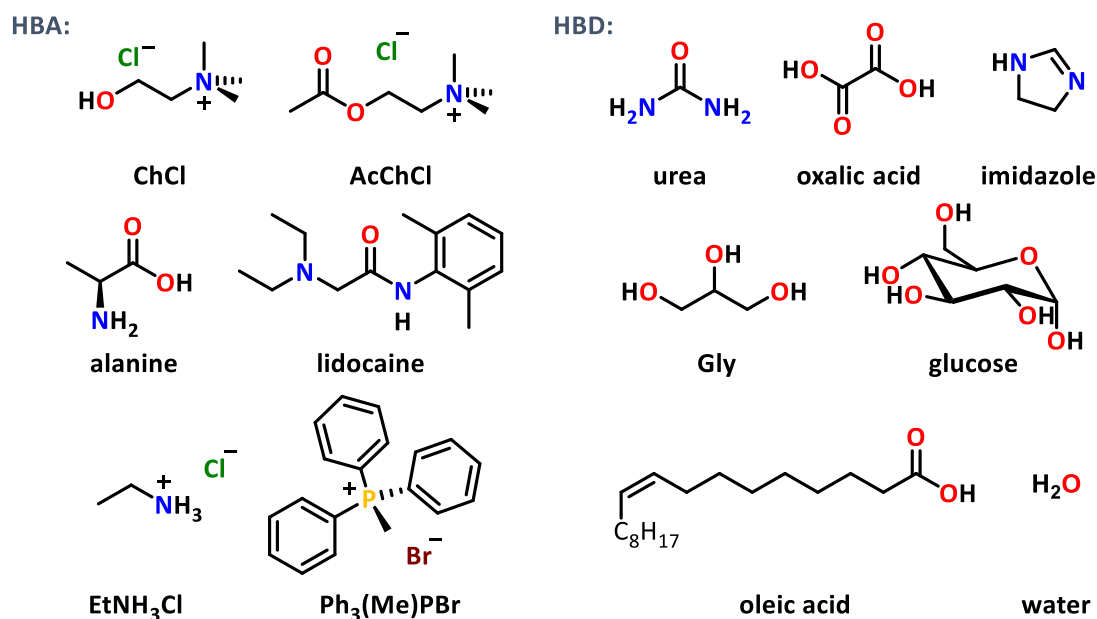


Figure 7 – Example constituents of a type III DES.

Type IV – A metal salt and a hydrogen bond donor.

The most recently defined and smallest type of DESs are those which are type IV, which consist of a metal salt and hydrogen bond donor. Few examples have been found, but zinc chloride has been shown to form room temperature eutectics with amides and alcohols.³⁸

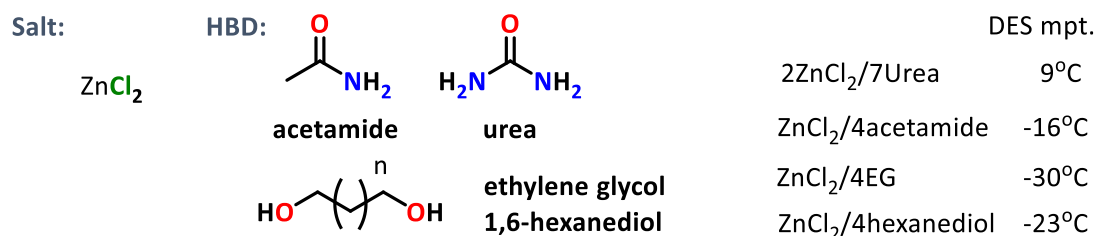


Figure 8 – Example constituents of a type IV DES.

Water is often included as a HBD in type III DESs, either alone or part of a three component mixture. The description of a water containing solvent mixture as DES and not simply a solution may appear contentious, but many studies have focussed on the nature of the interactions in DESs and compared these to water containing DESs, using techniques ranging from NMR spectroscopy³⁹ [Figure 9] to neutron scattering,^{22, 40, 41} and computational studies⁴² to probe interactions the H-bonding interactions in DESs and the effects upon the addition of water.

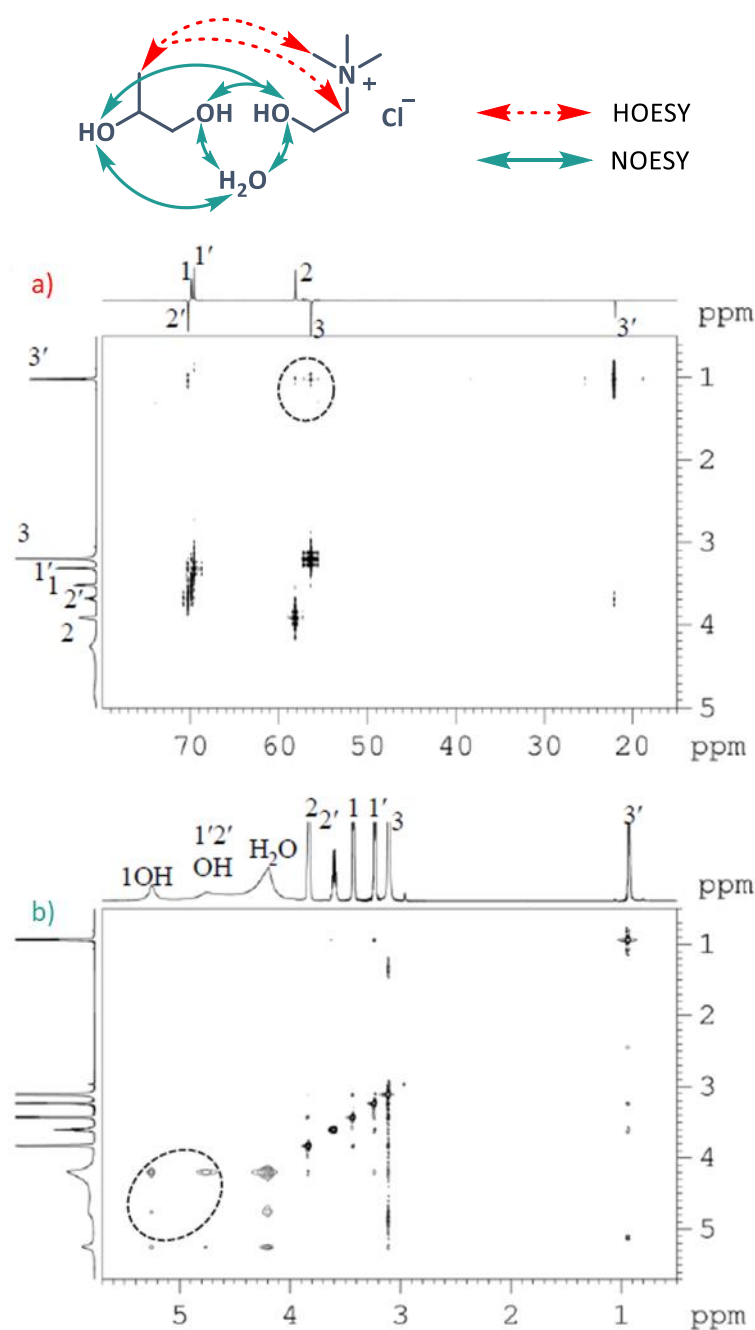


Figure 9 – ¹H NMR spectroscopy studies (HOESY, NOESY) of the interactions present in ChCl/1,2-propandiol/H₂O – From “Natural deep eutectic solvents as new potential media for green technology”.³⁹

The disruption of the H-bonding which forms the DESs appears to occur in stages upon addition of water. In the case of ChCl/2Urea the majority of DES interactions were found to remain intact experimentally up to around 42% w/w H₂O and remain so until 51% w/w (83 mol%) before solvating interactions became dominant, with the DES' H-bonding network initially able to accommodate water molecules interstitially.²¹ Although simulations have shown that other DESs such as ChCl/2Gly may already display a level of disruption of H-bonding as low as 5% w/w water as it is less able to interstitially accommodate the water molecules, with choline chloride instead showing a preference for solvation by water rather than glycerol. These apparent stages of water solvation, and the difference between the hydration of ionic liquids, DESs, and salts are illustrated in **Figure 10**.

The solvation by water has been suggested to be unequal amongst the DES components. Simulations of the addition of water to ChCl/2Urea mixtures have reported the strongest solvation to the chloride ions being primarily responsible for the disruption to H-bonding, although substantial urea-water interactions also form. Although interestingly one study has found by simulation that moving to high levels of water, even up to 90 mol% H₂O, in ChCl/2Urea the Cl⁻ anions were found to be not water saturated, with DES interactions still competing.¹⁹

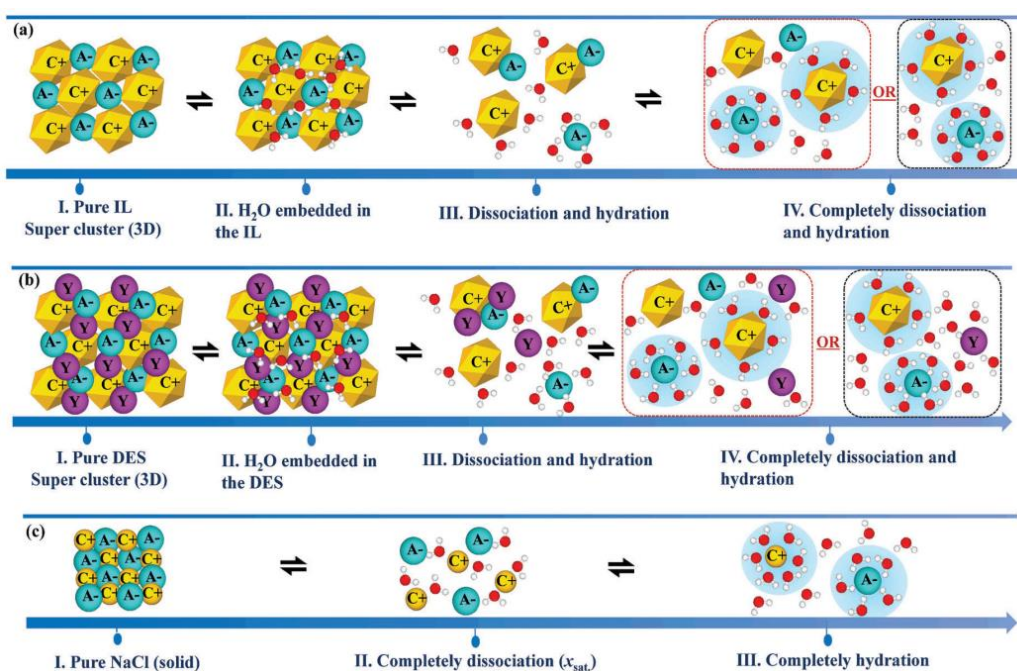


Figure 10 – IL and DES hydration vs NaCl hydration – From “The peculiar effect of water on ionic liquids and deep eutectic solvents”.¹⁹

I.III – Deep eutectic solvents, glycerol, and sustainability

Having introduced deep eutectic solvents, it now seems necessary to examine their green credentials to ascertain if they really are a sustainable alternative to traditional VOC solvents. For a large part of this thesis the DESs or components that are involved are type III (specifically choline chloride mixtures) therefore only chlorine chloride, glycerol, and ethylene glycol are examined here | **Figure 11** |. Although some DESs exclusively formed from natural (NADES)^{43, 44} and bio-mass (Bio-ILs)²⁴ derived components have been developed, with some even being hydrophobic (HESs),⁴⁵⁻⁴⁷ but these will not be considered in this thesis.

Choline chloride	ChCl is a quaternary ammonium salt, which is considered as an essential nutrient by the Food and Nutrition board of the US Institute of Medicine and widely produced for as an animal feed additive. ⁴⁸ Its innocuous nature complies with the green principles; however it is not currently renewably produced, with ethylene oxide which is petroleum derived, a feedstock for its current production. ^{49, 50}
Ethylene glycol	Unlike other DES components EG is toxic, being withdrawn from use in antifreeze due to the effects experienced by human consumption. ^{51, 52} It is also not currently renewable, being derived industrially from ethylene oxide similarly to choline chloride. However, an alternative method using carbon dioxide as a feedstock exists. ⁵³⁻⁵⁵
Glycerol	On the other hand Gly can be considered a fully green solvent as it is non-toxic, being used as a food additive, and produced from triglycerides coming from natural oils such as coconut, palm, rapeseed, and tallow from animals (which may have their own environmental considerations). These triglycerides are cleaved into desirable fatty acids and glycerol. The fatty acids produced are in high demand for a range of applications including biodiesel, making glycerol a highly produced side product. The triglycerides are normally split in three ways: high temperature/pressure hydrolysis, transesterification, or saponification with sodium hydroxide. ^{56, 57}

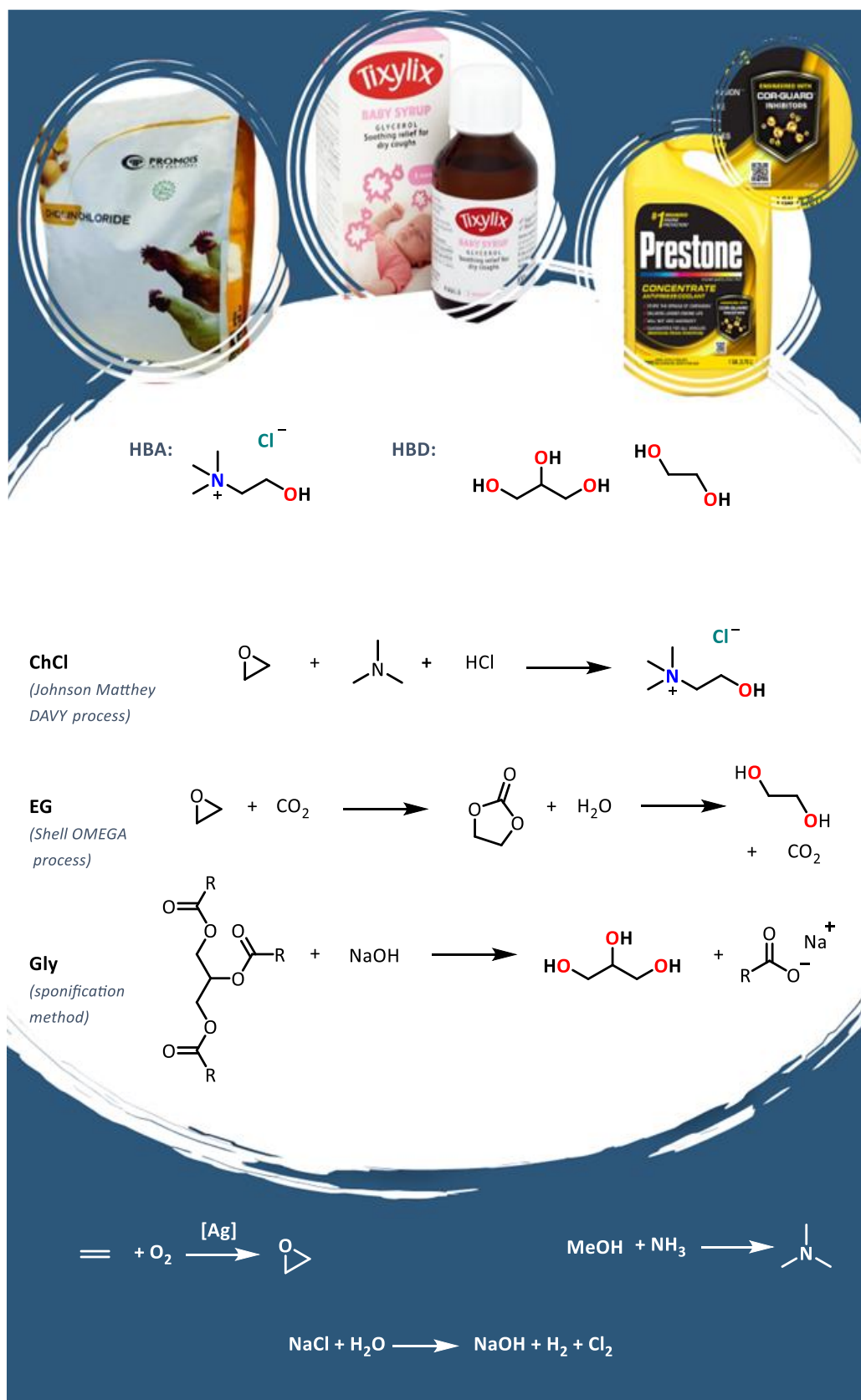


Figure 11 – The industrial production of choline chloride,⁵⁰ ethylene glycol,^{54, 55} and glycerol.^{56, 57} Including the formation of ethylene oxide,⁵⁸ trimethylamine,⁵⁹ and sodium hydroxide⁶⁰ reagents.

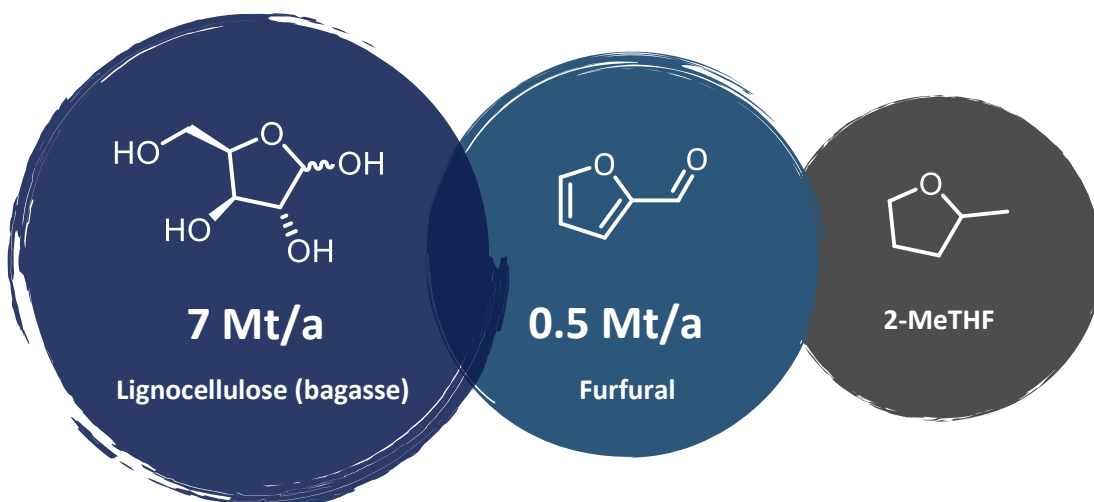
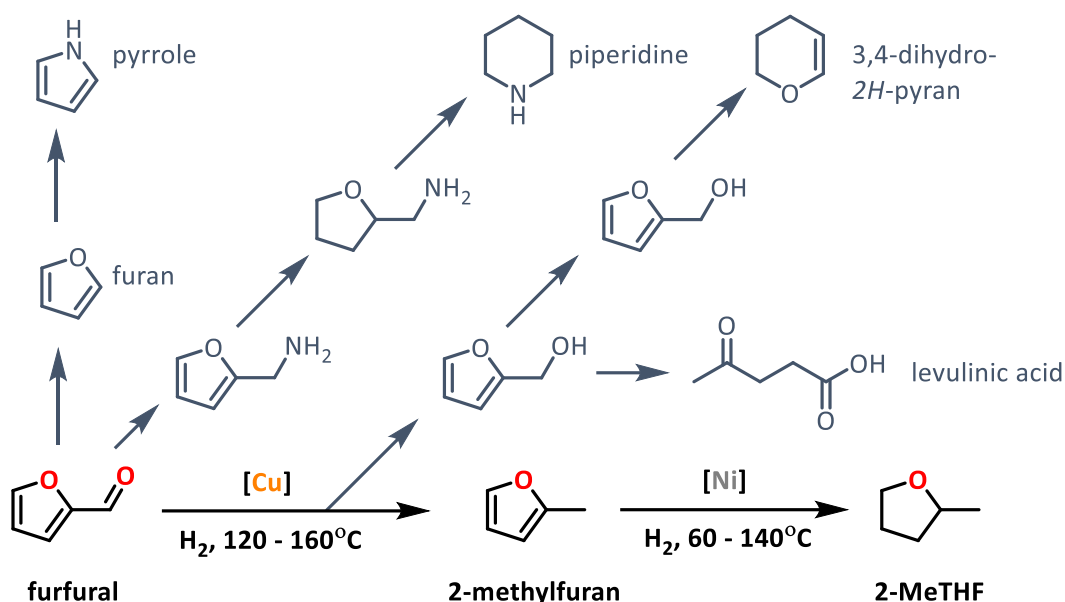


Figure 12 –The main species involved in the production of 2-MeTHF.⁶¹⁻⁶⁴

2-Methyltetrahydrofuran (2-MeTHF) is a bio-derived etheral solvent that is considered as (along with others such as cyclopentyl methyl ether, and 2,2,5,5-Me₄THF) one of the most promising alternative solvents to toluene and THF.^{65,66} Part of its success can be attributed to its relatively non-polar nature, which is uncommon amongst bio-derived solvents due to the large number of oxygen atoms that are often present in these compounds. The inherent relatively low polarity eliminates the need for removal of oxygen or incorporation of chlorine to reduce polarity as in other cases.⁶⁷

It is a derivative of furfural, which is produced from the lignocellulose from waste plant matter. Biomass offers a large scale renewable feedstock from which to produce solvents such as 2-MeTHF as, for example, around 7 million tonnes of biomass in the form of sugarcane bagasse was produced in the EU in 2017/2018 alone |**Figure 12**|.⁶¹ Furfural is one of the compounds commonly produced directly from lignocellulose by acid hydrolysis, with 500,000 tonnes being produced globally in 2015.^{62,63} Furfural is then transformed into a range of derivatives including 2-MeTHF, which is produced in two base metal catalysed hydrogenation steps, as shown in **Scheme 2**.⁶⁴



Scheme 2 – Scheme of some of the main furfural derivatives, highlighting the synthesis of 2-MeTHF.⁶⁴

The sustainable and non-toxic nature⁶⁸ of 2-MeTHF make it an attractive solvent option, but its properties are what makes it useful. It has a higher boiling point (80°C) than THF and a suitably low melting point, and is also mostly immiscible with water negating the necessity of solvent addition in reaction work ups and extractions.⁶⁹ Of particular relevance to solvent consideration in polar organometallic chemistry 2-MeTHF falls in between THF and Et₂O in terms of polarity and Lewis donor ability to alkyl lithium reagents. Furthermore, 2-MeTHF has been found to perform equally well or better than THF in reactions involving lithium aluminium hydride, alkyl lithium and Grignard reagents due to occasionally increased solubility of the organometallic species.⁶⁹

Despite all of the desirable properties of 2-MeTHF, one ‘problematic’ property that it shares with THF is the formation of peroxides.⁷⁰ 2-MeTHF, like other ethers, produces peroxides in the presence of air and is normally sold with the same quantity of inhibitor as THF, 250 ppm butylated hydroxytoluene. Other ethereal solvents require less inhibitor, with Et₂O normally sold with < 10 ppm, and cyclopentyl methyl ether (CPME) only 50 ppm. CPME is the main competitor to 2-MeTHF as a green solvent, with many similar properties. The only advantage that 2-MeTHF has is that currently CPME is produced (albeit with very high atom economy) from cyclopentene which is petroleum derived. However, it is possible to derive CPME from furfural, similarly to 2-MeTHF, which it may become in the future as green solvents gain momentum.⁶⁶

It should be noted however that, although currently produced in a non-renewable way, THF could also be produced as a derivative of furfural as outlined below in **Figure 13**.^{15, 71, 72}

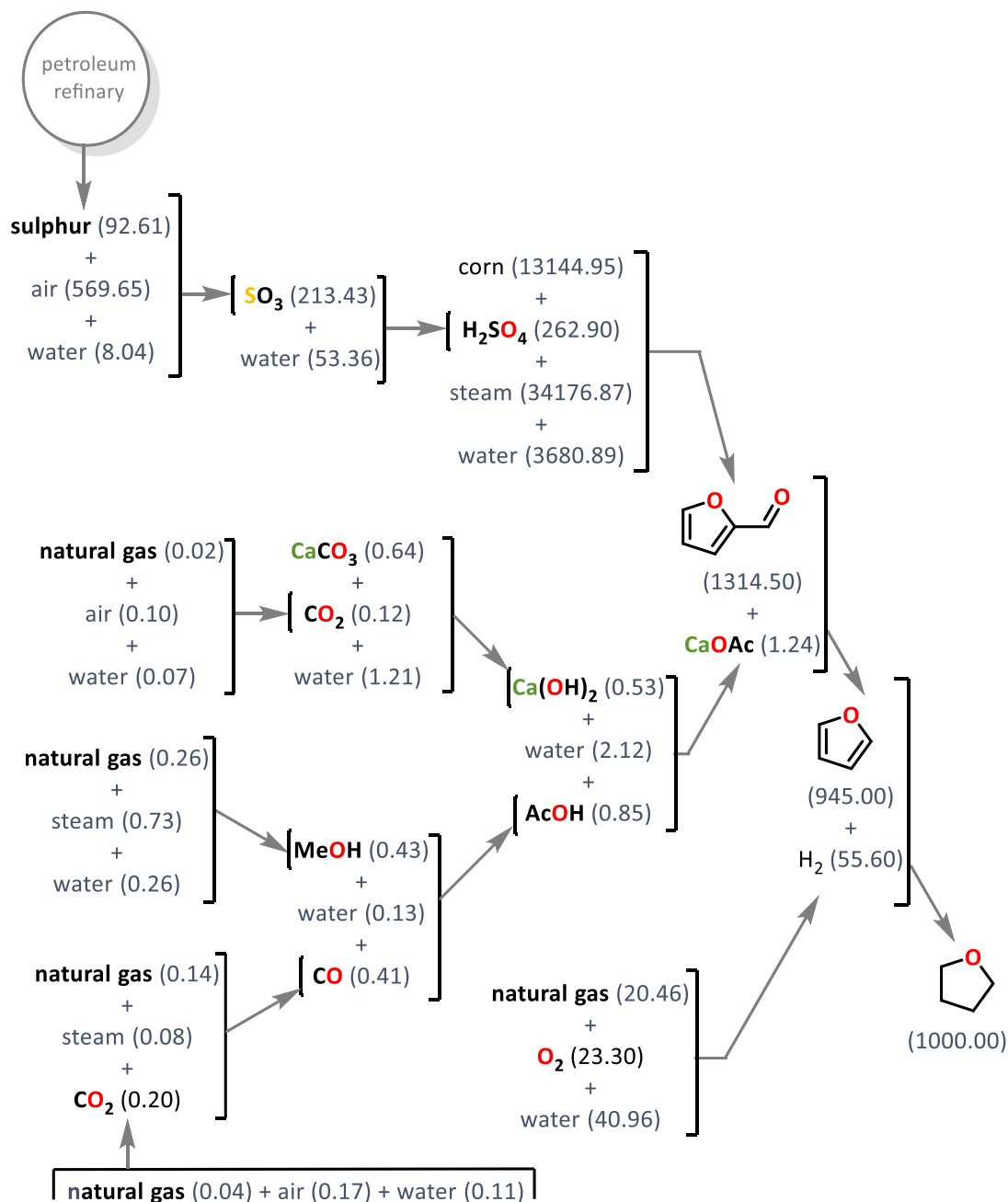
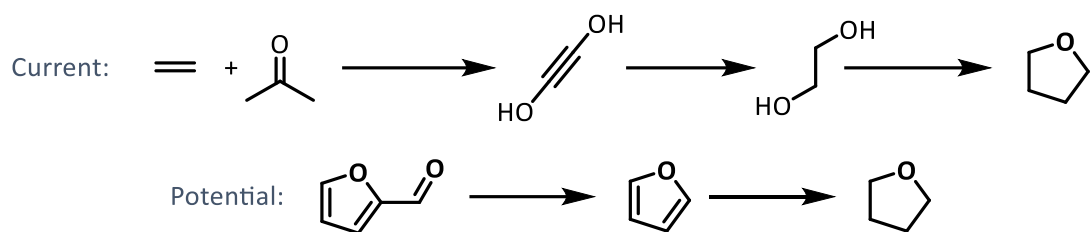


Figure 13 – The current and potentially renewable synthesis of THF,^{71, 72} including quantities required to produce 1000 kg THF vis furfural as outlined by GlaxoSmithKleine.¹⁵

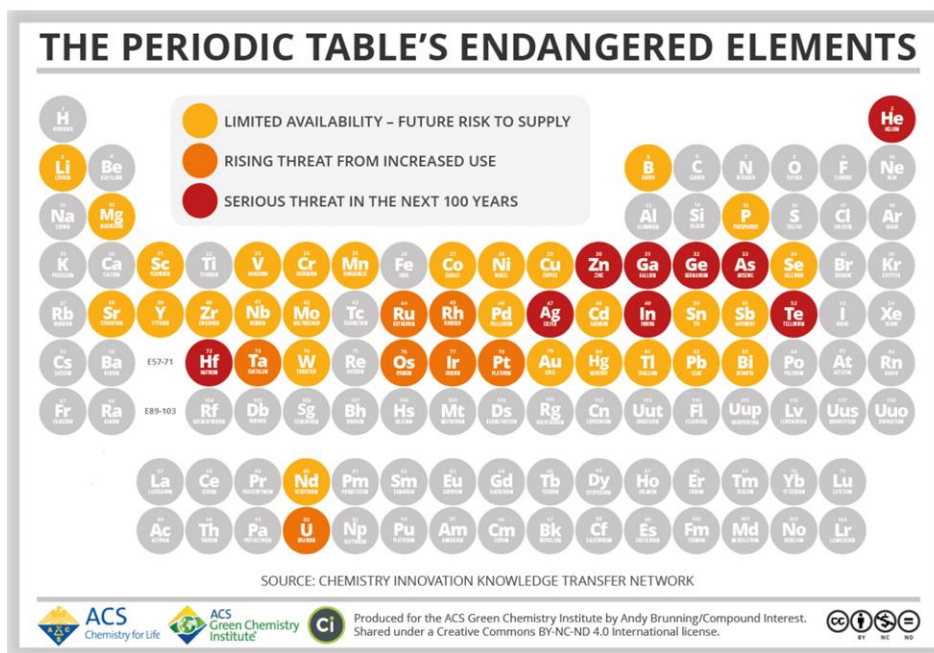


Figure 14 – “The periodic table’s endangered elements” by the ACS Green Chemistry Institute.⁷³

As already established one of the major concerns of green chemistry is the sustainable sourcing of materials. This extends all the way from solvents and chemical species down to the individual metals required as part of reagents or catalysts. 150 years after the creation of the periodic table by Mendeleev, 2019 was marked as the UNESCO International Year of the Periodic Table, in which there was a focus on the use and supply of individual elements. Both the American Chemical Society (ACS) |Figure 14| and the European Chemical Society (EuChemS) |Figure 15| have produced periodic tables outlining those elements have an endangered supply at current usage. In these is it clear to see that a large swathe of the transition metals are of limited availability or under extensive use. Therefore, it is clear that any move towards the use of more abundant main group elements can help alleviate the strain on some of the elements where demand rivals supply.

The main elements used in this work are the s-block metals, specifically the early alkali and alkaline earth metals: lithium, sodium, potassium, and magnesium. As can be seen by the size of the box in which each element is contained in Figure 15 the aforementioned elements are some of the more abundant on earth. Despite this lithium and magnesium are shown as of limited availability due to high use. To get the full picture however, sourcing, processing and cost should be considered.⁷⁰

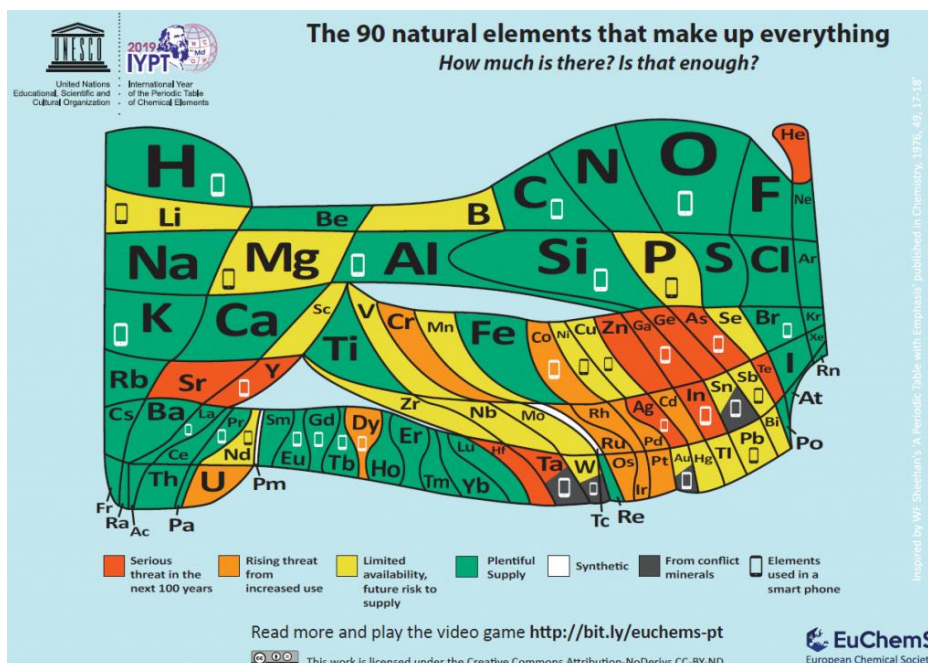


Figure 15 – “The 90 natural elements that make everything” by the European Chemical Society.⁷⁴

Lithium Originally sourced from by mining (petalite, $\text{LiAlSi}_4\text{O}_{10}$) lithium garners its name from ‘lithos’ (Greek: stone)⁷⁵ despite this it is now mostly produced from brines |Figure 16| which has become a more economical option. Although, due to the proliferation of lithium batteries previously unexplored sources are being examined to supply demand,⁷⁶ including the a number of mining operations, such as surface spodumene ($\text{LiAlSi}_4\text{O}_6$) mines.⁷⁶ World lithium extraction, supply and demand is elaborated in Figure 17.

Sodium Takes its name in English from ‘soda’, as in soda ash (Na_2CO_3) and caustic soda (NaOH).⁷⁵ Sodium compounds are also obtained during the extraction of lithium from brines |Figure 16|. Large deposits of trona ($\text{Na}_2\text{CO}_3 \cdot \text{NaHCO}_3 \cdot 2\text{H}_2\text{O}$) and salt are also readily available, therefore sodium is not considered endangered.⁷⁷

Potassium Takes its name in English from ‘potash’, which is mixture of soluble potassium salts (KCl , K_2CO_3).⁷⁵ Similarly to sodium it is obtained in the extraction of lithium from brines |Figure 16|. Due to this, and large sources of sylvinitite (mixture of KCl and NaCl) and langbeinite [$\text{K}_2\text{Mg}_2(\text{SO}_4)_3$] able for deep-well solution mining potassium is not considered endangered.⁷⁷

Magnesium Named from after the mineral ‘magnesia alba’ (Latin: white magnesia) from the Magnesia region of Greece (now known as periclase, MgO) [notably the similarity in name with manganese derives from here coming from ‘magnesia negra’ (black magnesia, now pyrolusite, MnO₂)].⁷⁵ A significant percentage of magnesium is also produced from brines [Figure 16], but also from the processing of magnesite (MgCO₃), brucite [Mg(OH)₂], and dolomite [CaMg(CO₃)₂] amongst other minerals.⁷⁸

Despite appearing as being of ‘limited availability’ in both ACS and EuChemS periodic tables the ‘Mineral Commodity Summaries 2019’ by the US Geological Survey (US Department of the Interior) lists magnesium supplies as “sufficient to supply current and future requirements”.⁷⁷ Although in the case of magnesium geopolitical concerns surface as, unlike the alkali metals mentioned which have relatively widespread production, magnesium (both metal and mineral forms) are mostly produced by China^{77, 78} raising some concerns over supply [Figure 17].

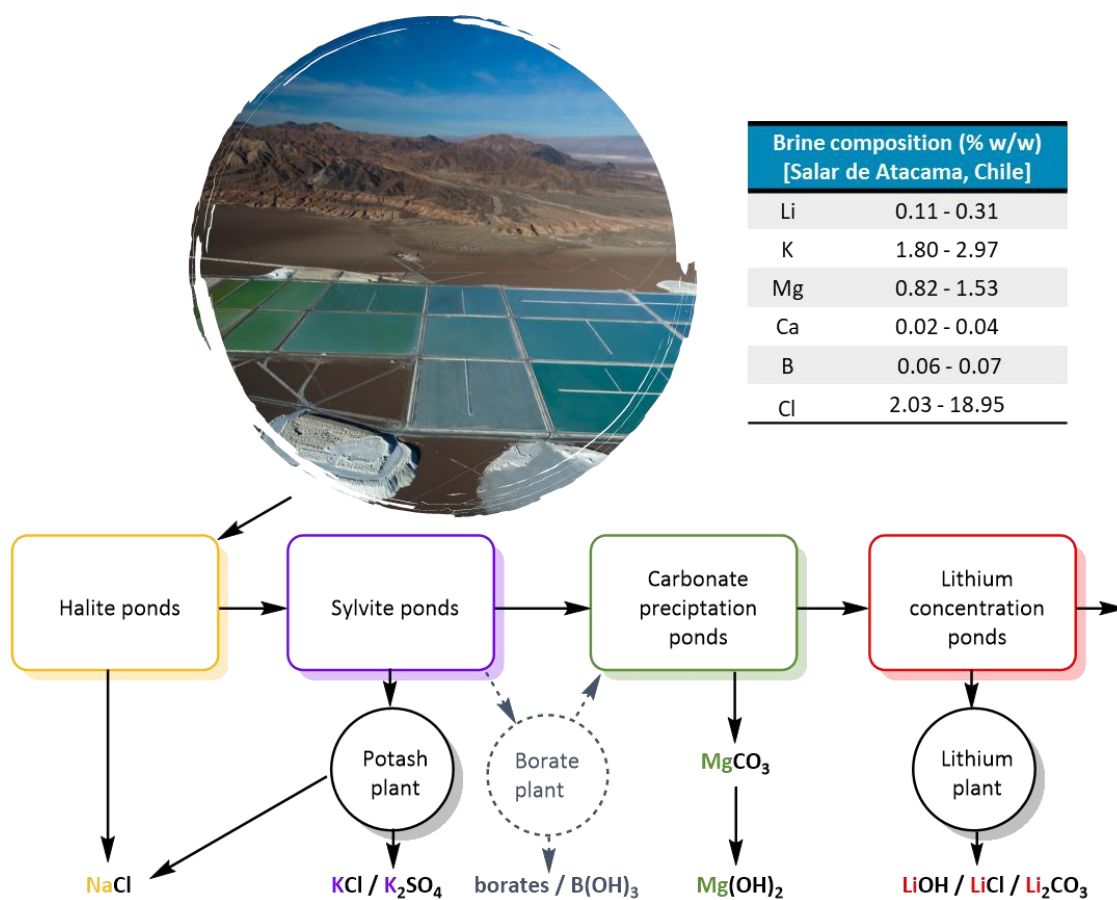


Figure 16 – Simplified lithium extraction process from continental brines, with example of ‘Salar de Atacama’.⁷⁶

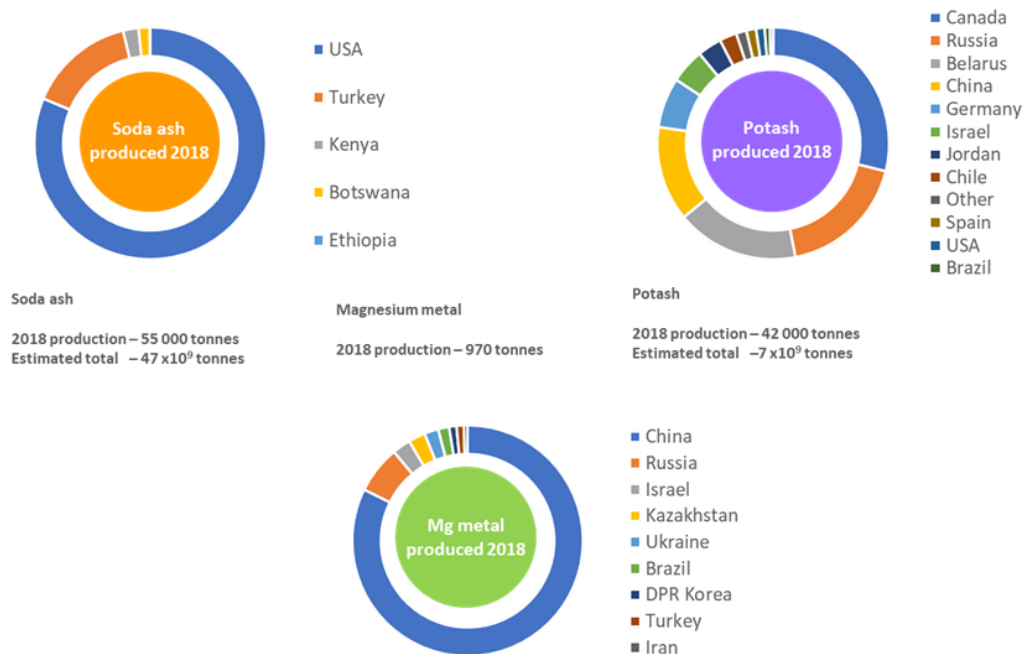
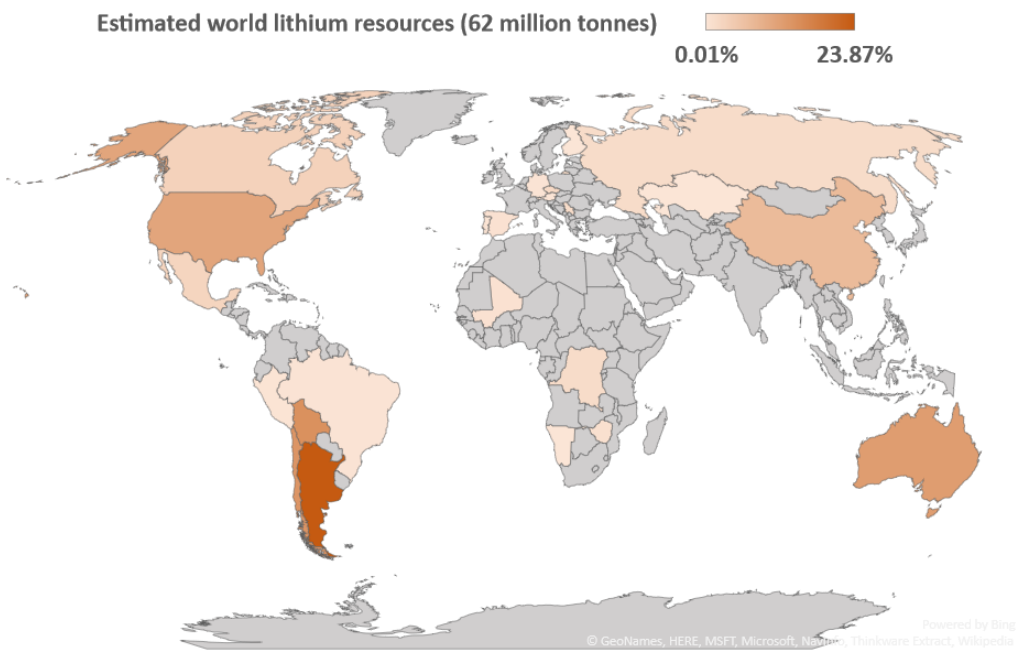
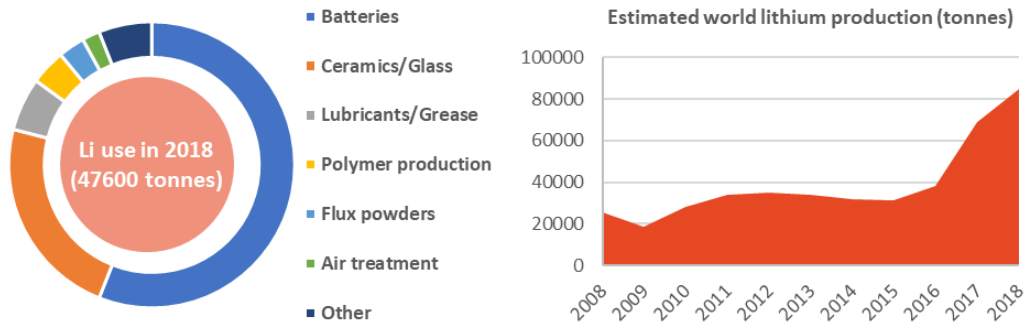


Figure 17 – Estimated global use, production, and supply of lithium, and 2018 production of sodium and potassium minerals and magnesium metal.^{76, 79}

I.VI – Polar main group organometallic reagents: reactivity, limitations and incompatibility

In order to appreciate the aptness of heterobimetallic compounds in catalysis it is necessary to initially consider homometallic organometallic reagents.

Polar main group organometallic compounds, in particular organolithium reagents, have been extensively used in metallation reactions in synthetic chemistry. Organolithium and lithium amide compounds have been known for around a century⁸⁰ and, although thought to be of limited use at the time, have grown to become involved in more than 90% of natural product synthesis,⁸¹ with some lithium amides even earning the name “utility amides”.⁸²⁻⁸⁴ Despite this widespread use, their high reactivity imposes severe limitations [Figure 18]; requiring low temperatures (-78°C or below) due to low functional group compatibility (reactivity with nitriles and nitro groups well below ambient temperature and esters even below -78°C)⁸⁵ and deprotonation of common organic solvents.^{82, 86} So overall these reagents require consideration of conditions to ensure selectivity and to avoid unwanted, detrimental side reactions.

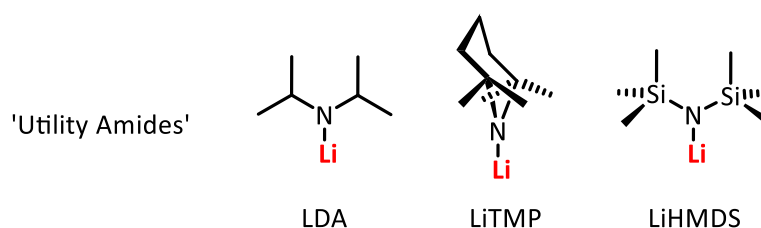
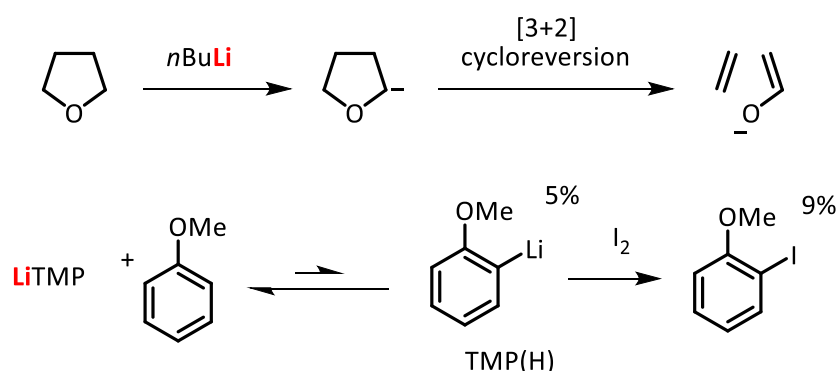


Figure 18 - |top| limitations of organolithium reagents: the decomposition of THF at ambient temperature and equilibrium limited deprotonative lithiation |bottom| the ‘utility amides’: lithium diisopropylamide, lithium 2,2,6,6-tetramethylpiperide, lithium hexamethyldisilazide.

A key fundamental aspect of organolithium chemistry is the ability for the species to exist in different aggregations states. Unlike the manner in which the organolithium species are represented in **Figure 19** they do not exist as discrete monomers. Instead they form aggregates, where the level of aggregation is dependent on the solvent, any additional Lewis donor molecules present, and the inherent nature of the organolithium species itself (sterics and ability to sustain π - or agostic interactions). The level of aggregation is influential in a species' reactivity, as a less aggregated state is generally associated with higher reactivity, although there is evidence that this is an oversimplification and not always the case.⁸⁷ Despite the passing of a century the identity of the aggregates present in many organolithium reagents are still being discovered,⁸⁸ such as the recently elucidated aggregates of isopropyllithium.⁸⁹ For the example of LiTMP the effect of environment on aggregate formed is highlighted in **Figure 19**.

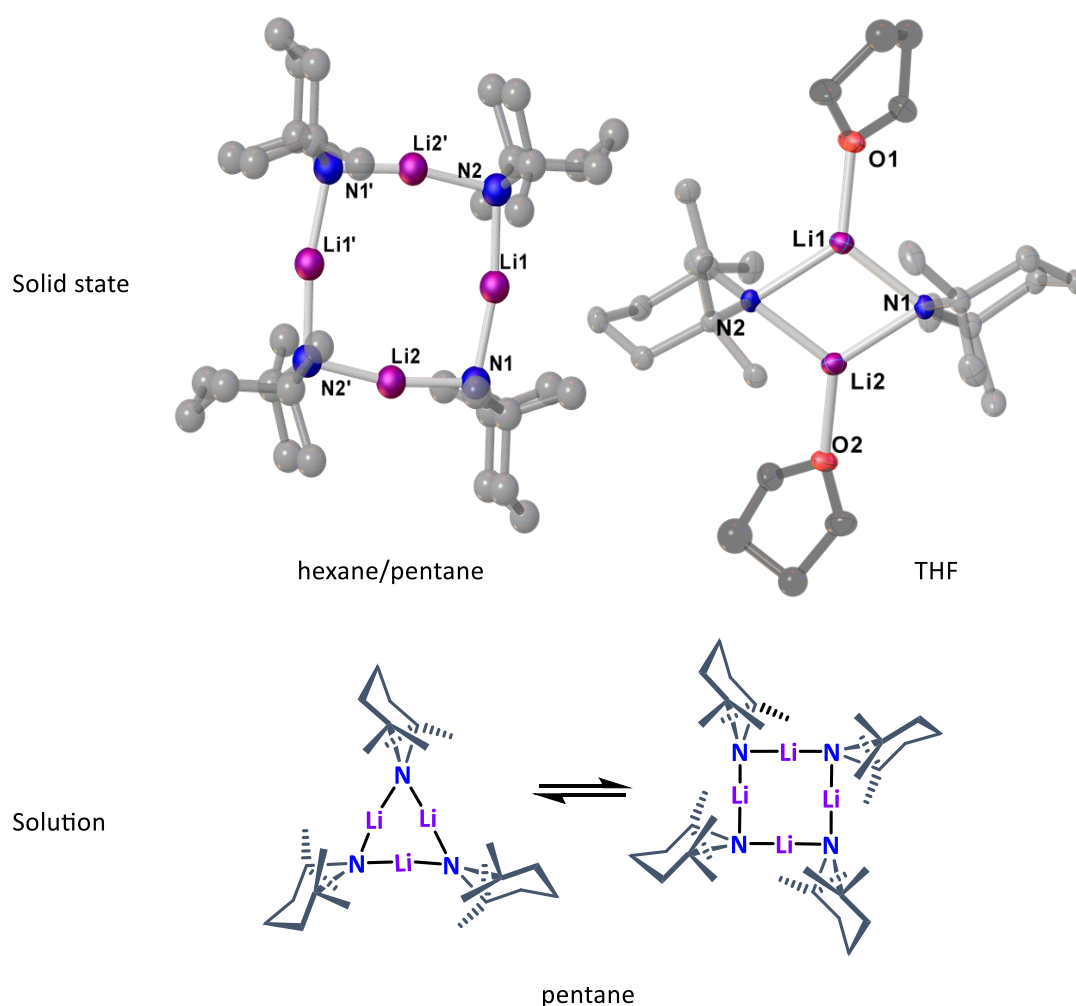


Figure 19 – Aggregates of lithium 2,2,6,6-tetramethylpiperidide from hydrocarbons,⁹⁰ THF⁹¹ and hydrocarbon solution.⁹²

Turning to organomagnesium compounds, they have been known for equally as long as organolithium compounds, with Grignard winning the Nobel Prize for the discovery of the 'RMgX' compounds which bear his name in 1912.⁹³ They differ from organolithium compounds in that magnesium is more electronegative: forming less polarised bonds with more covalent character than highly ionic Li-R bonds. This lower polarity causes a marked reduction in reactivity; and subsequently more user-friendly reaction conditions; indeed in some cases it is necessary to heat reaction for effective conversions to be obtained. Another benefit is that there is often an increase in functional group tolerance.⁸²

A key point in the chemistry of Grignard reagents is their fluxional nature in solution, as they partake in a process known as the Schlenk equilibrium, which results in as a complex mixture of species which are intermediate between heteroleptic and homoleptic magnesium compounds |Figure 20|. ⁹⁴

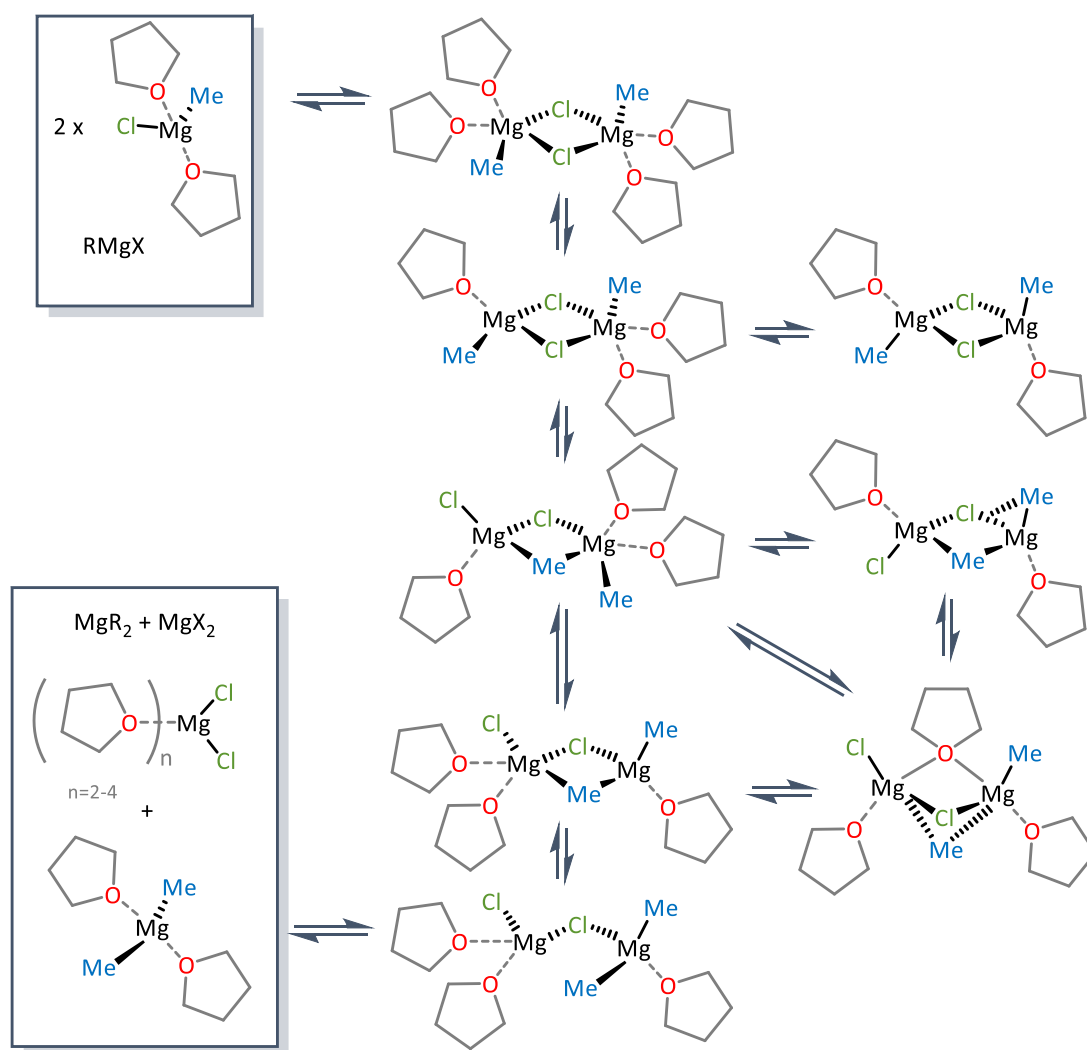


Figure 20 – The myriad of species which populate a solution of 'MeMgCl' in THF.

I.VII –Cooperativity in polar main group organometallic chemistry

Although over 150 years since the discovery of the first alkali metal metallate or ‘ate’ species by Wanklyn, namely NaZnEt_3 ,^{95, 96} these mixed metal organometallic species have remained little more than curiosities for most of the time that has passed since their inception. Even 100 years later when Wittig reported the first alkali metal magnesiate in 1951⁹⁷ the capability of these heterobimetallic species remain unexplored, but they have more recently developed into a new family of versatile organometallic reagents which is finding widespread applications in organic synthesis.⁹⁸⁻¹⁰²

In most cases an ate complex combines two different metals of distinct polarities, and can be defined as a mixture of a stoichiometric quantity of Lewis acid and base where the Lewis acid has formally increased its valency and become an anion.^{82, 103, 104} Combinations can include, but are by no means limited to, magnesium, zinc or aluminium as the more Lewis acidic part and an alkali-metal containing more Lewis basic component. In terms of structure, these ate complexes are found in two forms; solvent-separated ion pairs (SSIP) and contacted ion pairs (CIP). SSIP generally occur when strong Lewis donating solvents are employed and CIP in non-polar solvents, although the nature of the ligands and any other additive donor greatly impact the structure.⁸² The structure of CIP complexes is often linear with bridging ligands between the metals and the more Lewis acidic metal in the centre. This structure is known as a ‘Weiss motif’ [Figure 21], named such due to Weiss and co-workers’ discovery of this configuration as a preferred structure and highlighting the importance of knowing these compounds’ structure in order to understand their “true nature”.^{86, 105, 106}

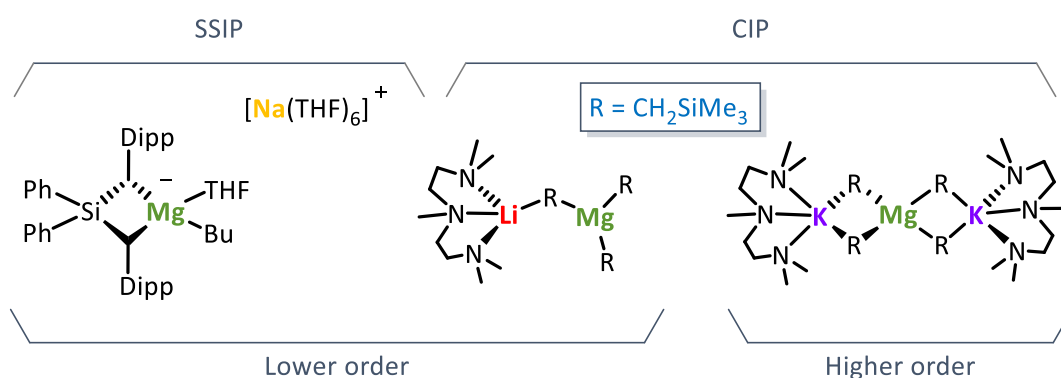


Figure 21 – Examples of solvent-separated, contacted ion-pair, lower-order- and higher-order alkali metal magnesiates.

Figure 21 also shows an example of a higher-order magnesiate, where the ratio of alkali metal to magnesium is greater than one, which is accomplished simply by mixing two equivalents of organo-alkali-metal to organomagnesium compound. It is also seen in **Figure 21** that theSSIP structure, in contrast to a Weiss motif, has no bridging ligands between sodium and magnesium and the sodium is solvated by six THF molecules.

There are two main methods of making ate complexes: co-complexation and salt metathesis [**Figure 22**]. Co-complexation involves nothing more than mixing an organometallic compound of each metal, and is a useful way of forming heteroleptic complexes as the two organometallic species being mixed can have different organic groups. Salt metathesis usually involving a metal halide salt of a low polarity metal which is reacted with a more polar organometallic reagent such as an organolithium; therefore using the formation of an alkali metal halide as the driving force for the formation of the ate.^{82, 86} Due to the various structures that can be obtained depending on the metals, ligands, solvent and donor used in their preparation there has been a great interest in the synthesis of different heterobimetallic complexes. This has sparked the investigation into the synthesis, structure, and reactivity of complexes ranging from alkali metal magnesiates, zincates, and aluminates,¹⁰⁷ to less common ferrates¹⁰⁸ and gallates,¹⁰⁹ even extending to calcium aluminates and gallates,¹¹⁰ and has shown the cooperative behaviour displayed by this class of compounds.¹¹¹

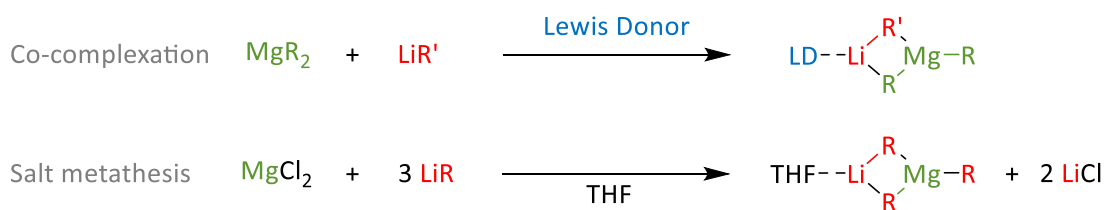
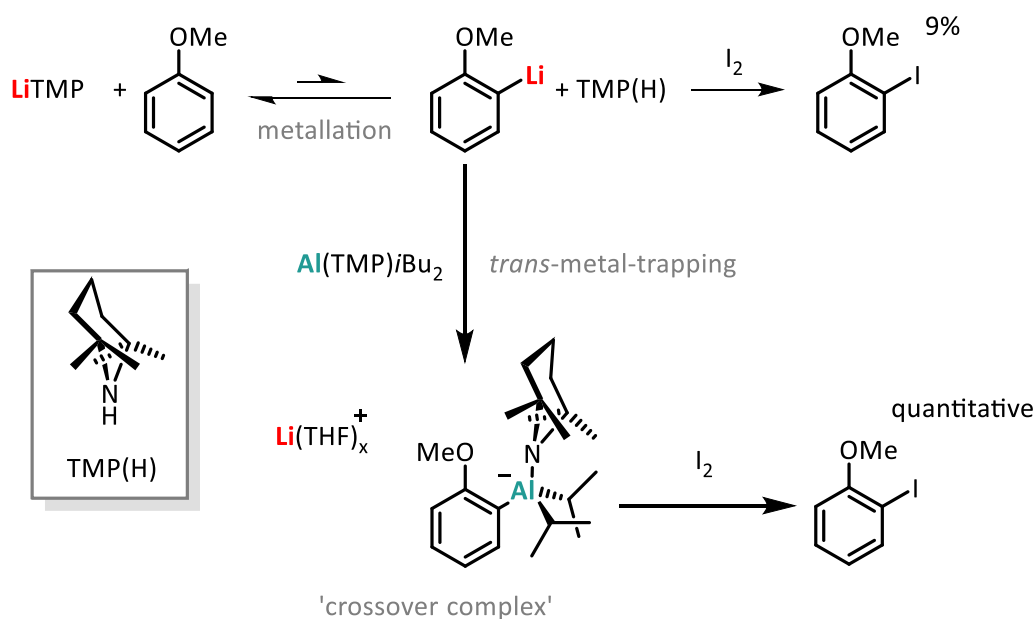


Figure 22 – Methods for the formation of ates: co-complexation and salt metathesis.

By engaging metal-metal cooperativities, these bimetallic systems can offer superior chemo- and regioselectivities and/or functional group tolerances to those of their monometallic counterparts.^{82, 112, 113} Most reactivity studies have focused on using these reagents as metallating reagents (via Mg-H or Mg-X exchange processes) as well as anionic transfer agents to unsaturated organic molecules.^{114, 115}

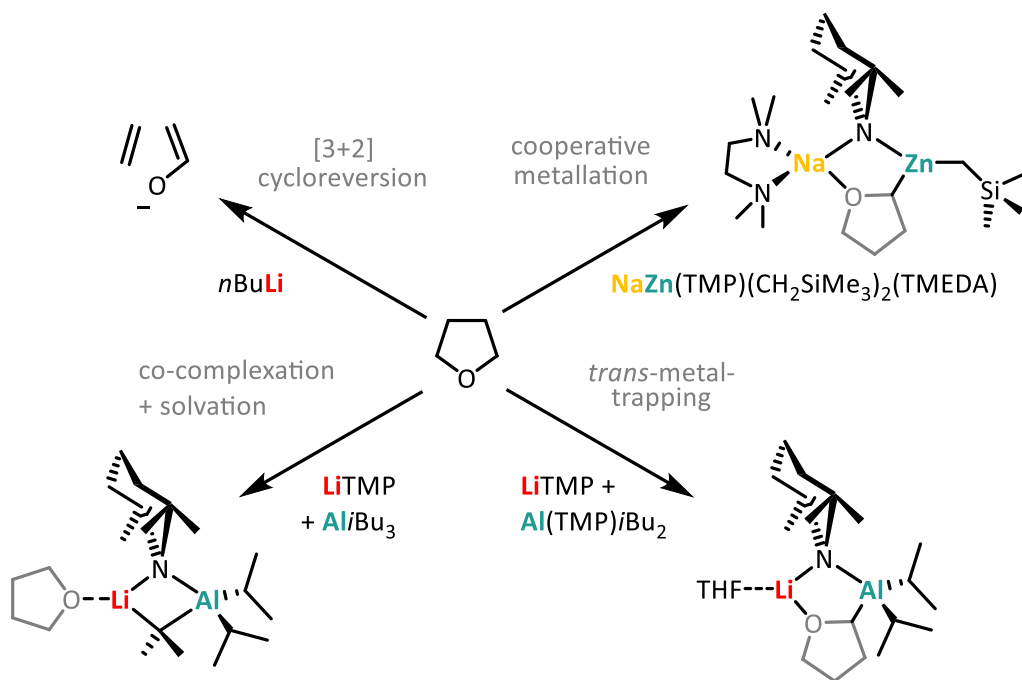
One of the ways in which the benefits of bimetallic cooperativity can be clearly seen is where enhanced reactivity is observed compared to a monometallic reagent. This cooperativity can be observed in *trans*-metal-trapping,¹¹⁶ where an alkali metal base and a 'trap' such as an organoaluminium or gallium species can effectively metallate compounds which are difficult for the alkali metal base to do so alone. The efficacy of the metallation stems from the bimetallic ate species or 'crossover complex' which is formed during the reaction that stabilises the reactive intermediate, providing a driving force for more complete metallation, and additionally an ability to metallate more sensitive substrates. In **Scheme 3** it can be observed that the formation of a bimetallic crossover complex drives the equilibrium towards lithiation in so furnishing, upon quenching, a near quantitative iodination of anisole. Notably, key to this *trans*-metal-trapping regime is the inability of base and trap to co-complex to form an ate, or else reactivity is shut down, as illustrated in **Scheme 4**.



Scheme 3 – The metallation and iodination of anisole via *trans*-metal-trapping using lithium 2,2,6,6-tetramethylpiperidide base and diisobutylaluminium(2,2,6,6-tetramethylpiperidide) 'trap'.

A similar *trans*-metal-trapping regime can also be used to carry out the deprotonation of THF. Here the formation of the stabilising crossover complex, rather than as a thermodynamic driving force as was the case with anisole, is instead used to stabilise the reactive THF anion which normally decomposes upon metallation with strong alkali metal bases [Scheme 4].¹¹⁷

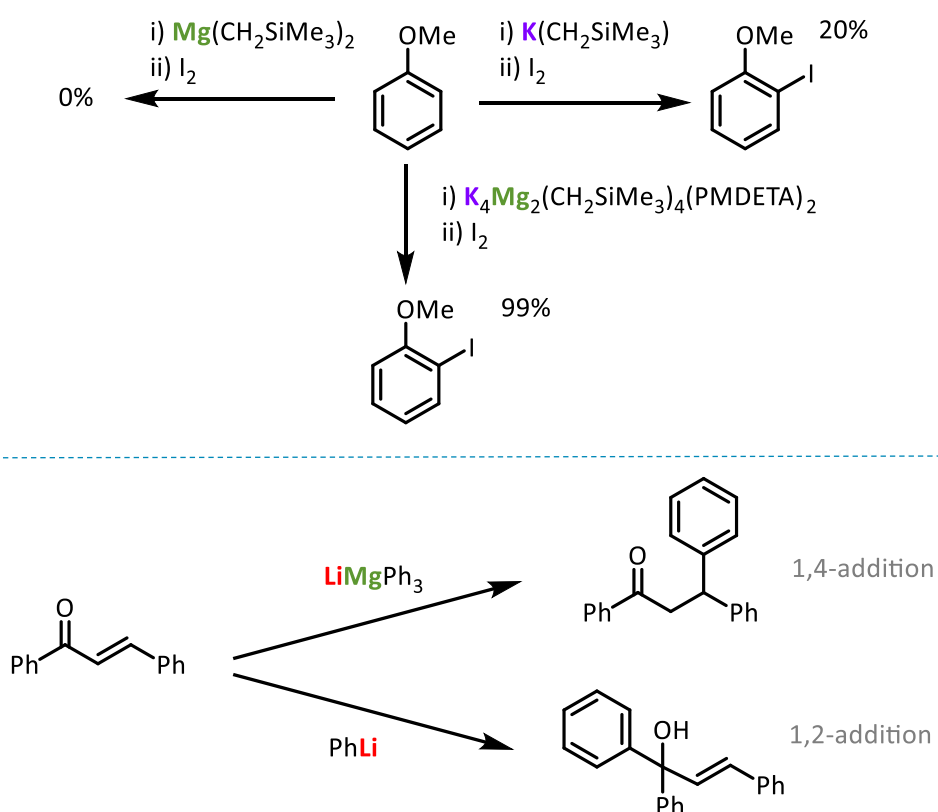
Trans-metal-trapping is a case of two monometallic complexes working synergistically, where the stabilising effect of a bimetallic complex can be used to enhance reactivity. It is also possible to achieve the same result using a bimetallic ate complex, directly making use of its bifaceted reactivity as an effective base and stabilising effects. Although aluminates formed from species similar to the *trans*-metal-trapping reagents shown are not sufficiently basic to perform many of these deprotonations, by employing $\text{NaZn}(\text{TMP})(\text{CH}_2\text{SiMe}_3)_2$ the effective metallation of THF is possible [Scheme 4] through a combination of the sodium enhanced basicity of its alkyl ligands and stabilising formation a relatively non-polar Zn-C bond.¹¹¹



Scheme 4 – The reaction of THF with: $n\text{BuLi}$, cycloreversion; $\text{NaZn}(\text{TMP})(\text{CH}_2\text{SiMe}_3)(\text{TMEDA})$, cooperative metallation; $\text{LiTMP} + \text{Al}i\text{Bu}_3$, solvation; $\text{LiTMP} + \text{Al}(\text{TMP})i\text{Bu}_2$, metallation via *trans*-metal-trapping.

The enhanced reactivity gained by cooperativity in heterobimetallic complexes can be further evidenced using the same example of the metallation of anisole. In **Scheme 5** the alkali metal base, (trimethylsilyl)methylpotassium, is seen to be only poorly capable of metallating anisole, and bis[(trimethylsilyl)methyl]magnesium completely unable to perform metallation. However, the tetraorganomagnesiates $K_4Mg_2(CH_2SiMe_3)_4(PMDETA)_2$ was able to do so almost quantitatively under the same conditions.¹¹⁸

This enhanced ability can also be seen in other examples such as: the Lochmann-Schlosser superbases, where a mixture of *n*-butyllithium and potassium *t*-butoxide create a bimetallic base with a higher reactivity than *n*-butyllithium but greater stability than *n*-butylpotassium;^{117, 119} and ‘turbo’ reagents, where the addition of lithium chloride or a lithium alkoxide appears to increase the solubility and basicity or nucleophilicity of Grignard and zinc reagents in metallation by metal-halogen exchange and deprotonation.^{102, 120, 121}



Scheme 5 – |top| the metallation and iodination of anisole by bis[(trimethylsilyl)methyl]magnesium, (trimethylsilyl)methylpotassium, and $K_4Mg_2(CH_2SiMe_3)_4(PMDETA)_2$. |bottom| the direct-addition of phenyllithium to chalcone and conjugate addition of lithiumtriphenylmagnesiates to chalcone.

Aside from enhanced reactivity and tolerance, bimetallic complexes can open up unique reactivity profiles to those of their monometallic components,^{106, 122, 123} such as in the example of the 1,2-addition of phenyllithium of chalcone but the different chemoselectivity of lithium triphenylmagnesiates where the 1,4-addition is instead observed [Scheme 5].

This ability to affect chemoselectivity can be even more stark, such as the ability to promote the regioselective dimetallation of aromatic substrates. Unique directed *ortho-meta'* and *meta-meta'* regioselectivities have been accomplished using a supramolecular sodium magnesiate base (inverse crown complex)¹²⁴ which is able to perform templated metallation [Figure 23].^{125, 126} The ability to execute directed dideprotonation is a synthetically very useful tool as this cannot be done with standard reagents, furthermore the ability to promote meta metallation should be highlighted as this is normally challenging, with directed *ortho* metallation much more common.^{82, 124}

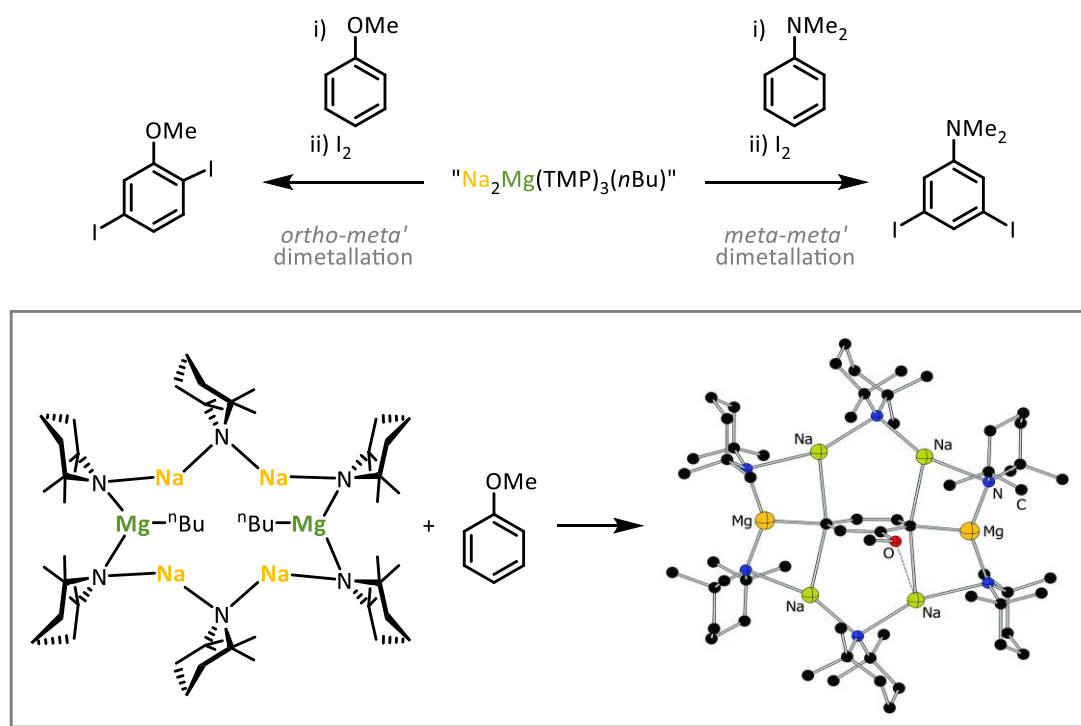


Figure 23 – The templated *ortho-meta'* metallation and iodination of anisole, and *meta-meta'* metallation and iodination of *N,N*-dimethylaniline through templated metallation by ' $\text{Na}_2\text{Mg}(\text{TMP})_3\text{nBu}$ ' (structure of the templated dimetallation of anisole shown).

Part 1 – Organolithium reagents in alternative solvents

Due to the inherent highly polarised bonds and reactive nature of polar main group organometallic species they are often pyrophoric, meaning they will react spontaneously and sometimes vigorously with the oxygen and moisture present in air and solvents. They therefore require handling under anhydrous conditions. This usually involves manipulation under inert atmosphere using a Schlenk line, storage of compounds in an inert atmosphere glovebox, and drying of reagents and solvent (normally by distillation over a desiccant and/or storage over molecular sieves). It has long been thought that these types of compounds were simply not compatible with standard bench conditions, i.e. open to air and ‘wet’ (protic) reagents/solvents, which has been said to be “one of the most formidable challenges in the field of organometallics”.¹²⁷ However, in recent years research is emerging that seems to show otherwise, and that it is possible to use these highly reactive reagents under bench conditions in some reactions.

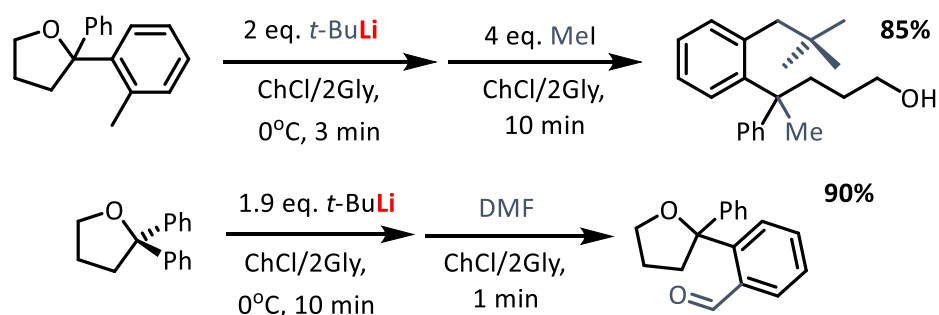


Figure 1.1 – Example inert atmosphere equipment: glovebox, dried reagents/solvent, and Schlenk line.

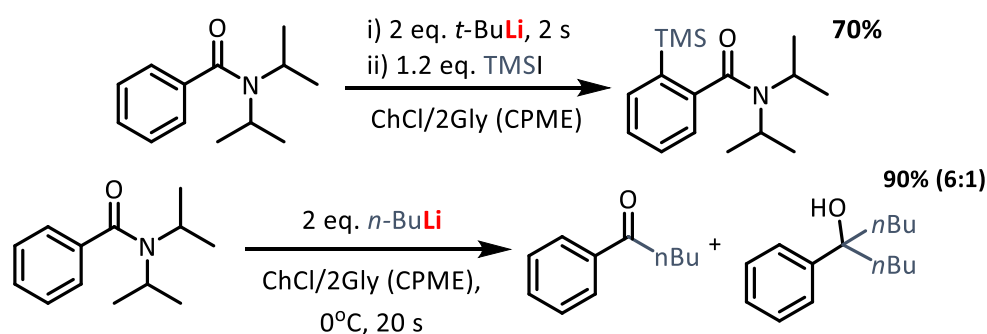
Recently organolithium reagents, workhorses of synthetic chemistry,^{128, 129} have been successfully employed in reactions under air in a range of alternative solvents including deep eutectic solvents, and water amongst others, demonstrating the ability for these reagents to be used more sustainably, under bench conditions in reactions which proceed more quickly than the competing hydrolysis.

One way in which organolithium and Grignard reagents have been successfully employed in alternative solvents is in deprotonation. In work by Capriati it has been demonstrated that aryl- and alkyl lithium reagents can be employed successfully in the lithiation and electrophilic quench of a range of alkyl and aryl compounds under air in both DESs and water.^{130, 131} Including recently reported switchable chemoselectivity, where the organolithium reagent can direct reactivity towards either *ortho*-metallation or acyl nucleophilic substitution.¹³² Most impressively these studies have even extended to the successful use of the extremely reactive *tert*-butyllithium [Scheme 1.1].

Capriati :



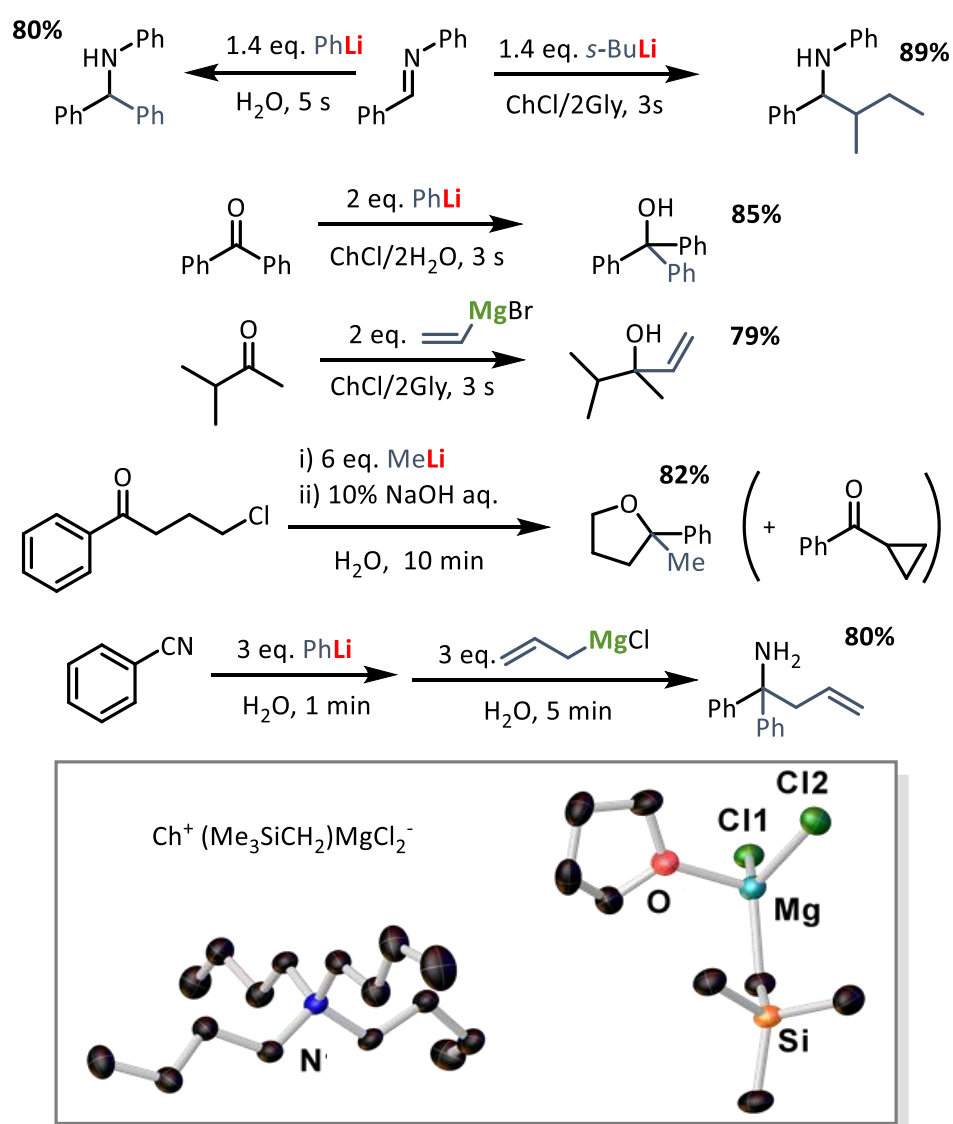
Capriati/Blangetti/Prandi :



Scheme 1.1 – The directed *ortho*-lithiation and electrophilic quench;^{130, 132} lateral lithiation and electrophilic quench;¹³¹ and nucleophilic acyl substitution¹³² under air in DESs and water.

In other work the ability for the addition of organolithium and Grignard reagents in alternative solvents has been explored. In these studies imines, ketones, and nitriles were shown to cleanly undergo nucleophilic addition in DESs and water. This has been demonstrated for a range of substrates using various alkyl- and aryllithium and Grignard reagents [Scheme 1.2].¹³³⁻¹³⁶ The possibility of the formation of ate species in DESs was investigated as a potential reason for the success of some of these addition reactions, with proof of the ability of choline chloride to form ates demonstrated by the isolation of a magnesiate formed between (trimethylsilyl)methylmagnesium chloride and choline chloride.¹³⁵

Capriati, Hevia/García-Álvarez :



Scheme 1.2 – The addition of: RLi to imines in water¹³³ and DESs;¹³⁴ RLi and RMgX to ketones in DESs¹³⁵ and water;¹³⁶ and nitriles in water.¹³³ Along with proposed ‘ate’ structure.¹³⁵

1.1 Addition of organolithium reagents to nitriles under air

As opposed to traditional organolithium chemistry, the addition reactions presented herein were carried out under air at ambient temperature. These reactions were therefore carried out in open vials or small flasks as shown in **Figure 1.2**. However, the synthesis of any organolithium species to be used in addition reactions was carried out using standard inert atmosphere techniques.

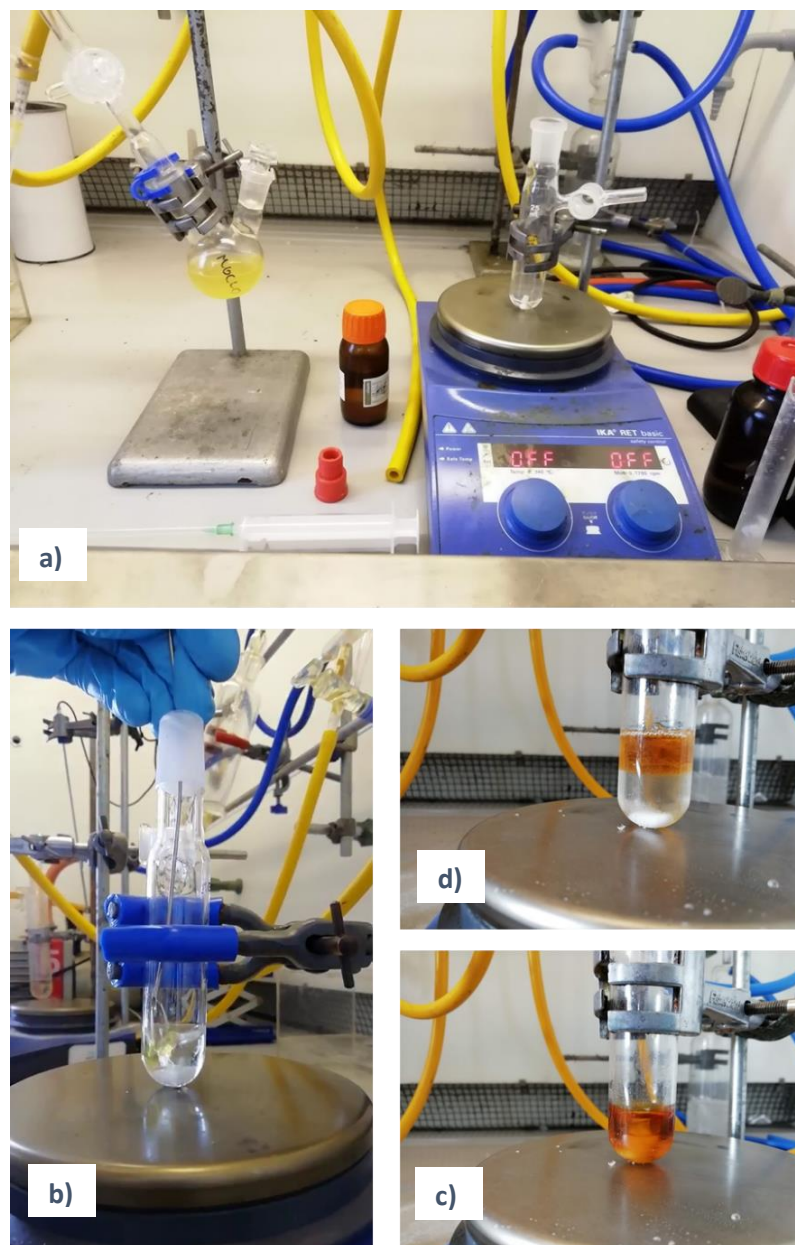
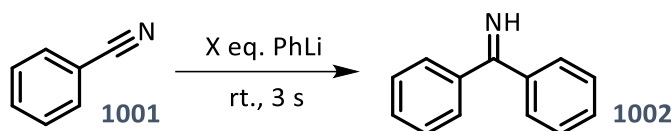


Figure 1.2 – Under air reaction set-up and addition. a) pre-addition, b) addition, c) reaction, d) post-quench

1.1.1 Initial reactions and solvent assessment

Aiming to extend the range of addition reactions of *s*-block organometallic reagents in green solvents under air, the addition to nitriles was chosen for investigation. As a model reaction the addition of phenyllithium to benzonitrile was chosen for initial parametrisation [Table 1.1]. Promising initial findings revealed >90% conversion of the parent nitrile to the corresponding imine able to be obtained in ChCl/2Gly using ≥ 1.5 eq. PhLi [Table 1.1, Entries 1-3]. Furthermore, similar conversions were found using water as a solvent when working under strict air and moisture-free conditions using as little as 1 eq. PhLi [Table 1.1, Entries 7-11]. These results align well with recent research by Capriati, investigating the addition of organolithium reagents to nitriles in water.¹³³ Interestingly high conversions were also observed using the eutectic mixtures ChCl/2H₂O and ChCl/2EG [Table 1.1, Entries 6 & 12].

Table 1.1 – The addition of phenyllithium to benzonitrile |1001| in green solvents (GC conversions).



Entry ^[a]	Eq. ^[b]	Solvent	Conversion (%) ^[c]	Entry ^[a]	Eq. ^[b]	Solvent	Conversion (%) ^[c]
1	2	ChCl/2Gly	92	7	2	H ₂ O	95
2	1.7		94	8	1.7		96
3	1.5		95	9	1.5		94
4	1.2		88	10	1.2		89
5	1		66	11	1		90
6	1.5	ChCl/2H ₂ O	90	12	1.5	ChCl/2EG	74

[a] Reactions performed under air, at ambient temperature. 1 g of solvent and 1 mmol benzonitrile |1001| used and reactions quenched with sat. Rochelle's salt sol. [b] Commercial PhLi (1.9 M in di-*n*-butyl ether) [c] Conversions by integral ration of starting material and product by GC-FID

It should be noted that conversions were obtained by integral ratio of product to starting material by GC-FID, with the only side products observed being a biphenyl and phenol from the quenching of excess phenyllithium. No double addition tertiary amine product was observed, although it has previously been shown that additions to imine (secondary aldimines and ketimines, vs. the primary ketimine products in the present case) under these conditions can occur.^{133, 134}

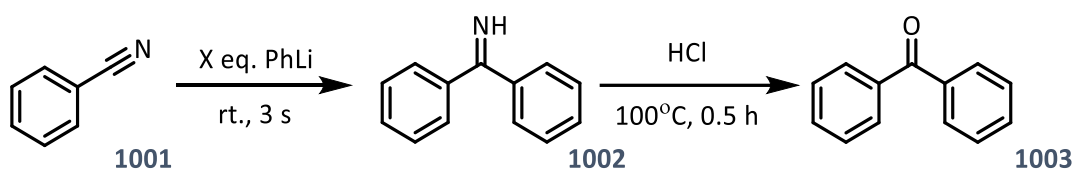
It was observed that reactions did not appear to occur homogeneously, with an indicative colour change occurring in the layer of organic solvent (di-*n*-butyl ether from phenyllithium solution) on the surface of the DES/water. From this it was then postulated that the unexpected compatibility with protic solvents could to a certain extent be due to the immiscibility of the reagents with the solvent. This appears to indeed be the case as benzonitrile is only sparingly soluble in water, and insoluble in the eutectic mixtures investigated (as generally were the other non-polar organic compounds used in the studies contained in this thesis). This sparing solubility in water however proved problematic, as when products were characterised by NMR spectroscopy the corresponding yield by integration against an internal standard did not match: with a lower product yield observed than that found using GC conversions. This discrepancy in yield appears to stem from the loss of remaining unreacted benzonitrile being lost to the aqueous phase during extraction from the reaction mixture before analysis by GC-FID. The result being that the ratio of starting material to product giving a falsely inflated conversion. From this juncture it was decided to analyse product yields quantitatively by ¹H NMR spectroscopy.

Now decided upon quantifying yields by NMR spectroscopy the problem arose of having a suitable resonance in ¹H NMR spectra to use as a handle for integration. As the model product imine, similar to others tested, and starting nitrile only contain aromatic protons it became quickly apparent that reliable crude yields would not be possible due to overlap of signals from starting material and product. Due to this, the isolation of the product imines was attempted by column chromatography. This was however found to not be a useful way of product quantification as during multiple attempts the product benzophenone imine was found to hydrolyse to the benzophenone. Partial product hydrolysis was observed during isolation attempts by silica column chromatography (including using basified silica and eluent) and alumina column chromatography.

Due to the sensitivity of the product imine it was decided that the easiest way forward would be to deliberately hydrolyse the product imines in the hope of easier purification of the more robust corresponding ketones. This was done by the addition of 2 M HCl and refluxing for 30 min. Using the new method of product hydrolysis, isolation, and NMR quantification of product yields it was apparent that initial optimisation reactions would have to be repeated to obtain true values for the reactions involved.

Using a quantitative method of GC analysis the yield of benzophenone imine was determined for the addition of various equivalents of phenyllithium to benzonitrile in glycerol [Table 1.2, Entries 7-11] where it was seen that the yield decreased with the addition of less than 2 eq.. After confirmation of yield by quantitative NMR other solvents were tested. Surprisingly, the eutectic mixture ChCl/2Gly (71%) furnished lower conversions than neat glycerol (83%).

Table 1.2 – The addition of phenyllithium to benzonitrile |1001| in green solvents (NMR yields).



Entry ^[a]	Eq. ^[b]	Solvent	Yield 1003 (%) ^[c]	Entry ^[a]	Eq. ^[b]	Solvent	Yield 1002 (%) ^[d]
1	2.0	Gly	83	7	3.0	Gly	85
2		ChCl/2Gly	71	8	2.5		85
3		H ₂ O	79	9	2.0		85
4		EG	53	10	1.5		80
5		MeOH	8	11	1.0		77
6		2-MeTHF	47				

[a] Reactions performed under air, at ambient temperature. 0.5 g of solvent and 0.5 mmol benzonitrile |1001| used and reactions quenched with sat. Rochelle's salt sol. [b] Commercial PhLi (1.9 M in di-n-butyl ether) [c] Yields determined by ¹H NMR spectroscopy by integration against a CH₂Br₂ internal standard [d] Yields by GC-FID using an external calibration curve of concentrations

Previously it has been proposed that in the DES the potential co-complexation of the organolithium reagent with the ammonium salt can lead to the formation of the more reactive 'ate' species^{134, 135} which would be predicted to be more nucleophilic, and therefore reactive, than the neutral organolithium reagent making it somewhat counterintuitive that a lower yield was obtained.

This lower yield can perhaps be explained by the reaction occurring under heterogeneous conditions, at the solvent interface, as the interactions present across the organic/aqueous interface can vary with the species present in each phase (*vide infra*). Previous studies with a similar scenario of heterogeneous conditions have been reported by Capriati^{130, 131, 133, 136} using organolithium and Grignard reagents in aqueous media, with addition reactions taking place "on water" conditions,¹³⁷⁻¹³⁹ rather than in the reaction medium, preferentially furnishing the relevant addition products instead of the hydrolysis of the organometallic reagent. "On water" reactions are thought to occur at the organic/liquid water interface with water insoluble reactants.¹³⁹

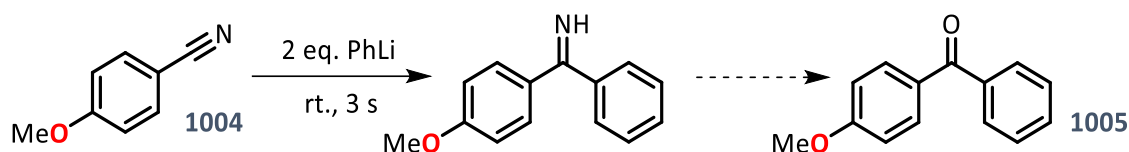
1.1.2 “On glycerol” reactions and surface phenomena

Similar to the heterogenous “on water” conditions mentioned it appears that the addition of phenyllithium to benzonitrile occurs in analogous heterogenous conditions “on glycerol”. Attempting to verify this “on glycerol” assumption, reactions were run in other protic reaction media with varying solubility of benzonitrile. Pleasingly, a good correlation between benzonitrile solubility and ketone product yield was observed [Table 1.2, Entries 3-5] with yields decreasing as solubility increased, confirming the “on solvent” hypothesis. Notably when the benzonitrile soluble non-protic solvent 2-MeTHF [Table 1.2, Entry 6] was employed the yield obtained was less than that of H₂O or glycerol, hinting at an rate acceleration gained from reacting on the surface of the glycerol or water rather than in the 2-MeTHF solvent bulk. Further evidence for a surface effect was gleaned from a comparison of the addition of 2 eq. of phenyllithium to benzonitrile [1001] carried out “on glycerol” without stirring where only a 51% yield was obtained compared to 83% with stirring. This result fits with previous reports of “on water” results showing that increased agitation affects the surface area of organic droplets in the aqueous phase increasing yields.¹³⁹

In addition to the effect of solubility, the effect of H-bonding was necessary to consider, as for example, benzonitrile is more soluble in methanol, but also methanol is less able to engage in hydrogen bonding than water or glycerol.¹⁴⁰ It has previously been reported that surface phenomena involving H-bonding can play a role in recent work involving “on water” reactions.^{133, 137-139} One proposed explanation is that “dangling” hydroxyl groups involved in trans-phase H-bonding at the water/organic interface to cause rate acceleration,¹⁴¹ although an alternative theory suggests proton transfer across the interface to be responsible.^{142, 143} In the case of glycerol, surface studies using broadband vibrational sum frequency generation (VSFG) spectroscopy have shown a lack of protruding OH group, unlike water, where many “dangle” into the vapour phase. It is however possible to disrupt this flat surface by introducing a salt, such as sodium bromide or -iodide where the halide anions disrupt the organisation of the glycerol, increasing the number of hydroxyl groups protruding at the interface.¹⁴⁴

To further investigate H-bonding effects at the interface the addition of phenyllithium to 4-methoxybenzonitrile |1004| was investigated in glycerol mixtures containing salt or water. The addition was seen to perform well on water (84%) but not on glycerol (32%) |Table 1.3, Entries 1-2| in contrast to benzonitrile due solubility |expanded upon in section 1.1.3 Assessing nitrile and aryllithium substrate scope|. Pertinent to the discussion of interfacial H-bonding is the slightly reduced yield obtained using NaCl:8Gly vs Gly |22%, Table 1.3, Entries 2-3| showing that disturbing the organisation of the glycerol to produce more protruding OH groups does not make for a more efficient addition process. The same trend was seen for the case of benzonitrile. In further support to this, performing the addition in D₂O does not decrease the reaction yield, as would be expected in the case where interfacial H-bonding had a strongly accelerating effect as O-D bonds are more orientated into the bulk compared to O-H bonds in H₂O.^{136, 138, 139} Less clear is the significance of yields of additions carried out in H₂O/Gly mixtures |58 - 70%, Table 1.3, Entries 4-5|, as intermediate yields between that of water and glycerol were obtained; possible due to varying dynamics of the H-bonding networks of these mixtures,¹⁴⁵ or simply solubility.

Table 1.3 – H-bonding effects in the addition of phenyllithium to 4-methoxybenzonitrile |1004|.



Entry ^[a]	Solvent	Yield (%) ^[c]
1	H ₂ O	84
2	Gly	32
3	NaCl/8Gly	22
4	H ₂ O/Gly	58
5	10H ₂ O/Gly	70

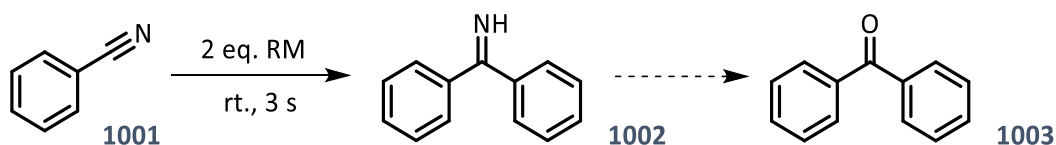
[a] Reactions performed under air, at ambient temperature. 0.5 g of solvent and 0.5 mmol benzonitrile |1001| used and reactions quenched with sat. Rochelle's salt sol. [b] Commercial PhLi (1.9 M in di-n-butyl ether) [c] Yields determined by ¹H NMR spectroscopy by integration against a CH₂Br₂ internal standard

1.1.3 Assessing nitrile and aryllithium substrate scope

After exploring solvents and their effect on the reaction, and the nature of this effect, the range of nitriles and organolithium reagents compatible with “on glycerol” and “on water” conditions were examined. As a starting point the possibility of using of an aryllithium or Grignard reagent in these addition reactions was considered. However, this was quickly discounted as *n*-BuLi [22%, Table 1.4, Entry 2] was seen to quench quickly in glycerol, likely due to being too reactive, but also possibly due to being solvated hexane as opposed to di-*n*-butyl ether. Likewise, Grignard reagents were considered unsuitable as phenylmagnesium bromide [Table 1.4, Entries 3-4] appeared not sufficiently reactive to undergo addition, with only traces of addition product obtained in glycerol (< 1%) or even the non-protic solvent 2-MeTHF (3%), suggesting that the higher polarity of Li-C bonds (vs. Mg-C) is crucial for successful addition, as has been previously seen^{134, 135}

Impressively the addition of phenyllithium to benzonitrile was found to produce comparable yields at higher scale (5 mmol) [87%, Table 1.4, Entry 5].

Table 1.4 – The addition of polar organometallic reagents to benzonitrile [1001] in green solvents.



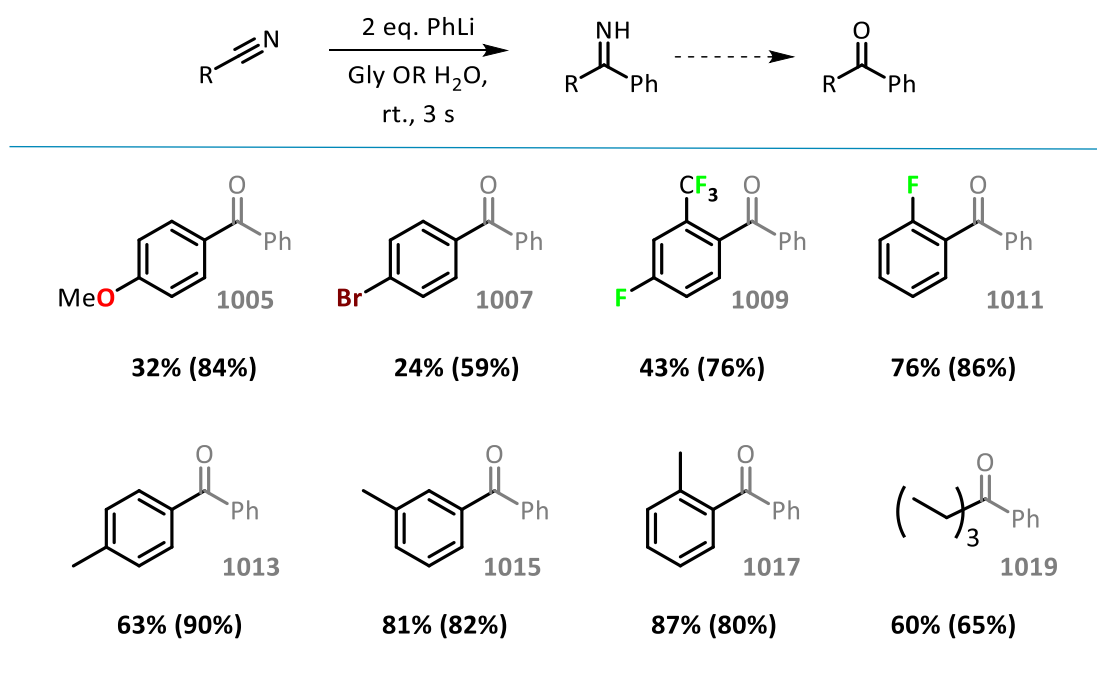
Entry ^[a]	RM ^[b]	Solvent	Yield (%) ^[c]
1	PhLi	Gly	83
2	<i>n</i> -BuLi		22
3	PhMgBr		trace
4	PhMgBr	2-MeTHF	3
5 ^[d]	PhLi	Gly	87

[a] Reactions performed under air, at ambient temperature. 0.5 g of solvent and 0.5 mmol benzonitrile [1001] used and reactions quenched with sat. Rochelle's salt sol. [b] Commercial PhLi (1.9 M in di-*n*-butyl ether), *n*-BuLi (1.6 M in hexanes), PhMgBr (1.0 M in THF) [c] Yields determined by ¹H NMR spectroscopy by integration against a CH₂Br₂ internal standard [d] Reaction performed under air, at ambient temperature. 5 g of solvent and 5 mmol benzonitrile [1001]

Moving to look at the nitriles involved, it was seen that moderate to good yields of addition products could be obtained in the near instantaneous time of 3 s across a variety of functionalised nitriles on both glycerol and water | **Table 1.5** |.

A clear trend in the solvent preference of the nitriles emerged with liquid nitriles | **1001, 1010, 1014, 1016** and **1018** | giving comparable yields on both glycerol and water, but solid nitriles | **1004, 1006, 1008** and **1012** | gave greater ketone conversions on water. This difference could be attributed to the solid remaining on the surface of the water throughout stirring (perhaps due to hydrophobic tendencies or the high surface tension of water), but suspending through the glycerol bulk upon stirring, making less of the nitrile easily available to react in the 3 s timescale. Nevertheless, the results show the tolerance of these “on glycerol” and “on water” additions to: electron-donating groups | **1005** |, electron-withdrawing halogens | **1007, 1009** and **1011** |, mild steric bulk across *ortho*- *meta*- and *para*-positions | **1011, 1013, 1015** and **1017** |, and alkyl groups | **1019** |. Electronic and steric effect, along with halogen exchange appearing not to be incompatible with this method of addition.

Table 1.5 – The addition of phenyllithium to various nitriles on glycerol (and water).^{[a][b][c]}



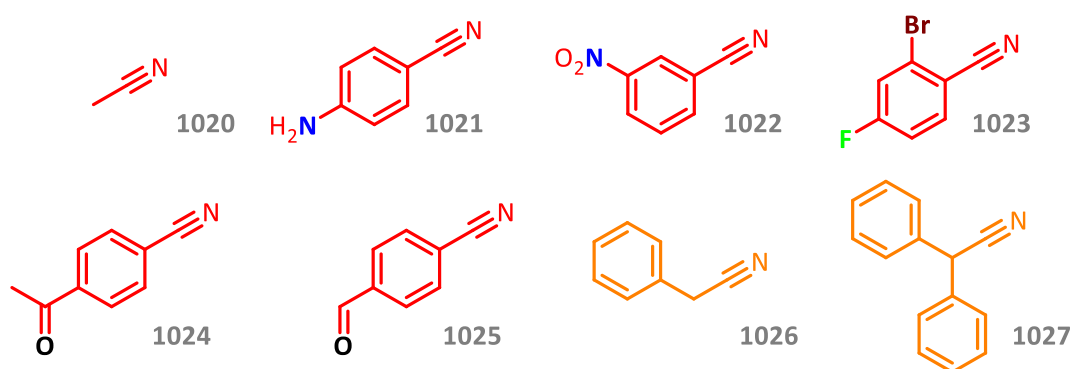
[a] Reactions performed under air, at ambient temperature. 0.5 g of solvent and 0.5 mmol nitrile |1004, 1006, 1008, 1010, 1012, 1014, 1016, 1018| used and reactions quenched with sat. Rochelle's salt sol. |b| Commercial PhLi (1.9 M in di-*n*-butyl ether) |c| Yields determined by ¹H NMR spectroscopy by integration against a CH₂Br₂ internal standard

Despite a general tolerance to a range of potentially problematic functional groups, many nitriles were seen to be incompatible with this method [Scheme 1.3].

No addition was seen with the use of acetonitrile [1020], suspected to be due to its solubility in both glycerol and water precluding the condition for heterogeneous reactions. For 4-aminobenzonitrile [1021] it is likely the reasonably acidic amine which impedes addition, as is likely the case that the reactive nitro group of 3-nitrobenzonitrile [1022] prevents addition. With 2-bromo-4-fluorobenzonitrile [1023] it may be that although an *ortho*-substituted methyl or fluorine is tolerated the much larger size of bromine is sufficiently hindering that no addition product was observed.

Substrates 4-formylbenzonitrile and 4-acetylbenzonitrile [1024 & 1025] were chosen to set up a competition reaction between addition to the carbonyl and nitrile moieties, as additions in green solvents have previously been investigated.¹³⁵ The expectation was that either single addition to one functionality or a mixture of di-addition products. However, curiously neither addition was observed and starting material was recovered. It is unclear why this should be the case.

Apart from these nitriles where no addition was observed, when phenylacetonitrile and diphenylacetonitrile [1026 & 1027] were subjected to the addition conditions a complex mixture of products were found to be produced. Also in this case it is not clear why such a mixture of products should be produced. The mixture was not further examined to identify its components.



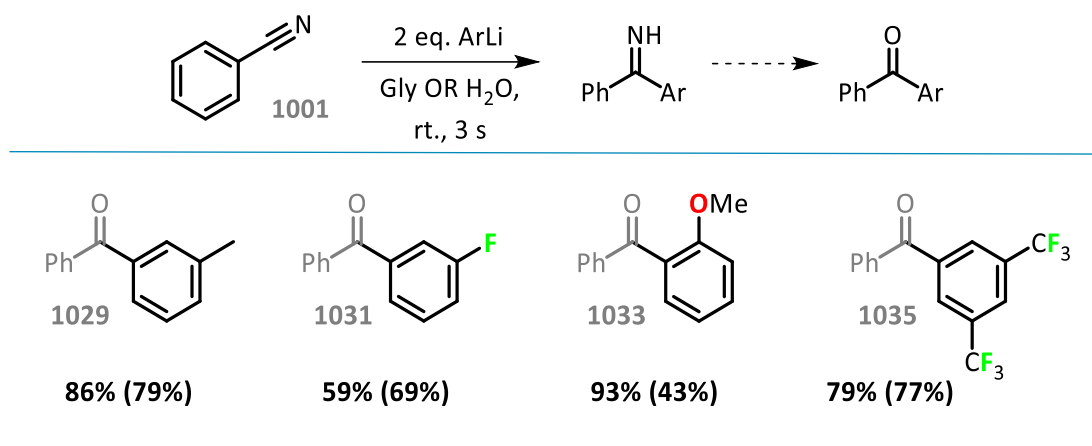
Scheme 1.3 – Failed nitrile scope for the addition of phenyllithium to various nitriles on glycerol and water.

|Red| No addition product was observed by GC-FID, |Orange| Multiple (addition) products were observed by GC-FID

Next the protocol was extended to functionalised aryllithium reagents. These aryllithium compounds were synthesised by lithium-halogen exchange from the corresponding aryl iodide and were added as a 1 M solution in diethyl ether/hexane. The benchmark nitrile, benzonitrile was used.

As previously observed addition occurred almost instantaneously (3 s), furnishing nonsymmetric diarylketones in moderate to excellent yields. No problems or by-products were observed across the small group of aryllithium compounds shown in **Table 1.6**. No clear trend in yields was observed with both glycerol and water, and only 2-methoxyphenyllithium |132| displayed a significant difference in yield, having a clear preference for glycerol, possibly due to detrimental H-bonding.

Table 1.6 – The addition of various aryl lithium reagents to benzonitrile |1001| on glycerol (and water).^{[a][b][c]}

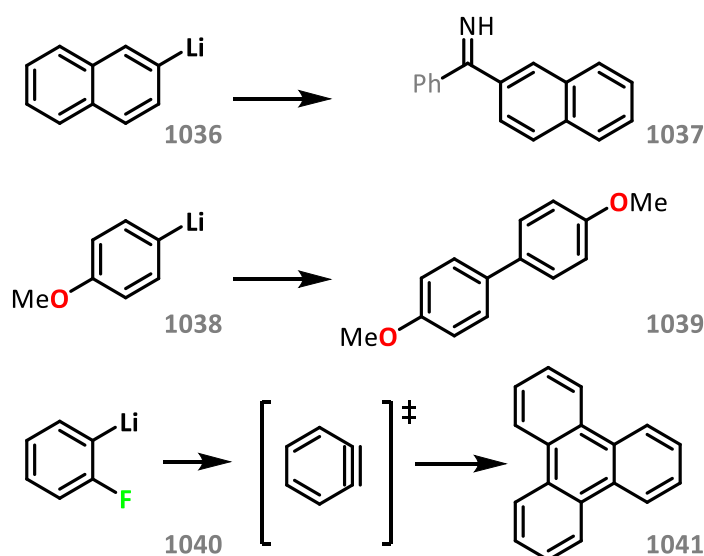


[a] Reactions performed under air, at ambient temperature. 0.5 g of solvent and 0.5 mmol nitrile used and reactions quenched with sat. Rochelle's salt sol. [b] Synthesised aryllithium reagents |1028, 1030, 1032, 1034| added as 1 M so. in diethyl ether/hexanes [c] Yields determined by ¹H NMR spectroscopy by integration against a CH₂Br₂ internal standard

Despite successful additions with some aryl lithium compounds, a more complex situation arose with others [Scheme 1.4]. In the case of 2-naphthyllithium [1036] insolubility prevented preparation of a solution of the organolithium reagent at a reasonable concentration. Although when added as a thick paste, imine product [1037] was observed. A meaningful yield cannot be given in this case as the quantity of 2-naphthyllithium added could not be accurately measured.

In the case of 4-methoxyphenyllithium [1038] homocoupled anisole [4,4'-dimethoxyphenyl, 1039] was instead seen as the major product. This was not the intention in this project but is an interesting result and merits further investigation itself.

2-Fluorophenyllithium [1040] was also synthesised with the intention of being used in addition reactions. It was instead seen to be thermally unstable. Lithium-halogen exchange was carried out at cryogenic temperatures, with clear formation of the lithiated arene evidenced by the appearance of bright colours, but upon warming to ambient temperature the lithium species is suspected to have undergone lithium fluoride elimination to form benzyne trimerisation to form triphenylene [1041] via benzyne trimerisation.



Scheme 1.4 – Aryllithium reagents unsuccessful in addition reactions to benzonitrile [1001] on glycerol and water.

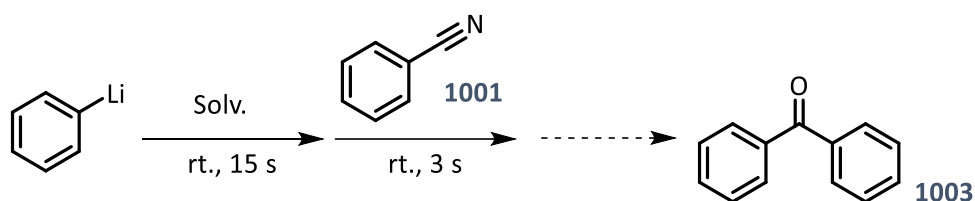
1.1.4 Aryllithium lifetime study

In exploration of substrate scope for the addition of aryllithium reagents to nitriles it has been shown that both glycerol and water are comparable solvents with a case by case basis for the preferential solvent. Therefore, in a final bid to more clearly differentiate the two the lifetime of phenyllithium on both solvents was considered.

To test the lifetime of the active organolithium species on both glycerol and water phenyllithium solution was added to stirring solvent, then after 15 s benzonitrile was added; the yield of addition product then indicative of the solvent's ability to prevent/cause hydrolysis of the organolithium species.

In this comparison it was finally able to clearly distinguish glycerol and water as solvents [Table 1.7] as slightly reduced yield of 74% benzophenone [1003] was still able to be obtained for glycerol, whereas with water only traces of addition product were detected. These findings illustrate the potential of glycerol to come out on top in kinetically favoured reactions of organolithium reagents.

Table 1.7 – The addition of polar organometallic reagents to benzonitrile [1001] in green solvents.



Entry ^{[a],[b]}	Solvent	Yield (%) ^[c]
1	Gly	74
2	H ₂ O	trace

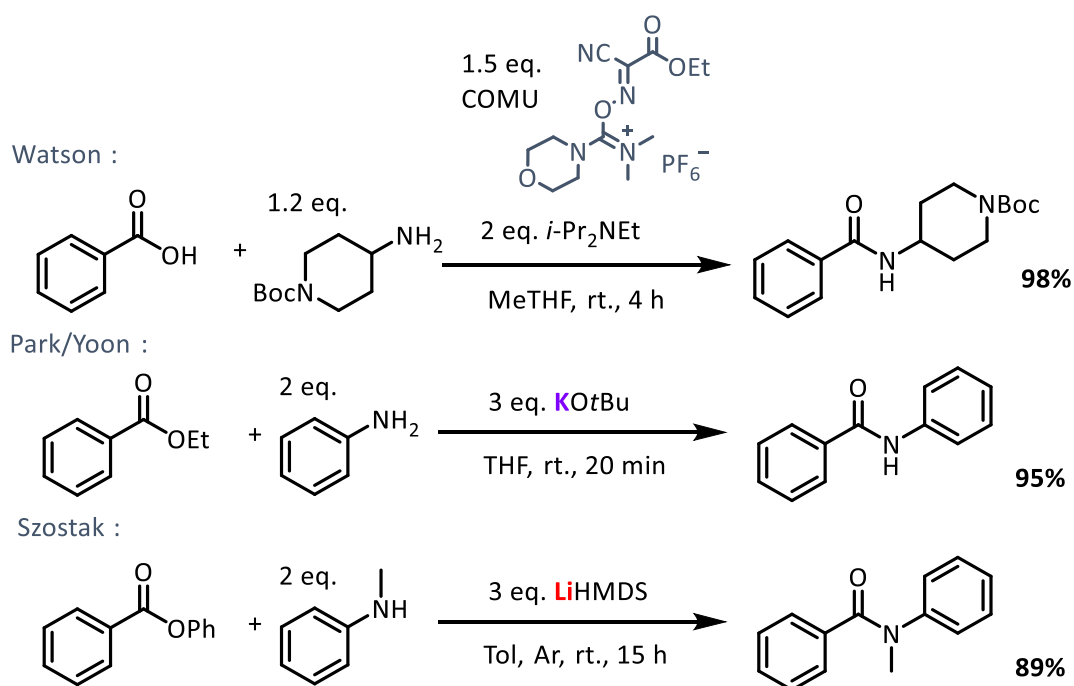
[a] Reactions performed under air, at ambient temperature. 0.5 g of solvent and 0.5 mmol benzonitrile [1001] used and reactions quenched with sat. Rochelle's salt sol. [b] Commercial PhLi (1.9 M in di-n-butyl ether) [c] Yields determined by ¹H NMR spectroscopy by integration against a CH₂Br₂ internal standard

1.2 Amidation of esters using lithium amides under air

Amide forming reactions are one of the most commonly found in pharmaceutical processes.¹⁴⁶ Due to this prevalence and their pivotal role in the synthetic processes,¹⁴⁷⁻¹⁵⁰ the investigation of a sustainable method for their formation has been identified by the ACS green chemistry institute as a key research area for the future of pharmaceuticals.^{151, 152} There is a large variety of amide bond forming reactions.¹⁵³⁻¹⁶³ Some seemingly simple tasks, however, still remain challenging, and standard amidation protocols often involve exceedingly expensive reagents. Only few of the methods address performing the reaction in sustainable conditions.

Avoiding expensive reagents and cooling procedures, some amidation procedures are outlined below in **Scheme 1.5**, including amidation: organo-mediated in green solvent,¹⁶⁴ by radical mechanism,¹⁶⁵ and by lithium amide.¹⁶⁶

Where lithium amides are used these amidation reactions occur exergonically due to the increased stability of the lithium alkoxide and carboxamide products over the reactive lithium amide and ester reactants, producing a thermodynamic driving force for the reaction.



Scheme 1.5 – Example amide forming reactions.^{164, 166}

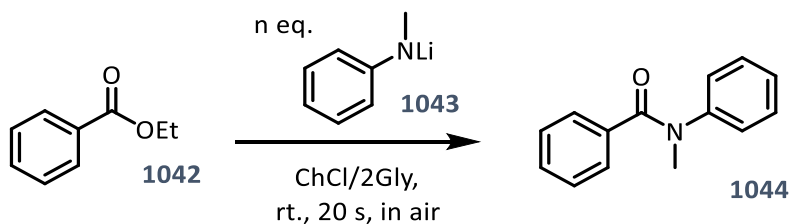
1.2.1 Initial reactions and solvent assessment

Initially the reaction of ethyl benzoate **|1042|** with lithium *N*-methylanilide **|1043|** was investigated in eutectic solvent mixtures at ambient temperature, under air as a model reaction in order to parameterise amidations in green solvents.

By employing 3 eq. of lithium amide as a THF solution, a high yield (90%) was obtained using ChCl/2Gly **|Table 1.8, Entry 1|** in a very short reaction time of 20 s, demonstrating the ability of the lithium amide to survive adequately under bench conditions to perform amide forming addition reactions to esters. Where less than 3 eq. were added yields were good but significantly lower ($\leq 70\%$).

It should be noted at this point that reactions were carried out with ambient temperatures (ca. 30°C). In addition, a dibromomethane standard was used for quantitative NMR yields and DCM for extractions.

Table 1.8 – The addition of various equivalents of lithium *N*-methylanilide **|1043|** to ethyl benzoate **|1042|** in ChCl/2Gly.



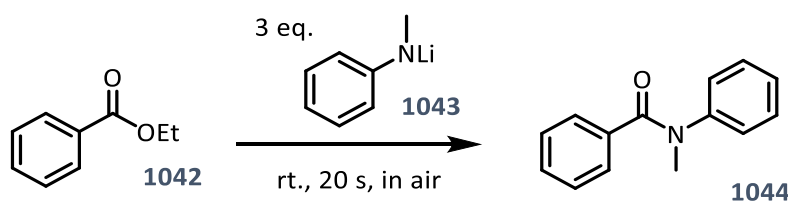
Entry ^{[a] [b]}	Eq.	Crude yield (%) ^[c]
1	3	90
2	2.5	70
3	2	60
4	1.5	52
5	1	37

[a] Reactions performed under air, at ambient temperature using 1 g ChCl/2Gly and 1 mmol ethyl benzoate **|1042|**. Reactions stirred at 480 rpm for 20 s then quenched with 5 mL sat. Rochelle's salt sol. and extracted into DCM [b] lithium *N*-methylanilide **|1043|** pre-isolated and added as a 0.5 M sol. In THF [c] Yields determined by ¹H NMR spectroscopy by integration against a CH₂Br₂ internal standard

With the success of the amidation using 3 eq. lithium *N*-methylanilide in ChCl/2Gly the possibility of using other solvents was investigated; including DESs, glycerol and water [Table 1.9]. It was however decided to move from DCM to 2-MeTHF as extraction solvent, as DCM is not environmentally friendly. Ferrocene was also chosen as the internal standard as it presents a clearer resonance for use in quantitative NMR (10x ¹H vs. 2x ¹H in CH₂Br₂).

A couple of things became immediately obvious with the yields obtained with these new conditions [Table 1.9]: a general inconsistency in yields across each of additions done in triplicate, and in the particular case of ChCl/2Gly [Table 1.9, Entry 1] where a comparison is available, yields were lower than those previously observed in Table 1.8, and inconstant. Four changes had occurred between this set of experiments and the previous round of additions, these were examined individually in turn.

Table 1.9 – The addition of lithium *N*-methylanilide [1043] to ethyl benzoate [1042] in various solvents and eutectic solvent mixtures.



Entry ^{[a][b]}	Solv.	Crude yield (%) ^[c]
1	ChCl/2Gly	36 / 69 / 77
2	ChCl/2EG	52 / 40 / 36
3	ChCl/2H ₂ O	61 / 37 / 43
4 ^[d]	LiCl/3Gly	68 / 33 / 30
5	Gly	85 / 71 / 74
6	H ₂ O	10 / 6 / 9

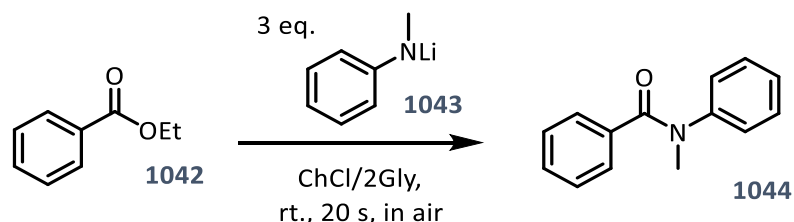
[a] Reactions performed under air, at ambient temperature using 1 g ChCl/2Gly and 1 mmol ethyl benzoate [1042]. Reactions stirred at 960 rpm for 20 s then quenched with 5 mL sat. Rochelle's salt sol. and extracted into 2-MeTHF [b] lithium *N*-methylanilide [1043] pre-isolated and added as a 0.5 M sol. In THF [c] Yields determined by ¹H NMR spectroscopy by integration against a FeCp₂ internal standard [d] Reactions carried out 53°C to due to viscosity

- Firstly, the stirrer speed had been increased from 480 to 960 rpm, this was done in an attempt to improve reproducibility, and in fact was found to slightly improved yields.
- Secondly, the product was extracted into 2-MeTHF instead of DCM. Upon investigation this was seen to have no effect on the yield of product obtained.
- Thirdly, the change of internal standard from dibromomethane to ferrocene. It was found that this change did affect yields, reducing them by ca. 10%. The cause for this was found to be due to a slower relaxation time (in ^1H NMR spectroscopy) of the dibromomethane standard compared to that of the methyl group protons of the product amide for which the yields were calculated. Due to the standard not having fully relaxed using standard relaxation times, but the amide had, an erroneously increased ratio of amide to standard was measured resulting in yields increased by ca. 10%. This could be easily resolved by increasing the relaxation time to allow the dibromomethane to express its true concentration in spectra. The yields obtained using a suitably long relaxation time with dibromomethane and those of the standard relaxation time using ferrocene were seen to matched. Therefore, it was seen that ferrocene was a good choice of standard and was used from this point on.
- Fourth and finally, an external factor that had not been considered appeared be the culprit of inconsistent yields. Initial reactions had been carried out when ambient temperature was a record breaking (30°C) but subsequent reactions when ambient temperature had returned to the standard summer range of 16-20°C. It appears that a 0.5 M concentration of lithium *N*-methylanilide in THF is on the limits of solubility at higher temperature and at the more moderate temperature a perfect solution is not obtained, and so it is likely due to this inconsistent quantities of lithium amide were being added to the reaction.

With the inconsistencies in yield and reproducibility in toe, the problem arose of requiring a significant volume of lithium amide solution due to reduced concentration [Table 1.10]. The maximum concentration of lithium *N*-methylanilide was found to be just over 0.2 M in THF and at standard ambient temperature [Table 1.10, Entry 1]. At this concentration 13.5 mL of lithium amide solution was required to be added to 1 mmol scale reactions, which was undesirable. In an effort to reduce this the addition of the donor TMEDA was considered [Table 1.10, Entry 2] with the intention of reducing the aggregation state of the lithium amide and increasing solubility. However, this was seen to have little to no effect likely due to an already relatively unaggregated state of the lithium amide in the inherently deaggregating donor THF.¹⁶⁷

Finally, the idea of solubilising the lithium amide in 2-MeTHF arose [Table 1.10, Entry 3]. This proving to be a much-improved solution, with concentrations in excess of 1 M possible at ambient temperature; only requiring the addition of a small amount of lithium amide solution to reactions. Using 2-MeTHF also improves the “greenness” of reactions with no non-renewable solvents now required for the amidation reaction (still required for pre-isolation of the lithium amide, although this could be carried out cryogenically in 2-MeTHF to create an *in-situ* 1 M solution).

Table 1.10 – The addition of various solutions of lithium *N*-methylanilide |1043| to ethyl benzoate |1042|.



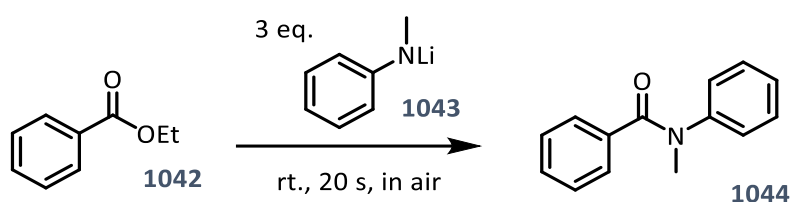
Entry ^{[a],[b]}	LiNMA 143 solvent	Max. conc.	Vol. required for 3 eq.	Crude yield (%) ^[c]
1	THF	0.22 M	13.5 mL	82
2	THF + 2 TMEDA	0.23 M	13.0 mL	76
3	2-MeTHF	(>)1.0 M	3.0 mL	99

[a] Reactions performed under air, at ambient temperature using 1 g ChCl/2Gly and 1 mmol ethyl benzoate |1042|. Reactions stirred at 960 rpm for 20 s then quenched with 5 mL sat. Rochelle's salt sol. and extracted into 2-MeTHF [b] lithium *N*-methylanilide |1043| pre-isolated [c] Yields determined by ¹H NMR spectroscopy by integration against a FeCp₂ internal standard

Upon establishing 2-MeTHF as the superior, and greener, solvent for the formation of lithium amide solution the reaction solvent was re-evaluated, considering the same group of DESs, glycerol and water as before [Table 1.11].

Again, it was quickly apparent that there was a problem; with supra-100% yields obtained. On this occasion it was easy to pinpoint the issue, i.e., the overlap of the N-H resonance of the excess (quenched) *N*-methylaniline and the product methyl group. This was resolved by isolation of the product by silica column chromatography.

Table 1.11 – The addition of lithium *N*-methylanilide |1043| (as a solution in 2-MeTHF) to ethyl benzoate |1042| in various solvents and eutectic solvent mixtures.



Entry ^{[a][b]}	Solv.	Crude yield (%) ^[c]
1	ChCl/2Gly	100 / 109 / 108
2	ChCl/2EG	66 / 67 / 93
3	ChCl/2H ₂ O	88 / 94 / 80
4 ^[d]	LiCl/3Gly	101 / 98 / 87
5	Gly	102
6	H ₂ O	43 / 50

[a] Reactions performed under air, at ambient temperature Using 1 g ChCl/2Gly and 1 mmol ethyl benzoate |1042|. Reactions stirred at 960 rpm for 20 s then quenched with 5 mL sat. Rochelle's salt sol. and extracted into 2-MeTHF [b] lithium *N*-methylanilide |1043| pre-isolated and added as a 1 M sol. In 2-MeTHF [c] Yields determined by ¹H NMR spectroscopy by integration against a FeCp₂ internal standard [d] Reactions carried out 53°C to due to viscosity

Finally, upon having established an adequate procedure to produce meaningful yields, the consideration and discussion of yields could begin.

First of all, four eutectic mixtures were considered for these amidation reactions; three choline-chloride-based, and one lithium-chloride-based. Of the choline-chloride-based DESs, ChCl/2Gly and ChCl/2H₂O | **Table 1.12, Entries 1-2** | both gave good yields of > 80% of | **1044** | with the addition of 3 eq. of lithium amide, whereas employing ChCl/2EG | **Table 1.12, Entry 3** | as solvent only 59% of the amide product was obtained. The trend of yields in these DESs is not easily rationalised, despite some insight in to the structural composition of these DESs. Investigation into the structural composition and H-bonding in these eutectic mixtures has provided clues to the aim of elucidating the inner workings and nature of the interactions of their components that govern the physical and chemical properties of these solvents. With the mixture ChCl/2Urea receiving the most focus, where it has been seen to form a strongly H-bonded network of both components.^{30,40} ChCl/2Urea was not used as it can be susceptible to addition reactions. The mixtures ChCl/2Gly and ChCl/2EG; however, have been seen to contain components that are less well matched to form effective hydrogen bonding, with more HBD self interaction¹⁶⁸ even to the point where ChCl/2Gly has been said to comprise mainly of a glycerol network with intercalated choline chloride, or some chloride bridges rather than an inter-H-bonded network.^{22,41} The internal interactions of ChCl/2H₂O even less well documented although the effect of adding water to a ChCl/2Urea mixture and the switching point between DES component interactions and solvating water interactions has been explored.²¹

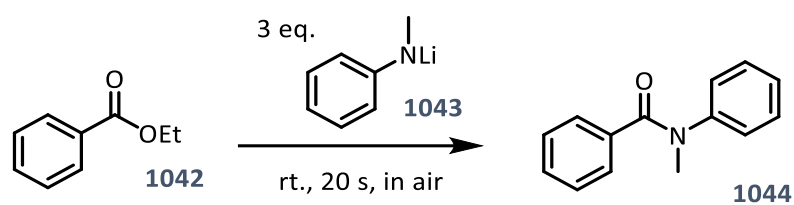
Unfortunately, these insights do not help rationalise the similarity/difference in yields obtained in the choline chloride based DESs. They do however help to rationalise the similarity in yields between ChCl/2Gly and glycerol | **Table 1.12, Entries 1 & 5** | where > 80% yields of the product amide were obtained in both. The similarity in yield appears to reflect the findings that ChCl/2Gly is comprised mainly of a self H-bonding glycerol network, as no increase in yield was obtained. Furthermore, it suggests that no 'ate' species was formed through interaction with the choline chloride as have been previously proposed.^{135, 169}

In attempt to form a lithiate species by a different method, the lithium-chloride-based DES LiCl/3Gly was employed.¹³ Lithium chloride has been previously seen to greatly enhance the reactivity of Schlenk and Grignard reagent, creating 'turbo reagents'.^{99, 102, 117, 121}

Unfortunately, it appears that the formation of a ‘turbo reagent’ or lithiate species did not occur [Table 1.12, Entry 4], evidenced by the a very similar yield (78%) being obtained to that in ChCl/2Gly (82%) and glycerol (85%).

As the ultimate green solvent, and having found to be successfully employed in other addition reactions involving pyrophoric reagents, water was considered as reaction solvent. In this case only very modest yields were obtained [Table 1.12, Entry 6] showing water to not be a suitable solvent for the addition of lithium amides (solution in 2-MeTHF) to esters. Noteworthy however, is the difference in yield between water (36%) and ChCl/2H₂O (81%), where a clear difference between water and a water-based DES is observed This appears to demonstrate the different make up of interactions in ‘neat’ water and a eutectic mixture/salt solution, and the ability that this affords to prevent or slow hydrolysis of reactive organolithium reagents.

Table 1.12 – The addition of lithium *N*-methylanilide |1043| (as a solution in 2-MeTHF with isolated yields) to ethyl benzoate |1042| in various solvents and eutectic solvent mixtures.



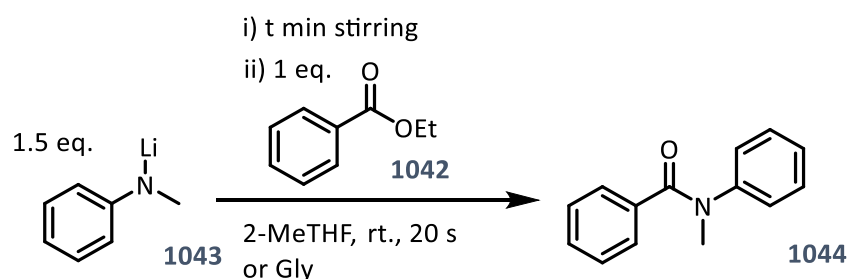
Entry ^{[a] [b]}	Eq.	Solvent	Yield (%) ^[c]	Entry ^{[a] [b]}	Eq.	Solvent	Yield (%) ^[d]
1	3.0	ChCl/2Gly	82	7	3.0	2-MeTHF	80
2		ChCl/2H ₂ O	81	8	2.0		80
3		ChCl/2EG	59	9	1.5		81
4 ^[d]		LiCl/3Gly	78	10	1.0		78
5		Gly	85	11 ^[e]	1.5	THF	93
6		H ₂ O	36				

[a] Reactions performed under air, at ambient temperature using 1 g ChCl/2Gly and 1 mmol ethyl benzoate |1042|. Reactions stirred at 960 rpm for 20 s then quenched with 5 mL sat. Rochelle’s salt sol. and extracted into 2-MeTHF [b] lithium *N*-methylanilide |1043| pre-isolated and added as a 1 M sol. in 2-MeTHF [c] Yields are of isolated product and are determined by ¹H NMR spectroscopy by integration against a FeCp₂ internal standard [d] Reactions carried out 53°C to due to viscosity [e] 0.2 M sol. of LiNMA in THF

Finally, 2-MeTHF was considered as a reaction solvent. 2-MeTHF was seen to perform equally well as glycerol and furnished high yields [Table 1.12, Entries 7-10] of *N*-methyl-*N*-phenylbenzamide [1044] upon the addition of 1.5 eq. of lithium amide (81%). It should be noted that the reaction can be carried out in THF as the reaction solvent (and the lithium amide solution solvent, although at 0.2 M vs. 1 M in 2-MeTHF due to poorer solubility of the lithium *N*-methylanilide in THF) achieving excellent yields [Table 1.12, Entry 11]. However, as THF is currently produced from petrochemicals and not a renewable 'green' solvent it was discounted as the preferred reaction solvent.

In order to discern between glycerol and 2-MeTHF as the best reaction solvent, lifetime studies were carried out [Table 1.13]. These entailed the pre-mixing of lithium *N*-methylanilide [1043] solution and the solvent in question in the reaction vessel, before the addition of ethyl benzoate [1042] after a set time interval, after a further 20 s the reactions were quenched.

Table 1.13 – Lifetime study of lithium *N*-methylanilide [1043] to ethyl benzoate [1042] in glycerol and 2-MeTHF.

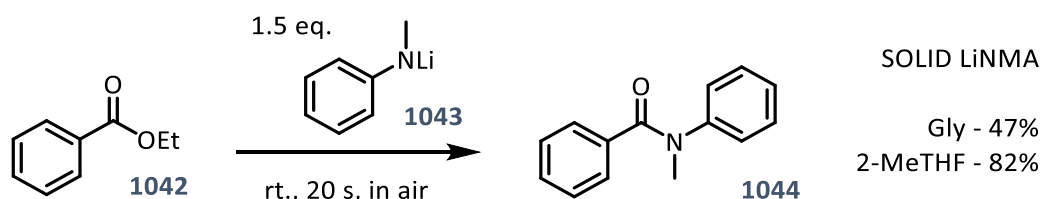


Entry ^{[a][b]}	Solv.	Time	Crude yield (%) ^[c]
1	Gly	10 s	19
2		30 s	3
3	2-MeTHF	1 min	70
4		2 min	61
5		5 min	42
6		10 min	13

[a] Reactions performed under air, at ambient temperature using 1 g solvent and 1 mmol ethyl benzoate [1042]. Reactions stirred at 960 rpm for 20 s then quenched with 5 mL sat. Rochelle's salt sol. and extracted into 2-MeTHF
 [b] lithium *N*-methylanilide [1043] pre-isolated and added as a 1 M sol. In 2-MeTHF [c] Yields determined by ¹H NMR spectroscopy by integration against a FeCp₂ internal standard

Through these reactions a dramatic difference in the lifetime of the lithium amide was observed. Glycerol performed very poorly at sustaining the integrity of the lithium amide [Table 1.13, Entries 1-2]. A yield of only 19% was obtained if the lithium amide was stirred for 10 s in the reaction medium before addition of the ester, and almost no reactivity was observed after 30 s with only traces of **1044** present at prolonged pre-mixing times. In striking contrast, in 2-MeTHF as reaction solvent little decomposition of the reactive lithium amide is seen for several minutes [Table 1.13, Entries 3-6]. Surprisingly after 10 min a yield comparable to that of 10 s in glycerol was still achieved. This result is in marked contrast to previous lifetime studies of phenyllithium on glycerol for the addition to benzonitrile.¹⁷⁰ The difference can be attributed to the addition of phenyllithium solution (in di-*n*-butyl ether) occurring ‘on glycerol’ as opposed to the present case with the addition of lithium *N*-methylanilide (in 2-MeTHF) occurring in the bulk solvent, therefore being highly susceptible to hydrolysis by the acidic hydroxyl protons of the glycerol and more so, by the water present in glycerol.

Further proof of the better adequacy of 2-MeTHF was observed upon the addition of solid lithium amide to the reaction in place of a 2-MeTHF solution [Scheme 1.6]. The reaction appeared to run smoothly, quickly mixing into 2-MeTHF giving an 82% yield, showing little difference in yield to the addition of the lithium amide as a solution [Table 1.12, Entry 9]. However, clear decomposition of the lithium amide was seen upon addition as a solid to glycerol, evidenced by the lower yield (47%). Due to the incredible lifetime of the lithium amide species and its highly advantageous ability to be the only solvent involved the reaction (reaction solvent, solvent for the lithium amide solution, and extraction solvent) allowing for easy recovery without purification, 2-MeTHF was selected as the best reaction solvent.



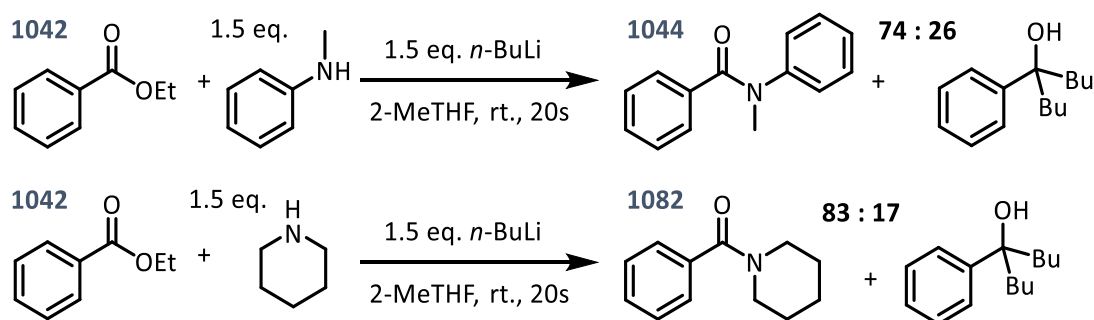
Scheme 1.6 – Addition of solid lithium *N*-methylanilide |**1043**| to ethyl benzoate |**1042**| in glycerol and 2-MeTHF.

Reactions performed under air at ambient temperature using 1 g of solvent and 1 mmol of ester |**142**|. Reactions stirred at 960 rpm for 20 s then quenched with sat. Rochelle’s salt soln. (5 mL). Product yields determined by ¹H NMR spectroscopy using a FeCp₂ standard.

In an attempt to avoid the pre-isolation of the lithium amide the feasibility of its *in-situ* formation through addition of *n*-butyllithium to an amine containing mixture was investigated [Scheme 1.7].

It was found that due to the lack of bulk, and the nucleophilicity of the *n*-butyllithium base, the double *n*-butyl addition product 5-phenylnonan-5-ol was observed alongside the desired amide product. Employing *N*-methylaniline a ratio of 74:24 amide:double alkyl addition was observed, and even by moving to a more nucleophilic amine, piperidine, an 83:17 amide:double alkyl addition ratio was observed. Due to the complication of the generation of an additional product even with more nucleophilic amines this *in-situ* generation of the lithium amide was discounted, being a less favourable method than pre-isolation.

In a final test to the model reaction scale up was attempted. With a 10 mmol scale reaction, scale up was successful and occurred with no problems and had little effect on the yield (84%) of amide isolated.



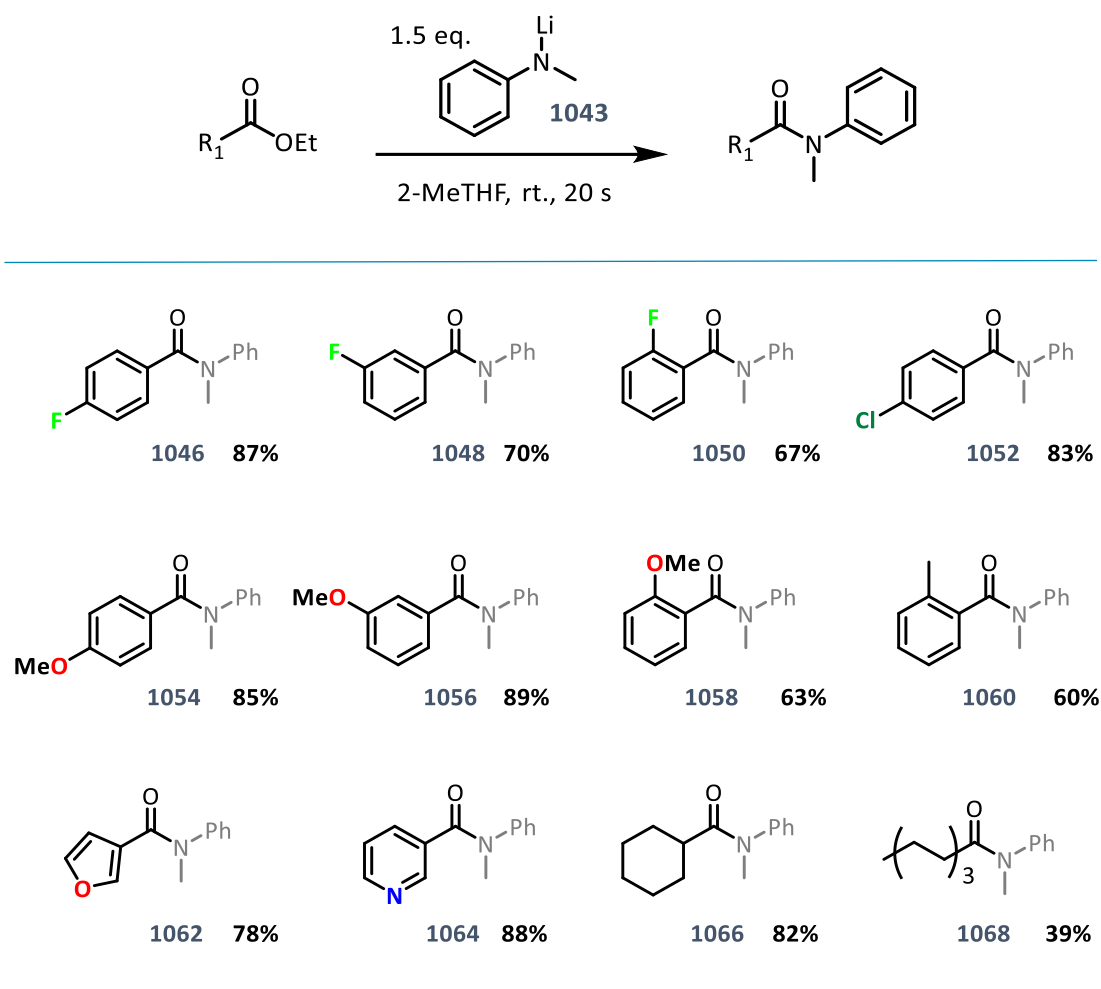
Scheme 1.7 – The *in-situ* formation of lithium *N*-methylanilide |1403| and lithium piperidide |1081| and reaction with ethyl benzoate |1042| in 2-MeTHF.

Reactions performed under air at ambient temperature using 1 g of 2-MeTHF and 1 mmol of ester |1042|. *n*-BuLi was added as a 1.4 M solution in hexanes. Reactions stirred at 960 rpm for 20 s then quenched with sat. Rochelle's salt soln. (5 mL). Product composition and ratios determined by GCMS

1.2.2 Assessing ester substrate scope

Encouraged by these initial findings and confident in the choice of 2-MeTHF as solvent we moved on to investigate the scope of esters that can undergo amidation via this method. A range of aromatic esters bearing different functional groups were tested for compatibility and most were found to convert in moderate to high yields in the 20 s reaction time [Table 1.14].

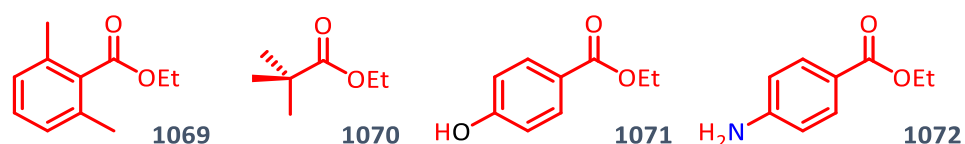
Table 1.14 – Addition of lithium *N*-methylanilide |1043| to various esters in 2-MeTHF. |a| |b| |c|



|a| Reactions performed under air at ambient temperature using 1 g of 2-MeTHF, 1 mmol of ester |1045, 1047, 1409, 1051, 1053, 1055, 1057, 1059, 1061, 1063, 1065, 1067|. Reactions stirred at 960 rpm for 20 s then quenched with sat. Rochelle's salt soln. (5 mL) |b| Lithium amide |1043| was pre-isolated and added as a 1 M soln. in 2-MeTHF. |c| Products determined by NMR spectroscopy and GCMS, yields determined by ^1H NMR spectroscopy using a FeCp_2 standard

Reactions involving halogen pendant aromatic esters achieved good yields (67 - 87%) with *p*-F, *m*-F, *o*-F and *p*-Cl [1045, 1047, 1049, 1051, Table 1.14], demonstrating a tolerance of mildly electron withdrawing groups and showing no evidence of lithium halogen exchange. A slight decrease in yield is apparent when an *ortho* substituent is introduced, even as small as fluorine. Moving to electron donating substituents *p*-MeO, *m*-MeO, *o*-MeO and *o*-Me [1053, 1055, 1057, 1059, Table 1.14], when a methoxy group is present in the *para* and *meta* positions the yield seems unaffected (85 – 89%) but *ortho* substituents see a drop in yield (60 - 63%). These results show that electronic effects are have a less prominent effect than steric effects which can be reasoned as due to the almost instantaneous nature of the reactions. The ester substrate scope was also extended successfully to both electron rich and poor heterocyclic substituents [3-furyl 1060 and 3-pyridyl 1602, Table 1.14], giving high yields (78 - 88%). Aliphatic esters [39 - 82%, 1065, 1067, Table 1.14], also proved compatible and showed no deprotonation of the mildly acid H_α of ethyl cyclohexanecarboxylate [1067].

The scope was however limited to less bulky esters, with di-*ortho*-substituted aromatic esters, such as ethyl *o,o*-dimethylbenzoate [1069] and quaternary carbon centres adjacent to carbonyl functionality, ethyl pivalate [1070], proving to be too sterically encumbered to allow nucleophilic attack of the ester. Esters bearing acid protons, i.e., such as ethyl 4-hydroxybenzoate [ethyl paraben, 1071] and ethyl 4-aminobenzoate [benzocaine, 1072] were also incompatible with this method of producing amides. In all cases of failed reactions the starting ester was recovered.



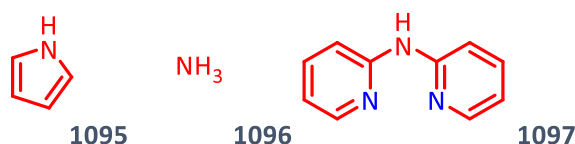
Scheme 1.8 – Failed ester scope for amidation by the addition of lithium *N*-methylanilide [1043] in 2-MeTHF.

1.2.3 Lithium amide assessment and synthesis of target products

After assessing the range of ester functionalities that could be tolerated by the system, the variation of lithium amides that could be successfully implicated was examined.

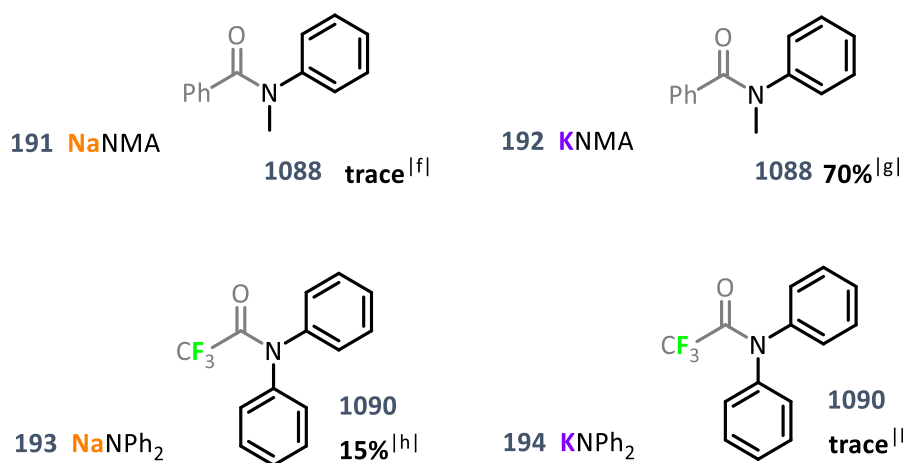
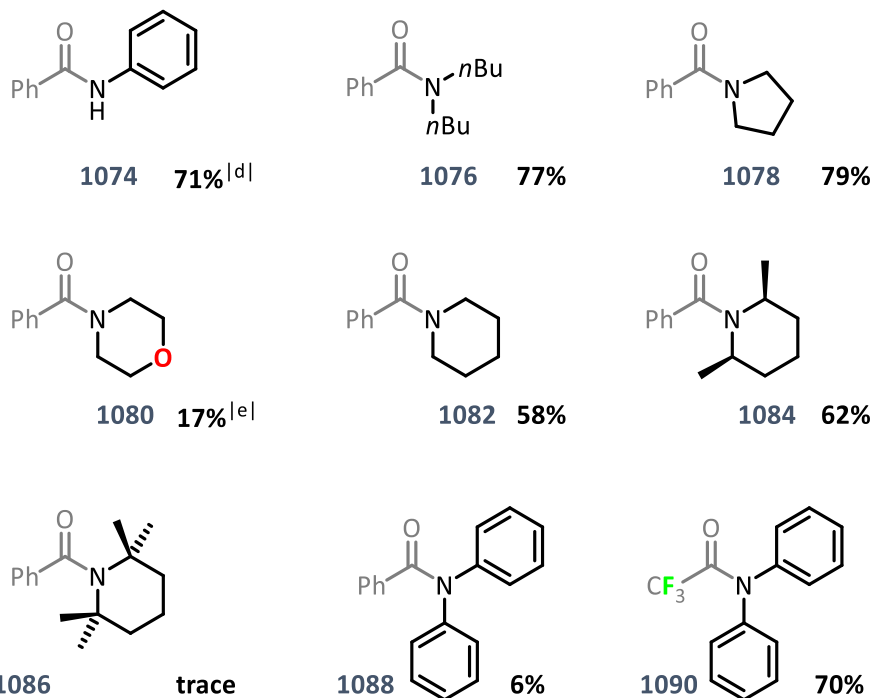
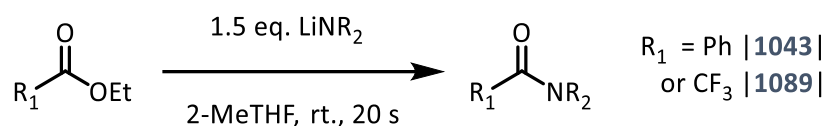
Initially the aromatic primary amine aniline |1073, Table 1.15| was found to achieve a good yield (71%) upon the addition of the higher load of 3eq. of lithium amide. The necessity for the use a larger excess of lithium anilide vs. lithium *N*-methylanilide could be due to the apparent increased reactivity of the lithium amide, giving rise to an increased rate of decomposition and subsequently a lower yield. A range of secondary aliphatic amines were found to give moderate to good yields |58 - 79%, 1075, 1077, 1079, 1081, Table 1.15| and even in the case of the di-*ortho*-substituted amine *cis*-2,6-dimethylpiperidine |1083, Table 1.15| the additional steric bulk seems to have little effect on the yield (62%). It is not until 2,2,6,6-tetramethylpiperidine |1085, Table 1.15| is employed that a severely limiting quantity of steric bulk can be observed. Moving to less nucleophilic aromatic secondary amines, lithium diphenylamide |1087| was seen to yield little amidated product with ethyl benzoate |1088, Table 1.15|, however, ethyl trifluoroacetate |1090, Table 1.15| was found to be a better electronic match and produce better yields.

It was however found that lithium amides of pyrrole |1095|, ammonia |1096| and 2,2'-bipyridylamine |1097| were not able to form a carboxamide using this method even when paired with ethyl trifluoroacetate.



Scheme 1.9 – Failed lithium amide scope for amidation of ethyl benzoate |1042| and ethyl trifluoroacetate |1089| in 2-MeTHF.

Table 1.15 – Addition various alkali metal amides to ethyl benzoate |1042| or ethyl trifluoroacetate |1089| to various in 2-MeTHF.^{[a][b][c]}



[a] Reactions performed under air at ambient temperature using 1 g of solvent, 1 mmol of ester |1043, 1089|. Reactions stirred at 960 rpm for 20 s then quenched with sat. Rochelle's salt soln. (5 mL). [b] Alkali metal amides |1073, 1075, 1077, 1079, 1081, 1083, 1085, 1087, 1089, 1091-1094| were pre-isolated and added as a 1 M solution in 2-MeTHF unless otherwise specified. [c] Products determined by NMR spectroscopy and GCMS, yields determined by ¹H NMR spectroscopy using a FeCp₂ standard. [d] 3 eq. lithium anilide, **1073** [e] 0.08 M lithium morpholide, **1079** [f] sodium N-methylanilide |1091| added as suspension ca. 3 eq. rude yield [g] 3 eq. potassium N-methylanilide |1092| added to butyl benzoate. Crude yield [h] Crude yields

The possibility of the addition of sodium or potassium amides was also explored. However, the heavier alkali metal amides were found to be less soluble than their lithium analogues. Sodium *N*-methylanilide **|1091|**, potassium diphenylamide **|1094|** were added at very high dilution and only yielded trace amounts of product. Potassium *N*-methylanilide **|1092|** and sodium diphenylamide **|1093|** proved more soluble, but yields lower than that of their analogous lithium amides, this could possibly be due to their higher reactivity making them more susceptible to decomposition under ambient conditions, or it is possible that side reactions with the 2-MeTHF solvent occur more quickly than their lithium analogues (as is the case with potassium 2,2,6,6-tetramethylpiperidide which reacts instantly with 2-MeTHF).

To further understand the reaction, the solid-state structures of 2-MeTHF solvates of the reactive lithium amide species were examined. The three of the lithium amides [lithium anilide **1073**, **Figure 1.3**, diphenylamide **1087**, **Figure 1.4**, and 2,2'-bipyridylamide **1095**, **Figure 1.5**], were found to exist as dimers, being tetra-, tri-, and di-solvated, respectively, with 2-MeTHF. The dimeric aggregation state is analogous to the THF solvated derivatives of lithium anilide^{171, 172} and to the 2-MeTHF solvated aggregate of lithium *N*-methylanilide.¹⁷³ In the case of lithium diphenylamide the 2-MeTHF solvate is dimeric as opposed to the monomeric (tri-solvated) THF analogue,¹⁶⁷ and it appears that a solid-state structure of lithium 2,2'-bipyridylamide has not previously been reported. These relatively low aggregation state may account for the high reactivity observed in these amidation reactions. The solution state aggregation of these species has so far not been investigated due to the lack of commercial availability deuterated 2-MeTHF and multi-step synthetic procedure.

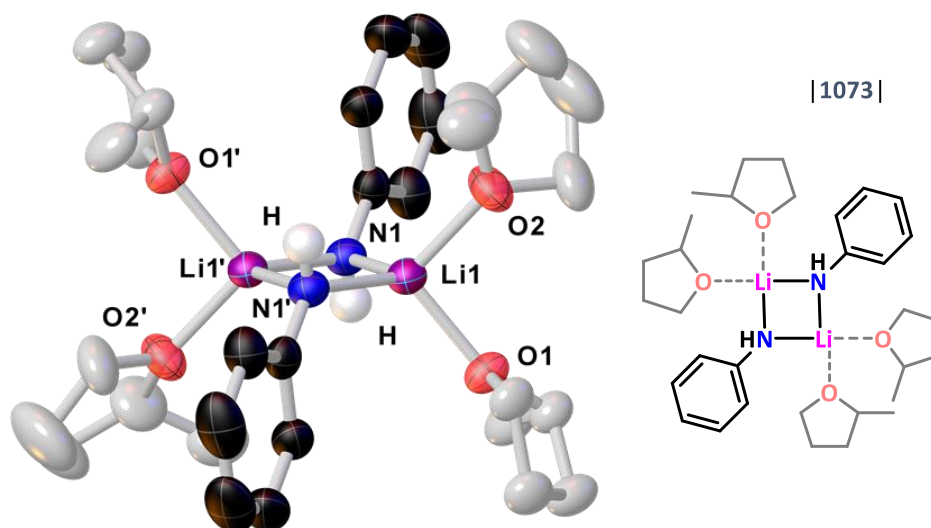


Figure 1.3 – Molecular structure of lithium anilide **|1073|** with displacement ellipsoids at 50% probability and hydrogen atoms omitted for clarity. Symmetry transformations used to generate equivalent atoms (1-X, 1-Y, 2-Z).

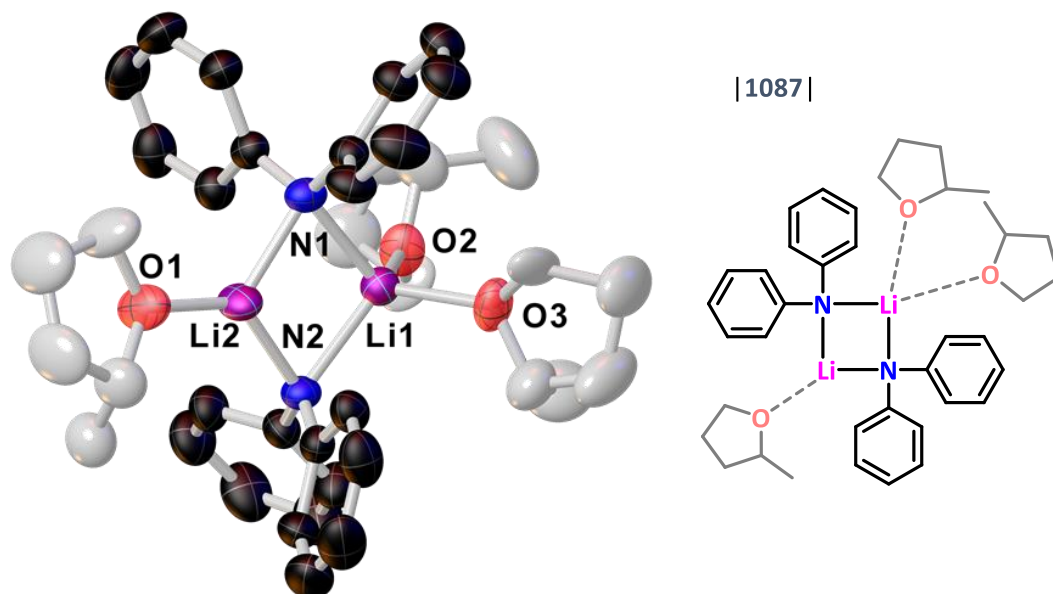


Figure 1.4 – Molecular structure of lithium diphenylamide [1087] with displacement ellipsoids at 50% probability and hydrogen atoms omitted for clarity.

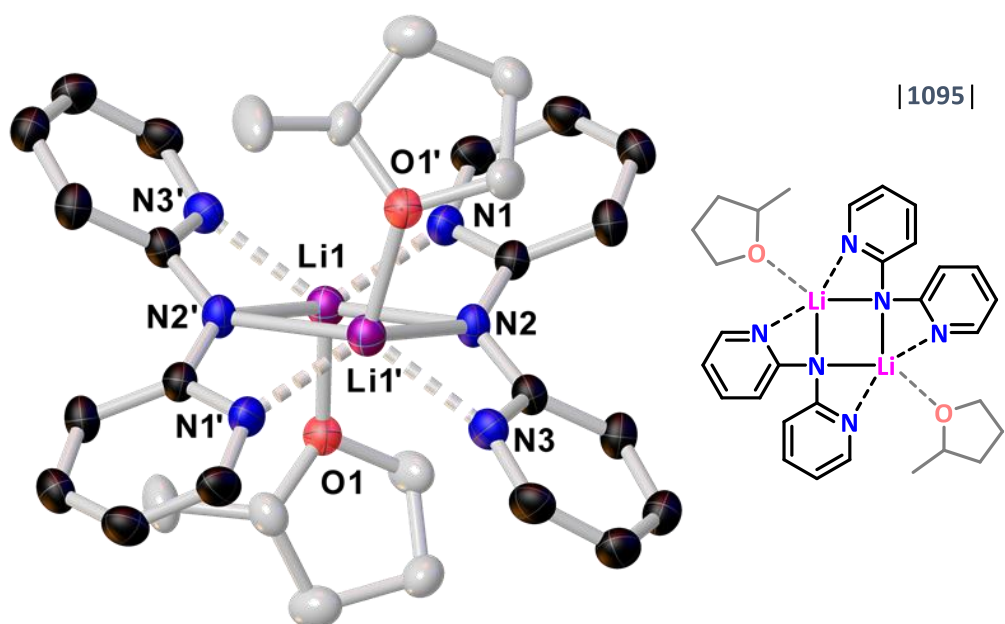


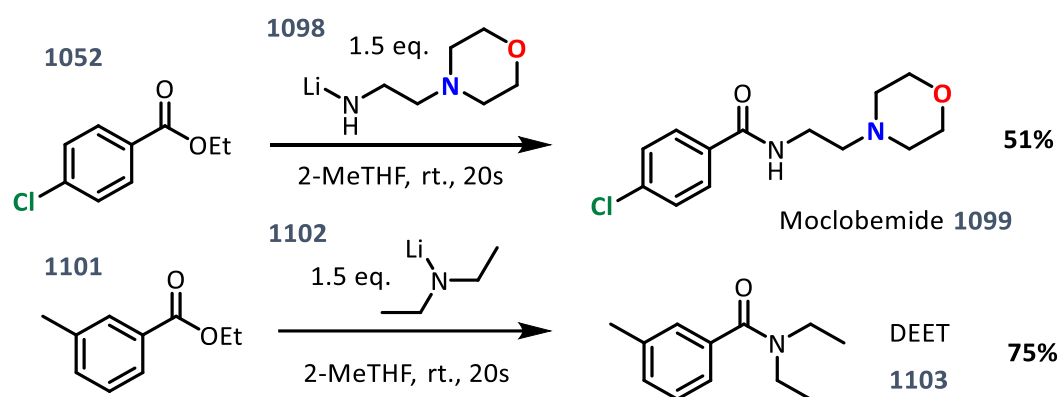
Figure 1.5 – Molecular structure of lithium 2,2'-bipyridylamide [1095] with displacement ellipsoids at 50% probability and hydrogen atoms omitted for clarity. Symmetry transformations used to generate equivalent atoms (-X, 1-Y, 1-Z).

Finally, after investigating a range of substrates and some technical aspects of these amidation reactions two target molecules were identified for synthesis by this lithium amide addition method. Both moclobemide [**1099**] and *N,N*-diethyl-*m*-toluamide [DEET, **1103**].

Moclobemide was first synthesised in 1972 but became commercially available in Europe in 1993 and is now widely used globally.¹⁷⁴ It is a reversible MAO inhibitor used to treat many depressive disorders, and proved to be more effective than older antidepressants.^{175, 176}

DEET is one of the most common active pharmaceutical ingredients in insect repellent. First developed by the US Department of Agriculture in 1944, it was used in jungle warfare by the US army during World War II, before becoming commercially available in 1956. DEET, as other insect repellents, forms a vapor barrier that is offensive in odour and taste to insects.¹⁷⁷

Both target compounds were synthesised in moderate to good yields as shown in [Scheme 1.10] demonstrating the ability of this amide forming method to obtain application relevant compounds.



Scheme 1.10 – The formation of synthetic targets moclobemide [**1099**] and *N,N*-diethyl-*m*-toluamide [**1103**] in 2-MeTHF.

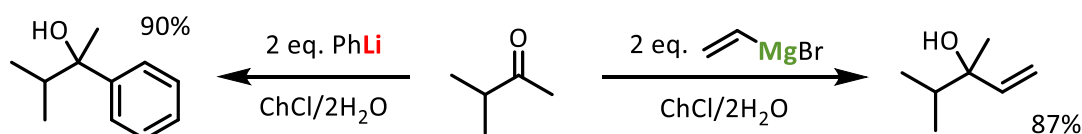
Reactions performed under air at ambient temperature using 1 g of solvent and 1 mmol of ester [**1052**, **1101**] and lithium amides [**1098**, **1102**] were pre-isolated and added as a 0.5 M solution in 2-MeTHF. Reactions stirred at 960 rpm for 20 s then quenched with sat. Rochelle's salt soln. (5 mL). Products determined by NMR spectroscopy and GCMS, yields determined by ¹H NMR spectroscopy using a FeCp₂ standard

1.3 Solvent directed reactivity using DESs

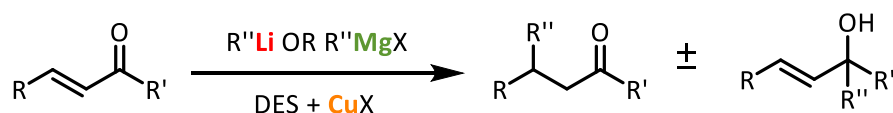
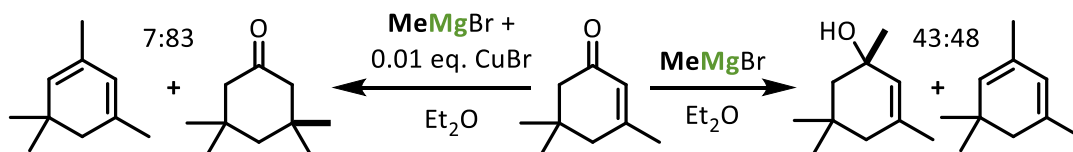
1.3.1 α,β -unsaturated ketones

Following on from previous successful additions of organolithium and Grignard reagents to carbonyl compounds, the possibility of performing regioselective additions to α,β -unsaturated carbonyls using the solvent to direct reactivity to either 1,2 or 1,4 addition. Organolithium and Grignard reagents are normally considered 'hard' nucleophiles (HSAB theory) and will usually undergo 1,2 to α,β -unsaturated ketones [Scheme 1.11]. Whereas addition of small amounts of copper allow for transmetallation to form organocopper species which are 'softer' due to the carbon metal bond being less polarised, due to this they undergo (1,4) conjugate addition. Organocopper species can also be pre-formed by reacting organolithium reagents stoichiometrically with a copper(I) salt to form a lithium cuprate, known as Gilman reagents.¹⁷⁸

García-Álvarez/Hevia :



Clayden :



Scheme 1.11 – [top] The addition of organolithium and Grignard reagents in ketones in green solvents.¹³⁵ [middle] The 1,2 and 1,4 addition of methyl magnesium bromide to an α,β -unsaturated ketone.¹⁷⁸ [bottom] The proposed conjugate addition of organolithium and Grignard reagents to α,β -unsaturated ketones in metal-salt-based DESs.

It was envisioned that using a type I, II or IV, metal salt containing DES might be able to direct the reactivity of organolithium and Grignard reagents as the combination of a catalytic amount of a copper salt (and often phosphine ligand) with Grignards,^{179, 180} organolithium,¹⁸¹ -zinc¹⁸² and -aluminium¹⁸¹ reagents has been shown to allow regioselective control, even allowing for asymmetric additions.¹⁸³⁻¹⁸⁵

It was envisaged that use of a copper salt in the eutectic mixture $\text{CuCl}_2/2\text{H}_2\text{O}$ would be a good choice for investigation due to the speciation of copper(II) chloride in this DES having previously been investigated.¹⁸⁶ The inner working of eutectic mixtures and their compositions have yet to be fully uncovered and the ability to estimate the species involved during reactions made these mixtures attractive. In said study, the composition of the copper species present in the mixture was able to be identified by EXAFS and UV-vis-near IR spectroscopic methods, with some species even examined by X-ray crystallography.

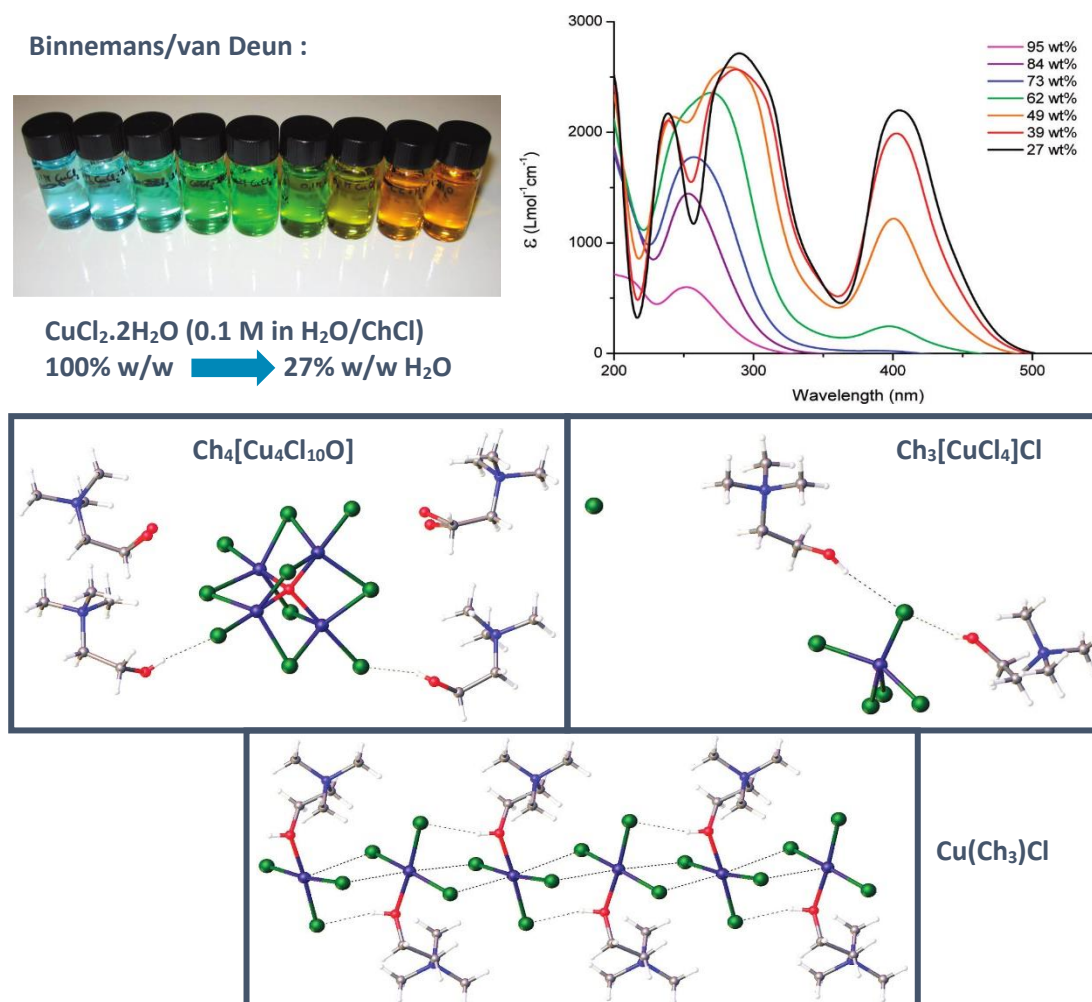
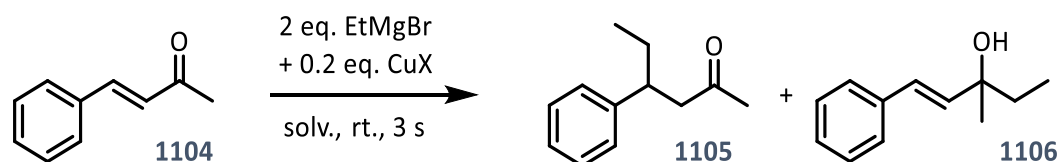


Figure 1.6 – UV-vis. spectra and solid state structures of species at different ratios of Cu(II)Cl_2 , ChCl and H_2O .¹⁸⁶

With this rationale in hand the addition of ethylmagnesium bromide to 4-phenylbut-3-ene-2-one **|1104|** was investigated under air in glycerol, water and DES mixture with the addition of a sub-stoichiometric quantity of a copper salt.

Initial reactions showed **|Table 1.16, Entries 1-6|** that even with the addition of 2 equivalents of ethylmagnesium bromide the major component obtained after reactions with **1104** was the starting ketone. This was thought to be simply due to a larger excess of Grignard reagent being required in the protic solvents used (glycerol and water) and perhaps a eutectic mixture would prove to be a better solvent choice. Comparing the selectivity across the three copper salts tested, no particular difference was noticed, with all producing around a 2:1 ratio of 1,4 to 1,2 addition product. Due to the better understood species in ChCl/2H₂O containing copper(II) chloride it was this salt that was chosen to be used in additions involving DESs.

Table 1.16 – The addition of ethylmagnesium bromide to 4-phenylbut-3-ene-2-one **|1104|** and sub-stoichiometric copper halide in glycerol, water and choline-chloride-based DESs.



Entry ^{[a][b]}	MX	Solv.	Ket. 1104	1,4-add. 1105	1,2-add. 1106	Mat. balance
1	Cu(I)Cl	Gly	38	: 44	: 18	-
2		H ₂ O	68	: 20	: 12	-
3	Cu(I)I	Gly	43	: 39	: 18	-
4		H ₂ O	77	: 16	: 8	-
5	Cu(II)Cl ₂	Gly	49	: 31	: 19	-
6		H ₂ O	85	: 10	: 5	-
7 ^[c]		ChCl/2Gly	4%	11%	6%	-73%
8 ^[c]		ChCl/2H ₂ O	31%	34%	14%	-20%

[a] Reactions performed under air at ambient temperature using 0.5 g of solvent and 0.5 mmol of ketone **|1104|** and commercial EtMgBr (1 M in THF). Reactions stirred for 3 s then quenched with sat. Rochelle's salt soln. [b] Conversions by integral ratio of starting material and product by GCMS [c] Yields determined by ¹H NMR spectroscopy by integration against a CH₂Br₂ internal standard

Additions in $\text{ChCl}/2\text{Gly}$ and $\text{ChCl}/2\text{H}_2\text{O}$ were seen to furnish a similar product selectivity with a 2:1 ratio of 1,4 to 1,2 product obtained [Table 1.16, Entries 7-8]. Somewhat some disappointment however, when measured quantitatively much of the material added was not recovered as starting material nor one of the two products, especially for the addition in $\text{ChCl}/2\text{Gly}$. This could be due to the loss of a known component during extraction or a further unknown side product being formed. Due to loss of material, addition conditions and reproducibility were examined.

Before checking reproducibility, the addition conditions were refined to define set reaction conditions [Table 1.17]. Firstly, the reaction vessel was examined with both '2-dram' (7.4 mL) and '4-dram' (14.8 mL) vials considered [Table 1.17, Entries 1-2]. It was seen that, although still low, a slightly higher yield was obtained using a '2-dram vial', but with a '4-dram vial' almost 100% of the material was recovered. The improved recovery of starting material and product was taken to signify that unreacted starting material was sometimes being lost during the extraction and not due to an unseen side reaction as it was deemed unlikely that a larger reaction flask would impact the ability of a side reaction to occur. Following on from this the amount of DES used was varied [Table 1.17, Entries 1-4]. This was seen to perhaps have a small effect on product yield, as with 2 g $\text{ChCl}/2\text{H}_2\text{O}$ in either size or reaction vessel less of the 1,4-product was obtained. It is unclear if this signifies products were formed in a different ratio or if an increased quantity of DES hinders the extraction of the 1,4-product [1105] (and starting material 1104) more than the 1,2 product [1106]. Next, pre-mixing was considered [Table 1.17, Entries 5-6] to see if having the ketone mixed through the solvent at the start of the reaction has any effect on product yield; it was found not to. Equally when stirring speed was varied [Table 1.17, Entries 7-9] it was seen that, although no stirring lowered yields, but faster or slower stirring had no noticeable effect. Finally, the rate of addition of the Grignard reagent was varied [Table 1.17, Entries 10-11] to assess if a slow addition or more rapid and turbulent addition would change any result, only a slightly higher yield was seen by performing the addition of the Grignard more slowly.

From variation of these parameters it was noted that in general conditions did not greatly affect the yield of ratio of product. Therefore, standard conditions of: 0.5 g $\text{ChCl}/2\text{H}_2\text{O}$, no pre-mixing, fast stirring and quite slow addition were chosen and the reproducibility of the reactions was further investigated.

Table 1.17 – Variation of addition parameters for the addition of ethylmagnesium bromide to 4-phenylbut-3-ene-2-one |1104| in $\text{CHCl}_2/2\text{H}_2\text{O}$ and sub-stoichiometric $\text{Cu}(\text{II})\text{Cl}_2 \cdot 2\text{H}_2\text{O}$.

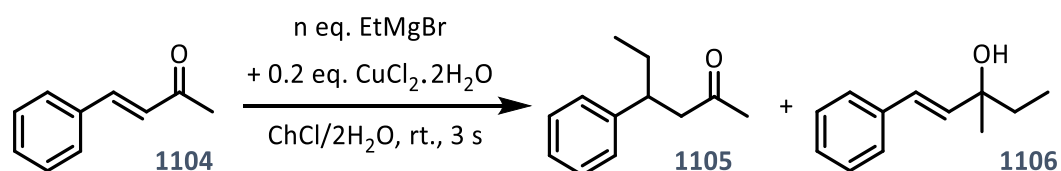
Entry ^{[a] b}	Variable	Condition	Ket.	1,4-add.	1,2-add.	Mat.
			1104	1105	1106	balance
1	Reaction vessel	2D vial	31%	34%	14%	-20%
		+ 0.5 g DES				
2		4D vial	61%	22%	11%	-6%
		+ 0.5 g DES				
3	DES quantity	2D vial	51%	17%	10%	-22%
		+ 2 g DES				
4		4D vial	56%	17%	10%	-16%
		+ 2 g DES				
5	Pre-mixing	Yes	46%	26%	10%	-18%
6		No	45%	27%	13%	-15%
7	Stirring	Slow	27%	28%	13%	-32%
8		Fast	34%	26%	10%	-30%
9		No	42%	16%	9%	-32%
10	Addition	Slow	23%	33%	14%	-30%
11		Fast	28%	24%	13%	-36%

[a] Reactions performed under air at ambient temperature using 0.5 g of solvent and 0.5 mmol of ketone |1104| and commercial EtMgBr (1 M in THF). Reactions stirred for 3 s then quenched with sat. Rochelle's salt soln. 2D = 7.4 mL, 4D = 14.8 mL |b| Yields determined by ^1H NMR spectroscopy by integration against a CH_2Br_2 internal standard

The reproducibility of the reaction was tested alongside optimisation of the number of equivalents of Grignard reagent required for a good yield |Table 1.18|.

It was seen that across the range of equivalents tested that reactions were fairly reproducible with the same approximately 2:1 ratio of 1,4 to 1,2 product seen. With the addition of 1.0 eq. EtMgBr ca. 15% of |1105| was obtained |Table 1.18, Entries 1-2|.

Table 1.18 – Variation of equivalent of ethylmagnesium bromide in the addition to 4-phenylbut-3-ene-2-one |1104| in $\text{CHCl}_2/2\text{H}_2\text{O}$ and sub-stoichiometric $\text{Cu}(\text{II})\text{Cl}_2 \cdot 2\text{H}_2\text{O}$.



Entry ^[a] b]	Eq. EtMgBr	Ket. 1104	1,4-add. 1105	1,2-add. 1106	Mat. balance
1	1.0	49%	16%	9%	-26%
2		40%	12%	8%	-41%
3	1.2	37%	21%	11%	-30%
4		39%	24%	11%	-26%
5	1.6	27%	28%	13%	-32%
6		23%	33%	14%	-30%
7	2.0	13%	34%	17%	-36%
8		11%	23%	15%	-51%
9	(d₁ = 4 s)	18%	24%	15%	-43%
10	2.5	12%	28%	14%	-46%
11		7%	31%	16%	-45%

[a] Reactions performed under air at ambient temperature using 0.5 g of solvent and 0.5 mmol of ketone |1104| and commercial EtMgBr (1 M in THF). Reactions stirred for 3 s then quenched with sat. Rochelle's salt soln. [b] Yields determined by ¹H NMR spectroscopy by integration against a CH₂Br₂ internal standard

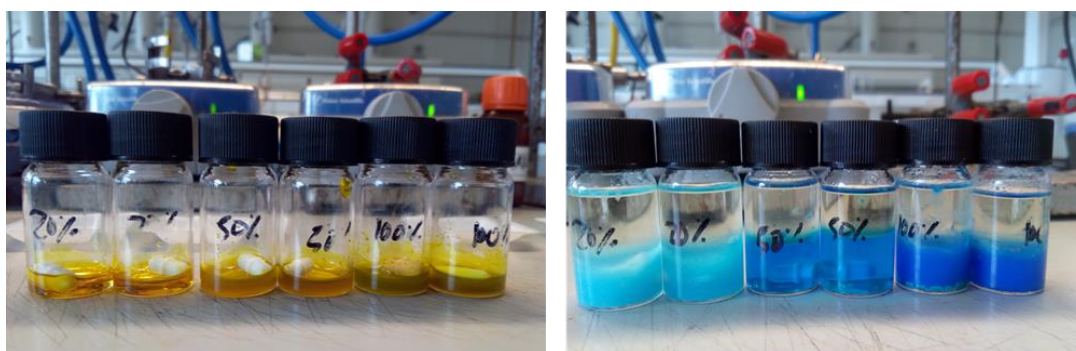
Moving to 1.5 eq. EtMgBr [Table 1.18, Entries 3-4], just over 20% of 1,4-addition product was obtained. Upon increasing to 1.6 eq. or more it was noted that a maximum of ca. 30% 1,4-addition product could be obtained [Table 1.18, Entries 5-11]. The legitimacy of the dibromomethane standard used to calculate yields was checked by increasing the relaxation time [Table 1.18, Entry 9] but no significant change in yield was observed, therefore the standard, and yields it produces, were deemed to be accurate.

Due to the inability to affect the ratio of 1,4- to 1,2-addition product the quantity of copper additive was next examined [Table 1.19].

With the variation of copper salt present it was quite clear to see the variation in colour of the DES + Cu [Table 1.19] from which it would have been possible to investigate speciation, with the orange colour visually suggesting the presence of CuCl_4 , likely in the form of $\text{CH}_3[\text{CuCl}_4]\text{Cl}$. Although this was not further investigated spectroscopically.

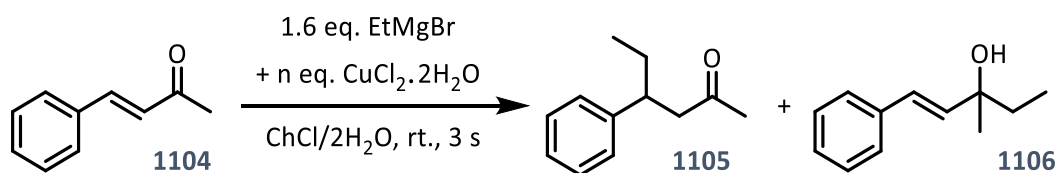
Unfortunately, it was quickly apparent that the quantity of $\text{Cu(II)Cl}_2 \cdot \text{H}_2\text{O}$ was unable to influence the ratio of conjugate [1105] to direct addition product [1106] as even with the addition of stoichiometric levels of copper salt the yields remained relatively unaffected [Table 1.19, Entries 1-6]. The decisive result came in the form of 0 eq. of copper additive [Table 1.19, Entry 7], even more disappointingly showing that the EtMgBr alone produced the same ration of 1,4- to 1,2- addition product without any copper present.

Table 1.19 – Variation of quantity of $\text{Cu(II)Cl}_2 \cdot 2\text{H}_2\text{O}$ in the addition of ethylmagnesium bromide to 4-phenylbut-3-ene-2-one |1104| in $\text{CHCl}_3/2\text{H}_2\text{O}$.



DES + CuCl_2 (pre-add.)

Post-addition & quench



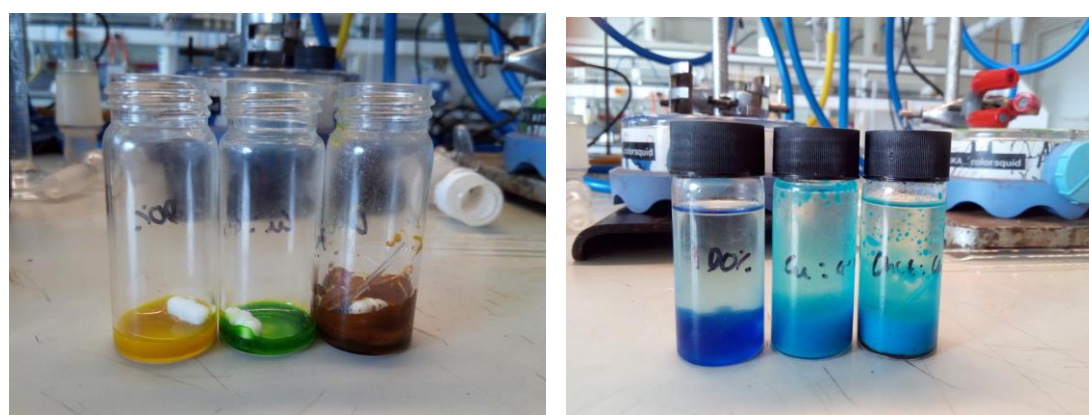
Entry ^{[a] [b]}	Eq. CuCl_2	Ket. 1104	1,4-add. 1105	1,2-add. 1106	Mat. balance
1	0.2	31%	34%	14%	-20%
2		34%	28%	13%	-26%
3	0.5	22%	38%	16%	-24%
4		37%	29%	13%	-22%
5	1.0	19%	16%	12%	-54%
6		36%	27%	12%	-25%
7	0.0	18%	27%	13%	-43%

[a] Reactions performed under air at ambient temperature using 0.5 g of solvent and 0.5 mmol of ketone |1104| and commercial EtMgBr (1 M in THF). Reactions stirred for 3 s then quenched with sat. Rochelle's salt soln. [b] Yields determined by ^1H NMR spectroscopy by integration against a CH_2Br_2 internal standard

Due to the inability to influence the regioselectivity of additions of ethylmagnesium bromide by addition of copper(II) chloride and the mixture of 1,4 and 1,2 addition products obtained under standard conditions, without a copper salt additive, investigation turned to the alkyllithium reagent ethyllithium.

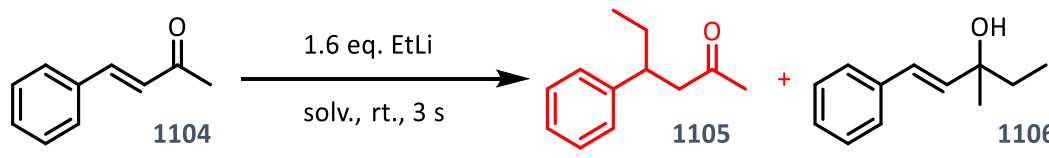
The addition of ethyllithium was tested in three different of copper-based DESs: the standard type III ChCl/2Gly with 1 eq. CuCl₂·2H₂O additive as was done before for ethylmagnesium bromide; (CuCl₂·2H₂O)/2Gly [type IV, metal salt + HBD]; and ChCl/2(CuCl₂·2H₂O) [type II, HBA + (hydrated) metal salt].

Table 1.20 – Variation eutectic solvent mixture in the addition of ethyllithium to 4-phenylbut-3-ene-2-one |1104|.



DES (pre-add.)

Post-addition & quench



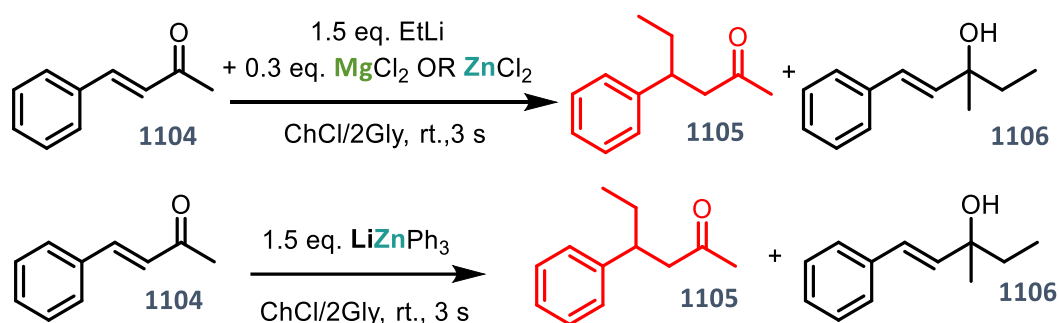
Entry ^{[a][b]}	DES	Ket. 1104	1,4-add. 1105	1,2-add. 1106	Mat. balance
1	ChCl/2Gly + 1.0 eq. CuCl ₂ ·2H ₂ O	26%	0%	25%	-50%
2	(CuCl ₂ ·2H ₂ O)/2Gly	13%	0%	43%	-44%
3	ChCl/2(CuCl ₂ ·2H ₂ O)	3%	0%	31%	-66%

[a] Reactions performed under air at ambient temperature using 0.5 g of solvent and 0.5 mmol of ketone |1104| and commercial EtLi (0.5 M in benzene:Cy). Reactions stirred for 3 s then quenched with sat. Rochelle's salt soln.
 [b] Yields determined by ¹H NMR spectroscopy by integration against a CH₂Br₂ internal standard

An apparent difference in DESs, even before the addition, was the different colours of the three eutectic mixtures (it should be noted that the HBD in this case is glycerol compared to the water previously used, and involved in the speciation study referenced)¹⁸⁶ [Figure 1.6]. The ChCl/2Gly + 1.0 eq. CuCl₂·2H₂O appeared orange, as it appears with ChCl/2H₂O, indicating the likely presence of CH₃[CuCl₄]Cl. The second [type IV] eutectic mixture (CuCl₂·2H₂O)/2Gly appeared bright green, which has previously been attributed to a mixed choline/chloro copper complex such as Cu(CH₃)Cl. The third [type II] eutectic mixture ChCl/2(CuCl₂·2H₂O) was rusty brown in appearance. This is not exactly the same in appearance to the crystalline solid [CH₄[Cu₄Cl₁₀O]] that has previously observed with the purely choline chloride/copper(II) chloride mixture (red in colour); however, this crystalline form was obtained after exposure to air over a few days and has a different stoichiometry from the eutectic mixture used in the present case, including an oxygen atom that could have been obtained from water or oxygen.

Again, despite the range of copper species, it was seen that the solvent was unable to influence the addition of the ethyllithium [Table 1.20]. In all three cases only direct (1,2) addition was observed, and poor yields were obtained. This result proved the inability for a simply copper containing DES to allow for the *in-situ* formation of an organocopper specie capable of undergoing conjugate addition using organolithium or Grignard reagents.

The use of other metal salts with the hope of forming ‘ate’ species *in-situ* was also attempted,¹⁸⁷ as was the direct addition of a zincate [Scheme 1.12]. However, all attempts to facilitate conjugate (1,4) addition were unsuccessful, with only 1,2 addition product observed.

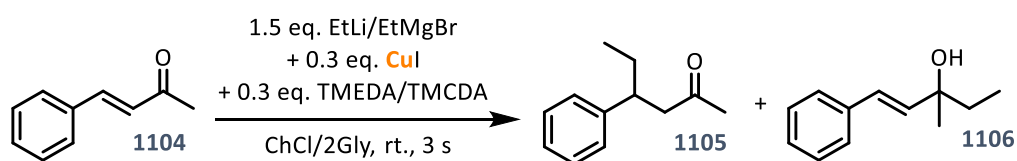
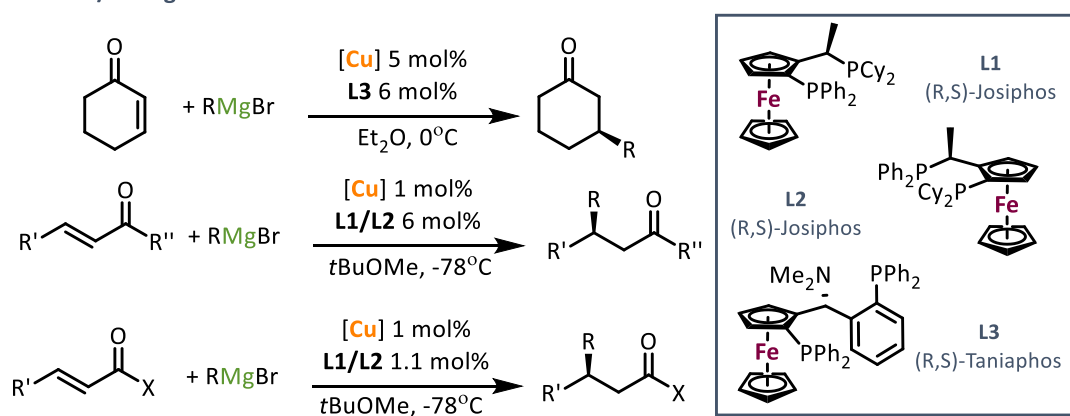


Scheme 1.12 – The addition of EtLi or LiZnPh₃ to 4-phenylbut-3-ene-2-one [1104] in ChCl/2Gly (in the presence of a metal salt).

Having seen that conjugate addition could not be directed by the inclusion of a metal salt or by the use of a metal-based DES, the investigation seemed to have drawn itself to a conclusion. However, it was noticed in the literature that in the most successful cases a phosphine ligand is also required with a copper salt when performing (asymmetric) conjugate addition of a Grignard reagent [Scheme 1.13]. It was therefore hypothesised that the inclusion of a Lewis donor ligand could help influence reactivity. In place of phosphine ligands cheaper amine ligands were considered, alongside a copper(I) salt, which appear to be more common for this type of addition reactions.

It was already initially apparent visually that there appeared to be different species involved using copper(I) iodide than copper(II) chloride, as would be expected, but there was also a clear visual difference between using TMEDA and (R,R)-TMCDA from start to finish through reactions [Figure 1.7] which is harder to explain.

Minaard/Feringa :



Scheme 1.13 – The conjugate addition of Grignard reagents to α,β -unsaturated ketones in the presence of a copper and phosphine ligand.¹⁸⁸

Curiously despite the colours observed for the reactions involving ethylmagnesium bromide mostly starting material was recovered, with the addition apparently hindered by the change of copper salt and addition of amine. In the case of ethyllithium however, we do see a difference in the products obtained upon the addition of an amine to the reaction mixture.

Looking at a GC-mass spectrum of the mixture obtained from the addition of EtLi with both TMEDA and (R,R)-TMEDA present [Figure 1.8] results look promising with a mixture of starting material (11.15/6 min) and 1,4 addition product (1.11 min) and an additional unknown product present in one of the cases (11.7 min). However, when NMR spectra of the same mixture are observed it is clear that that the GC-mass spectrum does not reflect the true extent of the species in the mixture.

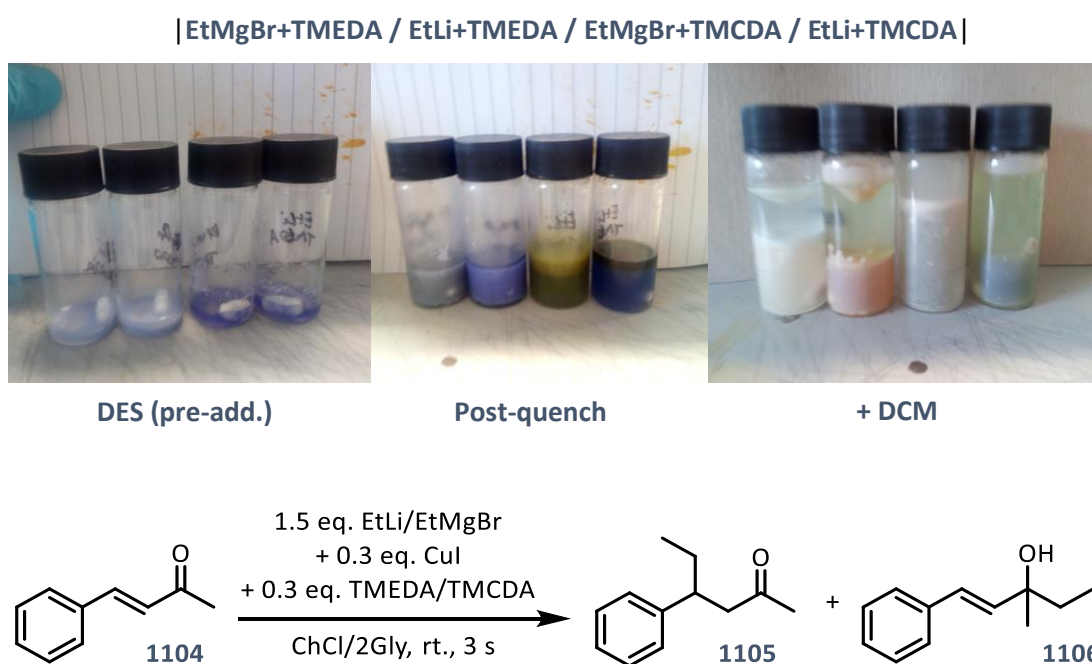


Figure 1.7 –The addition of EtLi and EtMgBr to 4-phenylbut-3-ene-2-one [1104] in ChCl/2Gly in the presence of Cu(I) and an amine donor (TMEDA or [R,R]-TMEDA).

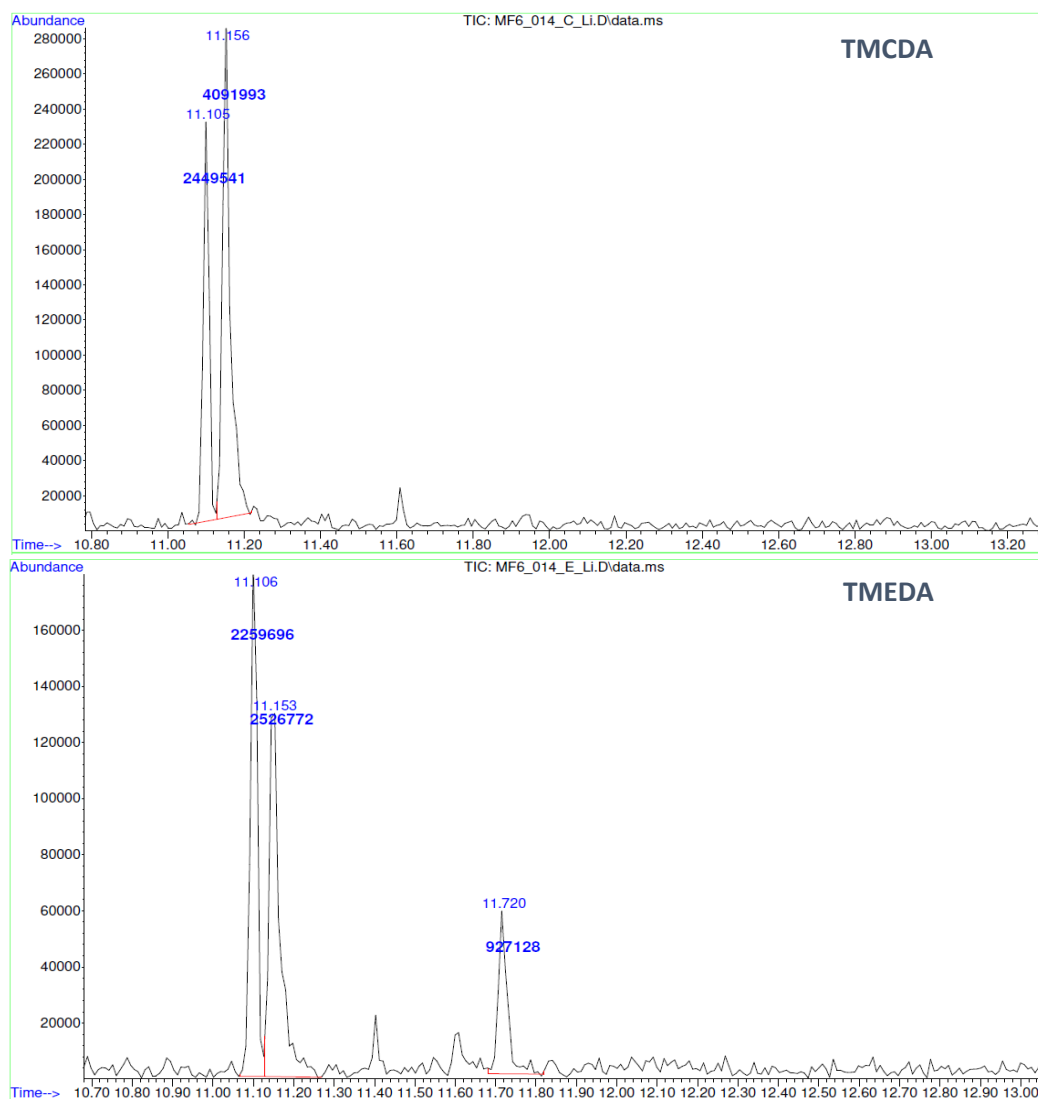
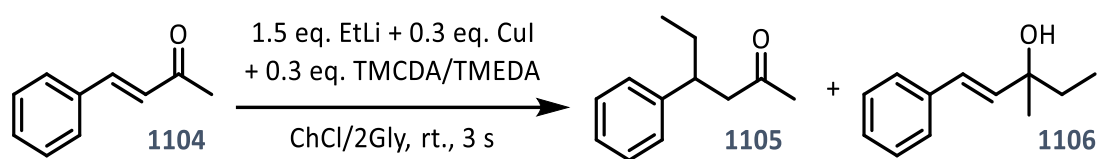


Figure 1.8 –GC-mass spectra of the addition of EtLi 4-phenylbut-3-ene-2-one [**1104**] in ChCl/2Gly in the presence of Cu(I) and an amine donor (TMEDA or [R,R]-TMCDA).

Observing the highlighted 1.5 – 2.5 ppm region | **Figure 1.9** | of a ^1H NMR spectrum of the product mixture and standards of the starting material and both 1,2 and 1,4 addition isomers it can be seen that the 1,4 addition product does seem to be present but not the 1,2 product as is observed in the GC mass spectrum, which would appear to indicate a successful reaction in where product regioselectivity has been influenced. However, there are also clearly peaks which do not correspond to either addition product or starting material.

Looking at a ^{13}C NMR of the same mixture provides further evidence of there being more species present than first appeared, with multiple carbonyl peaks visible ca. 220 ppm suggesting multiple ketone compounds to be present. It therefore seems that the reaction has been influenced by the addition of Cu(I)I and TMEDA, unlike Cu(II)Cl₂. Curious to why only two/three species were apparent in by GCMS the reaction mixture was analysed by LCMS. Using this technique it was possible to see copper species present in the mixture. It is unclear if these copper species are responsible of the suspected ketone resonances seen by the ^{13}C NMR spectroscopy. Attempts were made to remove the copper species present by filtration though Celite and a short column of silica but these were unsuccessful, making the prevailing copper species all the more mysterious.

The additional product species in reaction containing Cu(I)I and TMEDA/TMEDA are thought to possibly arise due to the amines functioning as a ligand to the copper and facilitating the production of different species, but also possibly due to the ability of Cu(I)I to participate in radical based reactions. If the rogue copper species can be contained, perhaps by used of a different copper salt to ensure they do not arise due to radicals, this apparent *in-situ* formation of a Gilman reagent type cuprate could be considered successful. However, no further investigation has been carried out into the topic.

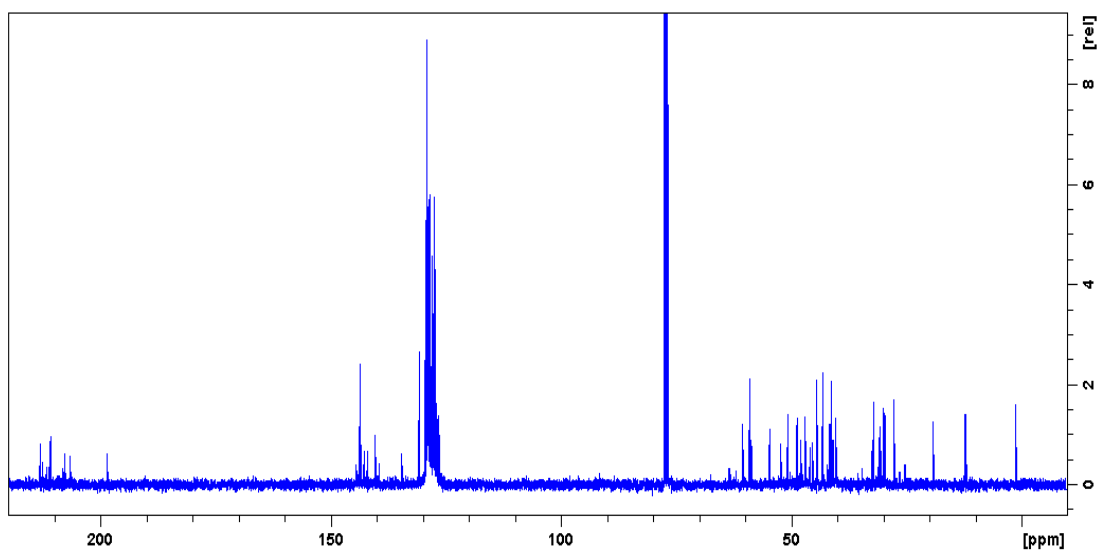
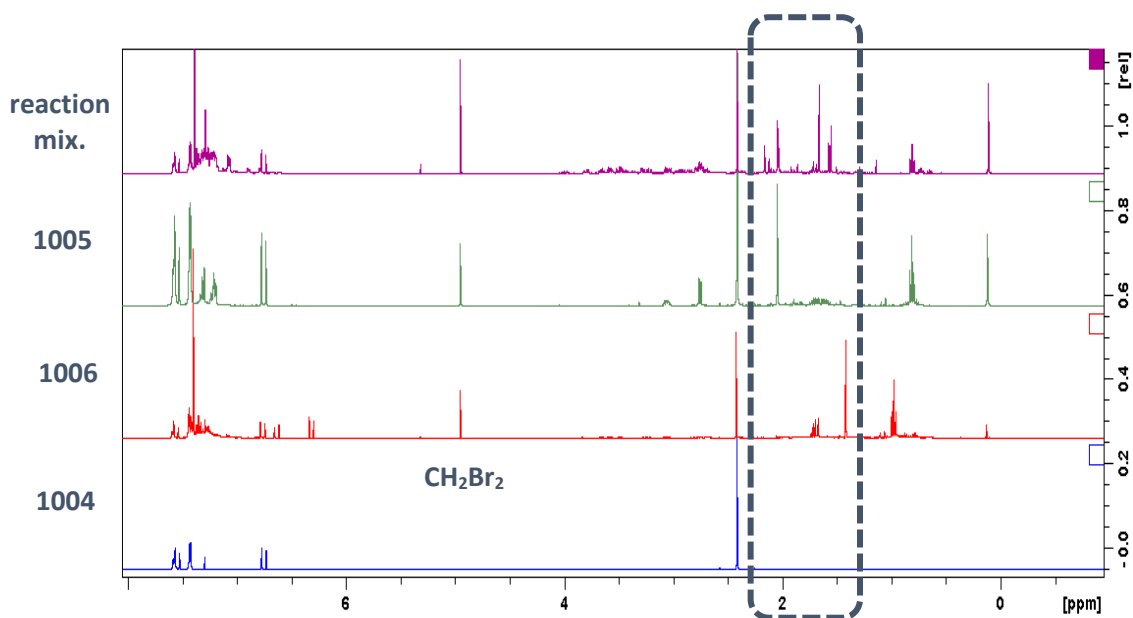
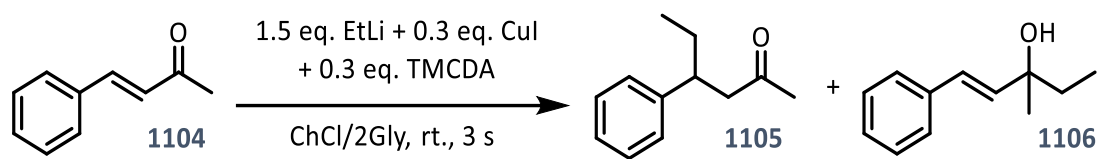


Figure 1.9 – |top| ¹H NMR spectra (400 MHz, CDCl₃) of the reaction of EtLi + CuI + TMCDA + 4-phenylbut-3-ene-2-one; 1.4 addition product **1105**; standard of 1.2 addition product **1106**; and |; 1.4 addition product **1105**. |bottom| ¹³C NMR spectrum (100 MHz, CDCl₃) of the reaction of EtLi + CuI + TMCDA + 4-phenylbut-3-ene-2-one.

1.3.2 Transition metal catalysed cross-couplings

In the hope of finding an alternative reaction in which metal base DESs could direct reactivity/form part of the reactive organometallic species cross-coupling reactions were investigated.

Transition-metal-catalysed cross-coupling reactions, in particular palladium catalysed carbon-carbon bond forming cross-coupling reactions are a cornerstone area of organometallic chemistry.¹⁸⁹⁻¹⁹² They generally involve aryl/alkyl halide and organometallic sections which are coupled together using most commonly, a platinum group catalyst (such as palladium or nickel), and have been developed over many years by many people employing a variety of different metals for the organometallic section involved in the coupling. The importance of these cross-coupling reactions and their ubiquity (particularly Suzuki-Miyaura)¹⁹³ in organic synthesis has even been recognised by the award of a Nobel Prize.¹⁹⁰

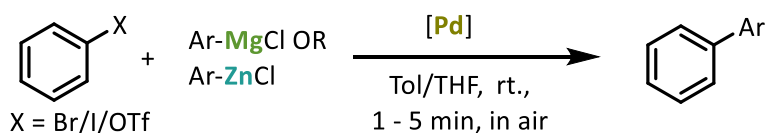
Of relevance to the project at hand, the cross-coupling of organozinc, Grignard and organolithium reagents has previously been investigated in air in traditional solvents, and non-pyrophoric reagents have been used in couplings in ionic liquids,¹⁹⁴ but it is only recently that the coupling of this class of reagents has been attempted in water or alternative solvents |**Scheme 1.14**|.^{127, 195, 196}

In investigations Schoenebeck¹⁹⁵ found that sp^2 -carbon-carbon bonds could be formed between aryl bromide, chloride or triflates and Grignard or organozinc reagents using a palladium(I) dimeric catalyst. Reactions could be carried out under argon or in air in less than 5 min at ambient temperature achieving good yields across a range of reactive and bulky functional groups.

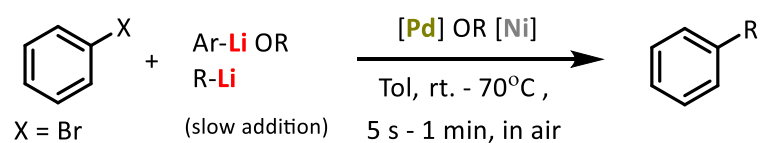
In work by Feringa¹⁹⁶ the ultrafast coupling of aryl and alkyllithium reagents with aryl bromides. It was found that the addition of organolithium reagents to a suitable palladium pre-catalyst in the presence of oxygen allowed for the formation of palladium nanoparticle that be capable of performing cross couplings in as little as 5 s with moderate catalyst loadings and 5 – 30 min at standard low palladium loadings.

Most recently, alongside Suzuki-Miyaura couplings,¹⁹⁷ Capriati¹²⁷ has investigated the palladium catalysed cross-coupling of organolithium compounds with aryl bromide and chloride compounds. It was seen that with the addition of 1 equivalent of sodium chloride a wide array of aryl halides could be coupled to sp^3 , sp^2 and sp organolithium reagents in water in as little as 20 s in good yields.

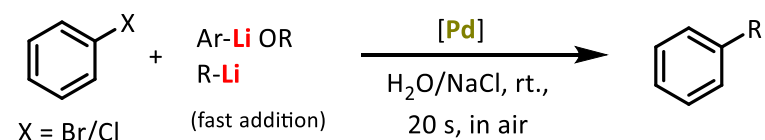
Schoenebeck :



Feringa :



Capriati:



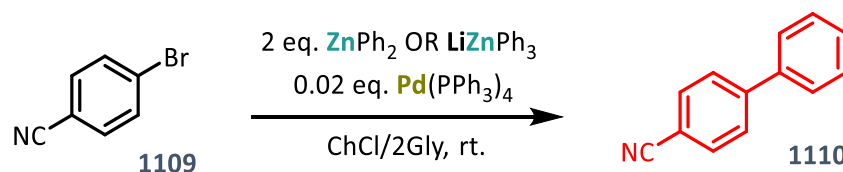
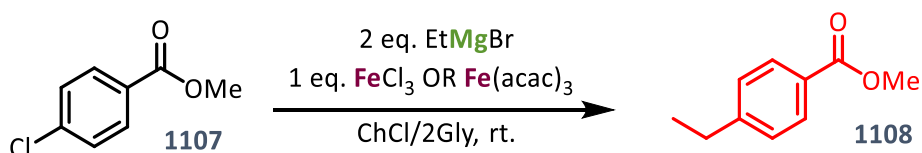
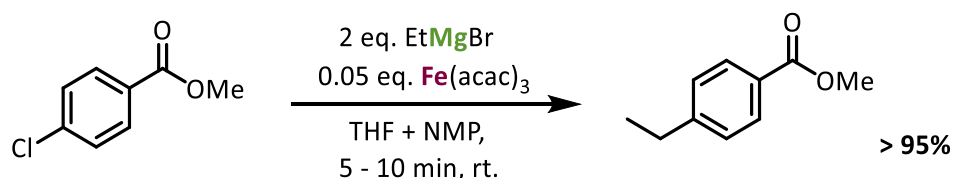
Scheme 1.14 – The palladium catalysed cross-coupling of: [Top] Grignard and organozinc reagents in air;¹⁹⁵ [Middle] Organolithium reagents in air;¹⁹⁶ [bottom] Organolithium reagents in air in brine.¹²⁷

Following on from these previous investigations the possibility of performing Kumada^{198, 199} and Negishi²⁰⁰ couplings in DESs was explored |Scheme 1.15|.

First the possibility of performing an iron-catalysed coupling of an aryl halide and a Grignard reagent was considered. This coupling has previously been undertaken under anhydrous conditions^{201, 202} and is additionally attractive due to the use of the abundant, base metal iron catalyst in place of palladium or nickel. Unfortunately, when attempted in DES no coupling was observed with only starting material obtained. This is likely due to a slightly longer reaction time being necessary, where under these conditions the Grignard reagent does not persist in high enough concentrations to be coupled. Next the possibility of performing a palladium catalysed coupling of an organozinc compound was attempted. Both an aryl zinc and a triaryl lithium zincate were tested as coupling partners for to 4-bromobenzonitrile in ChCl/2Gly with 2 mol% palladium(0) catalyst but in both cases starting material was obtained from the reaction mixture.

It is possible in the case of both types of cross-coupling that the reaction is not fast enough with decomposition of the 'air-sensitive' reagent occurring more quickly than the coupling reaction. Alternatively, it is possible that a suitable set of Lewis donor ligand is required to allow the coupling to occur. In any case it is likely that investigation of conditions and ligands would be required to find out if these coupling reactions are in fact possible under these conditions

Fürstner :

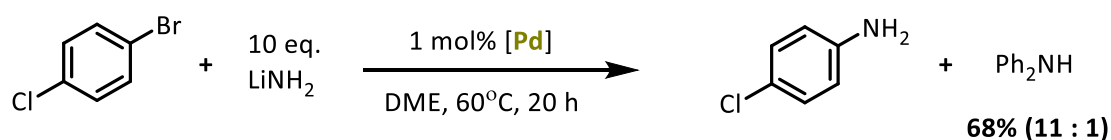


Scheme 1.15 — Kumada and Negishi style palladium catalysed cross-couplings in DESs using metal salt additives.

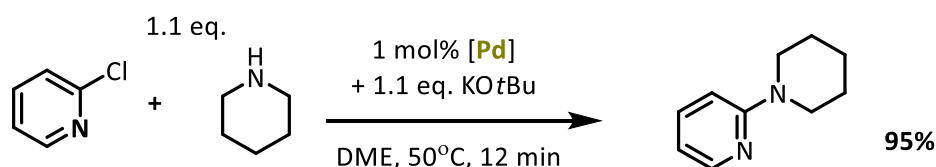
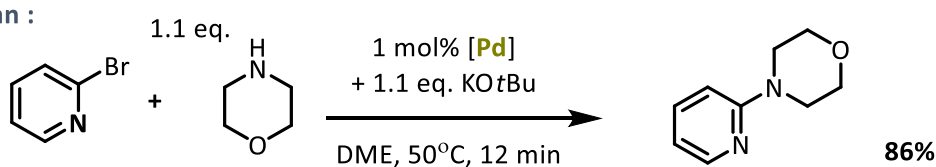
Based on findings of the lifetime of lithium amides in 2-MeTHF | **1.2 Amidation of esters using lithium amides under air** | an alternative cross-coupling reaction could perhaps be feasible using lithium amides in place of alkyl reagents.

Buchwald-Hartwig aminations involve the coupling of an amine and an aryl halide or triflate and could be a potential option.¹⁹² Although normally these reactions use an amine and base rather than metal amide and require much elevated temperatures for hours long reaction times meaning it is unlikely they are compatible with even the longest lithium amide lifetimes seen in 2-MeTHF (5 - 10 min). Despite this there have been a couple of examples that display potential compatibility | **Scheme 1.16** |. For example, the coupling of lithium amide and 1-bromo-4-chlorobenzene has been achieved showing this type of coupling possible, although it was seen to require slightly elevated temperature and only achieved moderate yields in 20 h,²⁰³ making the reaction too slow for consideration in air. However, lithium amide is relatively insoluble and was previously seen to be unreactive in addition reactions carried out in 2-MeTHF, therefore it is possible that the use of a more reactive lithium amide could give reduced reaction times although likely these would still be far in excess of the time needed to compete with decomposition processes.

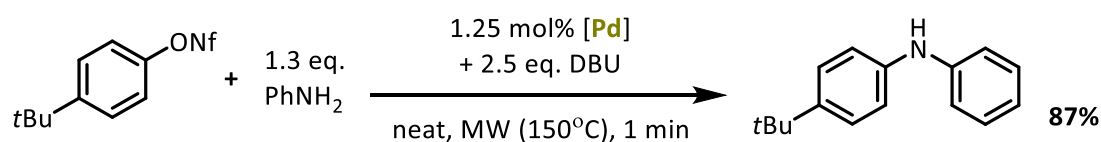
Hartwig :



Nolan :



Buchwald :



Scheme 1.16 — Buchwald-Hartwig aminations: |top| using lithium amide;²⁰³ |Middle| 12 min reaction times;²⁰⁴ |bottom| 1 min MW reactions.²⁰⁵

Apart from this example of the coupling of lithium amide to an aryl halide the coupling of amines (with use of a base) has been achieved in much shorter reaction times and have been achieved using amines similar to those previously used as alkali metal amides in DESs and 2-MeTHF [1.2 Amidation of esters using lithium amides under air].

These include the coupling of piperidine and morpholine to 2-chloro/bromo pyridine with the use of potassium *tert*-butoxide and palladium catalyst has been completed in just 12 min at 50°C.²⁰⁴ This approaches the reaction times possible using air sensitive reagents in air, although it may be that at 50°C the lifetime of organolithium species may already be much more severely limited than at standard temperature.

If the temperature is greatly increased by microwave heating to 150°C it has been seen possible to perform this type of Buchwald-Hartwig coupling in as little as 1 min using aniline and an aryl nonaflate instead of an aryl halide.²⁰⁵ Although the reaction time is now within an accessible range to in air reactions with organolithium reagents the high temperature used likely make the decomposition of the lithium species very fast and the working conditions dangerous to attempt to replicate the conditions used.

In conclusion this work has demonstrated that both glycerol and 2-MeTHF are suitable renewable solvents that can be used alongside deep eutectic solvent mixtures and water as a more environmentally friendly alternative to VOC based solvents in two types of addition reactions under standard bench conditions (ambient temperature and under air):

- The ultrafast, and chemoselective addition of organolithium reagents to nitriles
- The synthesis of carboxamides by addition of lithium amides to esters.

In the addition to nitriles reactions were shown to occur in heterogenous conditions “on glycerol” or “on water” with similar results across the board with a range of nitriles and aryl lithium reagents used. Although limited by a few very reactive or bulk functional groups the main key factor governing the success of these reactions was found to be the solubility of the species involved, although H-bonding may also play a role in the success of the “on solvent” regime.

In the case of amidations reactions occurred homogenously in 2-MeTHF. In 20 s, under these mild conditions fair to good yields of a wide range amide products could be obtained, including synthetically relevant molecules such as moclobemide and DEET. However, sterically bulky or acidic esters were not tolerated by this method, neither were the lithium amides of less nucleophilic amines. Sodium and potassium amides were also found to not be suitable in these additions due to reduced solubility compared to their lithium congeners and a potentially increased rate of hydrolysis.

Both in the case the addition of aryllithium reagents in glycerol and lithium amides in 2-MeTHF the lifetime of the organometallic species was examined. The stability of phenyllithium was considered on both glycerol and water where it was seen that glycerol was superior in preventing/causing hydrolysis of the active species, where it occurred in <15 s with water.

Investigating the lifetime of lithium amides it was seen that the amidation of ethyl benzoate with lithium *N*-methylanilide only yielded 19% in glycerol after only 10 s, whereas 70% was obtained in 2-MeTHF in 1 min. The amidation was still seen to proceed (at low yield, 13%) in 2-MeTHF after 10 min.

Further to the lifetime studies the solid-state structures of the 2-MeTHF aggregates of a few lithium amides used in the amidation work were obtained; these structures showing lithium anilide, lithium diphenylamide, and lithium 2,2'-bipyridylamide to be dimeric. Solution-state aggregations however were not investigated.

In addition to the investigation of aryllithium reagents and lithium amides in renewable solvents a short series of reactions investigating the use of metal salt additives and metal-salt-based type II & IV DESs to direct regioselectivity or participate in reactions by formation of organometallic species were attempted. This has been observed not to be a straightforward endeavour, with no successful reactions uncovered applying the style of in air additions used in previous work to the attempted reactions.

In the attempted *in-situ* formation of cuprates from organolithium and Grignard reagents to perform the conjugate addition of α,β -unsaturated ketones simply using a copper based eutectic mixture was found ineffective. Upon addition of a Lewis donating amine proligand to the reaction mixture it was however seen that cuprate species may be formed. The formation of new organocopper species was seen to influence reaction products but was ultimately not selective with numerous new unknown species observed. It is perhaps possible that an appropriate ligand and copper pairing could be found that selectively promote conjugate addition, but the studies completed do not make progress into uncovering the identity of appropriate compounds.

The possibility of performing transition-metal-catalysed cross-couplings in DESs was also briefly explored, with a range of organometallic species considered including organolithium, -magnesium and -zinc compounds. With the addition of a moderate loading of a palladium(0) catalyst or (sub-)stoichiometric iron no coupling products could be obtained using any of the organometallic compounds and an aryl halide coupling partner. Again, it appears likely that the addition of a Lewis donor (pro)ligand may be necessary to allow for the formation of a competent catalytic species, as the coupling of organolithium species has now been shown possible with the inclusion of a suitable phosphine ligand. It is possible that the coupling of lithium amides could also be carried out under similar conditions.

Further work for these projects involving alternative solvents could include the further examination of other nitriles or mixed carbonyl/nitrile species to determine if it is possible to perform selective double or sequential addition of aryllithium reagents. Otherwise the addition of turbo Grignard reagents to find out if the increase in reactivity can allow for addition to nitriles to occur.

Apart from widening the scope of additions possible the homocoupling of 4-methoxyphenyllithium could prove an interesting project on its own with the possibility of metal additives to the DESs or use of type I, II or IV DESs to increase the efficiency of this homocoupling

The trans-amidation of amides could also be investigated in 2-MeTHF as they have already been shown to occur (depending on relative amide nucleophilicity)¹⁶⁶ and the range of synthetically relevant molecules could be extended in either addition projects. In the case of amidations paracetamol or lignocaine are simple amides possible to synthesise by this method. Otherwise solution-based studies of the lithium amides involved in amidation reactions in either non-deuterated 2-MeTHF or deuterated THF could allow for more insight to be gleaned rather than just solid-state structures. Although as seen in the solid-state (for LiNPh_2) these aggregations are not always the same in both solvents.

Due to the almost instantaneous nature of the addition and amidation reactions, in turbulent conditions reactions may be able to be carried out in flow reactors, allowing for a simple and elegant continuous production method.

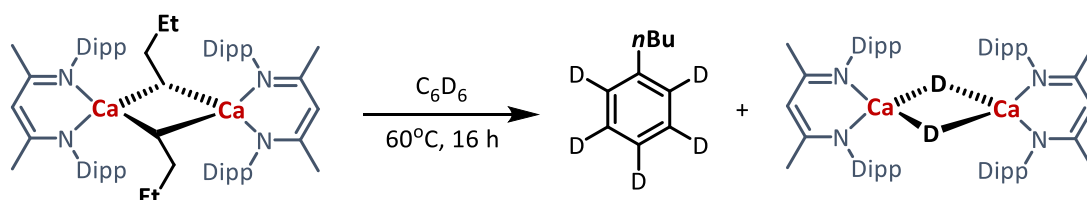
In DES directed additions exploration of the use of amine or phosphine ligands in the reactions could be carried out (stereochemical control could also possibly be achieved in this manner) or the feasibility of performing Buchwald Hartwig couplings using lithium amides could also be investigated.

Part 2 – s-Block cooperative catalysis

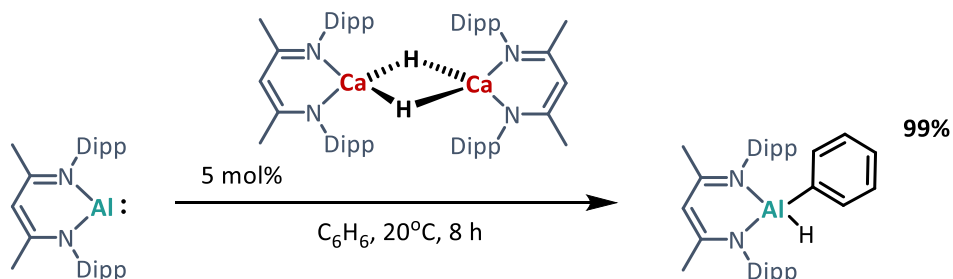
s-Block metals have long played second fiddle to their more illustrious transition metal counterparts in many areas of chemistry, especially in the field of catalysis due to their unavailable *d*-orbitals and so lack of participation in redox chemistry. However, in recent seminal work by Hill and Harder the capabilities of organo-s-block compounds are showcased in areas generally inaccessible to main group metals, for instance the power of (β -diketiminato)calcium complexes demonstrated in the mediation of nucleophilic alkylation of benzene,²⁰⁶ and by working in tandem with aluminium to reduce²⁰⁷ or catalytically C-H activate benzene²⁰⁸ [Scheme 2.1]. Additionally these (β -diketiminato)calcium complexes have been shown capable of the catalytic hydrogenation of unsaturated C-C and C-N bonds, highlighting the potential of s-block organometallic compounds in catalysis.²⁰⁹⁻²¹¹

As shown earlier in this thesis, enhanced and even new reactivities, unachievable by homometallic species, have been unlocked using bimetallic polar main group compounds, with the ability to harness cooperative effects generally across catalysis has already been established.^{212, 213} Thus, it is with this motivation that ability for bimetallic s-block compounds are here investigated in catalysis. A few currently known examples here presented.

Hill/Maron :



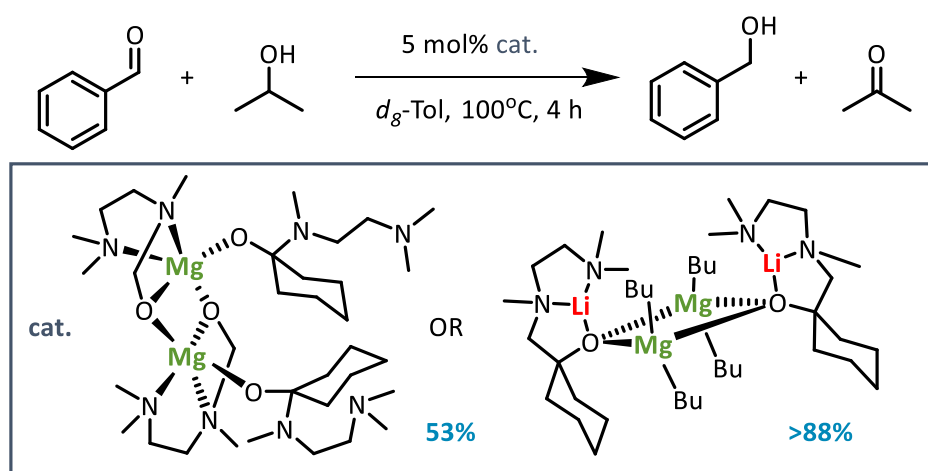
Harder :



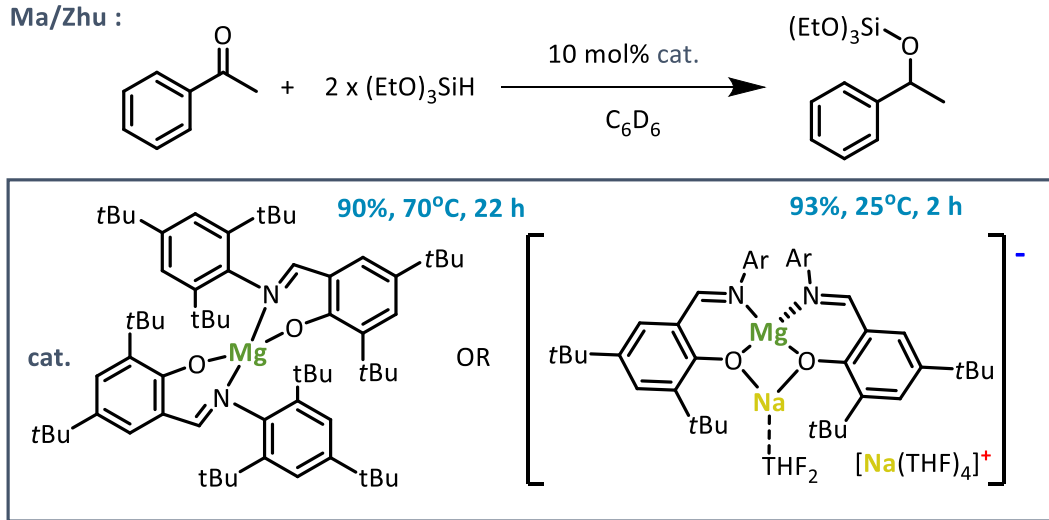
Scheme 2.1 – [top] the nucleophilic butylation of benzene mediated by an alkyl calcium- β -diketiminato. [bottom] the (β -diketiminato)calcium hydride catalysed C-H activation of benzene with low valent aluminium.

Some examples of cooperative *s*-block catalysis involve alkali metal magnesiates bearing Schiff-base ligands [Scheme 2.2], such as in an investigation of Meerwein-Ponndorf-Verley reactions by Wei.²¹⁴ This study found lithium magnesiates to display superior reactivity to a homometallic magnesium complex in the reaction of benzaldehyde and 2-propanol, achieving higher yields under the same conditions (>88% vs. 53%). Similarly Ma and Zhu²¹⁵ reported that through cooperative ability a sodium magnesiate proved a more potent catalyst than a comparable homometallic magnesium complex in the hydrosilylation of acetophenone, with the same yield of silyl ether achieved at a remarkably reduced temperature in a fraction of the time (70°C, 22 h vs. 25°C, 2 h).

Wei :



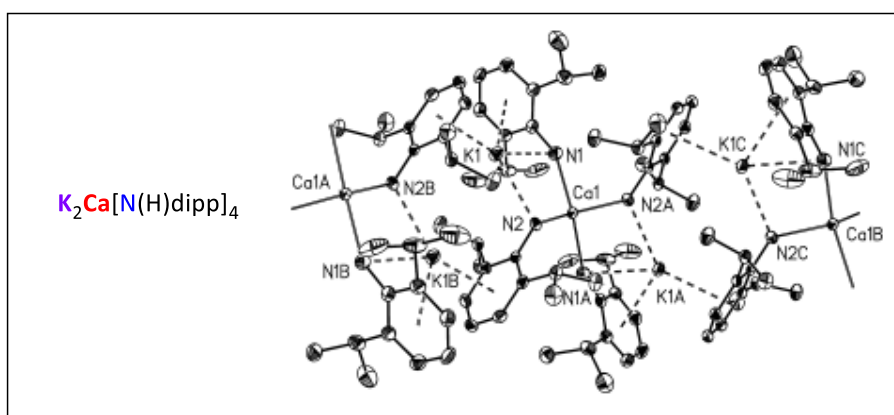
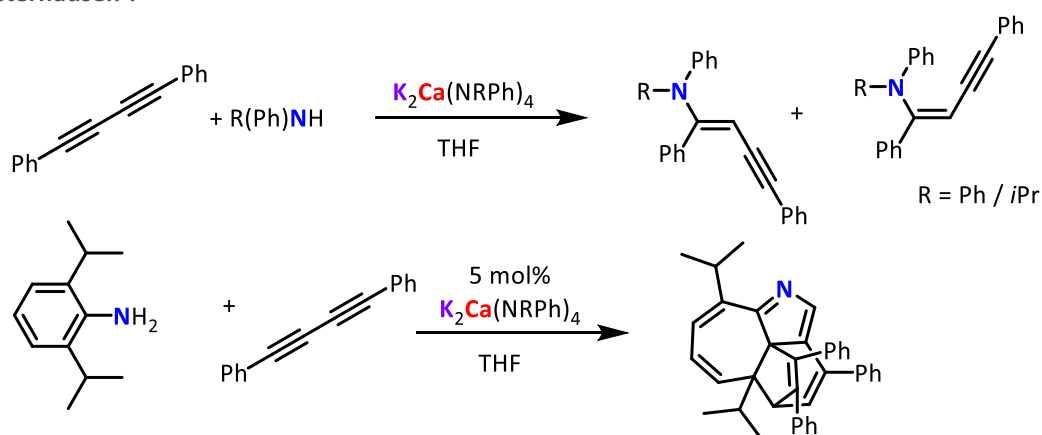
Ma/Zhu :



Scheme 2.2 – |top| the lithium magnesiate catalysed Meerwein-Ponndorf-Verley reaction of benzaldehyde and 2-propanol. | bottom| the sodium magnesiate catalysed hydrosilylation of acetophenone.

Another example of where the combination of two s-block metals were able to achieve reactivity out of reach of either metal on its own was discovered by Westerhausen. In attempting the hydroamination of diphenylbutadiene using potassium diphenylamide and calcium diphenylamide were ineffective and unable to mediate the reaction; however, the potassium calciate $K_2Ca(NPh_2)_4$ was able to do so effectively [Scheme 2.3].^{216, 217} It was observed that this disparity in reactivity was only applicable to less nucleophilic amides, as 2,6-diisopropylaniline was shown to be a suitable amine for hydroamination using either homometallic potassium or calcium amides or the potassium calciate.

Westerhausen :



Scheme 2.3 –the hydroamination of acetylenes catalysed by tetra(amido)potassium calciates.

Most pertinent to this thesis however is the catalytic work which has been previously carried out using the homoleptic alkali metal tri- and tetraorganomagnesiates bearing monosilyl groups. These magnesiates are formed by co-complexation of $AM(CH_2SiMe_3)$ ($AM = Li, Na, K$) and $Mg(CH_2SiMe_3)_2$ with the addition of a Lewis donor (TMEDA or PMDETA) necessary to for the isolation of higher-order variants. Two examples of higher-order magnesiates from this family are shown in **Figure 2.1**, both displaying a Weiss motif structure with bridging monosilyl groups. Monosilyl groups are employed in these magnesiates as they impart good solubility, and increased stability due to the lack of β -hydrogen; therefore not allowing for β -hydride elimination.²¹⁸ Additionally, upon reacting these monosilyl groups, they form volatile tetramethylsilane which will usually not participate or interfere with any subsequent steps.

These magnesiates have been mostly investigated in catalysing intermolecular hydroamination reactions. This includes: the formation of ureas,²¹⁹ the guanylation of amines,²²⁰ and the hydroamination of alkynes and olefins.²²¹

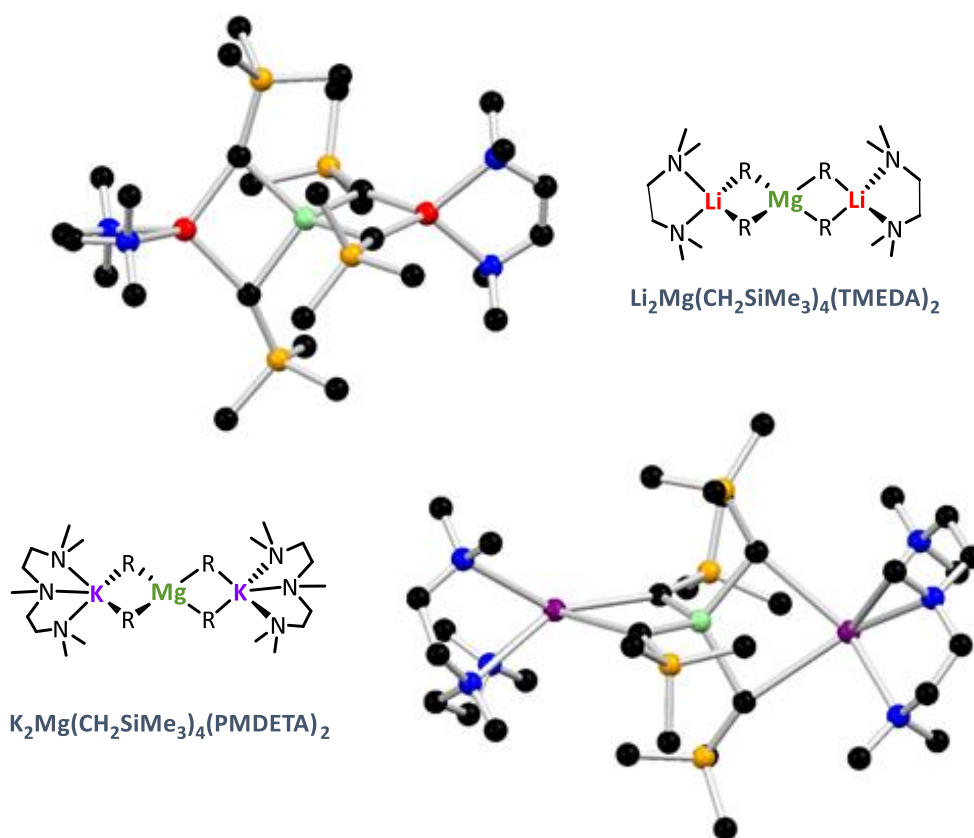
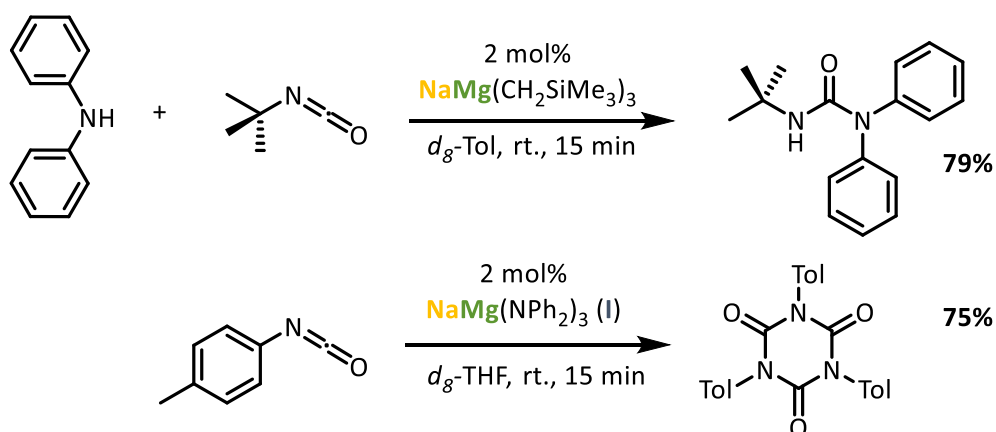


Figure 2.1 – the X-ray crystal structures of $Li_2Mg(CH_2SiMe_3)_4(TMEDA)_2$ and $K_2Mg(CH_2SiMe_3)_4(PMDETA)_2$.

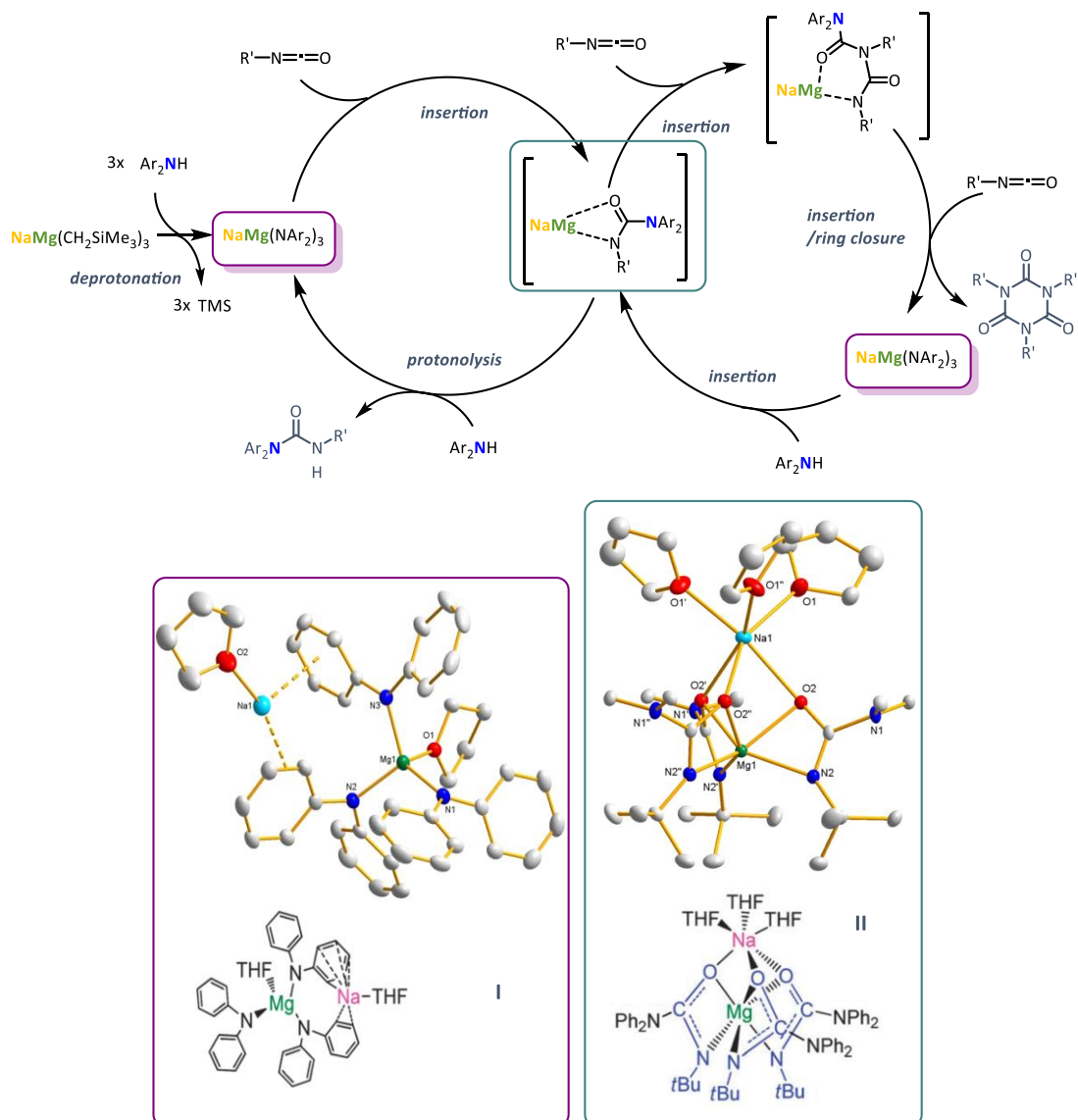
In the first of these reactions, the hydroamination of isocyanates to produce urea compounds,²¹⁹ it was found that the sodium magnesiate $\text{NaMg}(\text{CH}_2\text{SiMe}_3)_3$ was able to successfully catalyse this reaction at ambient temperature in just 15 min for a range of amines and isocyanates at a low catalyst loading of 2 mol% [Scheme 2.4]. A fast reaction time of 15 min was found sufficient for reactions involving aryl amines with alkyl isocyanates. Notably, where more electrophilic aryl isocyanates are used reactivity switches and a catalytic cyclotrimerisation producing isocyanurates occurs.

Through stoichiometric studies potential reaction intermediates were isolated, and from this a reaction pathway proposed [Scheme 2.5]. It involves two cycles, with cycle **A** in action with bulky alkyl isocyanates, and cycle **B** in action with less bulky, more electrophilic, aryl isocyanates. The first step in both cases is the formation of tris(amido)sodium magnesiate **I** by deprotonation of three equivalents of amine. Next the insertion of three equivalents of isocyanate yields tris(ureido)sodium magnesiate **II**. In the case of alkyl isocyanates, the ureido species undergoes protonolysis to release the product urea and close the catalytic cycle. In the case of aryl isocyanates two more subsequent insertions of three equivalents of isocyanate are proposed to occur, forming the isocyanurate product and reforming amido species **I**. From here reaction with three equivalents of isocyanate closes the cycle by reforming ureido species **II**.



Scheme 2.4 – |top| the sodium magnesiate mediated catalytic hydroamination of *t*-butylisocyanate, and |bottom| trimerisation of *p*-tolylisocyanate.

In this proposed mechanism the cooperative nature of the bimetallic catalyst can be seen through dual substrate activation. In ureido species **II**, sodium coordinates to the isocyanate performing Lewis acid activation, additionally in both ate complexes **I** and **II** the formally anionic nature of the magnesium imparts greater Lewis basicity than a neutral organomagnesium compound therefore enhancing nucleophilicity.

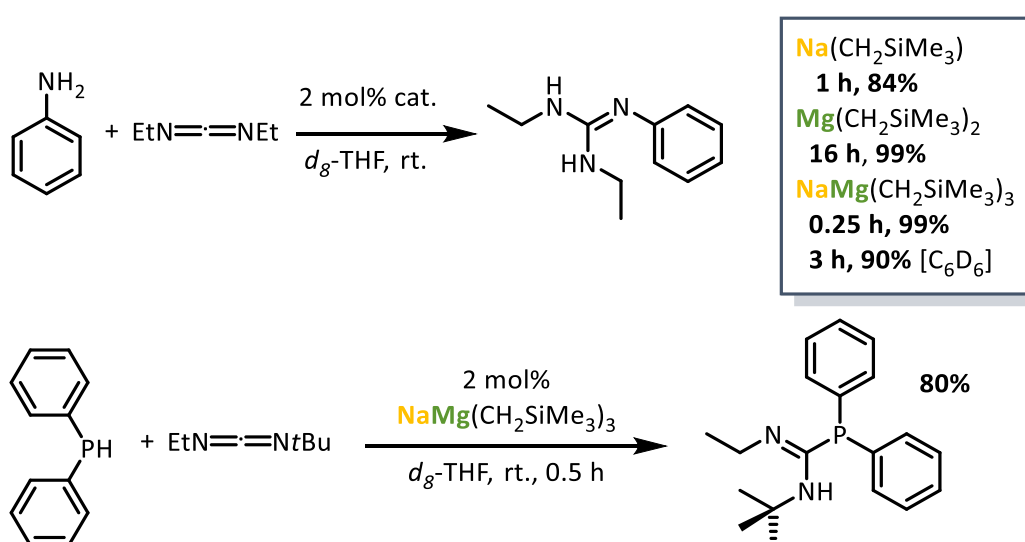


Scheme 2.5 – the proposed mechanism for the sodium magnesiate catalyzed hydroamination/cyclotrimerization of isocyanates.

A second example of catalysis mediated by the same family alkali metal magnesiates comes in the form of the guanylation of amines.²²² It was seen that the guanylation of a range of primary and secondary, aromatic and alkyl amines was possible with alkyl carbodiimides under mild conditions using a low catalyst loading of 2 mol% [Scheme 2.6]. When compared to its homometallic counterparts tris[(trimethylsilyl)methyl]sodium magnesiate (99%, 0.25 h) displayed enhanced reactivity; with moderate improvement in reaction times over (trimethylsilyl)methylsodium (84%, 1 h) and a marked improvement over bis[(trimethylsilyl)methyl]magnesium (99%, 16 h).

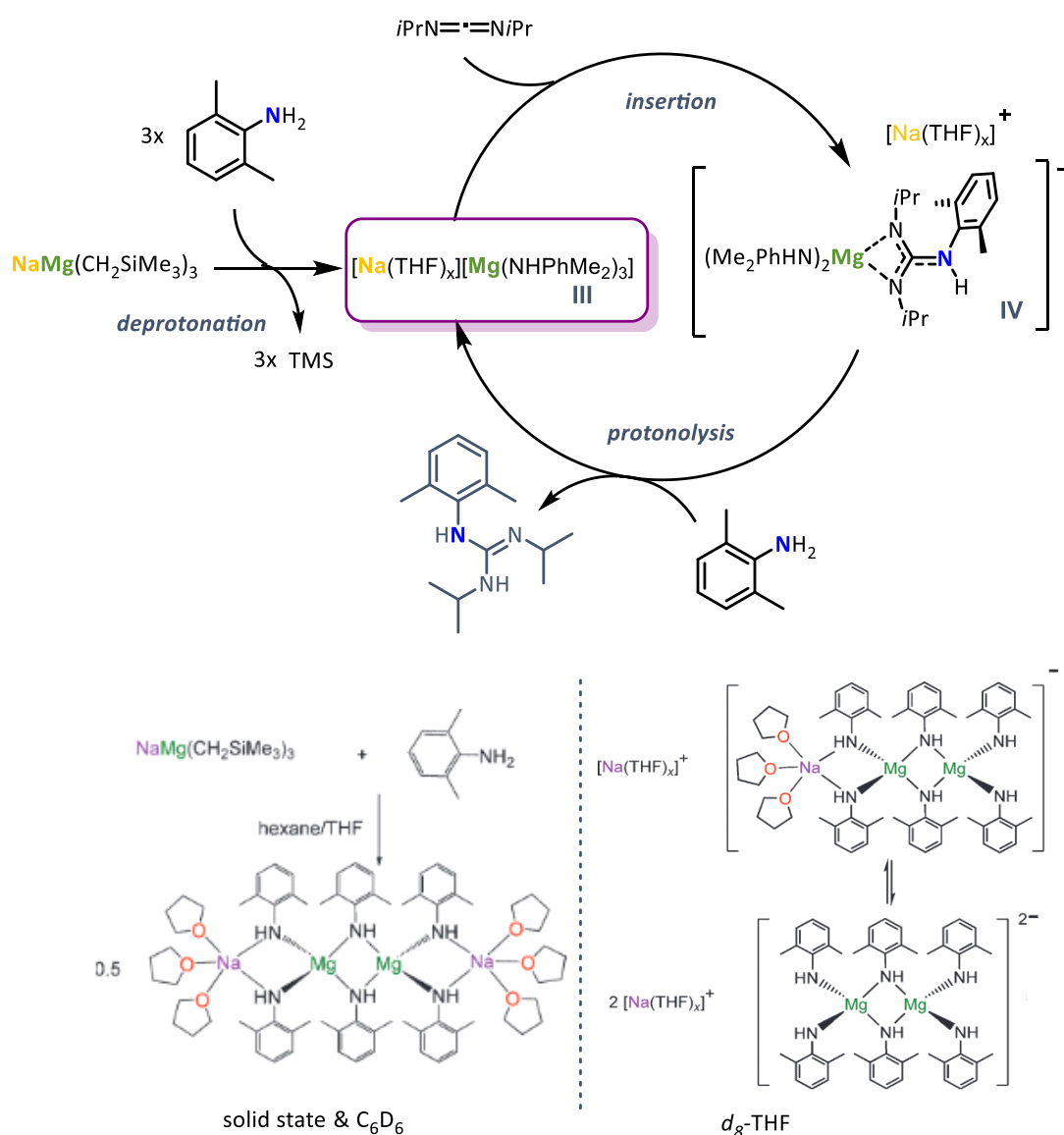
Reaction scope was also extended to include the first example of the hydrophosphination of a carbodiimide catalysed by a magnesium complex [Scheme 2.6].

Potential reaction intermediates were able to be isolated which, in conjunction with kinetic studies, allowed for the proposition of a mechanism [Scheme 2.7]. Kinetic investigations found a first order dependence in amine, carbodiimide and catalyst. This means that the rate of reaction is linearly dependent on the concentration of each of these species, and can additionally be interpreted that an equivalent of each is involved in the rate determining step. The proposed mechanism involves the formation of tris(amido)sodium magnesiate **III** by deprotonation of three equivalents of amine. Next the insertion of an equivalent of carbodiimide yields a heteroleptic (amido)(guanidinato)sodium magnesiate **IV**. From here protonolysis releases the product guanidine and closes the cycle, reforming amide species **III**.



Scheme 2.6 – |top| the sodium magnesiate mediates catalytic guanylation of aniline, and |bottom| hydrophosphination of N-ethyl-N'-t-butylcarbodiimide.

A key difference in this case compared to the hydroamination of isocyanates is the nature of the amido **III** and guanidinate **IV** species. Characterisation of the solid-state structure of tris(2,6-dimethylanilino)sodium magnesiate **III** demonstrated the complex to exist as a dimeric contacted ion-pair, this same aggregate was observed in benzene solution by ^1H DOSY NMR spectroscopy [Scheme 2.7]. However, in the preferred reaction solvent, THF, a mixture of two dimeric solvent separated ion pair were instead observed. This change from CIP to SSIP in the more Lewis donating solvent is perhaps also reflected in the accelerated rate of reaction in THF (0.25 h) vs. benzene (3 h), hinting that the rate determining step may be more facile where a SSIP is present rather than a CIP (*vide infra*).



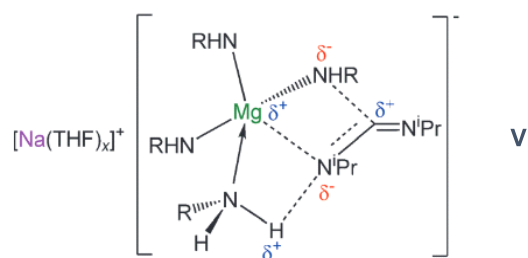
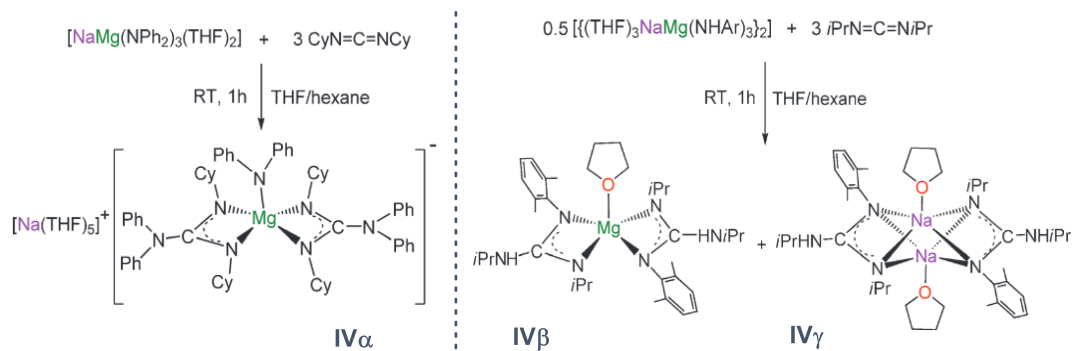
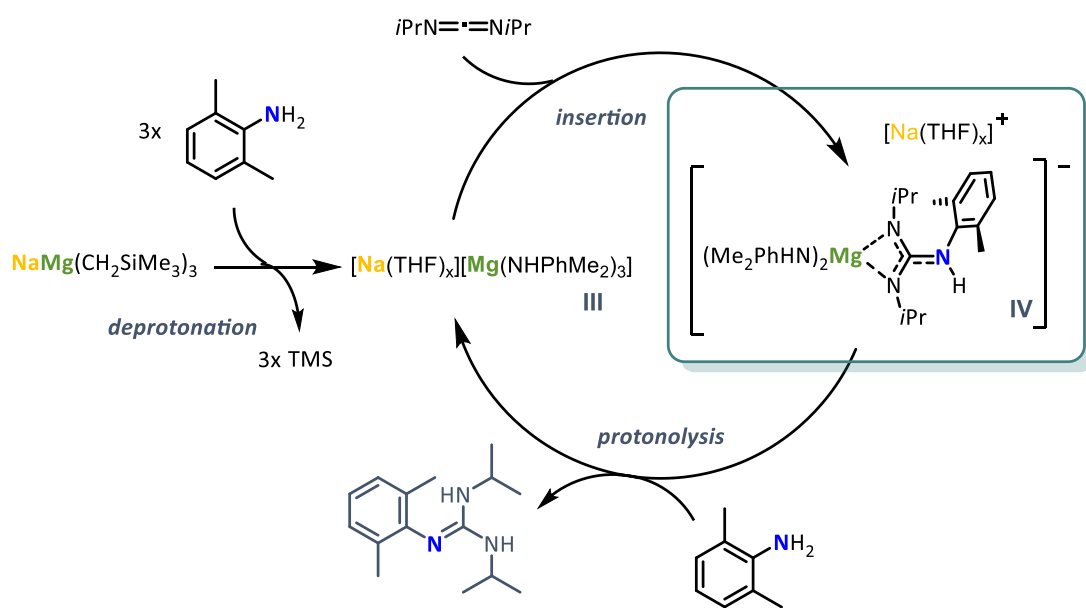
Scheme 2.7 - the proposed mechanism for the sodium magnesiate catalyzed guanylation of amines, focussing on intermediate bis(amido)sodium magnesiate **III**.

An examination of the (guanidinato)sodium magnesiate **IV** by stoichiometric studies gave mixed results |**Scheme 2.8**| with theSSIP (monoamido)(bisguanidinato)sodium magnesiate **IV α** obtained with diphenylamine and *N,N'*-dicyclohexylcarbodiimide, but a neutral sodium guanidinate **IV γ** and neutral magnesium guanidinate **IV β** formed via disproportionation with 2,6-dimethylaniline and *N,N'*-diisopropylcarbodiimide. When tested the homometallic guanidinates |**IV γ** , **IV γ** | were found to be much poorer catalysts than the tris(alkyl)- or tris(amido)sodium magnesiate, even when used as a mixture. However, the heteroleptic sodium magnesiate **IV α** performed as well as the initial tris(alkyl)sodium magnesiate. This discrepancy highlights the necessity for the enhanced nucleophilicity of the anionic moiety rather than neutral magnesium centre species, and also the possible misguidance of comparing stoichiometric and catalytic conditions.

Due to the solvent separated nature of the complexes obtained by stoichiometric studies, the role of the sodium, beyond allowing for the formation of the anionic magnesium centre, was investigated. Addition of 15-crown-5 to sequester the sodium, or substituting the sodium magnesiate for its lithium congener were found to have very little effect on the rate of reaction, suggesting that in this system the anionic magnesium centre is required to promote catalysis but not the additional Lewis acid activation from the alkali metal as is observed in other cases.

In a bid to gain insight into the rate determining step, kinetic isotope studies were performed, with a primary kinetic isotope effect being found indicative of a N-H bond breaking in the limiting step. This suggested the rate determining step to be either the formation of the amido species **III**, or the protonolysis step. Due to the generally facile nature of the deprotonation of an amine with these organometallic species and the first order dependence observed for amine, carbodiimide, and catalyst, the postulated turn over step is the protonolysis of the guanidinate species **V** |**Scheme 2.8**|.

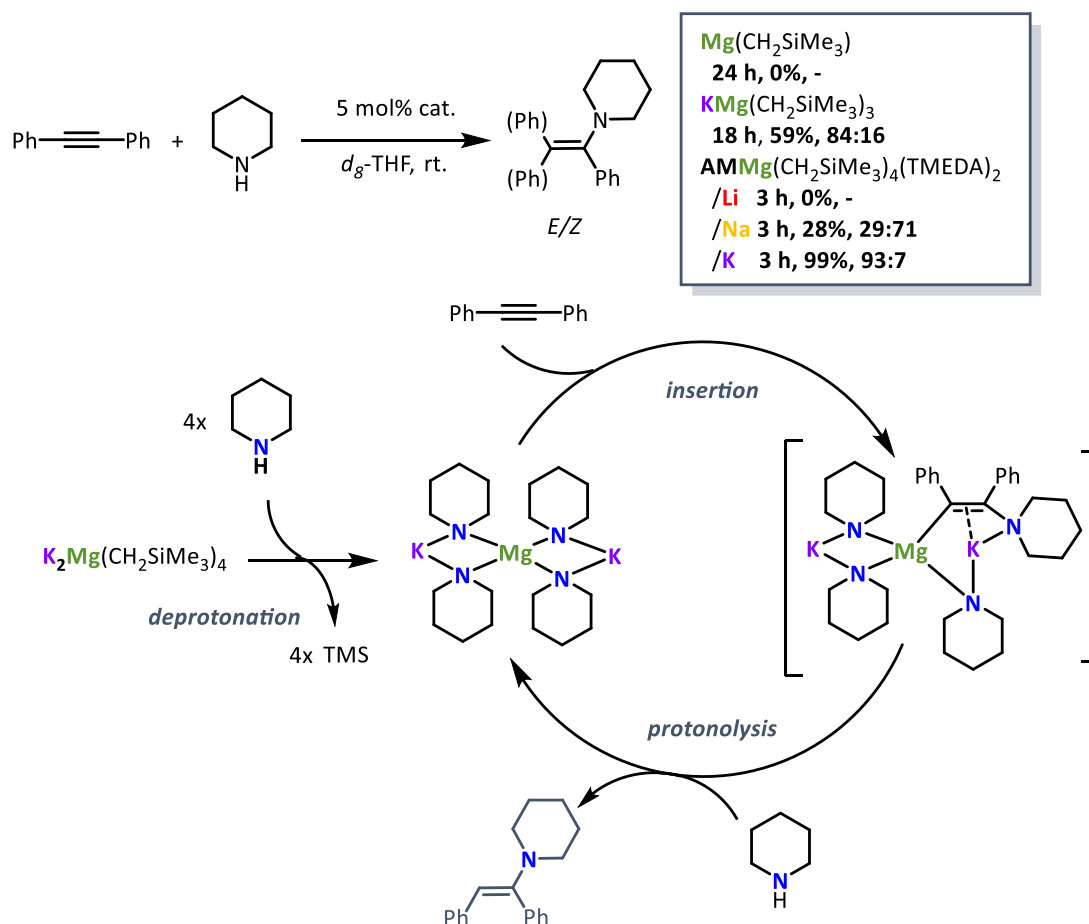
Complex **IV** is depicted here as bearing one amide and two guanidinate ligands due to the stoichiometric evidence pointing towards incomplete insertion of carbodiimide into the amide ligands of **III**, and an experimentally observed inability to force this third carbodiimide insertion into complex **III**. Additional evidence from the kinetic studies suggesting that only one guanidinate ligand undergoes protonolysis corroborates protonolysis potentially being the rate limiting step.



Scheme 2.8 - the proposed mechanism for the sodium magnesiate catalyzed guanylation of amines, focussing on intermediate sodium magnesiate **IV**.

A final application of this family of homoleptic (monosilyl)alkali metal magnesiates is the hydroamination of C-C unsaturated bonds in alkenes and alkynes.²²¹ In this study it was shown that a homometallic magnesium compound was unable to mediate catalysis where alkali metal magnesiates were. Various magnesiates were compared [Scheme 2.9], observing an increased rate of reaction with higher-order magnesiates, with $\text{KMg}(\text{CH}_2\text{SiMe}_3)_3$ (18 h, 59%) performing more poorly than its higher-order analogue $\text{K}_2\text{Mg}(\text{CH}_2\text{SiMe}_3)_4(\text{PMDETA})_2$ (3 h, 99%) in promoting the reaction of diphenylacetylene and piperidine. Additionally, an alkali metal effect was observed with $\text{K} > \text{Na} \gg \text{Li}$, fitting with the observation in heavier main group metals and lanthanides that larger, more polarisable metals are more apt for this catalysis.²²¹

As in the other hydroamination studies a bimetallic amide species was able to be isolated as part of stoichiometric studies of potential reaction intermediates, and from this a catalytic cycle was proposed.



Scheme 2.9 - the potassium magnesiate mediated catalytic hydroamination of diphenylacetylene and proposed catalytic cycle.

2.1 Hydroalkoxylation/cyclisation of alkynols

Hydroalkoxylation is defined as the addition of an O-H bond across a C-C unsaturated multiple bond.²²³ It is a 100% atom efficient process,²²⁴ and therefore intramolecular hydroalkoxylation (cyclisation) of alkynyl alcohols is a highly desirable route to provide straightforward access to a series of synthetically significant *O*-heterocycles such as hydrofurans, pyrans, benzofurans, *etc.* which are fundamentally important to many natural products²²⁵ and pharmaceutical²²⁶ compounds [Figure 2.2]. However the large bond enthalpy of typical O-H bonds and the modest reactivity of electron-rich olefins with nucleophiles can make these transformations especially challenging.²²⁷ Thus, intramolecular hydroalkoxylation appears a suitable step up from intermolecular hydroamination to explore the limits of cooperative alkali metal magnesiate mediated catalysis.

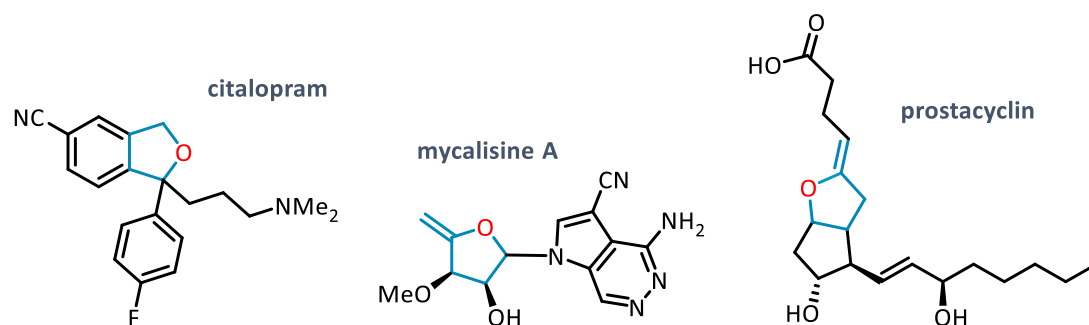
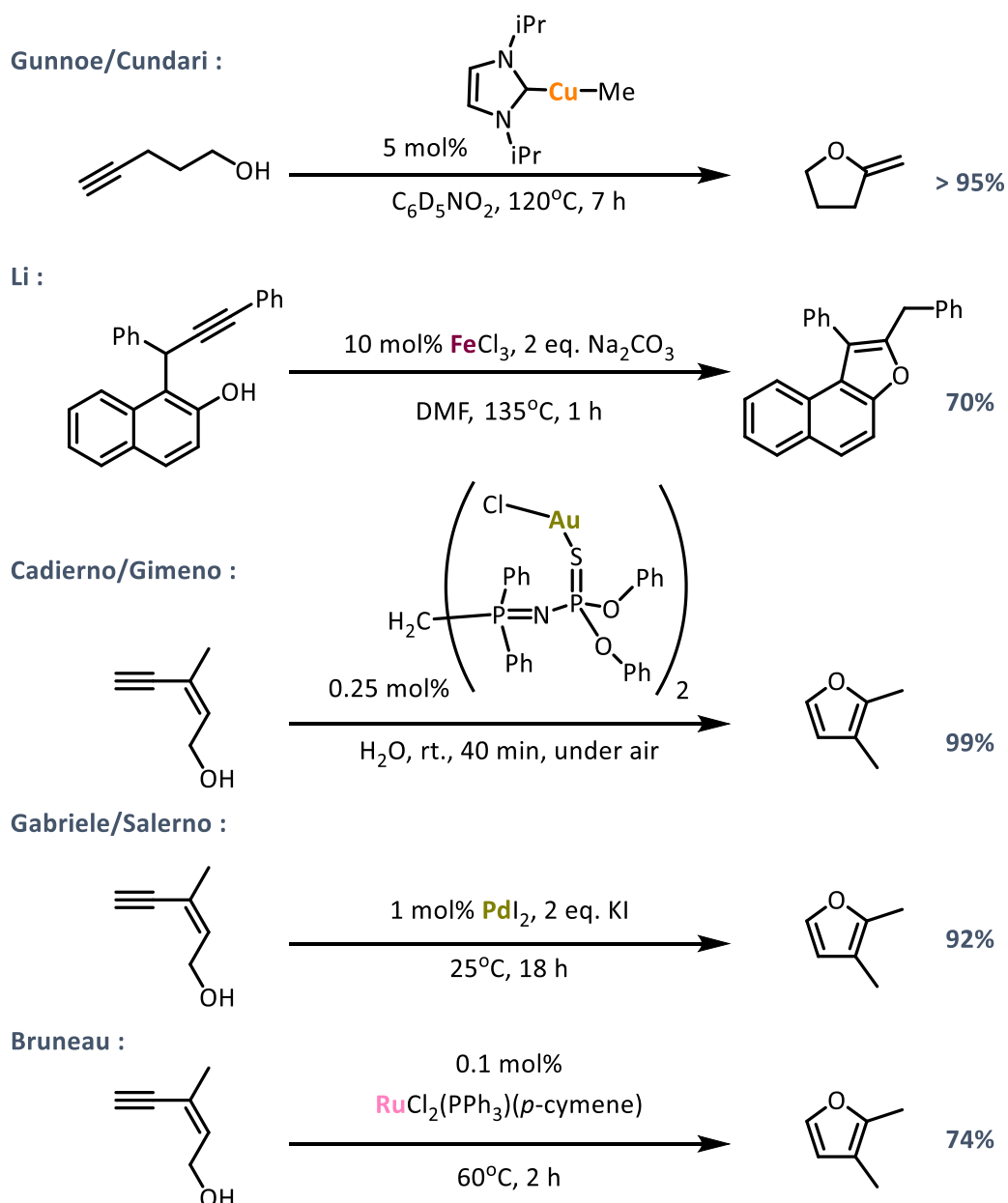


Figure 2.2 – Cyclic enol ether containing natural products: [left] citalopram, a popular antidepressant,^{228, 229} [centre] mycalisines, nucleosides which have been found to inhibit cell division in star fish,^{230, 231} [right] prostacyclin (epoprostenol) which can be used to prevent blood clotting during kidney dialysis.^{232, 233}

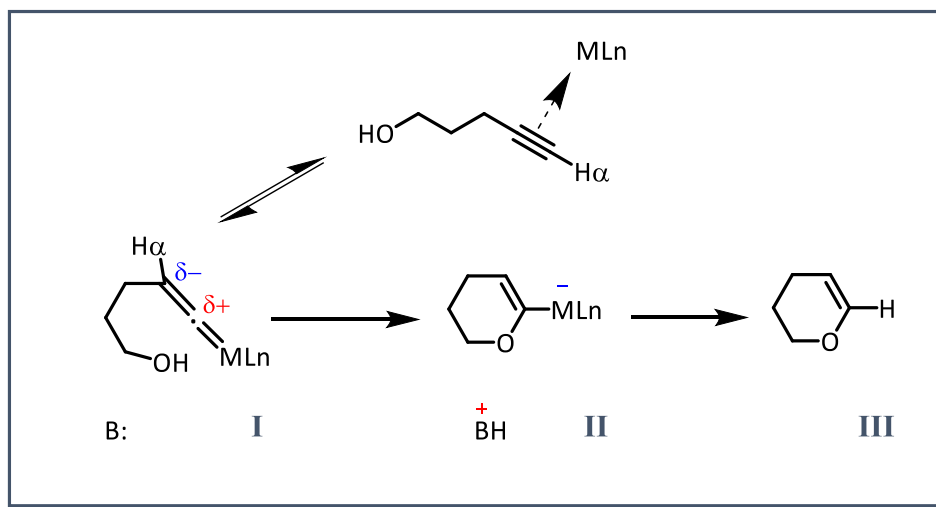
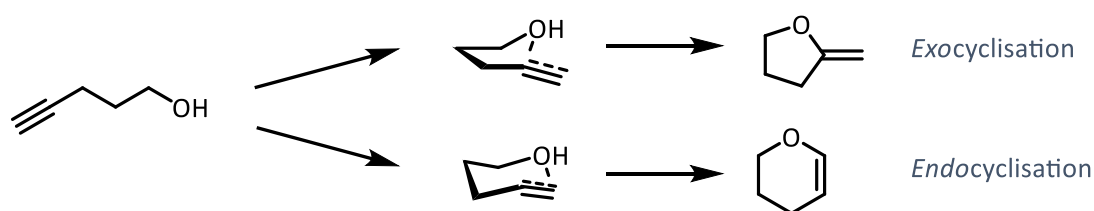
A catalogue of catalysts has been developed for the cyclisation of alkynols. Starting from initial catalytically selective work by Villemin²³⁴ using mercury oxide and boron trifluoride etherate the number of catalytic systems has greatly expanded; growing to include various transition metal complexes, as well as alkaline earth- and *f*-block metal compounds. Of these transition metals previously used to promote the transformation are mostly precious metals including ruthenium,²³⁵⁻²³⁷ palladium,²³⁸⁻²⁴² and gold²⁴³⁻²⁴⁸ amongst others,^{169, 249-254} but a few others such as copper,²⁵⁵ iron,²⁵⁶ and tungsten^{257, 258} have also been investigated [Scheme 2.2].



Scheme 2.10 – Transition metal mediated exocyclisation of alkynols.^{235, 238, 239, 259, 260}

Different metal complexes have been seen to offer different product selectivities, as there are two distinct cyclisation routes for hydroalkoxylation of alkynols as illustrated for 4-pentynol [**Scheme 2.11**], where the isomers can be denoted as 5-*exo*-dig and 6-*endo*-dig, according to Baldwin's rules,²⁶¹ and so will be referred to *exo*- and *endocyclisation* products.

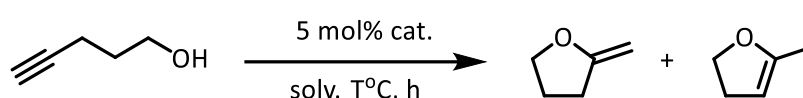
For instance, tungsten, ruthenium and molybdenum complexes have been used to produce *endocyclised* enol ether products. This occurs due to the proposed formation of a η^2 -vinylidene metal complex intermediate [**I**, **Scheme 2.11**], which is then susceptible to nucleophilic addition to generate a Fischer oxacarbene [**II**, **Scheme 2.11**] that ultimately yields the endocyclised product [**III**, **Scheme 2.11**].²⁶²⁻²⁶⁵ However more commonly, where no electronically-biased intermediate is formed, exocyclisation occurs due to the more favourable approach of the nucleophile with respect to the π -system.^{266, 267}



Scheme 2.11 –Conversion of 4-pentynol to respective five-membered *exo*-, and six-membered *endocyclised* products. The latter conversion proceeds via vinylidene [**I**] and Fischer oxacarbene [**II**] intermediates.

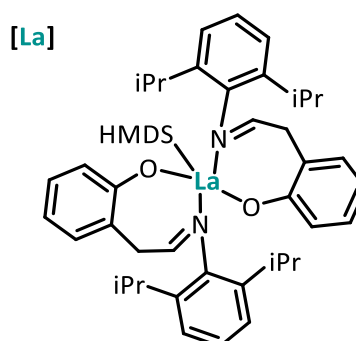
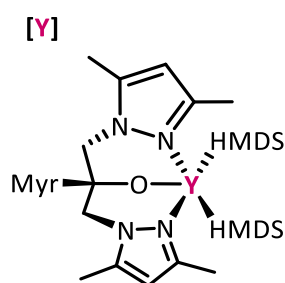
Besides the numerous examples of transition metal catalysts, the use of *f*- and *s*-block catalysts for this reaction has been recently investigated. Thus, Marks has utilised lanthanide amide catalysts, such as LaHMDS²⁶⁸ and Cp*₂Th(CH₂SiMe₃),²²³ while Otero and Lara-Sánchez have employed heteroscorpionate yttrium and lutetium catalysts.²⁶⁹ Alternatively, heavier alkaline earth metal complexes have also shown great promise as demonstrated by Hill using calcium, strontium and barium amides as catalysts,²⁷⁰ as illustrated in **Table 2.1**. Exocyclisation was seen to occur in all non-transition metal examples, although using alkaline earth metal amides two different product isomers were observed, an internal and external alkene.

Table 2.1 – Hydroalkoxylation 4-pentynol | **201** | catalysed by *f*- and *s*-block catalysts.²⁷⁰⁻²⁷³



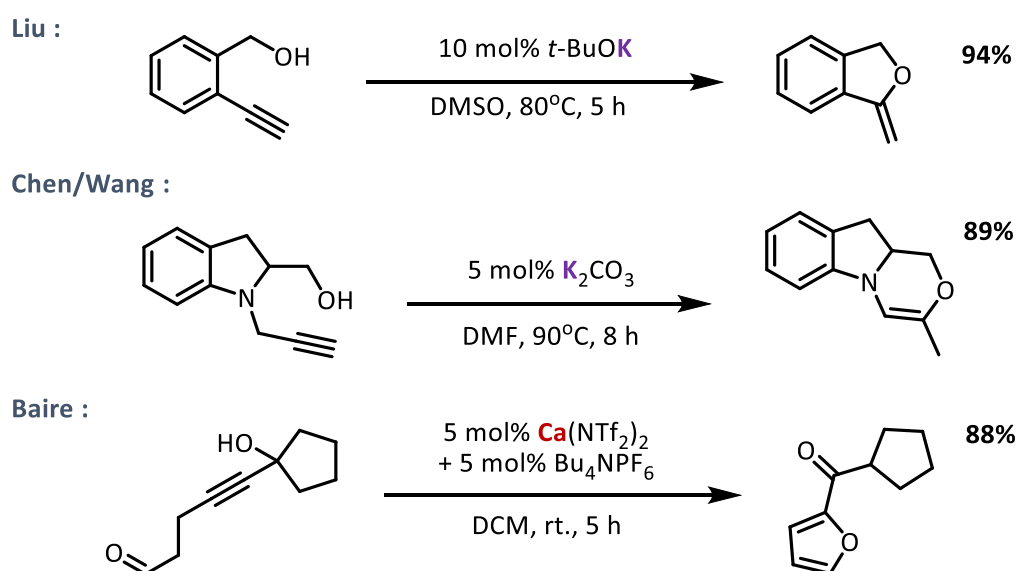
Entry	Catalyst	Conditions	Time (h)	Yield (%) & Isomer ratio
1	La(HMDS) ₃	C ₆ D ₆ , 70°C	≈ 2.5	≥ 95% (100 : 0)
2	[Y]	<i>d</i> ₈ -Tol, 90°C	3	96% (100 : 0)
3	[La] [*]	C ₆ D ₆ , 75°C	12	78% (100 : 0)
4	Ca(HMDS) ₂	C ₆ D ₆ , 90°C	4.5	≥ 95% (98 : 2)
5	Sr(HMDS) ₂	C ₆ D ₆ , 90°C	2.5	≥ 95% (90 : 10)
6	Ba(HMDS) ₂	C ₆ D ₆ , 90°C	6	≥ 95% (97 : 3)

^{*} 6 mol% cat.



Since Hill's initial study in 2012, new studies focusing on alkali metal and alkaline earth catalysts have been reported [Scheme 2.12]. Liu has shown that potassium *tert*-butoxide is an effective and selective catalyst for cyclisation of aromatic alkynyl amines and alkynols,²⁷⁴ albeit with the need of elevated temperatures and highly polar solvents. Utilising similar reaction conditions, Wang employed potassium carbonate to prepare indole/pyrrole-fused 1,4-oxazines.²⁷⁵ Baire has also recently reported that cycloisomerisation of *cis*-6-hydroxy- and *cis*-6-acyloxyhex-2-en-4-ynals to 2-acylfurans and 2-(1-acyloxyalkenyl)furans is achievable using calcium catalysis.²⁷⁶ In contrast magnesium-based reagents have not followed suite by showing very little promise to catalyse these type of transformations; whereas the catalytic properties of *s*-block bimetallic complexes remains unexplored in this context.

Expanding the scope of *s*-block cooperative catalysis, here the first catalytic applications of alkali metal magnesiates to promote cyclisation reactions are reported, focussing on intramolecular hydroalkoxylation of alkynols. Profiting from the enhanced metallating and nucleophilic abilities of these synergistic systems, playing a dual role in overcoming the main challenges encountered in these transformations, facilitating not only OH activation, but also the required addition across C≡C bonds. Combining kinetic experiments with reactivity studies, to provide informative mechanistic insights on how cooperative effects can be maximised as well as on the key role that each metal plays in these novel ate-catalysed transformations.



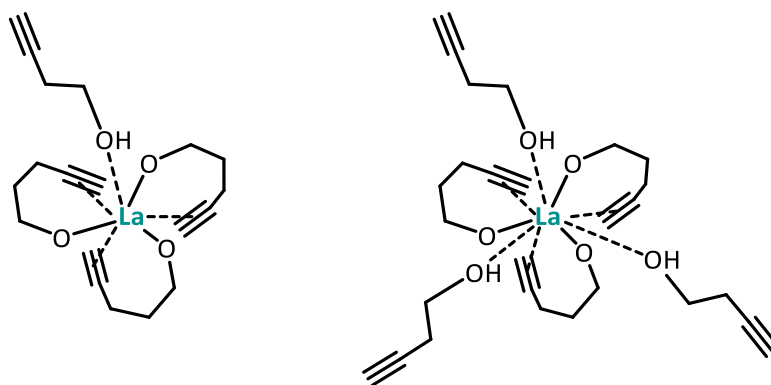
Scheme 2.12 – Cyclisation of alkynyl alcohols and aldehydes by *s*-block metal catalysts. ²⁷⁴⁻²⁷⁶

2.1.1 Assessing Alkali metal and Stoichiometric effects

In the same line as previous *s*-block and *f*-block catalysis 4-pentynol |**201**| was selected as the benchmark reagent for the optimisation of hydroalkoxylation reactions. Led by the curious absence of magnesium from the alkaline earth amides employed by Hill,²⁷⁰ $\text{Mg}(\text{CH}_2\text{SiMe}_3)_2$ was chosen as a starting point. When heated at 75°C for 36 h no reaction was observed |**Table 2.2, Entry 1**|, confirming the suspected reason for its absence from the aforementioned work. It does however raise the question of why should it not be able to mediate the cyclisation where, only one period below, calcium can.

It appears likely that the difference is predominantly due to difference in ionic radii and π -philicity.²⁷⁷ When we look at DFT studies by Marks²⁷⁸ on the active species in catalytic work using $\text{La}(\text{HMDS})_3$ we see it is likely tetra-coordinated; with three alkynoxide ligands binding via their O atom and also forming a close-range π -interaction with the alkyne unit to achieve coordinative saturation. Importantly this π -interaction activates the alkyne for insertion into the La-O bond whilst holding it in position to easily cyclise. The lowest energy ‘resting’ state for the lanthanum catalyst was also calculated as a similar but more coordinatively saturated species.

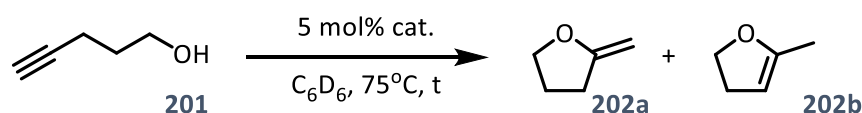
The ability to form such good π -interactions is notably what gives gold its ability to perform the cyclisation without activation of the alcohol by forming metal oxygen bonds, allowing it to cyclise even alkynyl aldehydes and acids.¹⁶⁹ With this in mind it is potentially due to magnesium not being sufficiently large, nor π -philic, to accommodate this ‘dual activation’ of the alkynol by simultaneously being bonded to both the oxide anion and hold the π -density of the alkyne in close proximity.



Scheme 2.13 – DFT predicted |left| ‘catalytically active’ and |right| ‘resting state’ species involved in the lanthanum amide mediated cyclisation catalysis of 4-pentynol.²⁷⁸

With the cyclisation of 4-pentynol a potential candidate for effective cooperative catalysis due to this lack of activity observed with $\text{Mg}(\text{CH}_2\text{SiMe}_3)_2$, it was then necessary to evaluate the catalytic capabilities of the other half of the partnership, the alkali metals. With the idea of size and π -philicity in mind $\text{K}(\text{CH}_2\text{SiMe}_3)$ was chosen as a suitable candidate. Promisingly, this proved capable of promoting exocyclisation, although poorly only achieving an 11% yield in 36 h |Table 2.2, Entry 2| allowing a lot of room for potential improvement through cooperativity. It was envisaged that by employing a bimetallic catalyst the task of ‘dual activation’ could be split: with the formation of a magnesium alkoxide, and the alkali metal providing the necessary π -interactions with the carbon-carbon triple bond, therefore together cooperatively activating the molecule for cyclisation.

Table 2.2 – Pre-catalyst selection for the cyclisation of 4-pentynol |201|.

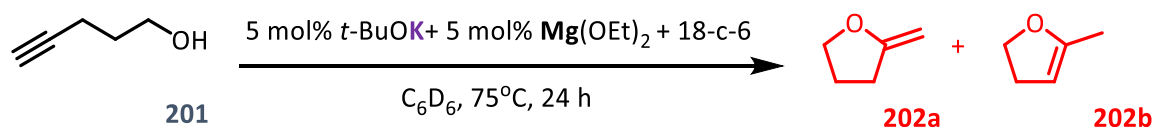


Entry	Pre-catalyst R = CH_2SiMe_3	Time (h)	Yield (%) ^c	Isomer ratio 202a : 202b
1	MgR_2 ^a	36	0	-
2	KR ^a	36	11	99 : 1
3	LiMgR_3 ^a	36	3	- ^d
4	NaMgR_3 ^a	36	12	97 : 3
5	KMgR_3 ^a	36	16	99 : 1
6	$\text{Li}_2\text{MgR}_4(\text{TMEDA})_2$ ^b	36	3	- ^d
7	$\text{Na}_2\text{MgR}_4(\text{TMEDA})_2$ ^b	36	83	91 : 9
8	$\text{K}_2\text{MgR}_4(\text{PMDETA})_2$ ^b	22	91	86 : 14

|a| Reactions were performed in a Young's cap NMR tube, using 0.5 mmol of substrate (4-pentynol) |201| and 0.025 mmol (5 mol%) pre-catalyst. |b| Reactions were performed in a Young's cap NMR tube, using 0.6 mmol (1.2 eq.) of substrate (4-pentynol) |201| and 0.025 (5 mol%) pre-catalyst. This additional 0.1 mmol (20 mol% / 0.2 eq.) of 201 was employed to convert the pre-catalyst to 'active catalyst' (vide infra). |c| Calculated from ^1H NMR spectroscopic data by integration against an internal standard (0.05mmol / 10 mol% 1,2,3,4-tetraphenylnaphthalene). |d| Due to low yields obtained and the inherent error within the measurement, an isomer ratio is not reported

With the catalytic ability of both group 1 and 2 monometallic compounds evaluated, and the opportunity for a heterobimetallic catalyst identified, the search began by looking at triorganomagnesiates. Initial findings were disappointing with negligible improvement in yield in moving from $\text{K}(\text{CH}_2\text{SiMe}_3)$ to $\text{KMg}(\text{CH}_2\text{SiMe}_3)_3$ |16%, Table 2.2, Entry 5|, and as suspected upon interrogation of the lighter group 1 metals they were found less capable, with $\text{NaMg}(\text{CH}_2\text{SiMe}_3)_3$ producing an only slightly reduced yield to potassium |12%, Table 2.2, Entry 4| but $\text{LiMg}(\text{CH}_2\text{SiMe}_3)_3$ proving almost entirely ineffective |3%, Table 2.2, Entry 3|. In the hope of seeing major improvements, tetraorganomagnesiates were tested, where the formally dianionic magnesiates were expected to be more powerful nucleophiles and more potent catalysts. In the case of $\text{Li}_2\text{Mg}(\text{CH}_2\text{SiMe}_3)_4(\text{TMEDA})_2$ |3%, Table 2.2, Entry 6| no discernible improvement was seen, and so it appears lithium is not able to suitably activate the alkyne despite previously having been shown to engage in meaningful π -interactions. However, finally the cyclisation was successfully catalysed by the sodium (83%) and potassium higher-order magnesiates (91%), nearing completion in 36 and 22 h respectively. At this point it is non-trivial to address the selectivity of the reaction. A good isomer selectivity of >85% external alkene isomer |2-methylenetetrahydrofuran, 202a| was yielded in both cases. Notably both products observed were exocyclic, in line with what has been previously seen with non-transition metals.

Although established that the combination of potassium and magnesium allows for more efficient catalysis through cooperativity, the necessity of synthesising such reactive, pyrophoric, compounds (such as the alkali metal magnesiates investigated in this work) should be addressed. To illustrate the benefits of using $\text{K}_2\text{Mg}(\text{CH}_2\text{SiMe}_3)_4(\text{PMDETA})_2$ the experiment was run under the same conditions but using air stable alkoxides of both metals |Scheme 2.14|. No product was observed after 24 h, presumably due to lack of solubility of the alkoxides and the unlikelihood that a bimetallic compound was formed in this way. This lack of reactivity nicely displays the benefit of these particular alkali metal magnesiates, in that although it has previously been proven possible to promote the cyclisation of alkynols using a simple base²⁷⁴ the conditions, in terms of solvent and temperature, are much more limited.

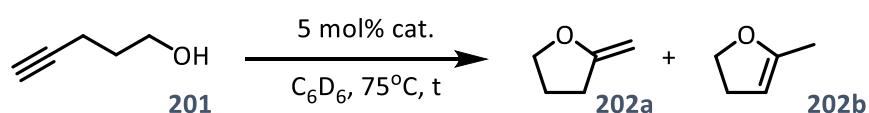


Scheme 2.14 – The failed hydroalkoxylation of 4-pentynol |201| by potassium and magnesium alkoxides.

2.1.2 Assessing the role of Lewis donors as co-catalysts

Upon establishing higher-order magnesiates as best placed to perform as catalysts, the question remained if cooperative catalysis was truly occurring. We next focussed our attention on assessing the importance of the coordination of Lewis donors in order to facilitate (or hinder) the hydroalkoxylation reactions.

Table 2.3 – The role of crown ethers in the cyclisation of 4-pentynol |201| mediated by alkali metal magnesiates.



Entry	Pre-catalyst R = CH ₂ SiMe ₃	Time (h)	Yield (%) ^c	Isomer ratio 202a : 202b
1	MgR ₂ + 18-c-6 ^a	36	0	-
2	KR + 18-c-6 ^a	16	70	99 : 1
3	KMgR ₃ + 18-c-6 ^a	10	77	81 : 19
4	Li ₂ MgR ₄ (TMEDA) ₂ + 4 x 12-c-4 ^{b e}	36	4	- ^d
5	Na ₂ MgR ₄ (TMEDA) ₂ + 2 x 15-c-5 ^{b e}	5	88	95 : 5
6	K ₂ MgR ₄ (PMDETA) ₂ + 2 x 18-c-6 ^{b e}	3	94	90 : 10

|a| Reactions were performed in a Young's cap NMR tube, using 0.5 mmol of substrate (4-pentynol) |201| and 0.025 mmol (5 mol%) pre-catalyst. |b| Reactions were performed in a Young's cap NMR tube, using 0.6 mmol (1.2 eq.) of substrate (4-pentynol) |201| and 0.025 (5 mol%) pre-catalyst. This additional 0.1 mmol (20 mol% / 0.2 eq.) of 201 was employed to convert the pre-catalyst to 'active catalyst' (vide infra). |c| Calculated from ¹H NMR spectroscopic data by integration against an internal standard (0.05mmol / 10 mol% 1,2,3,4-tetraphenylanthracene). |d| Due to low yields obtained and the inherent error within the measurement, an isomer ratio is not reported. |e| A stoichiometric quantity of crown ether co-catalyst used according to the alkali metal [i.e., 2 x 18-c-6 = 10 mol% for 5 mol% K₂MgR₄(PMDETA)₂]

Initially a catalytic amount of crown ether was added as co-catalyst, with the presumable effect of sequestering the alkali metal, leaving the remaining $\text{Mg}(\text{OR})_3^-$ or $\text{Mg}(\text{OR})_4^{2-}$ (now solvent separated). This could have the possible effect of rendering the magnesiate unable to perform the catalysis, in so demonstrating the necessity of both metals to work cooperatively to successfully carry out the catalysis. To great surprise no hindering of the reaction occurred, contrary to expectation a dramatic increase in reactivity was observed.

Addition of a catalytic quantity (stoichiometric to catalyst) of 15-crown-5 or 18-crown-6 to the sodium and potassium systems respectively greatly increased their reactivity with reaction completion occurring around 5 h (vs. 36 h without 15-c-5) for $\text{Na}_2\text{MgR}_4(\text{TMEDA})_2$ | **88%, Table 2.3, Entry 5** | and around 3 h (vs. 22 h without 18-c-6) for $\text{K}_2\text{MgR}_4(\text{PMDETA})_2$ | **94%, Table 2.3, Entry 6** |. This trend of increasing reactivity was also seen with homometallic $\text{K}(\text{CH}_2\text{SiMe}_3)$ | **70%, Table 2.3, Entry 2** |. and lower-order $\text{KMg}(\text{CH}_2\text{SiMe}_3)_3$ | **77%, Table 2.3, Entry 3** |. Notably $\text{Li}_2\text{MgR}_4(\text{TMEDA})_2$ showed no improvement | **4%, Table 2.3, Entry 4** | upon addition of a crown ether co-catalyst and was still seen to be ineffective at a 1:1 of 2:1 stoichiometry of 12-crown-4 to magnesiate, further confirming the inadequacy of lithium to play its part in the partnership by being unable to sufficiently activate the alkyne for cyclisation. Similarly it was seen to be the case that $\text{Mg}(\text{CH}_2\text{SiMe}_3)_2$ | **0%, Table 2.3, Entry 1** | remained completely ineffective with the addition of crown ether co-catalyst. This result also ascertaining that 18-crown-6 is not catalytically active in itself.

Due to the significant difference in rate of the sodium and potassium higher-order magnesiates it seems unlikely that a solvent separated $\text{Mg}(\text{OR})_4^{2-}$ and crown-ether-captured alkali metal complex is formed. Instead a contacted pair with alkali-metal- π -interactions appears more probable, otherwise no difference in reactivity should be apparent between sodium and potassium analogues as they would both essentially only consist of a $\text{Mg}(\text{OR})_4^{2-}$ active component. Although the crown ethers are often expected to mostly sequester the alkali metal there are a few examples of structures where the alkali metal can be seen to reach out and form π -interactions.²⁷⁹⁻²⁸⁵

The ability for an alkali metal to sustain π -interactions whilst encircled by a crown ether can be observed in work by Maron and Okuda,²⁸⁶ where an x-ray crystal structure was obtained of a higher-order potassium zincate bearing 4-*n*-butylpyridine ligands [Figure 2.3] in which the potassium is coordinated by the 18-c-6 and is still able to sustain η^5 coordination to a pyridine ring. This highly coordinated environment in which potassium is encircled by 18-c-6 and further lateral π -interactions could also be in operation in the present case.

Maron/Okuda:

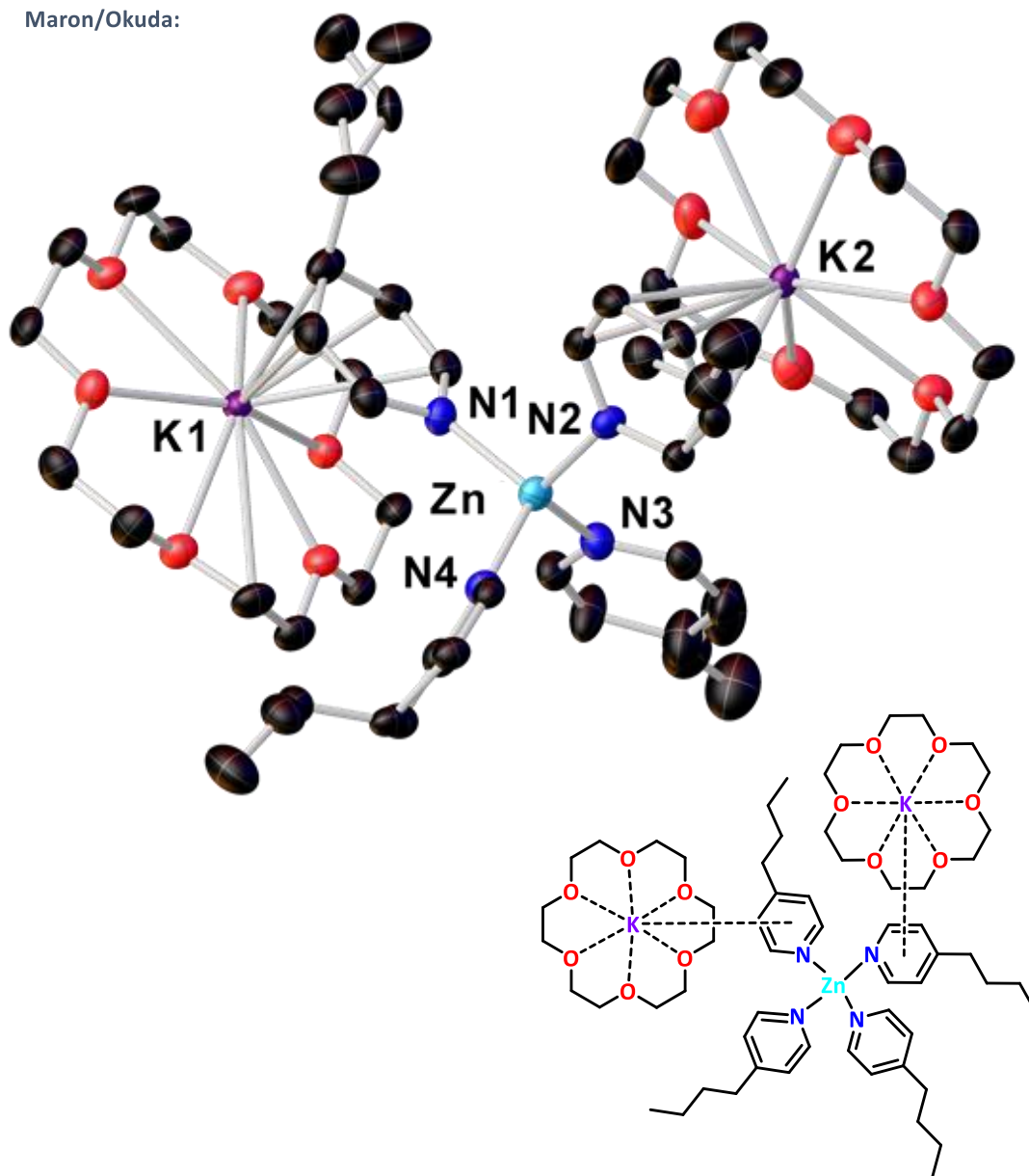


Figure 2.3 – X-ray crystal structure of a potassium tetraorganozincate, where potassium is coordinated by 18-c-6 and 4-*n*-butylpyridine.²⁸⁶

It therefore appears that under these conditions the addition of a crown ether is important in tuning the coordination of the alkali metal to make it a more competent catalyst, possibly through Lewis acidity and protecting it sterically |2.1.5 Mechanistic studies| whilst allowing it to remain intimately involved in the catalysis.

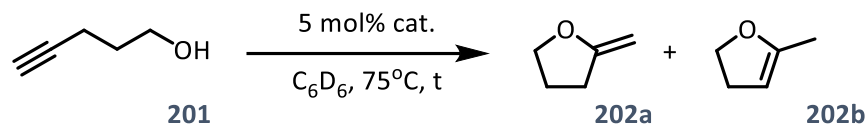
In a final bid to ensure the legitimacy of the apparent trends (alkali metal effect between the sodium and potassium higher order magnesiate, and higher-order vs. lower-order) the Lewis donors involved were investigated.

Firstly, to ensure the apparent increase in rate upon moving from lower-order to higher order magnesiate was not due to the change between TMEDA or PMDETA (these donors are necessary for the formation/isolation of higher-order magnesiate) they were added to $\text{Mg}(\text{CH}_2\text{SiMe}_3)_2$, $\text{NaMg}(\text{CH}_2\text{SiMe}_3)_3$ and $\text{KMg}(\text{CH}_2\text{SiMe}_3)_3$ |Table 2.4, Entries 1-3|. No difference in reactivity was observed with the addition of these donors.

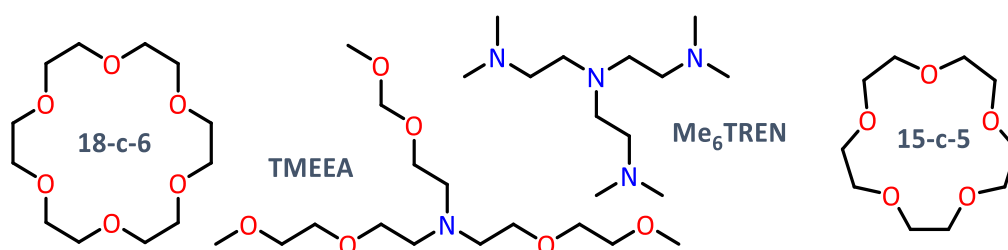
Secondly to negate any effect in Lewis donor attributing to the observed alkali metal effect between $\text{Na}_2\text{MgR}_4(\text{TMEDA})_2$ and $\text{K}_2\text{MgR}_4(\text{PMDETA})_2$ the TMEDA analogue $\text{K}_2\text{MgR}_4(\text{TMEDA})_2$ was compared. A negligible difference was observed with 88% yield of cyclised product achieved in 3 h by the PMDETA analogue |Table 2.4, Entry 5| and 94% in 3 h by the TMEDA analogue |Table 2.4, Entry 4|, substantiating the difference in rate as an alkali metal effect and not due to the Lewis donor present.

Curious of the effect produced by the crown ether it was questioned if other chelating Lewis donors could reproduce this rate acceleration. The clear starting point was the addition of the 'mismatched' crown ether to both the sodium and potassium higher-order magnesiate to ascertain if the acceleration was due to the use of a specific crown ether, or the pairing of crown ether and alkali metal. Oddly it was noted that 'mismatching' of the crown and alkali metal produced intermediate reaction times between no crown ether and the 'appropriate' one. $\text{K}_2\text{MgR}_4(\text{PMDETA})_2$ + 15-c-5 achieved a 96% yield in 12 h compared with 3 h with 18-c-6, and $\text{Na}_2\text{MgR}_4(\text{TMEDA})_2$ + 18-c-6 reaching 81% in 11 h and 5 h respectively with 15-c-5 |Table 2.4, Entries 5-8| displaying a clear rate increase with the 'matched' crown ether. This unsuitability of 'mismatching' appears to demonstrate that it is the pairing of alkali metal and crown that is crucial in the activation of the alkynol for cyclisation rather than an inherent property of the crown ether itself.

Table 2.4 – The role of Lewis donors in the cyclisation of 4-pentynol |201| mediated by alkali metal magnesiates.



Entry	Pre-catalyst R = CH ₂ SiMe ₃	Time (h)	Yield (%) ^c	Isomer ratio 202a : 202b
1	MgR ₂ + 18-c-6 (± PMDETA) ^a	36	0	-
2	NaMgR ₃ (TMEDA) ^a	36	13	96 : 4
3	KMgR ₃ (PMDETA) ^a	36	20	94 : 6
4	K ₂ MgR ₄ (TMEDA) ₂ + 2 x 18-c-6 ^{b d}	3	94	90 : 10
5	K ₂ MgR ₄ (PMDETA) ₂ + 2 x 18-c-6 ^{b d}	3	88	90 : 10
6	K ₂ MgR ₄ (PMDETA) ₂ + 4 x 15-c-5 ^{b d}	12	96	75 : 25
7	Na ₂ MgR ₄ (TMEDA) ₂ + 2 x 15-c-5 ^{b d}	5	88	95 : 5
8	Na ₂ MgR ₄ (TMEDA) ₂ + 2 x 18-c-6 ^{b d}	11	81	89 : 11
9	K ₂ MgR ₄ (PMDETA) ₂ + 4 x Me ₆ TREN ^{b d}	21	90	82 : 18
10	K ₂ MgR ₄ (PMDETA) ₂ + 4 x TMEEA ^{b d}	10	86	79 : 21



|a| Reactions were performed in a Young's cap NMR tube, using 0.5 mmol of substrate (4-pentynol) |201| and 0.025 mmol (5 mol%) pre-catalyst. |b| Reactions were performed in a Young's cap NMR tube, using 0.6 mmol (1.2 eq.) of substrate (4-pentynol) |201| and 0.025 (5 mol%) pre-catalyst. This additional 0.1 mmol (20 mol% / 0.2 eq.) of 201 was employed to convert the pre-catalyst to 'active catalyst' (vide infra). |c| Calculated from ¹H NMR spectroscopic data by integration against an internal standard (0.05mmol / 10 mol% 1,2,3,4-tetraphenyl-naphthalene). |d| A stoichiometric quantity of crown ether co-catalyst used according to the alkali metal [i.e., 2 x 18-c-6 = 10 mol% for 5 mol% K₂MgR₄(PMDETA)₂]

In an effort to further improve reaction times $K_2MgR_4(PMDETA)_2$ was taken with other chelating Lewis donors but no effect was observed after the addition of Me_6TREN [90%, 21 h, Table 2.4, Entry 9], and only a limited effect, similar to 15-c-5, was observed with TMEEA [86%, 10 h, Table 2.4, Entry 10]. TMEEA was hoped to be a comparable donor to 18-c-6 due to its high denticity, itself containing 6x O atoms the same as 18-c-6. The higher rate observed with the crown ether seems likely due to its ring geometry, where the more planar ring of 18-c-6 may be advantageous due to steric effects and more energetically unfavourable decoordination due to the macrocyclic effect.²⁸⁷ Due to a bulkier 'encapsulation' style of coordination (instead of 'encircling' as with 18-c-6) and lower barrier to (partial) decoordination than the macrocycle 18-c-6 it is likely that TMEEA is less strongly coordinated to potassium, possibly having only one or two 'arms' engaged in coordination. This increased Lewis donating ability of 18-c-6 compared to TMEEA could account for the observed difference in reactivity despite the similar denticity.

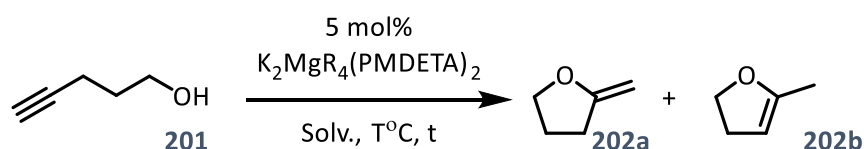
Apparent that $K_2MgR_4(PMDETA)_2 + 18-c-6$ was the most effective catalyst, an attempt was made at the synthesis of $K_2MgR_4(18-c-6)_2$, however, this was found not to be possible using the method to produce the PMDETA and TMEDA analogues of the magnesiate as an insoluble solid was formed. It was also observed that addition of 18-c-6 to a solution of $K_2MgR_4(PMDETA)_2$ caused the decomposition of the 18-c-6, imposing an order of addition to catalytic reactions where magnesiate must be added to alkynol before or simultaneously with crown ether.

2.1.3 Optimisation of reaction conditions and substrate compatibility

Alongside optimisation of the catalyst, different reaction conditions and substrates were evaluated. Three common deuterated solvents were considered; benzene, THF and toluene. Solvent selection posed little difficulty, with benzene easily identified as the best choice. In toluene degradation of the catalyst by reaction with the solvent was quickly apparent as a bright red colour indicative of metallated toluene was produced rapidly upon addition of the magnesiate, and so it was instantly discounted. In THF [12 h, 93%, Table 2.5, Entry 3], although the reaction occurred more quickly, the product isomer selectivity was much poorer leaving benzene as the only suitable candidate.

Temperature selection also transpired as a simple task due to the reaction employing $K_2MgR_4(PMDETA)_2$ without crown ether co-catalyst at 90°C [4 h, 97%, Table 2.5, Entry 2] occurring in the same 3 h time frame as at 75°C with $K_2MgR_4(PMDETA)_2 + 18-c-6$. The milder reaction temperature required in the presence of co-crown catalyst was judged to be the more economical option, and additionally could potentially be advantageous to thermally sensitive alkynol substrates.

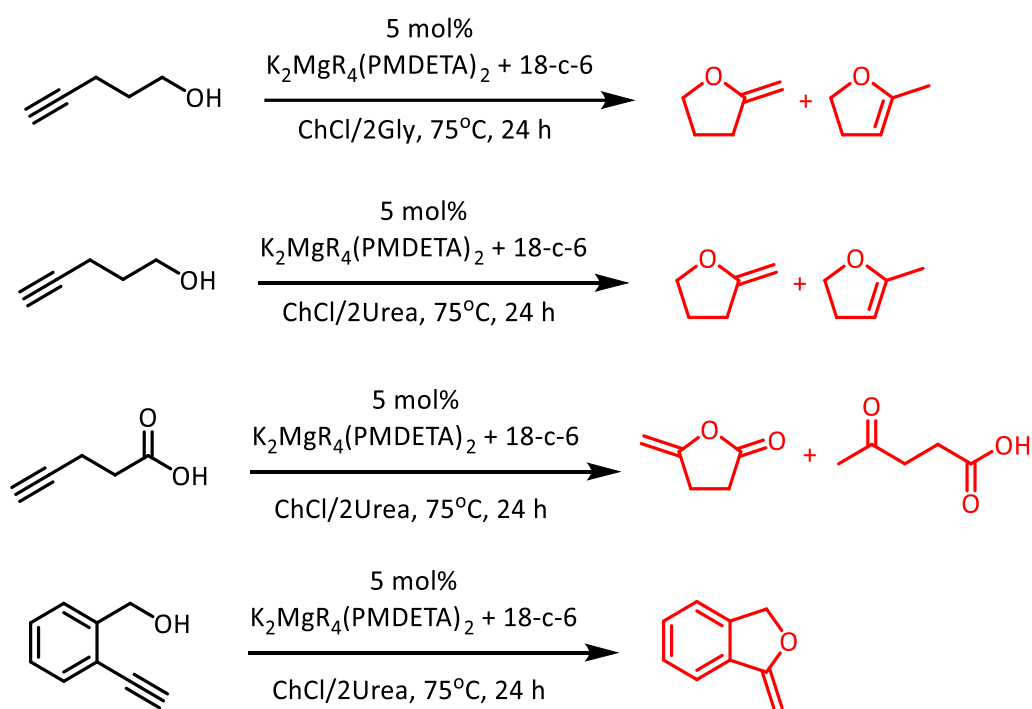
Table 2.5 – The role of solvent in the cyclisation of 4-pentynol |201| mediated by alkali metal magnesiates.



Entry	Solvent ^[a]	Temp (°C)	Time (h)	Yield (%) ^[b]	Isomer ratio 202a : 202b
1	<i>d</i> ₆ - benzene	75	22	91	86 : 14
2	<i>d</i> ₆ - benzene	90	4	97	83 : 17
3	<i>d</i> ₈ - THF	75	12	93	63 : 37
4	<i>d</i> ₈ - toluene	75	-	catalyst degradation	-

[a] Reactions were performed in a Young's cap NMR tube, using 0.6 mmol (1.2 eq.) of substrate (4-pentynol) |201| and 0.025 mmol (5 mol%) pre-catalyst. This additional 0.1 mmol (20 mol% / 0.2 eq.) of 201 was employed to convert the pre-catalyst to 'active catalyst' (vide infra). [b] Calculated from ¹H NMR spectroscopic data by integration against an internal standard (0.05mmol / 10 mol% 1,2,3,4-tetraphenyl naphthalene).

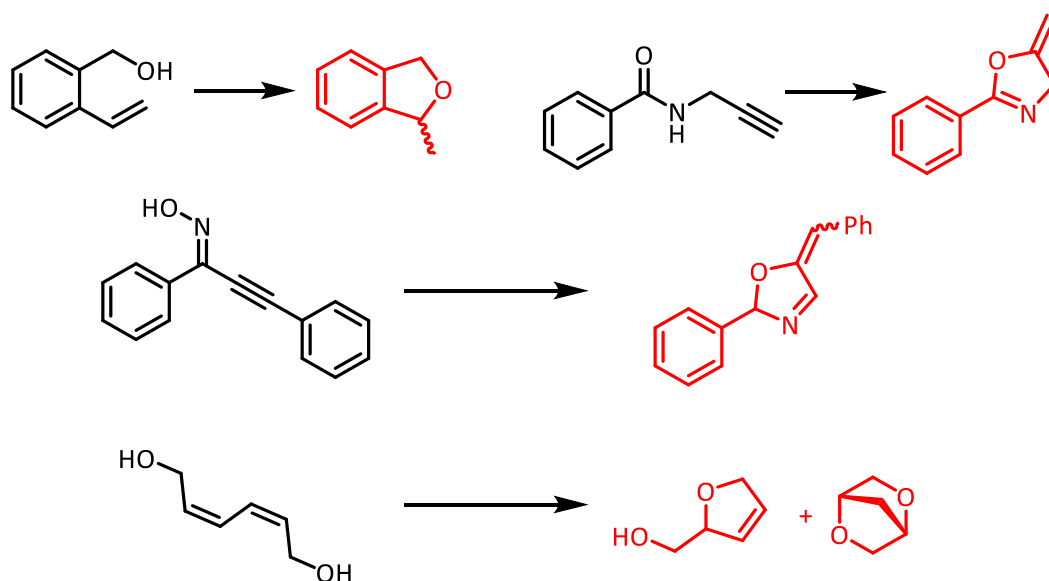
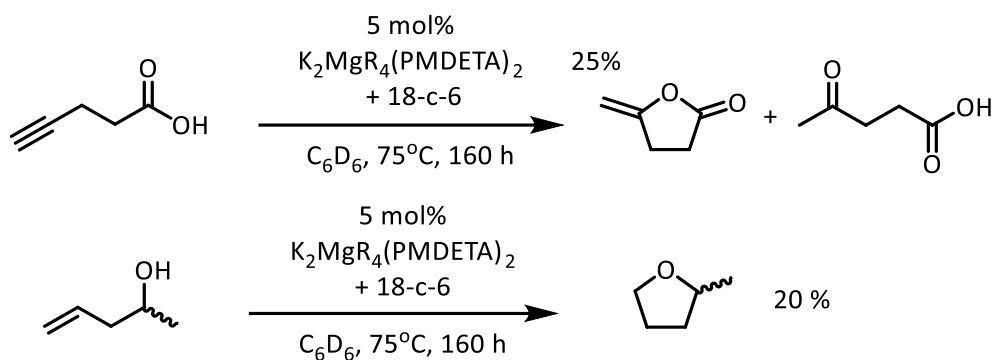
In parallel to other work included in this thesis |Part 1 – Organolithium reagents in alternative solvents| the catalysis of a few different substrates was explored in ChCl/2Gly and ChCl/2Urea |Scheme 2.15|. These reactions were found to be unsuccessful with no evidence of product formation when heated for 24 h. This is presumably due to the reaction being slower than the possible side reactions that quench the organometallic active species in the DESs.



Scheme 2.15 – Exploration of the alkali metal magnesiate mediated hydroalkoxylation in DESs

Reactions were performed using 1 mmol of substrate and 0.05 mmol pre-catalyst in 1 g of DESs and the reaction was monitored by GC-FID. A stoichiometric quantity of crown ether co-catalyst used according to the alkali metal [i.e., 2 x 18-c-6 = 10 mol% for 5 mol% $K_2MgR_4(PMDETA)_2$]

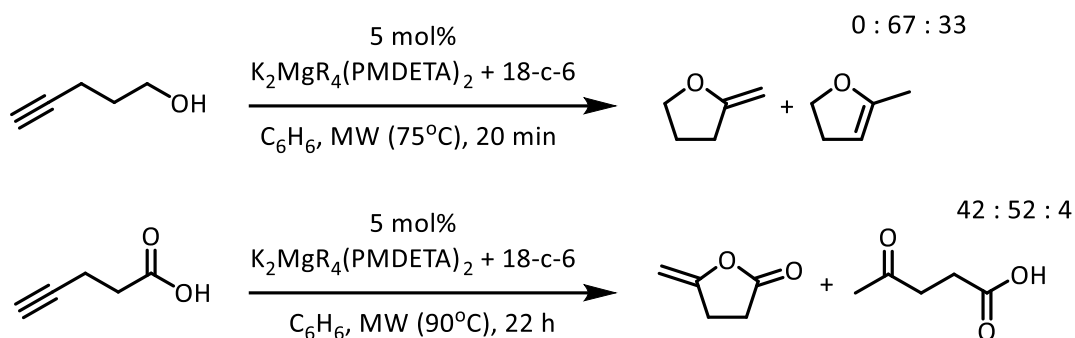
Other related compounds to alkynols such as aldehydes, acids and alkenes were also tested as potential substrates for catalysis under standard conditions [Scheme 2.16]. In the case of 4-pentynoic acid and 2-methyl-3-buten-1-ol progress was so slow that although product was detected catalytic turnover could not be confirmed. In other cases, substrates were simply unsuitable for catalysis due to insolubility in benzene, due to its low polarity, at standard concentrations, even upon heating. As benzene was previously established as the best placed solvent in which to perform catalytic reactions no alternative was explored instead the range of substrates was limited to alkynols.



Scheme 2.16 – Exploration of substrate scaffolds suitable for alkali metal magnesiate mediated hydroalkoxylation. |top| compounds with long reaction times |bottom| substrates insoluble in benzene at standard concentrations.

Reactions were performed in a Young's cap NMR tube, using 0.6 mmol (1.2 eq.) of substrate and 0.025 mmol pre-catalyst. Yields calculated from 1H NMR spectroscopic data by integration against an internal standard (0.05 mmol / 10 mol% 1,2,3,4-tetraphenyl naphthalene). A stoichiometric quantity of crown ether co-catalyst used according to the alkali metal [i.e., $2 \times 18-c-6 = 10 \text{ mol\%}$ for 5 mol% $K_2MgR_4(PMDETA)_2$]

Microwave heating was employed [Scheme 2.17] as an aid to reach a catalytic turnover more quickly as it allows the potential to somewhat superheat the reaction mixture. This method of heating showed some promise as it appeared to facilitate an increased rate of cyclisation of 4-pentynol and allow for the cyclisation of other types of substrate such as 4-pentynoic acid. Despite increased reaction rates microwave heating was not pursued for cyclisation reactions, with thermal heating instead chosen going forward.



Scheme 2.17 – Exploration of the use of microwave heating in alkali metal magnesiate mediated hydroalkoxylation.

Reactions were performed using 1 mmol of substrate and 0.05 mmol pre-catalyst in 1.04 mL benzene and the reaction was monitored by GC-FID. A stoichiometric quantity of crown ether co-catalyst used according to the alkali metal [i.e., 2 x 18-c-6 = 10 mol% for 5 mol% $K_2MgR_4(PMDETA)_2$]

2.1.4 Exploration of alkynol substrate scope & functional group tolerance

Having established optimal conditions for the cyclisation of 4-pentynol |201| as 5 mol% $K_2MgR_4(PMDETA)_2$ + 18-c-6 in C_6D_6 at 75°C, and the most suitable family of substrates to explore as alkynols, the range and robustness of the system was investigated with a selection of different alkynol scaffolds and a variety of functional groups.

Even looking only at a few terminal and internal alkynols it was soon apparent that the ease of cyclisation varies greatly between substrates. Employing 5-hexynol |203, Table 2.6, Entry 1|, with an increased chain length of only one, a higher temperature of 90°C becomes necessary to push through the reaction, and interestingly the major product obtained is not a cyclised enol ether |204a, 14% or 204b, 7%| but an isomerised alkynol |204c, 76%|, where the triple bond has migrated one carbon atom along the chain. This isomerisation is envisaged to be due to an unfavourable angle of ring closure,^{261, 288} hence due to the formation of an allene intermediate |4,5-hexadien-1-ol, Figure 2.4| during the reaction and lack of cyclisation the alkyne preferentially reforms in the internal position rather than terminal, being its more stable isomer due to hyperconjugation.²⁸⁹ The evidence for and consequences of this allene intermediate are further discussed in |2.1.6

Mechanistic interpretation| and |2.2 Isomerisation of terminal alkynes|.

Notably 4-hexynol, internal isomer product 204c, is also capable of being exocyclised to form a 5-membered cyclic enol ether. It does however not appear to occur over the same 24 h time scale of the isomerisation of 5-hexynol. Therefore, curious to the ability of the magnesiate to cyclise internal alkynols, 4-hexynol |204c| was isolated from the reaction mixture and used as a substrate |Table 2.6, Entry 2|. The cyclisation of this aliphatic internal alkynol proved very challenging, evidenced by the 600 h (25 d) reaction time. Nevertheless, cyclised products 204d and 204e were however obtained demonstrating it to be possible, however slow. It is unclear if full conversion of these products was achieved. NMR yields indicate only 50% of product isomers were obtained and turnover ceased, even upon the addition of a second 0.025 mmol of $K_2MgR_4(PMDETA)_2$ upon recommencing heating no further increase in yield was achieved. It is unclear if this is due to another, unidentified product, having been formed or simply that beyond this point catalytic turnover is not possible. Sound identification of products from 1H NMR spectra of the reaction mixture proved difficult, and the volatility, lack of easily distinguishable functional groups, and similarity of boiling point to the benzene solvent (ca. 80°C) precluded isolation and more thorough characterisation.

Table 2.6 – Exploration of structurally diverse alkynols for alkali metal magnesiate mediated hydroalkoxylation.

Entry	Substrate ^{[a][b][c]}	Yield ^[d]
1	<p> $\text{K}_2\text{MgR}_4(\text{PMDETA})_2$ $+ 18\text{-c-6}$ $90^\circ\text{C}, 26 \text{ h}$ </p>	99% (14 : 9 : 77)
2	<p> $\text{K}_2\text{MgR}_4(\text{PMDETA})_2$ $+ 18\text{-c-6}$ $90^\circ\text{C}, 600 \text{ h}$ </p>	50%
3	<p> $\text{K}_2\text{MgR}_4(\text{PMDETA})_2$ $+ 18\text{-c-6}$ $\text{rt.}, 1 \text{ h}$ </p>	86%
4	<p> $\text{K}_2\text{MgR}_4(\text{PMDETA})_2$ $+ 18\text{-c-6}$ $75^\circ\text{C}, 1 \text{ h}$ </p>	89%
5	<p> $\text{K}_2\text{MgR}_4(\text{PMDETA})_2$ $+ 18\text{-c-6}$ $75^\circ\text{C}, 1 \text{ h}$ </p>	90%

[a] $R = (\text{CH}_2\text{SiMe}_3)$. [b] Reactions were performed in a Young's cap NMR tube, using 0.6 mmol (1.2 eq.) of substrate (4-pentynol) |201| and 0.025 mmol (5 mol%) pre-catalyst. This additional 0.1 mmol (20 mol% / 0.2 eq.) of **201** was employed to convert the pre-catalyst to 'active catalyst' (vide infra). [c] A stoichiometric quantity of crown ether co-catalyst used according to the alkali metal [i.e., $2 \times 18\text{-c-6} = 10 \text{ mol\%}$ for 5 mol% $\text{K}_2\text{MgR}_4(\text{PMDETA})_2$]. [d] Calculated from ^1H NMR spectroscopic data by integration against an internal standard (0.05mmol / 10 mol% 1,2,3,4-tetraphenylanthracene)

Continuing with alkynol substrate scope, where both alkyne and hydroxyl group are already held in a manner partially aligned to that of the cyclised product, the cyclisation progresses much more readily, as seen with 2-ethynylbenzyl alcohol [205, Table 2.6, Entry 3]. This occurs even at ambient temperature in 1 h. A similar effect is observed in cyclisation of Z-enynols [207 and 209, Table 2.6, Entries 4-5] along with interesting product selectivity. Employing the optimised conditions, we see only the production of aromatic furan products 208a, 210a. This differs from the product previously reported using heavier alkaline earth^{223, 268, 290} or lanthanide amides.^{227, 266, 267} With these catalytic systems only the non-aromatic products, 3-methyl-2-methylene-2,5-dihydrofuran and 3-methyl-2-benzylidene-2,5-dihydrofuran [208b, 210b], were observed, and it is only by moving to transition metal catalysts,¹⁶⁹ we see formation of the aromatic furan product. Even more curiously it was seen that the non-aromatic products [208b, 210b] could be obtained by employing KMgR_3 or $\text{Na}_2\text{MgR}_4(\text{TMEDA})_2$ as catalyst but use of $\text{KMgR}_3 + 18\text{-c-6}$, $\text{Na}_2\text{MgR}_4(\text{TMEDA})_2 + 15\text{-c-5}$ or $\text{K}_2\text{MgR}_4(\text{PMDETA})_2 \pm 18\text{-c-6}$ all furnished the aromatic furan product [208a, 210a].

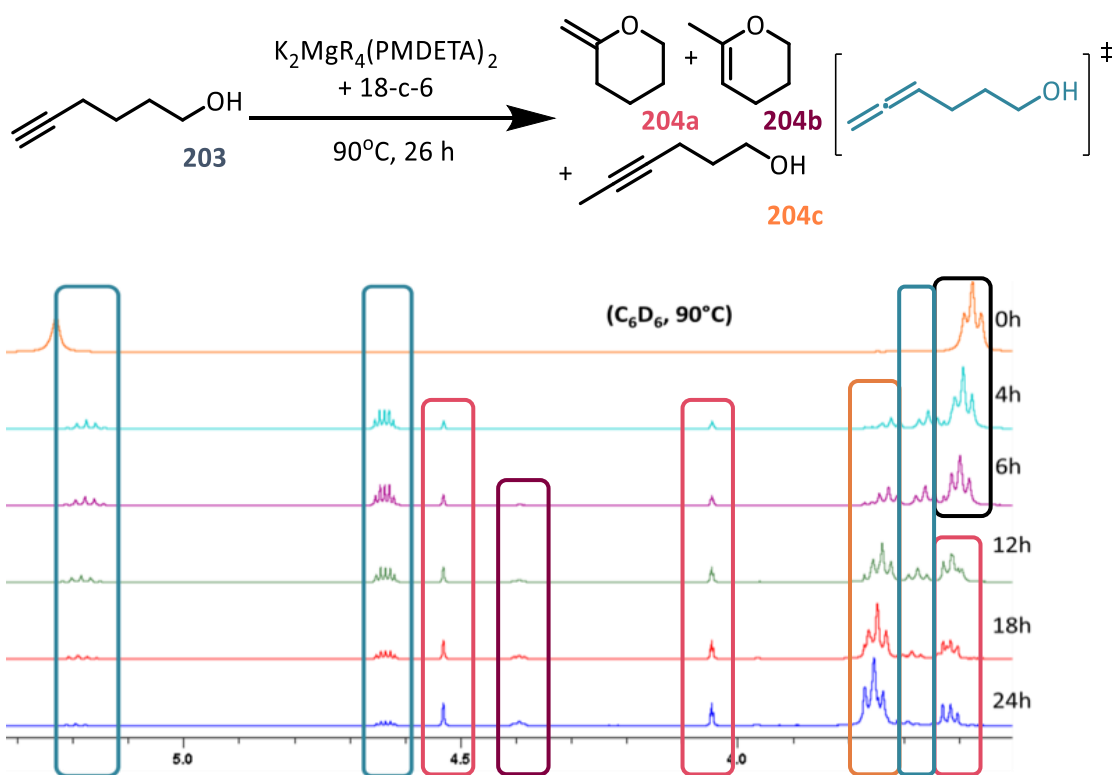
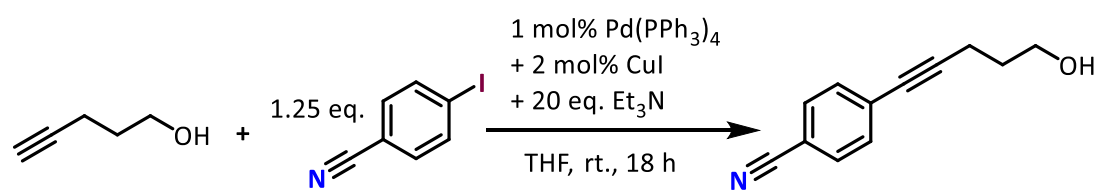
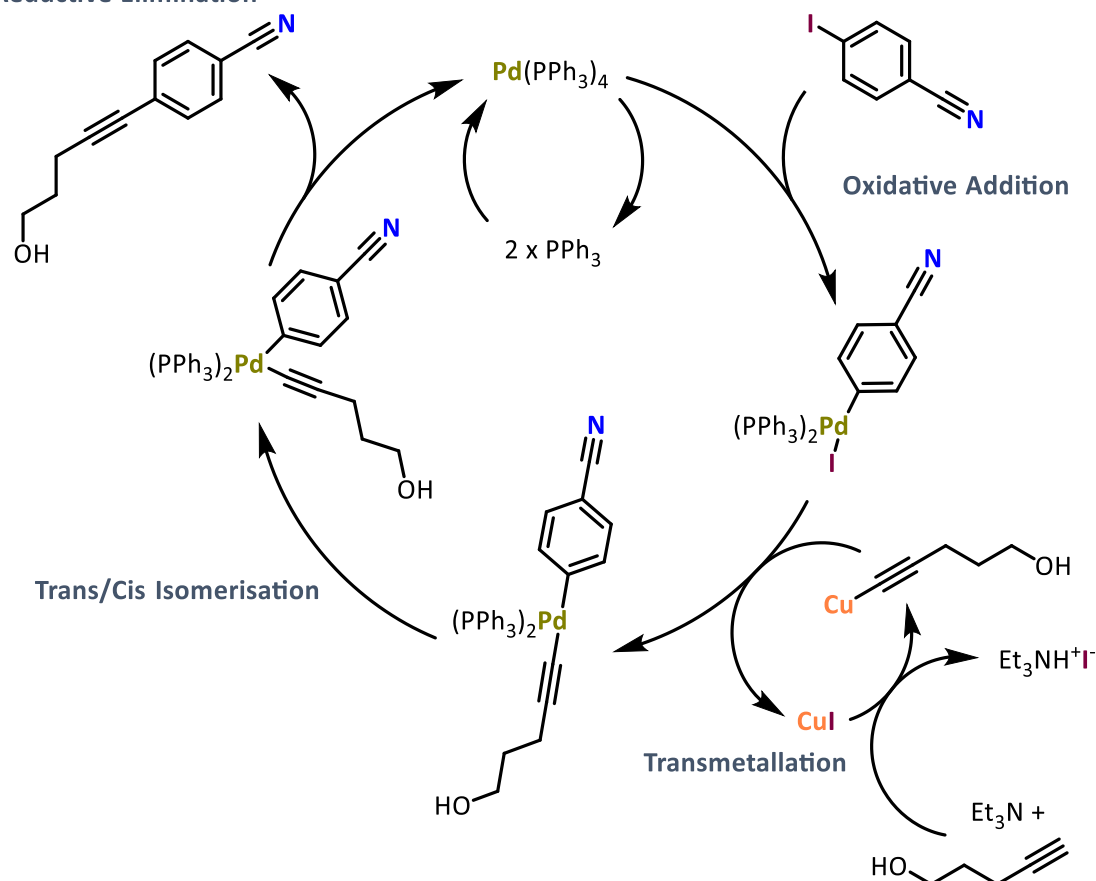


Figure 2.4 –Selected region of ^1H NMR spectrum (400.1 MHz, C_6D_6) of the (cyclo)isomerisation of 5-hexynol [203, Table 2.5, Entry 1] displaying the presence of 4,5-hexadien-1-ol as an intermediate.

In order to further probe the functional group tolerance of the catalytic magnesiumate system, a range of internal alkynes were synthesised with different pendant functional groups, including halogens, electron-donating and electron-withdrawing groups. These compounds [213, 215, 217, 219, 221, 223 and 225] were synthesised *via* Sonogashira coupling [Scheme 2.18] of 4-pentynol and the relevant iodo- or bromo-aryl and were fully characterised as compound were not reported in the literature. The major products from these cyclisations [214b, 216b, 218b, 220b, 222b and 224b] were also novel, requiring isolation and full characterisation. Products isomers could be identified by 2D NMR spectroscopic methods as outlined herein using the example of 4-(5-hydroxypent-1-yn-1-yl)benzonitrile [223].



Reductive Elimination



Scheme 2.18 – Sonogashira coupling of 4-pentynol and 4-iodobenzonitrile.

Looking at a ^1H NMR spectrum of the completed reaction of **223**, **Figure 2.5** predominately one component can be seen with two sets of roofing doublets observed in the aromatic region characteristic of the *para* substituted phenyl ring. Although reassuring that the mixture is likely comprised of one component, alone it does not indicate which compound it may be.

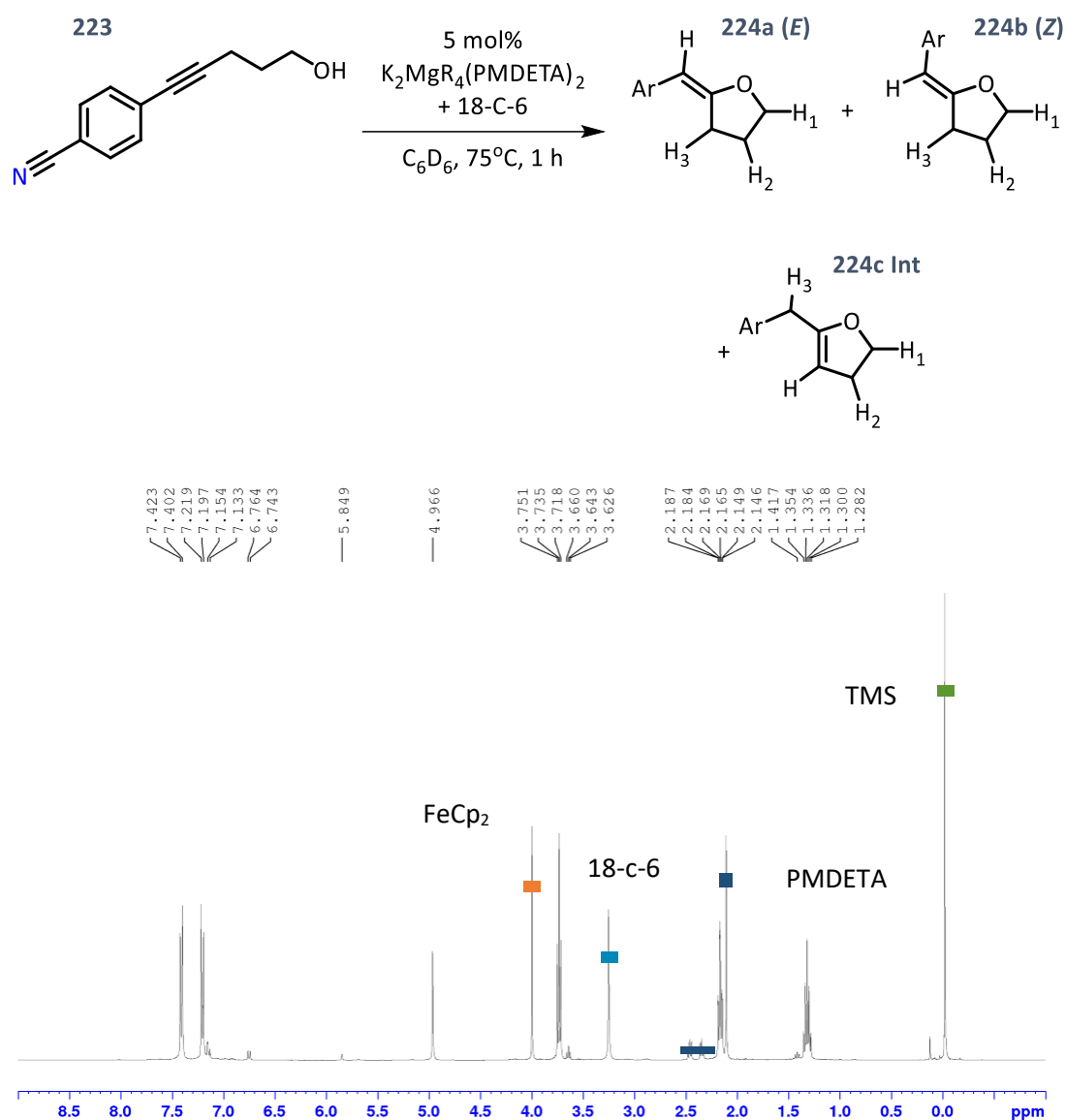


Figure 2.5 – ^1H NMR spectrum (400.1 MHz, C_6D_6) of the reaction mixture after the cyclisation of **223**.

By comparing the chemical shift of the peaks with the starting alkynol a slight difference indicates a transformation of sorts has occurred, but more substantial evidence of cyclisation having occurred could be gathered by IR spectroscopy. Comparing spectra of starting alkynol and product mixture [Figure 2.6] the disappearance of the OH stretch around 3500 wavenumbers is indicative of cyclisation.

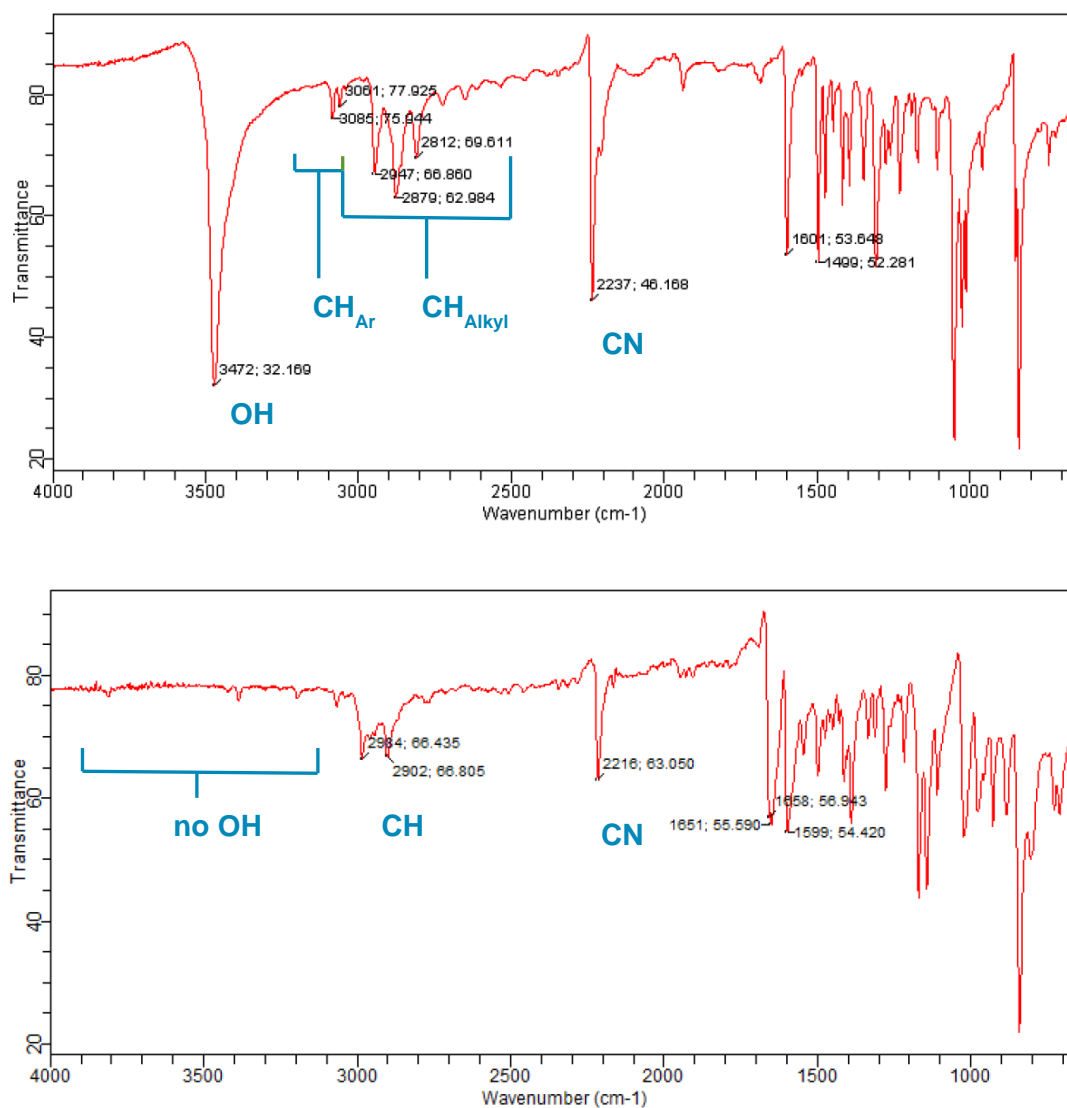


Figure 2.6 –|top| IR spectrum of **223**, and |bottom| the reaction mixture after the cyclisation of **223**.

Having established that cyclisation had occurred it was then possible to discern between external isomers **223a-b** and internal isomer **223c** by ^1H COSY NMR spectroscopy [Figure 2.7].

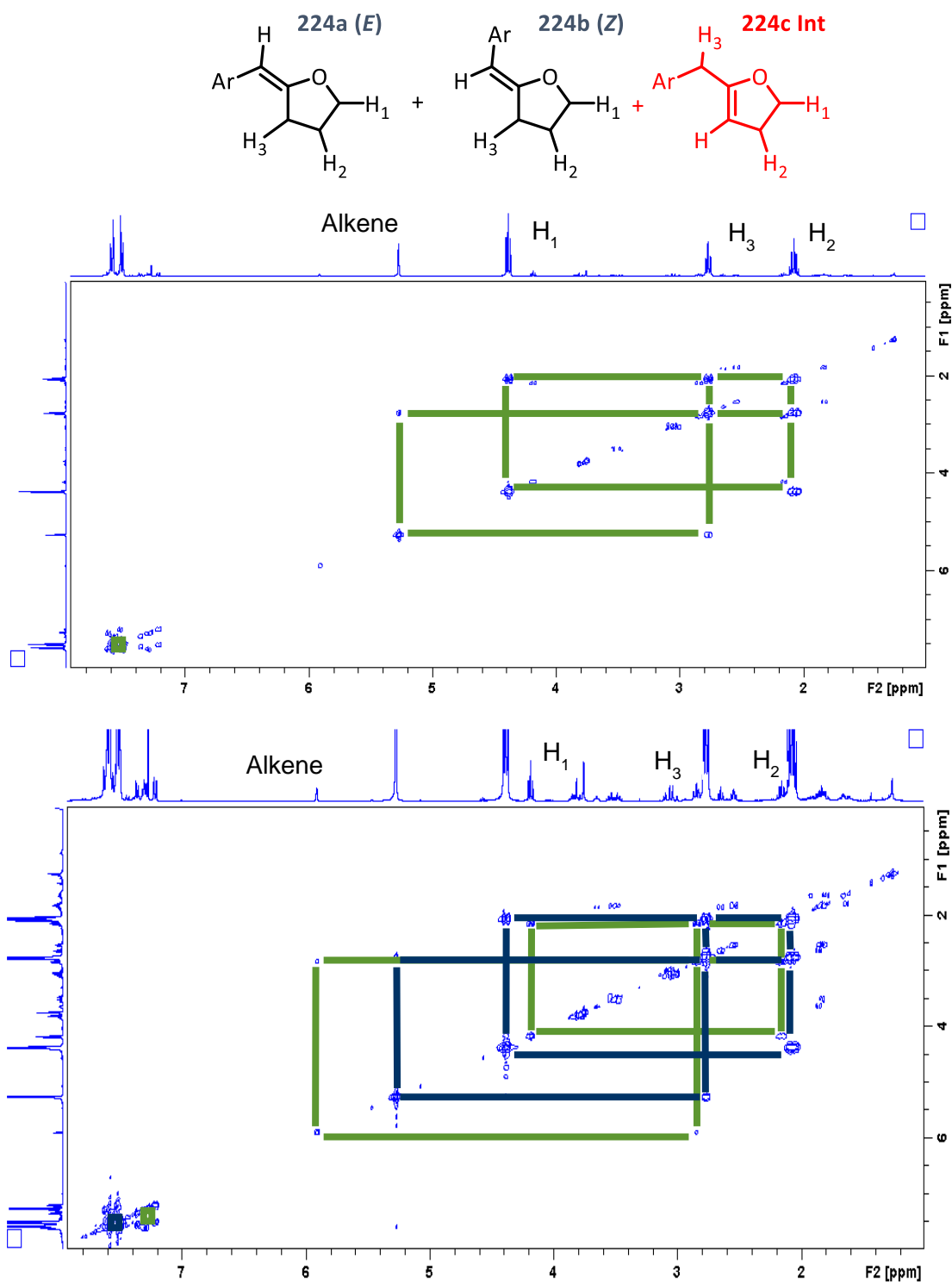


Figure 2.7 – ^1H COSY spectrum (400.1 MHz, C_6D_6) showing ^1H – ^1H bonding interactions of the major product (above), and minor product (below) of the cyclisation of the cyclisation of **223**.

The interactions between $H_1 - H_2$, $H_3 - H_2$ and $H_3 - H_{alk}$ are clear for the major isomer present in the mixture, with, upon closer inspection, the same interactions in a second isomer. From the appearance of an $H_3 - H_2$ and the lack of a $H_2 - H_{alk}$ interaction the internal alkene isomer can be ruled out as either of the two products. Despite remaining, unassigned, resonances suspected to be internal alkene product **224c** in the 1H NMR spectrum, the expected proton interactions could not be identified in the 1H COSY NMR spectrum. Due to the same proton bonding ‘through-bond’ interactions being present in both stereoisomers of the external alkene product ($H_3 - H_{alk}$ as a 4J coupling in both), it was necessary to examine ‘through-space’ interactions in order to differentiate between *E* and *Z* isomers. Looking at a 1H NOESY NMR spectrum [Figure 2.8] these ‘through space’ interactions can be observed. In this spectrum presented below the key $H_3 - H_{alk}$ interaction is observed for the major product but not for the minor, clearly demonstrating the major product to be the *Z* isomer.

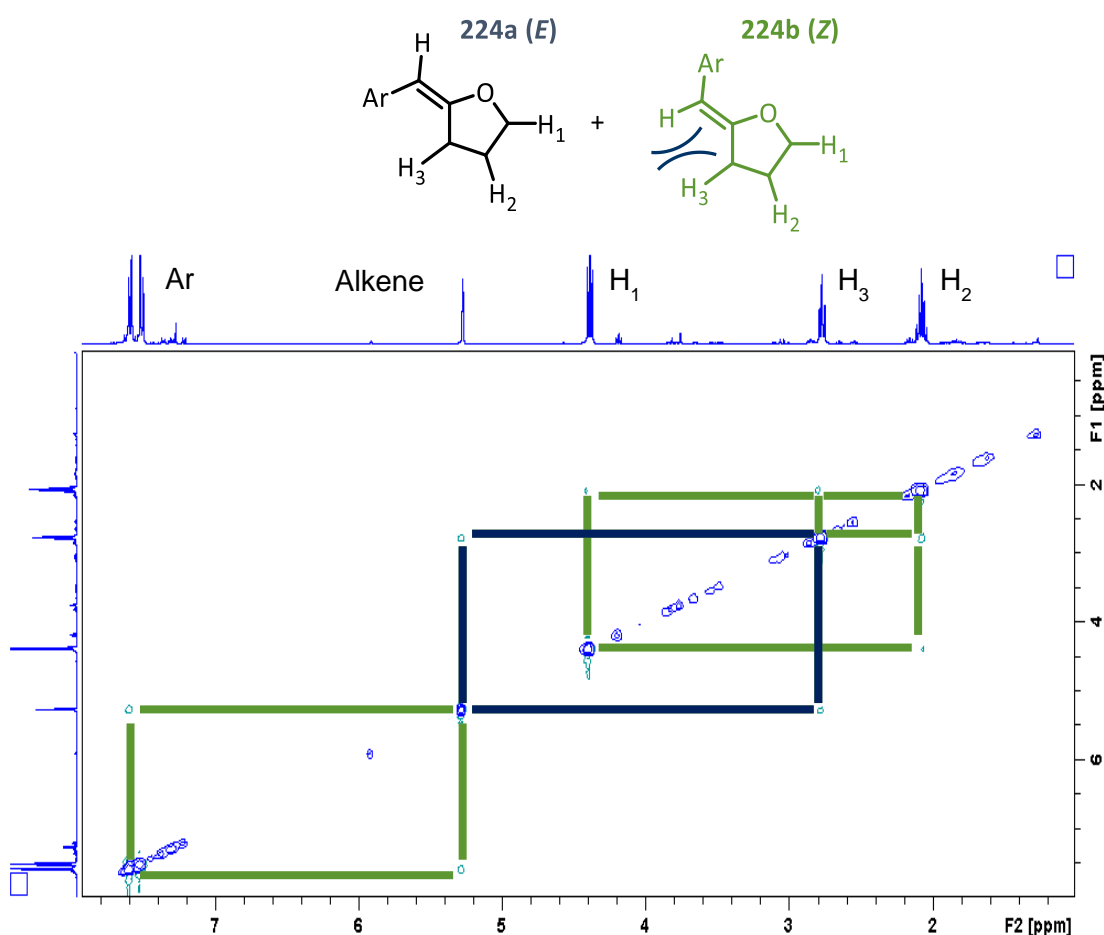


Figure 2.8 – 1H NOESY spectrum (400.1 MHz, C_6D_6) showing $^1H - ^1H$ through-space interactions of the major of the cyclisation of **223**.

It was found, to some despair, that all cyclised products [**214b**, **216b**, **218b**, **220b**, **222b** and **224b**] were not stable under bench conditions and once isolated would decompose, rapidly if an oil. Therefore, it was necessary to store all products at -33°C in an argon filled glove box to enable full characterisation. The extent of decomposition is illustrated below for (Z)-2-(3-fluorobenzylidene)tetrahydrofuran [**220a**, **Figure 2.9**] with a multitude of resonances appearing in ^{19}F NMR spectra taken over an few hours timescale.

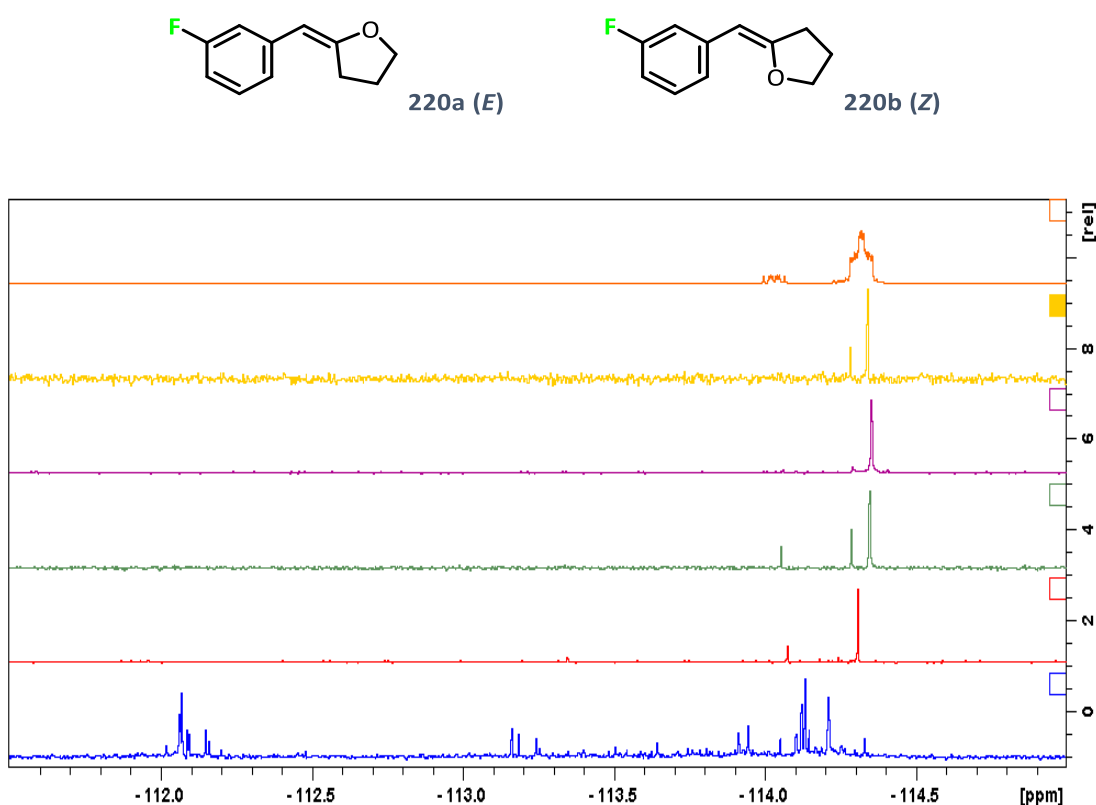


Figure 2.9 – ^{19}F NMR spectrum (128.4 MHz, CDCl_3) of the decomposition of [**220a** and **220b**] (E/Z)-2-(3-fluorobenzylidene)tetrahydrofuran.

Table 2.7 – Exploration of functional group compatibility for alkali metal magnesiate mediated hydroalkoxylation.

Entry	Substrate	Products	Conditions [a]	Yield [b]
1		Ar-CH=CH-O-CH ₂ -CH ₂ -CH ₂ -OH (E) 212a + Ar-CH=CH-O-CH ₂ -CH ₂ -CH ₂ -OH (Z) 212b + Ar-CH=CH-O-CH ₂ -CH ₂ -CH ₂ -OH (Int) 212c (Int)	75°C, 1 h 40°C, 36 h	84% (10:90:0) 6%
2		Ar-CH=CH-O-CH ₂ -CH ₂ -CH ₂ -OH (E) 214a + Ar-CH=CH-O-CH ₂ -CH ₂ -CH ₂ -OH (Z) 214b	75°C, 6 h 40°C, 36 h	87% (11:89) 2%
3		Ar-CH=CH-O-CH ₂ -CH ₂ -CH ₂ -OH (E) 216a + Ar-CH=CH-O-CH ₂ -CH ₂ -CH ₂ -OH (Z) 216b	75°C, 36 h 40°C, 36 h	64% (31:69) ^[a] 1%
4		Ar-CH=CH-O-CH ₂ -CH ₂ -CH ₂ -OH (E) 218a + Ar-CH=CH-O-CH ₂ -CH ₂ -CH ₂ -OH (Z) 218b	75°C, 1 h 40°C, 36 h	99% (9:91) 51%
5		Ar-CH=CH-O-CH ₂ -CH ₂ -CH ₂ -OH (E) 220a + Ar-CH=CH-O-CH ₂ -CH ₂ -CH ₂ -OH (Z) 220b	75°C, 0.5 h 40°C, 24 h	95% (8:92) 82%
6		Ar-CH=CH-O-CH ₂ -CH ₂ -CH ₂ -OH (E) 222a + Ar-CH=CH-O-CH ₂ -CH ₂ -CH ₂ -OH (Z) 222b	75°C, 0.5 h 40°C, 2 h	97% (4:96) 93%
7		Ar-CH=CH-O-CH ₂ -CH ₂ -CH ₂ -OH (E) 224a + Ar-CH=CH-O-CH ₂ -CH ₂ -CH ₂ -OH (Z) 224b	75°C, 0.5 h 40°C, 0.5 h	84% (6:94) 76%
8		Ar-CH=CH-O-CH ₂ -CH ₂ -CH ₂ -OH (E) 226a + Ar-CH=CH-O-CH ₂ -CH ₂ -CH ₂ -OH (Z) 226b		

[a] Reactions were performed in a Young's cap NMR tube, using 0.6 mmol (1.2 eq.) of substrate and 0.025 mmol (5 mol%) $K_2MgR_4(PMDETA)_2$ and 0.05 mmol 18-c-6. [b] Calculated from 1H NMR spectroscopic data by integration against an internal standard (0.05 mmol / 10 mol% ferrocene). [c] Lower selectivity presumed to be symptomatic of low conversion at the current stage of reaction (as it seen with other substrates) and higher selectivity is assumed if completion were reached

Of the *t*-butyl, MeO, Cl, F, CF₃, CN and CO₂Et groups that were incorporated into the substrate, with the only incompatible group being CO₂Et. However, as the ester containing substrate was *ortho* substituted and no other *ortho* pendant alkynols were tested it is unclear if the incompatibility stems from the ester functionality, the *ortho* substitution or both.

Firstly, looking at 5-phenylpent-4-yn-1-ol |**211, Table 2.7, entry 1**| the reaction reached completion in 1 h at 75°C yielding only two product isomers. The major product being the external *Z*-alkene |**212b**| and the minor external *E* isomer |**212a**|. In the aforementioned studies by Hill,²⁷⁰ a mixture of three product isomers was obtained, the external alkene isomers |**212a, 212b**| and an internal alkene |**212c**| (note these three products are all exocyclic). It was also noted that the product ratio appeared to have a degree of temperature dependence and required significantly harsher reaction conditions (90-110°C, 16-40 h). Despite altering the reaction temperature (reactions performed at both 40 and 75°C), the same isomer ratios were obtained for all the reactions which tended towards completion |**Table 2.7, Entries 6-7**|.

Focusing on the specific substrates when the mildly electron donating *t*-butyl group |**Table 2.7, Entry 2**| is incorporated onto the 5-phenylpent-4-yn-1-ol scaffold, the reaction rate is reasonably reduced with 87% yield only being achieved after 6 h compared to 1 h for the non-functionalised substrate |**Table 2.7, Entries 1**|. This effect is seen even more acutely upon the incorporation of a stronger electron donating methoxy group |**Table 2.7, Entry 3**| where a dramatic reduction in reaction rate has it limping to an only 64% in the cut off time of 36 h. When mildly withdrawing halides are incorporated within the substrate |**Table 2.7, Entries 4-5**| the reaction is complete in less than 1 h. At this juncture, it was deemed necessary to consider reaction times at 40°C to ascertain if any difference in relative rates was observed. With a Cl substituent |**Table 2.7, Entry 4**|, the yield was 51% after 36 h compared to 6% for the non-substituted alkynol at this temperature. Using a F substituent, this yield can be increased to 82% in 24 h |**Table 2.7, Entry 5**|. Moving to stronger electron withdrawing groups, incorporating trifluoromethyl brings the reaction time down to only 2 h at 40°C |**Table 2.7, Entry 6**|, and if a cyano substituent is utilised this is further reduced to 30 min |**Table 2.7, Entry 7**|.

X =	σ_{para} or σ_{meta}	X =	σ_{para} or σ_{meta}
<i>p</i> - OMe	-0.268	<i>p</i> - Cl	0.227
<i>p</i> - tBu	-0.197	<i>m</i> - F	0.337
H	0.000	<i>m,m</i> -di-CF ₃	0.430
		<i>p</i> - CN	0.660

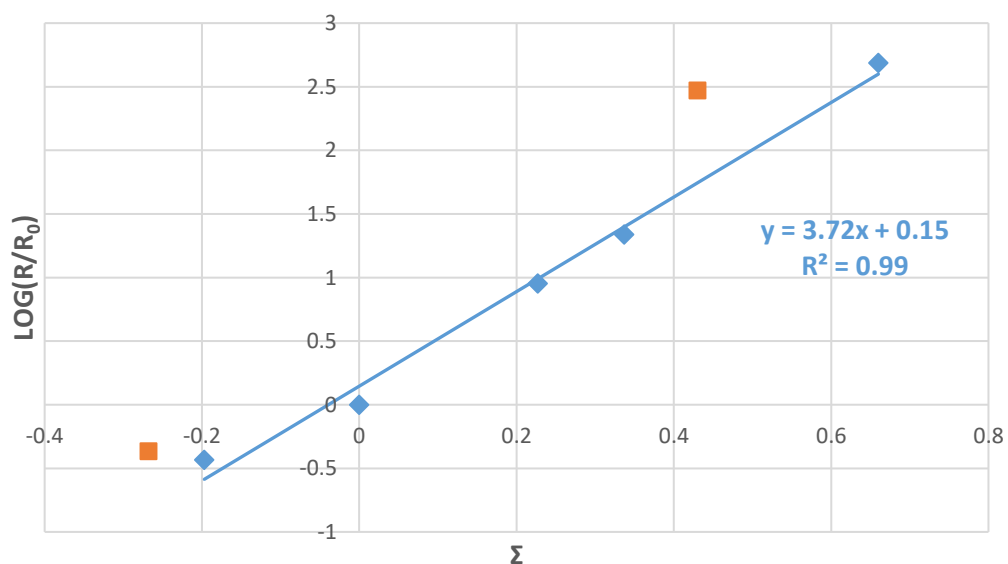
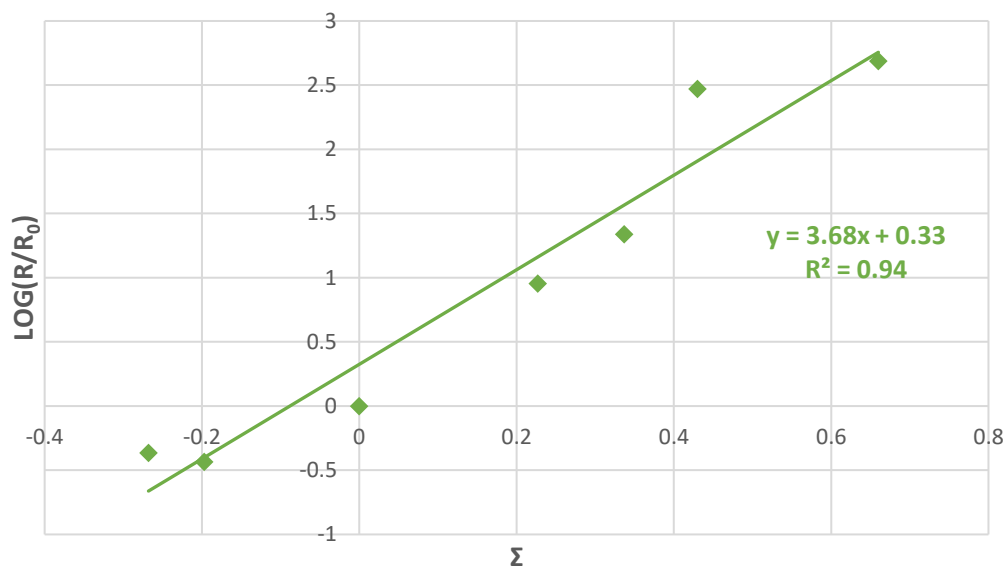
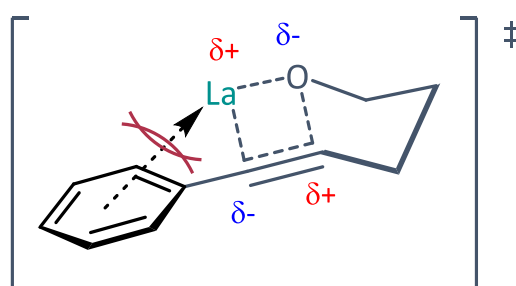


Figure 2.10 – Hammett style plot of the cyclisation reactions included in **Table 2.7** created from data from said table (blue trend line does not include orange points *p*-OMe and *m,m*-di-CF₃).

Plotted on a Hammett style plot | **Figure 2.10** | the rate accelerating effect of electron withdrawing groups is clearly displayed. A reasonably good linear fit was seen, which could be improved to a very good fit by not including the points for 5-(4-methoxyphenyl)pent-4-yn-1-ol | **215** | or 5-[3,5-(trifluoromethyl)phenyl]pent-4-yn-1-ol | **221** |. The positive gradient in this plot alludes to a negatively charged intermediate in the rate-determining step that is stabilised by reduction of charge density. This fits well with expectations of these reactions as during the cyclisation two electron rich groups (alkyne and hydroxyl) are being brought in close proximity, no doubt aided by any reduction in charge density. Of note, if the reaction were radical mediated this plot should, ideally, be flat with no gradient, positive or negative.

These functional group bearing substrates based upon 5-phenylpent-4-yn-1-ol | **211** | show nicely the benefit of using a bimetallic system for these cyclisation reactions. With the heavier alkaline earth metal amides and lanthanide amides, substrate | **211** | is more challenging to cyclise, taking 16 h at 90°C with $\text{Ca}(\text{HMDS})_2$ and about 15 h at 120°C with $\text{La}(\text{HMDS})_2$. Marks^{223, 227} has suggested that the reason for this sluggish reaction time with $\text{La}(\text{HMDS})_3$ is sterically-driven, due to the phenyl substituent preventing interaction between the metal and the internal alkyne. He also notes that potential π -interactions with the aryl ring and electrophilic metal centre also help prearrange the alkynol into a favourable geometry for cyclisation, therefore cyclisation occurring more rapidly with aryl substituted alkynes than aliphatic substituted | **Scheme 2.19** |. Using a bimetallic system, it appears that the favourable π -interactions which aid the geometry of the ring closing can be maintained whilst the steric clash is somewhat circumvented; so giving rise to faster reaction times than the other two systems mentioned.



Scheme 2.19 – Illustration of the simultaneous activating and sterically hindering π -interactions incurred by homometallic catalysts during the cyclisation of aryl substituted internal alkynols.

2.1.5 Mechanistic studies

Prime motivations in investigating reaction kinetics were to determine the reaction order of the alkynol substrate and catalyst present in the reaction; with the aim of providing insights into the reaction mechanism. The substrate chosen for these studies was 4-pentynol |**201**|, as this was used for the initial parameterisation studies.

Initially the concentration of major product isomer **202b** was monitored (continuously by ^1H NMR spectroscopy) until at least 75% yield under similar conditions to those used previously. Firstly, the reaction was plotted as concentration of **201** against time |**Figure 2.11**| in which a constant gradient demonstrates an overall reaction order of zero. A good linear fit was observed until half conversion, after this point a deviation in the form of rate acceleration is observed. This increase in rate could be due to acceleration caused by increasing product concentration or a reduction in inhibition alleviated by decreasing substrate concentration. The reaction was plotted as $[\mathbf{201}]^2$ versus time |**Figure 2.11**|, in which a straight line indicates a reaction order of -1 and so indicates the presence of inhibition. In this plot a good linear fit was observed consistent with inhibition, indicating the substrate likely inhibiting.

In order to gather further evidence, initial rate studies were conducted to investigate the individual rate order dependence on the concentration of alkynol and catalyst. These individual rate order studies involved monitoring (continuously by ^1H NMR spectroscopy) the concentration of major isomer product **202b** formed over the first 6% of the reaction. Concentrations of substrate **201** and $\text{K}_2\text{Mg}(\text{CH}_2\text{SiMe}_3)_4(\text{PMDETA})_2$ were chosen to allow for the collection at least 20 data points (concentrations of **202b**) to be measured before the reaction reached 6% yield. To find the rate dependence of a particular species a series of reactions were run varying the concentration of the compound in question, whilst maintaining the reaction conditions and concentrations of other species constant. For investigation of rate dependence on alkynol this involved five different concentrations of 4-pentynol (1.0 – 2.5 M), and for catalyst four different concentrations of $\text{K}_2\text{Mg}(\text{CH}_2\text{SiMe}_3)_4(\text{PMDETA})_2$ (0.033 – 0.058 M).

Using an initial rates approach is usually advantageous in intermolecular reactions in negating the necessity for employing high excesses of the other reagent(s) not under investigation (although newer ‘visual’ analysis methods can circumvent this).²⁹¹⁻²⁹³

This use of an initial rate method to avoid using high reagent excesses was not necessary in this case, being an intramolecular transformation, but this approach was decided more suitable in avoiding any complication arising from the apparent substrate inhibition present.

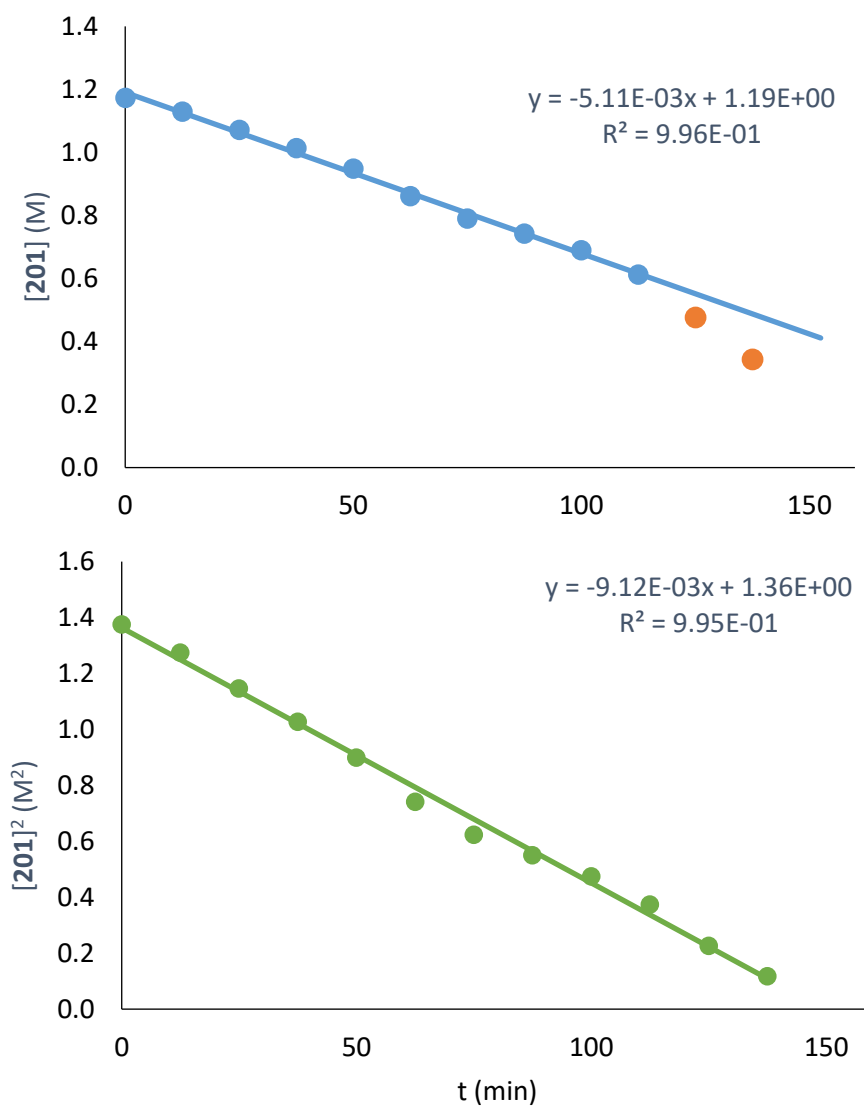
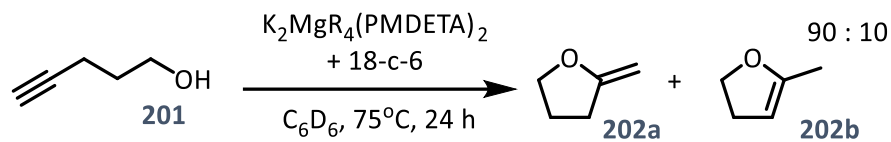


Figure 2.11 –|top| Plot of the consumption of 4-pentynol **201** versus time (0.040 M cat., C_6D_6 , 343 K) |below| $[4\text{-pentynol } \mathbf{201}]^2$ versus time (0.040 M cat., C_6D_6 , 343 K).

Plotting the concentration of major isomer product **202b** at varied alkynol concentration [Figure 2.12] a clear decrease in rate was observed with increasing alkynol concentration (2.50 M omitted from for clarity). This confirms that the substrate alkynol inhibits cyclisation in some way and is likely responsible for the apparent rate acceleration toward the end of the reaction seen in Figure 2.11.

In previous studies of the same reaction by Hill²⁷⁰ employing heavier group 2 amide catalysts a negative first order was observed in alkynol, where its origin is proposed to be the decoordination of a substrate molecule from the active catalyst being required before cyclisation can occur [Scheme 2.20]. When coordination occurs (IV), it appears that the cyclisation process is hindered. As the reaction is inverse first order in substrate it is assumed that the incoming alkynol coordinates to the single Mg centre rather than the K centres, which are already highly coordinated by bonding to the crown ether. In previous studies, the addition of 18-crown-6 has had both beneficial^{285, 294} and detrimental²⁸⁴ impacts on synthetic performance. Here we observe an improvement in catalytic activity, which could perhaps be explained by the 18-crown-6 sufficiently satisfying the coordination environment of the metal, preventing further excess alcohol coordination from occurring which would cause inhibition.

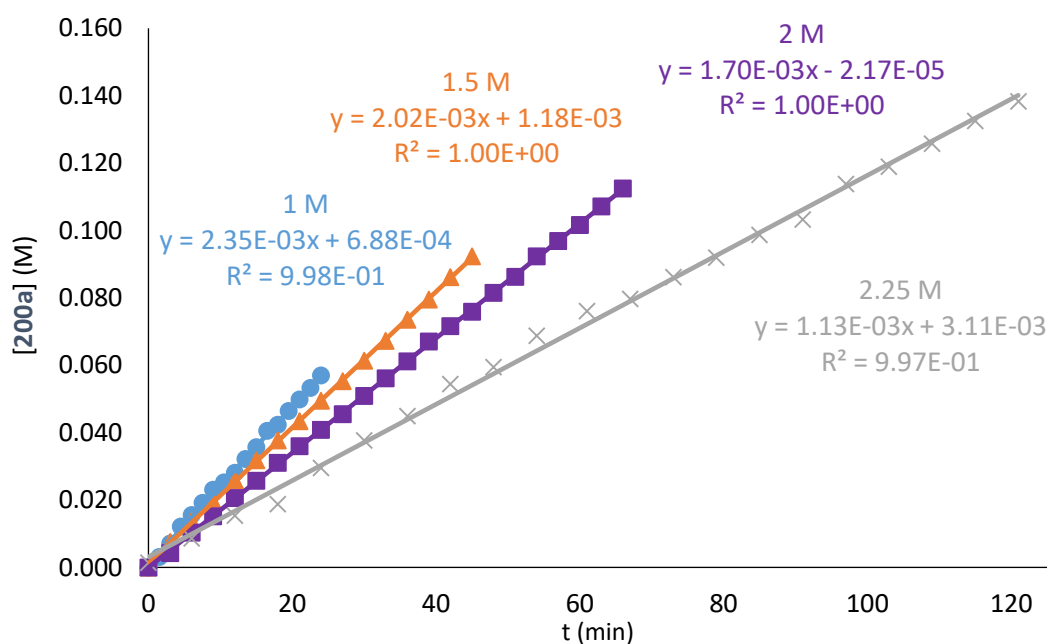


Figure 2.12 – Production of product **202a** (0.033 M cat., C₆D₆, 343 K) at varied substrate concentrations |201| (1.0 - 2.25 M).

This catalytic process can be considered as an initial association/dissociation of alkynol **201** (k_1 and k_{-1}) followed by cyclisation reaction (k_2) as illustrated in **Scheme 2.20**. To obtain a rate equation for this two-step process two different approximations can be made.

The first option is to use a steady-state approximation, this assumes that there is negligible variation in the concentration of intermediate **V**, which remains small.²⁹⁵ It is an appropriate assumption when the first step (in this case dissociation) is slower than the second (cyclisation), and results in rate **eqn. 1**. At low concentrations of **201** the term ' k_2 ' becomes much greater than the term ' $k_{-1}[201]$ ' and the rate equation simplifies to **eqn. 2**.

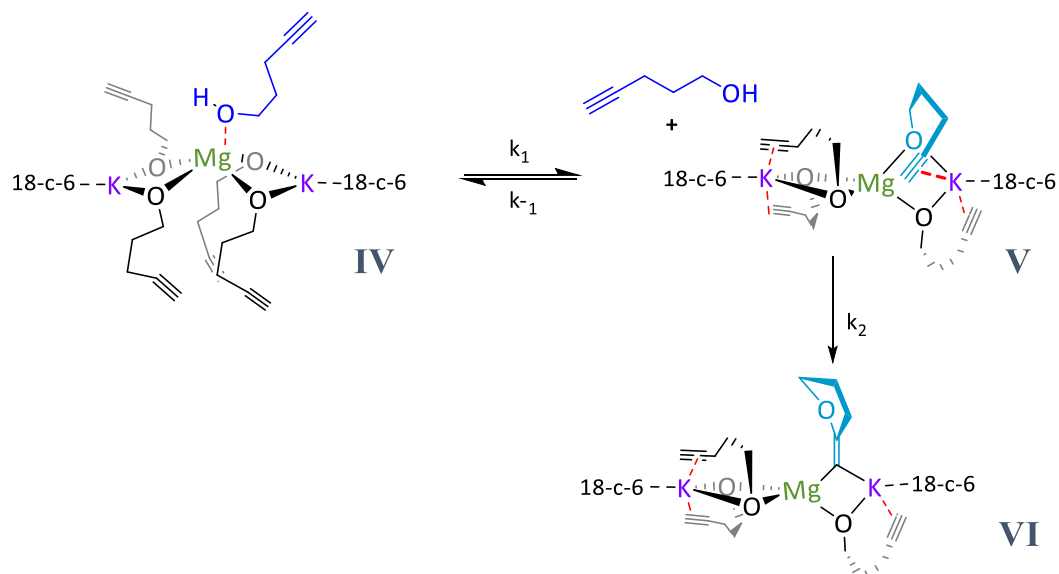
Steady-state approximation
First step slow

$$d[\text{VI}]/dt = \frac{k_1 k_2 [\text{IV}]}{k_{-1}[\text{201}] + k_2} \quad (1) \quad d[\text{VI}]/dt = k_1 [\text{IV}] \quad (2)$$

Pre-equilibrium approximation
First step fast

$$d[\text{VI}]/dt = \frac{k_1 k_2 [\text{IV}]}{k_{-1}[\text{201}]} \quad (3)$$

Alternatively, a pre-equilibrium approximation can be applied which assumes that the species involved in the first step are in equilibrium (in this case a fast association/dissociation step) and the second step (cyclisation) is slower.²⁹⁵ In this case dissociation of **201** from magnesium does not influence the reaction rate, with only cyclisation rate limiting. A good inverse first order relationship in **201** at any concentration of this ligand (as is apparent from rate equation **eq. 3**) should be obtained if this is the case.



Scheme 2.20 – The proposed coordination/decoordination of an additional alkynol molecule responsible for the experimentally observed inhibition term.

Rearranging these equations to the form of the equation of a straight line eqns. 4-5 are obtained, where it can be seen by plotting observed rates (the gradient from plot of [201] vs time assuming steps subsequent to the generation of VI are facile) against 1/[201] in the pre-equilibrium case the plot obtained should be linear. If not, it is likely the steady-state approximation is more fitting for this system.

Steady-state approximation

First step slow

Pre-equilibrium approximation

First step fast

$$d[\text{VI}]/dt = \frac{k_1 k_2 [\text{IV}][\text{201}]}{k_{-1}[\text{201}] + k_2} \quad (1/[\text{201}]) \quad (4)$$

$$d[\text{VI}]/dt = \frac{k_1 k_2 [\text{IV}]}{k_{-1}} \quad (1/[\text{201}]) \quad (5)$$

$$y = mx + c$$

A plot of observed rate against 1/[201] | Figure 2.13 | shows an overall non-linear fit, as this is inconsistent with eqn. 5 a slow ligand dissociation step followed by rapid cyclisation process as described in the steady-state case is a better fit for the system. The extent of the inhibition present at 2.25 M and 2.5 M suggests that above a concentration of 2.0 M in alkynol [201] a further, more strongly inhibiting process is likely at play. As the standard conditions used throughout this study of alkynol cyclisation are circa 1 M this greater level of inhibition at high substrate concentrations was not further investigated, focussing instead on the apparent mechanistic processes at concentrations more relevant to this study.

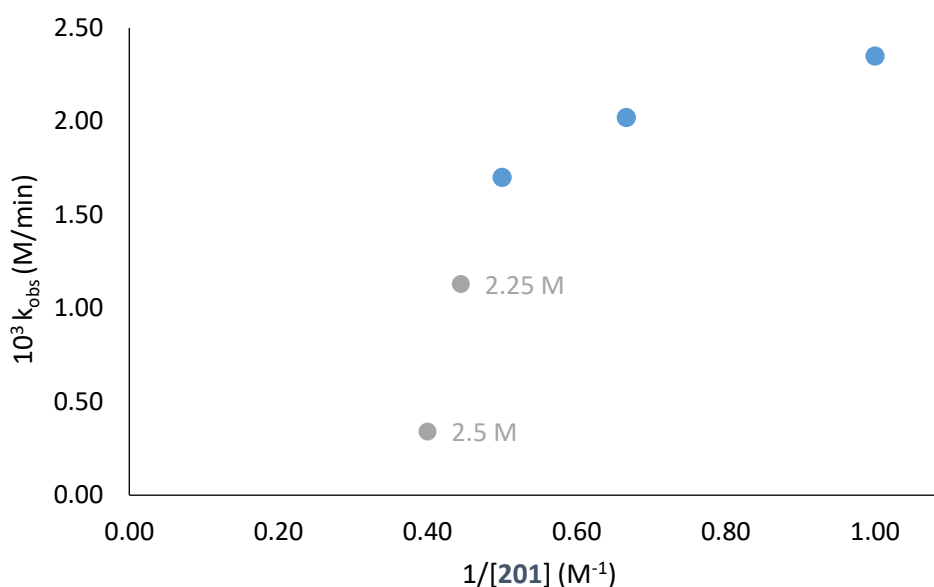


Figure 2.13 – Observed rate constant at varied substrate concentrations versus inverse substrate concentration.

After examining the complex rate dependency of the reaction on alkynol concentration catalyst order was examined, transpiring to be more straightforward.

The concentration of **201** was plotted against time at varied precatalyst concentrations [Figure 2.14]. From this the observed rates (gradient at each catalyst loading) were then plotted against precatalyst concentration [Figure 2.15], with a good linear fit and a positive gradient being obtained. A linear fit and positive gradient are indicative that the reaction has first order dependence on catalyst, with rate increasing linearly with increase catalyst concentration.

A first order dependence on the alkali metal magnesiate precatalyst was also observed here as has previously in the hydroamination of carbodiimides.²²⁰ The order of dependence of the catalyst can also be dependent on the nature of the precatalyst as in studies using heavier alkaline-earth metal amides by Hill²⁷⁰ a second order dependence on precatalyst concentration was found due to the dimeric nature of these amides. By this logic the monomeric nature of $K_2Mg(CH_2SiMe_3)_4(PMDETA)_2$ appears to fit with the observed first order dependence.

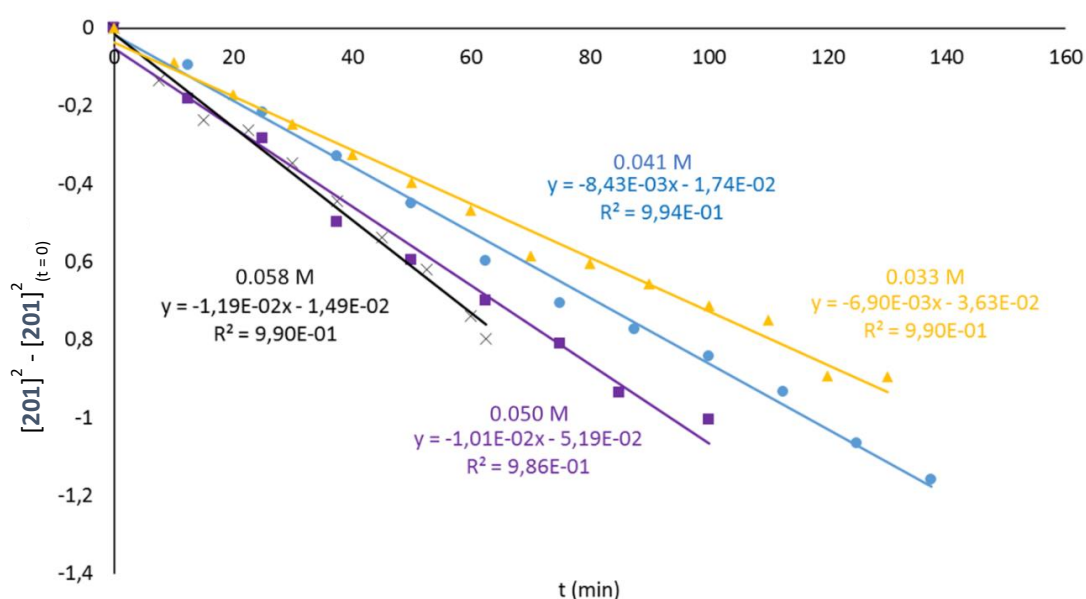


Figure 2.14 – Consumption of 4-pentynol **201** (C_6D_6 , 343 K) at varied catalyst loadings (0.033 - 0.058 M).

To summarise this section mechanistic studies using the reaction kinetics has shed light on the reaction dependency of the concentration of alkyne and precatalyst. They have shown that although a simple first order dependence on the concentration of magnesiate was observed the effect of alkyne concentration on reaction rate is more complicated, involving an inhibition term which likely forms part of the rate determining step. The rate determining step is postulated to consist of a two-step process: dissociation of a molecule of alkyne to the active catalytic magnesiate species, and cyclisation of an alkynoxide arm of the active magnesiate catalyst. The cyclisation itself would seem to intuitively be the highest energy barrier step, and this does appear to be true at low concentrations, where it is likely rate limiting; but at higher alkyne concentrations the inhibiting decoordination term becomes more prevalent and must also be considered part of the rate determining step. At concentrations > 2 M it is likely that an additional inhibiting effect is present. This could be hypothesised to be due to the coordination of a further (second) alkyne molecule causing a second order inhibition, however, this possibility has not been explored and is only speculative.

The reaction dependence of the crown ether co-catalyst has not been studied, in all reactions run as part of these kinetic studies 2 equivalents of 18-c-6 were added per $K_2Mg(CH_2SiMe_3)_4(PMDETA)_2$, as is represented in the species shown in |Scheme 2.20|.

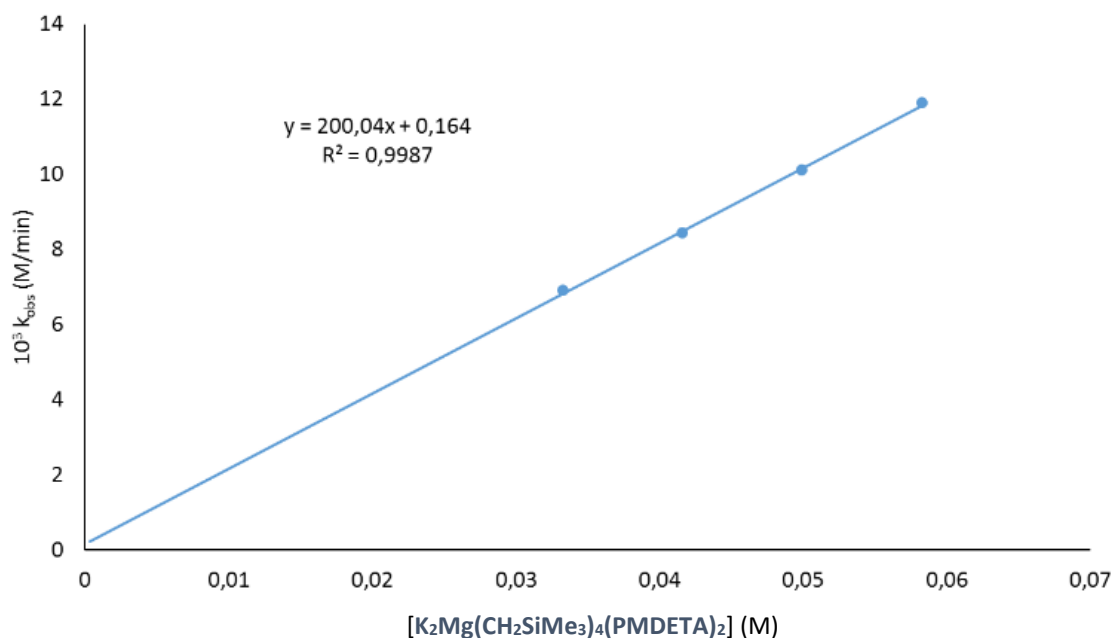


Figure 2.15 – Plot of the observed rate constant at varied catalyst loadings versus catalyst concentration.

2.1.6 Mechanistic interpretation

In terms of mechanism, there has been a previous proposition by Hill²⁷⁰ building upon the work of Marks.²²⁷ It reasons that there are two catalytic cycles at work simultaneously to allow for the production of the two product isomers observed. One cycle involves the alkyne passing through an allene intermediate, where it was demonstrated that starting from an allenyl alcohol instead of the alkynyl alcohol yielded the same products in a similar yield and ratio. In this work utilising alkali metal magnesiate in combination with substrate **203**, we detected the presence of an allene intermediate (by ¹H NMR spectroscopy, at δ 5.19 and 4.63 ppm) during the course of the reaction |**Figure 2.16**|. As such we believe that a similar two-cycle reaction mechanism is likely to be at play. The findings from the kinetics were also included with the other results to form a proposed mechanism for this alkali metal magnesiate-mediated catalysis |**Scheme 2.21**|.

Attempts were made at isolating a catalytically active intermediate with the hopes of determining its structure through single crystal x-ray diffraction, however despite multiple attempts no crystalline solid could be obtained. Despite this it was possible to carry out a solution study on the proposed active species in the form of ¹H DOSY NMR |**Figure 2.17**|. This type of diffusion-based NMR can show which species diffuse together and through a method developed by Stalke²⁹⁶⁻²⁹⁸ can estimate the molecular mass of species in solution. The spectrum clearly shows three diffusing species; TMS, PMDETA, and 4-pentynol and 18-crown-6 diffusing together. This seems to support what was seen in the optimisation |**2.1.2**

Assessing the role of Lewis donors as co-catalysts| where an alkali metal effect between sodium and potassium higher-order magnesiate suggested that the alkali metal (and by extension likely crown ether) remained contacted with the rest of the complex, it also suggests that the PMDETA is non-coordinated. However, when molecular masses were calculated using this method for (using TMS as standard) no satisfactory molecular masses were obtained. The molecular mass found for the diffusing fragments well exceeded the acceptable error making them of little value. As 18-crown-6 was seen to only exist in one environment no acceptable configurations of the magnesiate could be found, with an equilibrium of coordination of 18-c-6 and potassium being the closest. Even the value calculated for the suspected 'free' PMDETA did not fall within the acceptable error range. Therefore, from this ¹H DOSY NMR spectrum only the diffusion of 18-c-6 and 4-pentynol as part of the same species can be taken as significant.

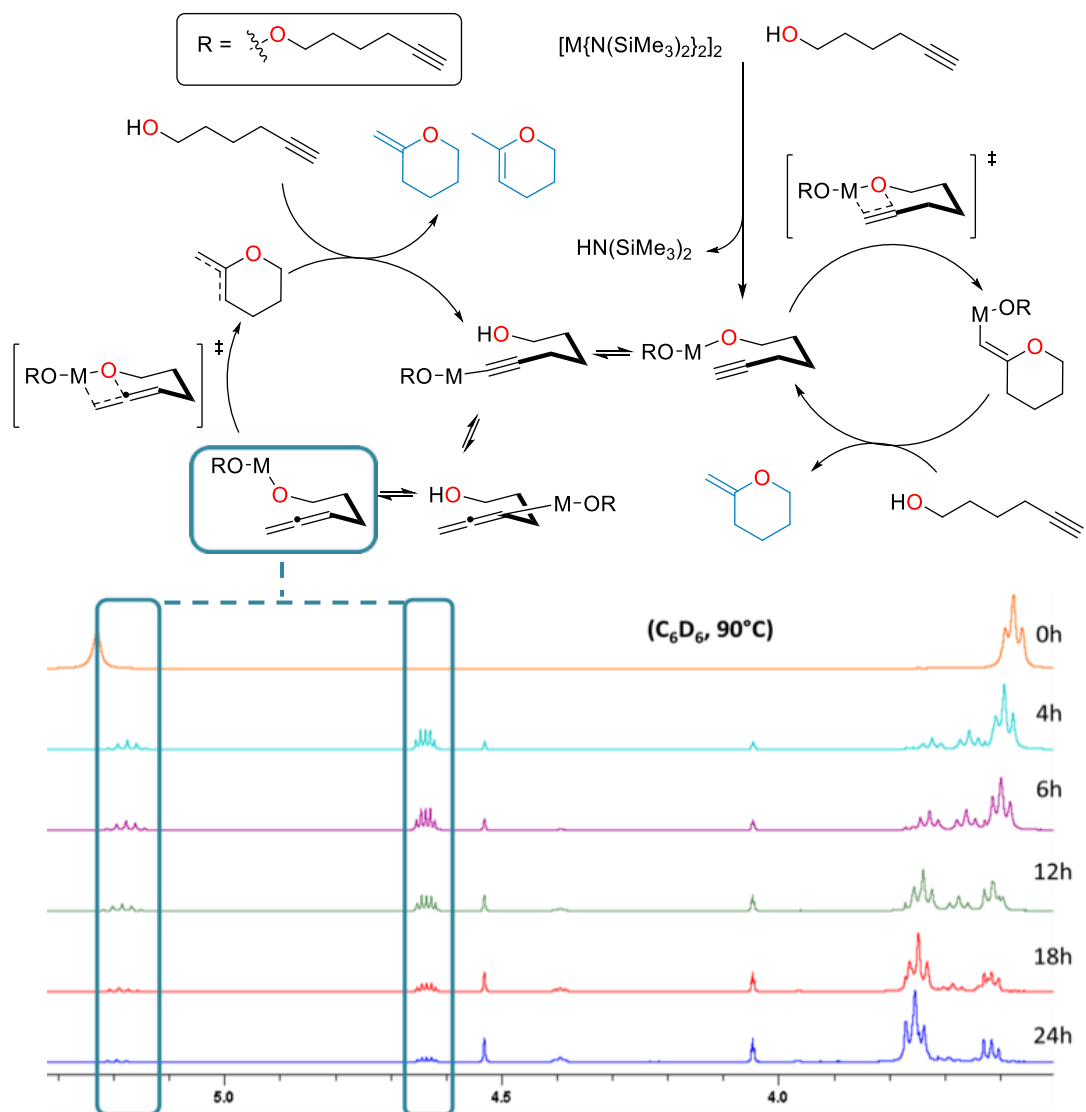
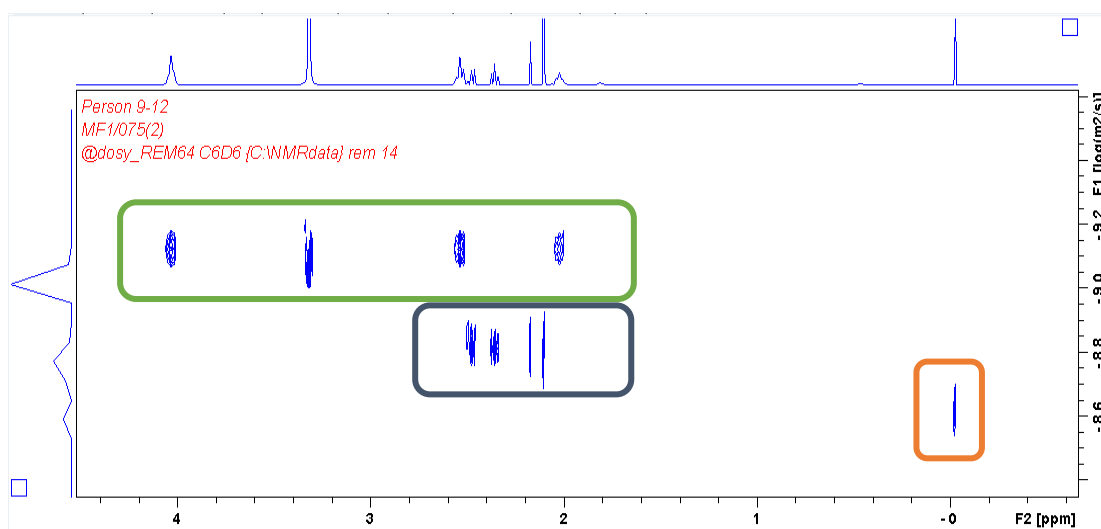


Figure 2.16 – Evidence for the allene intermediate (via 1H NMR spectroscopy, C_6D_6 , 400.1 MHz) produced during cyclisation of 5-hexynol |203, Table 2.6, Entry 1| as proposed by Hill.²⁷⁰



Species	Predicted	Proposed	Error
PMDETA	194	173	+ 12%
$K_2Mg(OR)_4$	600	330	+ 82%
$K_2Mg(OR)_4 + 2$ 18-c-6	600	964	- 38%
$K_2Mg(OR)_4$ (+ 2 18-c-6) in equilibrium	600	661	- 9%

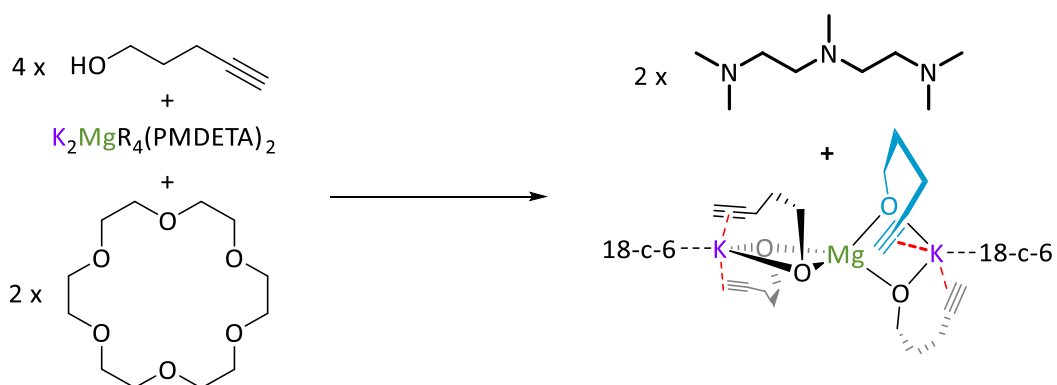


Figure 2.17 – 1H DOSY NMR spectrum (C_6D_6) of $K_2MgR_4(PMDETA)_2 + 4$ x 4-pentynol + 2 x 18-c-6 and suspected species present in mixture.

One final element of the mechanism was observed in the production of a brightly coloured intermediate in the cyclisation of the internal aryl alkynols [Figure 2.18]. This colour intermediate appears toward the end of the reaction and is extinguished upon exposure to air in a matter of seconds. It was initially considered that the bright colour may have been produced by a radical species, however, the sharpness of a ^1H NMR spectrum of the reaction mixture and the inability of the radical trap TEMPO to eliminate the colour appeared to prove otherwise. A radical base mechanism is also unsupported by any other evidence gathered, notably with the Hammett style plot [Figure 2.10] suggesting a negatively charged intermediate rather than positively charged or radical in nature. Thus, it was proposed that the colour is generated by a conjugated anion intermediate.

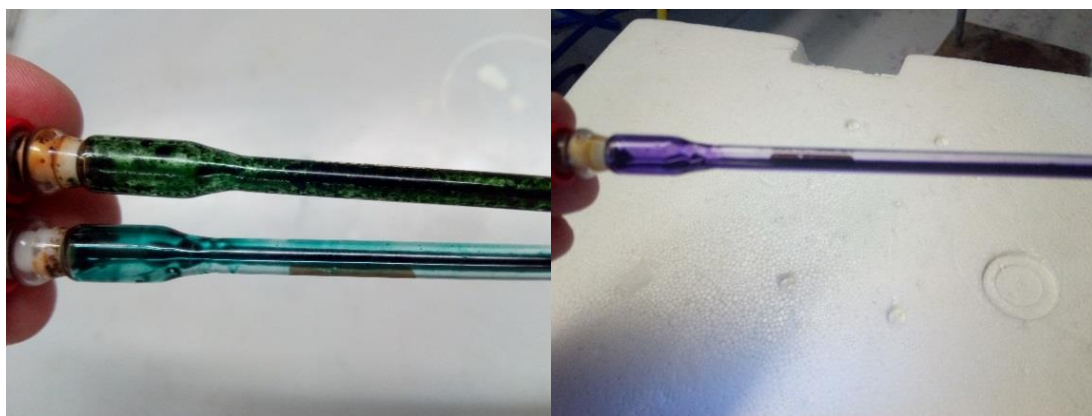
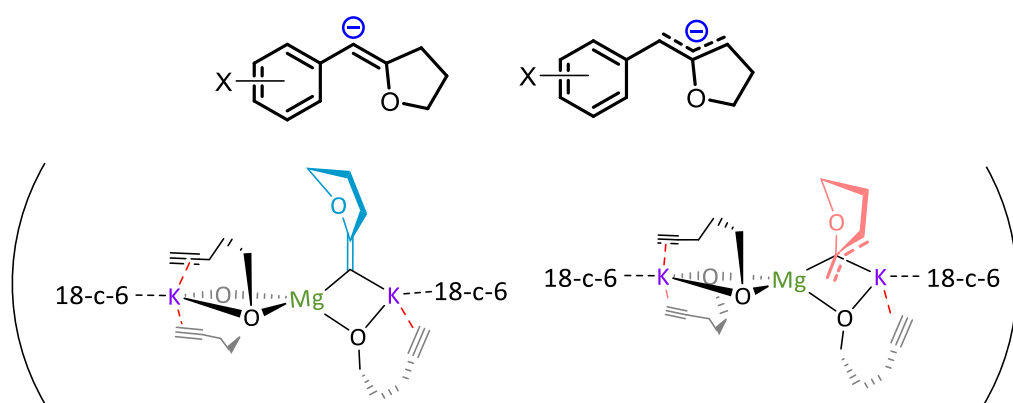


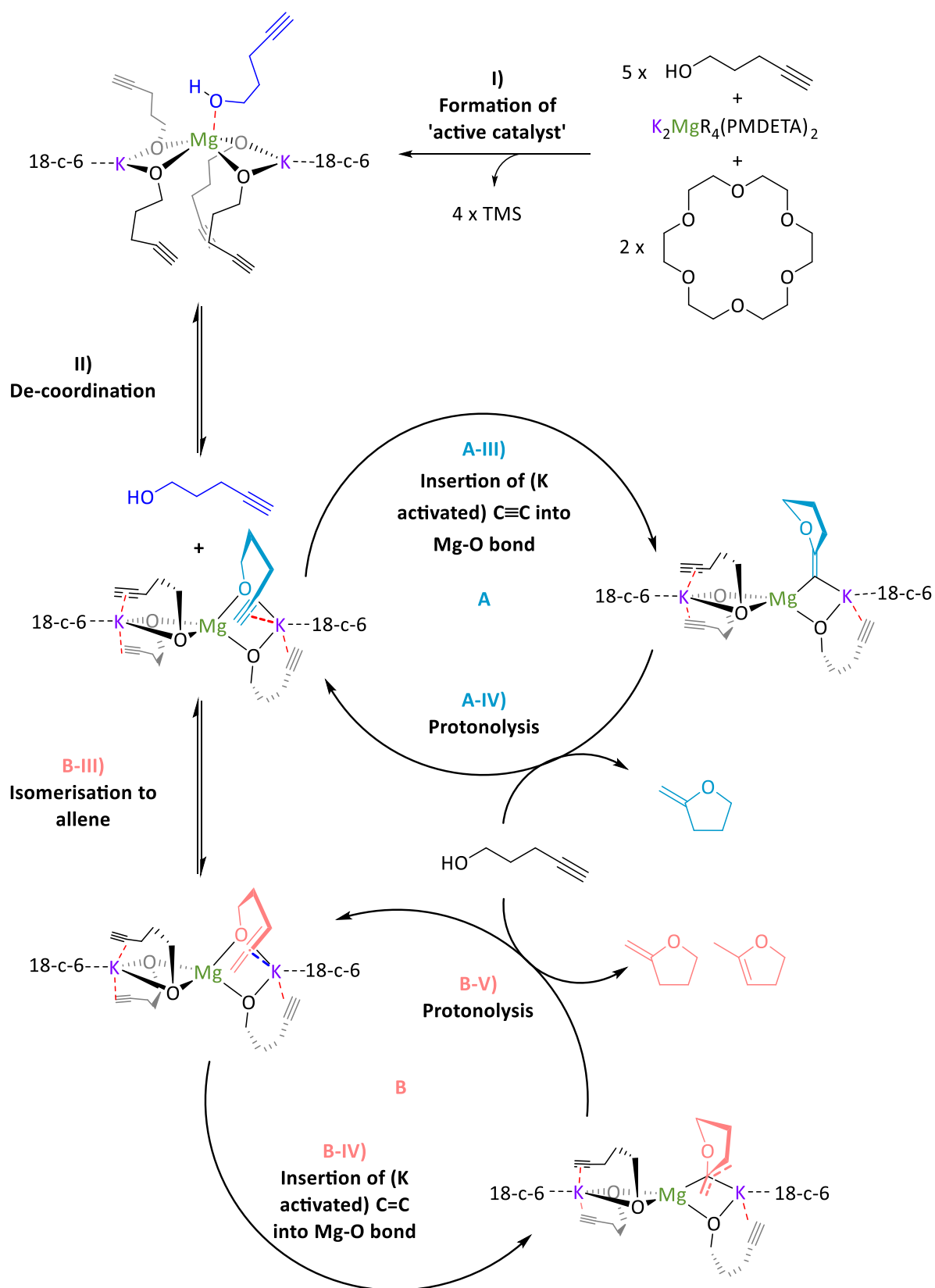
Figure 2.18 – Coloured species produced in the cyclisation of: |Green| $X = m\text{-F}$ [219], internal standard = Hexamethylcyclotrisiloxane; |Blue| $X = m\text{-F}$ [219], IS = 4-bromobenzaldehyde; |Purple| $X = p\text{-CN}$ [223], IS = FeCp_2

With these considerations of intermediates and kinetic studies carried out a mechanism was proposed for these hydroalkoxylation reactions | [Scheme 2.21](#) |.

Overall the deduced mechanism starts with formation of the active catalyst from the magnesiate pre-catalyst. This involves the deprotonation of four alcohol substrate molecules to form a magnesiate alkoxide, liberating tetramethylsilane. This 'active catalyst' is then involved in a coordination/decoordination process with an additional substrate molecule as suggested by the kinetic studies. This additional molecule of **201** occupies the coordination sphere of the magnesium inhibiting cyclisation, giving rise to an inverse first order term in the substrate. Cyclisation (insertion of the carbon-carbon multiple bond into the magnesium oxygen bond) only occurs upon its decoordination.

In cycle A the carbon-carbon triple bond of the alkyne is directly inserted into the metal-oxygen bond, leading to the formation of only one product upon protonolysis. Cycle B on the other hand involves an equilibrium isomerisation from alkyne to allene which upon insertion into the metal-oxygen bond, and subsequent protonolysis, can yield two product isomers. Protonolysis releases the cyclised products and reforms the active catalyst completing the cycle.

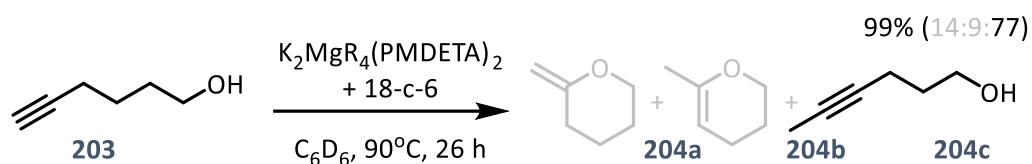
Disclosing a unique cooperative behaviour under catalytic conditions, each of the metals plays a key role in this process, by simultaneously activating the O-H and C≡C bond of the substrate. Thus, coordination of the C≡C bond to the larger more π-philic potassium centre enables further activation of this unsaturated group and brings it into close proximity to the di-anionic (magnesiate) $[\text{Mg}(\text{OR})_4]^{2-}$ component, which is significantly more nucleophilic than a charge-neutral magnesium compound, facilitating the intramolecular ring-closure to furnish the relevant oxygen-heterocycle.



Scheme 2.21 – Proposed mechanism for the alkali metal magnesiate + crown ether co-catalyst mediated catalytic cyclisation of alkynols via dual activation.

2.2 Isomerisation of terminal alkynes

In the cyclisation of 5-hexynol |203| it was observed that the major product was not the cyclised 6-membered cyclic enol ether but in fact the internal alkyne isomer 5-hexynol |204c, Scheme 2.22|. It was not in any way unique, having previously been observed but it did raise the question of if there was value to be gained in performing isomerisations of terminal alkynes.



Scheme 2.22 – The alkali metal magnesiate mediated Isomerisation of 5-hexynol |203|.

It has previously been reported by Tsurugi²⁹⁹ that organomagnesium complexes can promote alkyne isomerisation of benzylic alkynes, occurring in two steps with the relevant allene being first produced before being converted through to the internal allene |Figure 2.19| through temporarily separated auto tandem catalysis.

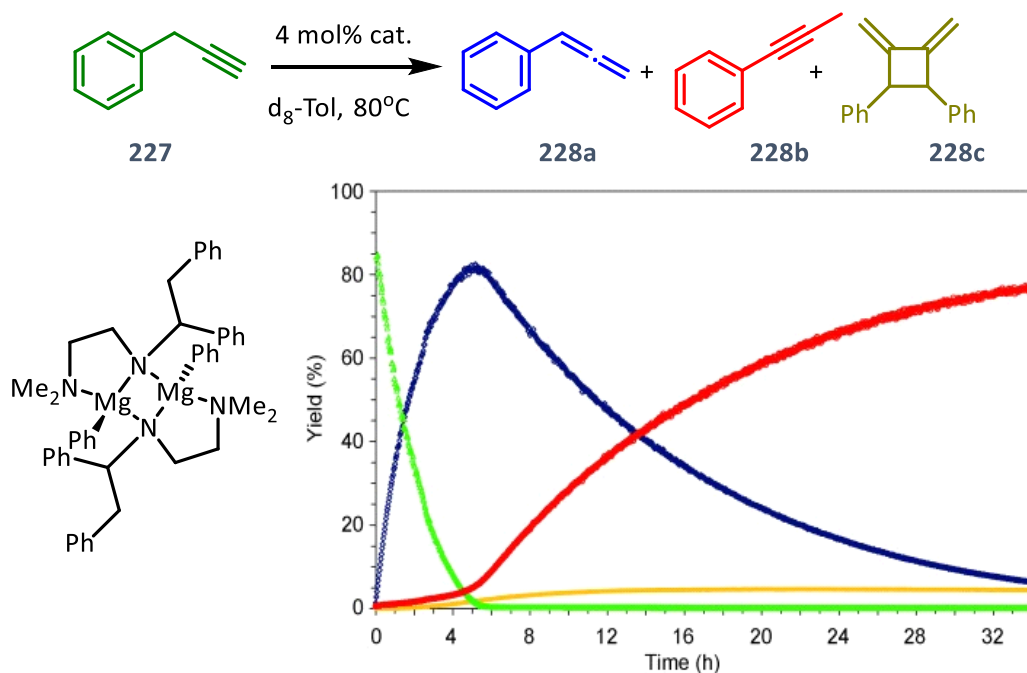


Figure 2.19 – The autotandem catalysis of 3-phenylpropyne |227| by Tsurugi²⁹⁹

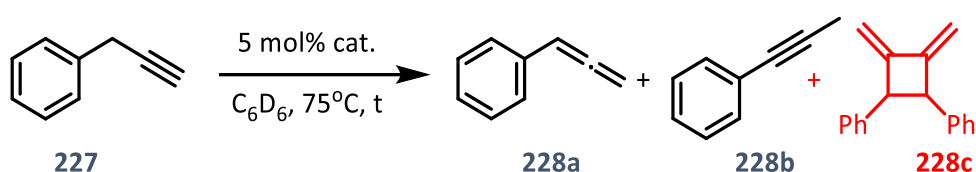
2.2.1 – Optimisation & Substrate scope

It was hoped that using the heterobimetallic alkali metal magnesiate system that the isomerisation of (non-activated) non-benzylic alkynes would be possible given the evidence in the isomerisation of 5-hexynol. Firstly, however, the isomerisation of 3-phenylpropyne was investigated to ensure benzylic alkynes could be satisfactorily isomerised. As with previous work by Tsurugi²⁹⁹ the monometallic compound $\text{Mg}(\text{CH}_2\text{SiMe}_3)_2$ |Table 2.8, Entry 1| was found to promote the formation of allene **228a** but in contrast was not seen to facilitate the second step producing the internal alkyne **228b**. When the monometallic $\text{K}(\text{CH}_2\text{SiMe}_3)$ |Table 2.8, Entry 2| was employed the internal alkyne product |**228b**| was observed with good most 3 h but the second step of transformation of the allene |**228a**| to internal alkyne |**228b**| still incomplete. Moving to the lower-order magnesiate $\text{KMg}(\text{CH}_2\text{SiMe}_3)_3$ |Table 2.8, Entry 3| it is clearer to see the conversion of internal alkyne to allene then to internal alkyne as almost all 3-phenylpropyne |**227**| is converted to phenylpropa-1,2-diene/phenylallene |**228a**| in 1 h and by 3 h has been further isomerised to 3-phenylpropyne |**228b**|. This reaction nicely shows the ability of the two metals to work together to achieve increased reactivity as the reaction time of 3 h is less than that of the homometallic $\text{K}(\text{CH}_2\text{SiMe}_3)$ and much faster than $\text{Mg}(\text{CH}_2\text{SiMe}_3)_2$ or the homometallic organomagnesium complex utilised by Tsurugi, additionally advantageous no homo-coupled product **228d** was observed. This said, it does however appear curious that the overall product yield (97 – 75%) appears to drop between 2- 3 h |Table 2.7, Entries 4-5|, this can only be mainly attributed to a side reaction of the phenylallene **228b** as between these time points (2 – 3 h) the quantity of internal alkyne **228c** remains reasonably constant (0.48 – 0.44 mmol). As no evidence of production of the homo-coupled (3,4-dimethylenecyclobutane-1,2-diyl)dibenzene |**228d**| or any other species was apparent the side product was initially puzzling, however, the same situation arose in the case of $\text{K}_2\text{Mg}(\text{CH}_2\text{SiMe}_3)_4(\text{PMDETA})_2$ but this time ¹H NMR spectroscopy alluding a possible side product. A broad, humping baseline in the aromatic region suggests the occurrence of polymerisation. It is perhaps not surprising that polymerisation can occur with conjugated allenyl and alkynyl compounds such as these.

Currently no further characterisation of the product mixtures, or substantiation of this suspected polymerisation has been carried out. It is also possible that this polymerisation can be avoided by carrying out the reaction at lower temperatures.

Faced with the obstacle of polymerisation using benzylic terminal alkynes, next simple alkyl alkynes were investigated. As 5-hexynol |203| had been previously successfully isomerised 1-hexyne was chosen as a suitable candidate for test reactions/optimisation. The isomerisation of 1-hexyne was seen, as expected, to be more challenging than 3-propyne, however, by applying the conditions used in the cyclisation of 5-hexynol |Scheme 2.22| isomerisation was achieved in 4 h |Table 2.9, Entry 3|.

Table 2.8 – Pre-catalyst selection for the isomerisation of 3-phenylpropyne |227|.

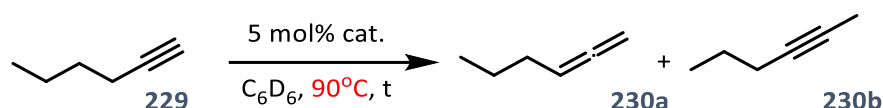


Entry	Pre-catalyst ^[a]	Time (h)	Yield (%) ^[e]	Isomer ratio 228a : 228b
1	MgR₂ ^[b]	6	22	100 : 0
2	KR ^[b]	3	90	33 : 67
3	KMgR₃ ^[c]	1	96	77 : 23
4		2	97	25 : 75
5		3	75	10 : 99
6	K₂MgR₄(PMDETA)₂ ^[d]	1	53	0 : 100

[a] R = (CH₂SiMe₃). [b] Reactions were performed in a Young's cap NMR tube, using 0.5 mmol of substrate (3-phenylpropyne) |227| and 0.025 mmol (5 mol%) pre-catalyst. [c] Reactions were performed in a Young's cap NMR tube, using 0.575 mmol (1.15 eq.) of substrate (3-phenylpropyne) |227| and 0.025 (5 mol%) pre-catalyst. [d] Reactions were performed in a Young's cap NMR tube, using 0.6 mmol (1.2 eq.) of substrate (3-phenylpropyne) |227| and 0.025 (5 mol%) pre-catalyst. [e] Calculated from ¹H NMR spectroscopic data by integration against an internal standard (0.05mmol / 10 mol% ferrocene)

This reaction clearly shows the benefits of a heterobimetallic system as 1-hexyne was previously found unable to be catalytically isomerised with Tsurugi homometallic organomagnesium complex. Interestingly, the same trends in catalyst efficacy observed in the cyclisation of alkynols were observed in isomerisation reactions. The lithium lower-order magnesiate [Table 2.9, Entry 1] and even sodium lower-order magnesiate [Table 2.9, Entry 2] were found to be completely ineffective (on the same time scale) as the potassium lower-order magnesiate [Table 2.9, Entry 3], demonstrating a similar alkali metal effect as was previously [2.1 Hydroalkoxylation/cyclisation of alkynols]. The dependence of the pairing of a crown ether as co-catalyst was also observed, with a lack of 18-crown-6 having a detrimental effect to the reactivity of $K_2Mg(CH_2SiMe_3)_4(PMDETA)_2$ [Table 2.9, Entries 4-5]. The one nuance to the addition of 18-c-6 co-catalyst was seen to be that, in its absence it is possible to form a significant concentration of 1,2-hexadiene [230a], whereas upon addition of 18-c-6, the reaction appears to progress directly to 2-hexyne [230b].

Table 2.9 – Pre-catalyst selection for the isomerisation of 1-hexyne [229].

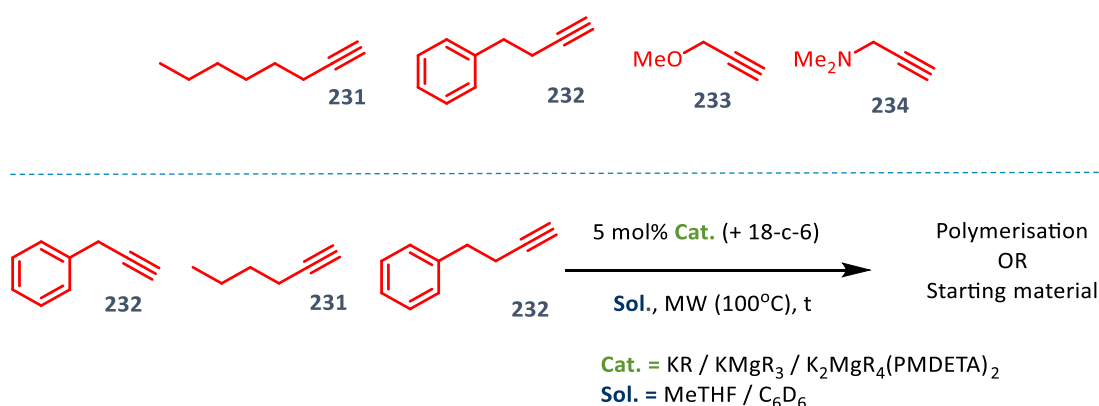


Entry	Pre-catalyst ^[a]	Time (h)	Yield (%) ^[c]	Isomer ratio 230a : 230b
1	$Li_2MgR_4(TMEDA)_2 + 4 \times 12\text{-c-4}$ ^[b]	2	0	-
2	$Na_2MgR_4(TMEDA)_2 + 2 \times 15\text{-c-5}$ ^[b]	2	2	100 : 0
3	$K_2MgR_4(PMDETA)_2 + 2 \times 18\text{-c-6}$ ^[b]	1	46	7 : 93
4		4	98	0 : 100
5	$K_2MgR_4(PMDETA)_2$	24	5	60 : 40

[a] $R = (CH_2SiMe_3)$. Reactions were performed in a Young's cap NMR tube, using 0.6 mmol (1.2 eq.) of substrate (1-hexyne) [229] and 0.025 (5 mol%) pre-catalyst. [b] A stoichiometric quantity of crown ether co-catalyst used according to the alkali metal [i.e., $2 \times 18\text{-c-6} = 10 \text{ mol\%}$ for 5 mol% $K_2MgR_4(PMDETA)_2$]. [c] Calculated from 1H NMR spectroscopic data by integration against an internal standard (0.05 mmol / 10 mol% 1,2,3,4-tetraphenylnaphthalene)

Unfortunately, if these more forcing conditions employed with 1-hexyne are applied to the isomerisation of 3-phenylpropyne it is suspected that polymerisation occurs to an even greater extent. After initial reactions with 3-phenylpropyne and 1-hexyne showing alkali magnesiate as promising catalysts for their isomerisation if suitable conditions can be found, a few, slightly more varied substrates, specifically of those alkynes unable to be cyclised by Tsurugi, were chosen for investigation. [Scheme 2.23]. Both heteroatom containing substrates 3-methoxypropyne/methyl propargyl ether [233] and 3-dimethylaminopropyne/*N,N*-dimethylpropargylamine [234] were found to give unexpected, and unidentified, products. Initially decomposition of the starting material or oligomerisation was suspected as discrete resonances can be observed by ¹H NMR spectroscopy. However, 233 and 234 were seen to be stable to heating overnight at the 90°C reaction temperature without catalyst. It therefore seems possible that oligomerisation of intermediates of products has occurred, or if not there is the possibility of hydroelementation of the carbon-carbon triple bond, however products remain unidentified with low molecular weight/volatility hindering characterisation.

In an attempt to increase the 'greenness' of these isomerisation reactions microwave heating was explored as an option [Scheme 2.23]. 3-Phenylpropyne [227], 1-hexyne [229] and 4-phenylbutyne [232] were heated at 100°C in either C₆D₆ or 2-MeTHF, employing 5 mol% KR, KMgR₃ or KMgR₄(PMDETA)₂ ± 18C6 as pre-catalyst. All cases were unsuccessful, with either recovery of starting material or polymerisation observed. The recovery of starting material could be due to difference in concentration from reactions involving conductive heating or solvent incompatibility.



Scheme 2.23 – Failed substrate scope for alkali metal magnesiate mediated isomerisation.

In summary, alkali metal magnesiates have been shown to successfully promote the catalytic intramolecular hydroalkoxylation of alkynols through cooperative bimetallic catalysis, and show promise in the isomerisation of terminal alkynes.

The role of both magnesium and potassium components are crucial for the success of the process, affording a unique type of substrate activation that is not possible in conventional single-metal systems. Through cooperativity, the utilisation of an alkali metal magnesiate has overcome the inherent problems associated with homometallic magnesium systems. The optimised catalyst system for the cyclisation of alkynols, $K_2Mg(CH_2SiMe_3)_4(PMDETA)_2$ paired with 18-crown-6 has been shown to function well with both terminal and internal alkyne substrates bearing a range of functional groups. Kinetic studies have revealed an inhibition effect of the substrate over the catalyst under standard conditions by the formation of a coordination adduct which requires dissociation prior to the cyclisation step. Initial reactivity studies suggest coordination of the 18-crown-6 to potassium finely tunes the reactivity of the bimetallic system, probably minimising the coordination of additional substrate molecules to the catalyst.

In the case of catalytic cyclisation kinetic studies were conducted that found a first order dependence on the concentration of magnesiate but a more complicated situation with the effect of alkynol concentration, involving an inhibition term arising due to alkynol decoordination, which likely forms part the rate determining step. A mechanism was also produced outlining two catalytic cycles proposed to be responsible for the two different cyclic product isomers obtained.

The case of catalytic terminal alkyne isomerisation, however, remains less well explored. The range of difficulty of isomerisation was seen to result in different conditions being necessary and likely precludes a universal set of optimised conditions. Substrates were found susceptible to side reactions as oligomer- and polymerisation, along with suspected hydroelementation of heteroatom containing alkynes. In all, the catalytic isomerisation of terminal alkynes remains at preliminary stages with no firm grasp of its applicability and limitations.

Further work for these projects involving cooperative catalysis could include the use of an alternative solvent to d_6 -benzene due to its toxicity and derivation from petrochemical sources. Any improvement in either of safety or renewability would greatly improve the methodology of cyclisation. The substrate scope could be widened to include the hydroalkoxylation directly from allenes, instead of the minor products or isomerisations that were seen as a consequence of their generation during the reaction. The cyclisation of allenyl alcohols shows every possibility of being successful as it is suspected to already occur *in-situ*. More challenging, however, would be the successful cyclisation of alkenyl alcohols with the carbon-carbon double bond being harder to hydrofunctionalise than the carbon-carbon triple bond of alkynes. Evidence for the ability to promote the hydroalkoxylation of alkenes was seen, although long reaction times may make the process unsuitable for all but the most activated alkenols.

Also, all reactions carried out have so far involved cyclisation/intramolecular hydroalkoxylation. The next step would therefore seem to be to attempt intermolecular hydroalkoxylation of alkynes/allenes/alkenes with alcohols similar to that already been achieved in the hydroamination of said unsaturated species.

Although tempting to propose the use of heavier alkali metal magnesiates, alkali metal calciates or group 2 heterobimetallic complexes (i.e. a calcium magnesiate) for catalysis these avenues were ruled out due to: the even more hazardous reactivity of the heavier group 1 metals, and the organocalcium compound which would be required to synthesise calcium homologues, $\text{Ca}(\text{CH}_2\text{SiMe}_3)_2$, having a very short half-life (4 at rt. and 30 h at $^\circ\text{C}$ in a pentane/THP/ d_6 -benzene solvent mixture).³⁰⁰

In the isomerisation of terminal alkynes, the use of higher-order magnesiates + crown ether at lower temperatures for the isomerisation of benzylic alkynes could allow for better chemoselectivity and improved reaction times. Also, the use of less volatile alkynes would facilitate product isolation and characterisation. The two catalytic transformations investigated could also be combined by first performing the isomerisation of terminal alkynes to allenes or internal alkynes then addition of an alcohol (or amine / phosphine / thiol) to perform a second catalytic functionalisation step.

II – Global conclusions and further work

In this thesis sustainable methods in the use of polar main group organometallic compounds has been investigated. Two routes have been considered to this end:

1. The investigation of alternative, more sustainable, solvents rather than traditional VOCs for use in selected addition reactions of pyrophoric organolithium reagents in air.
2. The investigation of *s*-block bimetallic cooperative catalysis in isomerisation reactions in which monometallic compounds struggle, as an alternative to less abundant and more expensive transition metal catalysts.

This thesis submits that with regards to consideration 1 the range of reactions involving the addition of organolithium compounds in sustainable solvents in air has been extended. Glycerol and 2-methyltetrahydrofuran, both bio-derived solvents, were found to be compatible with the use of alkyl- and aryllithium, and Grignard reagents under air at ambient temperature. It was found that the addition of aryllithium reagents to nitriles and lithium amides to esters could be successfully carried out under these conditions, therefore, extending the range of reaction known possible for organo-*s*-block reagents not requiring strict inert atmosphere protocols.

In regard to consideration 2 this thesis submits that the alkali metal magnesiate mediated catalytic hydroalkoxylation of alkynols was demonstrated successful; proving that more abundant and cheaper, non-transition metals can be better able to perform catalysis when paired together to exploit cooperativity. In so demonstrating cooperative catalysis to a competent strategy for the reduction in use of rare, toxic, or expensive metal catalysts.

Over all further work which could build upon the findings of this work could involve some of the following.

Additions in glycerol, 2-MeTHF and DESs show potential as being adaptable to flow systems. This could allow for the continuous processes based from these reactions. Equally the use of chiral species in eutectic mixtures could potentially allow for the asymmetric synthesis of compounds. If it is possible to promote asymmetric addition by modification of the solvent it could allow for the production of chiral alcohols or amide by this method. Asymmetric synthesis by this method would also follow 'principle 8 – reduce derivation' by not relying on the temporary modification of substrates to template asymmetric synthesis.

One of the steps in the use of polar main group organometallic compounds that is not carried out in sustainable solvent, and does not have and requires a clear alternative is the formation of the various organometallic species themselves. In this work all synthesised variations of aryllithium compounds and lithium amides were synthesised in hexane, a petroleum derived solvents. Although it may be possible to synthesise these species THF and by extension in 2-MeTHF at low temperatures this is neither ideal. A viable non-protic, non-polar solvent for use in these reactions would allow for the development of more sustainable practices.

In the case of the cyclisation of alkynols, this catalysis work was carried out using benzene as a solvent and thermal heating. Investigation in other solvents would be a clear next step, with microwave irradiation a possible option. Unfortunately, deuterated versions of many of the green solvents are not currently commercially available which impedes NMR studies into the use these solvents. Furthermore, due to the homogenous nature of the catalysis work presented in this thesis it is not readily applicable to larger scale or continuous processes. Catalyst separation and recycling, or immobilisation studies could allow for this to be a possibility.

III - Experimental

Organometallic species were synthesised under a protective atmosphere of argon (or nitrogen) using standard Schlenk techniques³⁰¹ to ensure anhydrous and oxygen free conditions.

Hexane, THF, toluene and diethyl ether used in anhydrous reactions were dried by heating to reflux over sodium ketyl radical under nitrogen, or alternatively dried using a solvent purification system. Other non-deuterated solvents and other organic liquid compounds required to be used in anhydrous conditions were distilled over sodium, calcium hydride or barium oxide, depending on the compound, under a nitrogen atmosphere and stored over molecular sieves. Deuterated solvents used for NMR spectroscopy were degassed (freeze pump thaw) and stored over molecular sieves.

The storage and manipulation of air sensitive solids was carried out in a glovebox filled with an argon atmosphere, with thermally sensitive compounds stored at -18°C in a freezer within the glovebox.

Non-synthesised reagents were obtained from one of the following commercial sources: Merck (formerly Sigma-Aldrich), Alfa Aesar, Fluorochem, TCI (Tokyo Chemical Industry).

NMR spectra were recorded on a Bruker AVIII 400 MHz spectrometer operating at 400.1 MHz for ¹H, 100.6 MHz for ¹³C[¹H], 128.4 MHz for ¹⁹F or 155.5 MHz for ⁷Li.

GC-FID measurements were made on an Agilent Technologies 7820A chromatograph and GCMS on an Agilent Technologies 5975C GC/MS detector. High resolution mass spectrometry was carried out by the EPSRC National Mass Spectrometry Facility, Swansea, or the University of Edinburgh Mass Spectrometry Facility.

III.I Addition of organolithium reagents to nitriles

Phenyllithium was commercially obtained as a 1.9 M solution in di-*n*-butyl ether, and *n*-butyllithium as a 1.6 M solution in hexanes. DESs were prepared following literature procedures.^{13, 302} Aryllithium reagents were synthesised as outlined below.

General procedure for the addition reactions of phenyllithium to nitriles in alternative solvents

Syntheses were performed under air and at room temperature. In a '4D' 14.8 mL vial, the appropriate nitrile (0.5 mmol) was added to the corresponding alternative solvent (0.5 g) under air, followed by the addition of PhLi (1 mmol) at room temperature, and the reaction mixture was stirred for 2–3 s. The reaction was then stopped by addition of a saturated solution of the Rochelle salt (sodium potassium tartrate tetrahydrate). The reaction mixture was transferred to a round-bottom flask, 2 M HCl (5 mL) was added and heated at 100°C for 30 min. After cooling down to room temperature, the reaction mixture was neutralized by addition of NaHCO₃ and the organic products were extracted with dichloromethane (3x 5mL). The combined organic extracts were dried over MgSO₄ and the solvent removed under reduced pressure. Yields of the reaction crudes were determined by ¹H NMR methodology by using dibromomethane as an internal standard. The identity of obtained ketones (**1003**, **1005**, **1007**, **1011**, **1013**, **1015**, **1017**, **1303**),³⁰³ **1003**(*n*Bu),³⁰⁴ **1019**,³⁰⁵ **1031**,³⁰⁶ and **1035**³⁰⁷ was assessed by comparison of their ¹H and ¹³C NMR spectroscopic data with those reported in the literature. Compound 3i was isolated and fully characterized. All reactions were done in triplicate to ensure good reproducibility of the obtained yields.

General procedure for the synthesis of aryllithium reagents

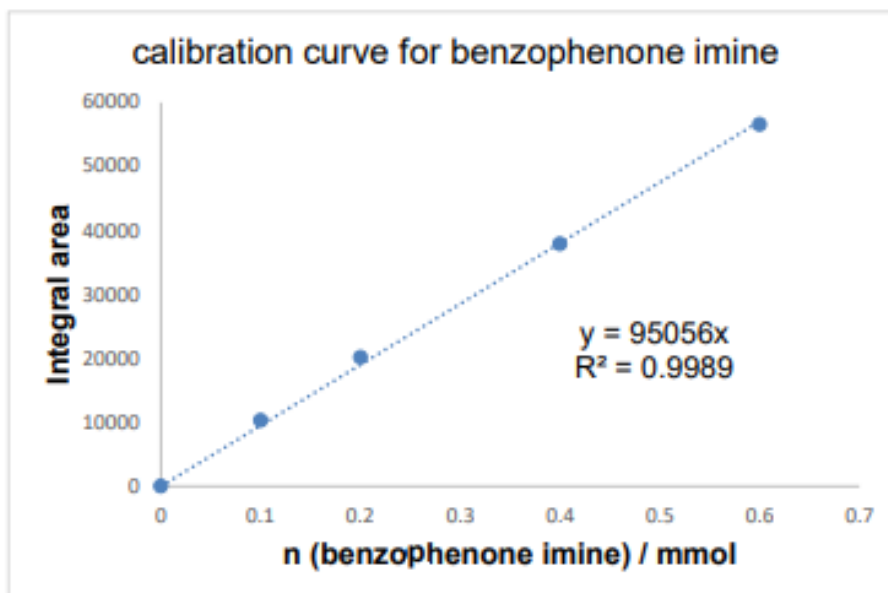
In addition to commercially available PhLi, other aryllithium reagents were tested as reagents that can undergo addition to benzonitrile. These were prepared under protective argon atmosphere by using standard Schleck techniques and solvent dried by heating to reflux over sodium benzophenone ketyl and then distilled under nitrogen prior to use. To a stirring solution of the chosen aryl iodide (6 mmol) in 2.2 mL of diethyl ether at -78°C, *n*-butyllithium (3.8 mL, 6 mmol) was added drop-wise. The reaction mixture was warmed up and stirred at room temperature for 2 h before it was used as a 1 M solution of aryllithium reagent for the addition reactions. The following additions were, as described above, performed under air in triplicate.

Comparison of the stability of phenyllithium in glycerol and water

Phenyllithium (0.53 mL, 1 mmol) was added to glycerol or water (0.5 g) and stirred under air. After 15 s, benzonitrile (0.051 g, 0.5 mmol) was added under air at room temperature and the reaction mixture was stirred for 2–3 s. The reaction was then stopped by addition of a saturated solution of the Rochelle salt and the product was hydrolysed, isolated, identified and quantified as previously described.

Addition of various equivalents of phenyllithium to benzonitrile in glycerol (GC-FID calibration)

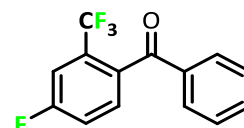
Ph ₂ NH (mmol)	Peak area
0	0
0.1	10299.9
0.2	20180
0.4	37903.4
0.6	56590.6
0	0



Eq. PhLi	Peak area	Ph ₂ NH (mmol)	Conversion (%)
1.0	36627.1	0.385	77
1.5	38060.8	0.400	80
2.0	40426.9	0.425	85
2.5	40369.8	0.424	85
3.0	40682.9	0.427	85

Characterisation of new addition products

2-(trifluoromethyl)-4-fluorobenzophenone | 1009 |



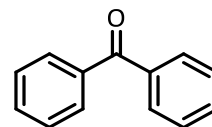
NMR: ¹H (400.1 MHz, CDCl₃): δ 7.77 (m, 2H), 7.62 (tt, 7.4 Hz, 1.3 Hz), 7.48 (m, 3H), 7.41 (dd, 8.7 Hz, 5.3 Hz), 7.33 (td, 8.1 Hz, 2.6 Hz); ¹³C[¹H] (100.6 MHz, CDCl₃): δ 194.2, 162.5 (d, 252 Hz), 136.1, 134.3 (m), 133.5, 130.6 (d, 8.3 Hz), 130.3, 128.1, 124.0, 121.2 (q, 275 Hz), 118.4 (d, 21.5 Hz), 114.3 (dq, 25 Hz, 4.8 Hz); ¹⁹F (128.4 MHz, CDCl₃): δ -58.5 (s, 3F), -108.2 (td, 8.4 Hz, 5.5 Hz).

MS (ASAP/TOF-MS): m/z: 269.0590 (M+H), 249.0527 (M-F) – C₁₄H₈O F₄

Other addition products

benzophenone

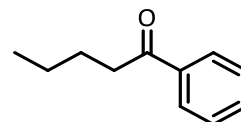
| 1003 |



^1H (400.1 MHz, CDCl_3): δ 7.81 (2H, m, Ar), 7.58 (1H, t, $J = 7.4$ Hz, Ar), 7.48 (2H, t, $J = 7.5$ Hz, Ar).

1-phenylpentan-1-one

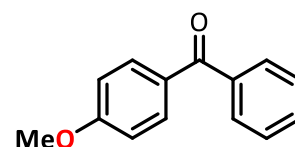
| 1003(nBu) |



^1H (400.1 MHz, CDCl_3): δ 7.94 (2H, m, Ar), 7.58 (1H, t, $J = 7.3$ Hz, Ar), 7.43 (2H, t, $J = 7.3$, Ar).

4-methoxybenzophenone

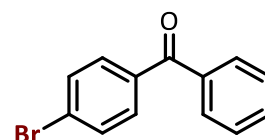
| 1005 |



^1H (400.1 MHz, CDCl_3): δ 7.82 (2H, d, $J = 8.8$ Hz, Ar), 7.75 (2H, m, Ar), 7.57 (1H, t, $J = 8.8$ Hz, Ar), 7.44 (2H, m, Ar), 6.94 (2H, m, Ar), 3.87 (3H, s, CH_3).

4-bromobenzophenone

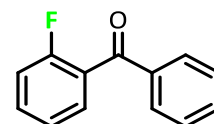
| 1007 |



^1H (400.1 MHz, CDCl_3): δ 7.75 (2H, m, Ar), 7.66 (2H, dt, $J = 8.7, 2.0$ Hz), 7.60 (2H, dt, $J = 8.7, 2.0$ Hz), 7.58 (1H, m, Ar), 7.46 (2H, t, $J = 7.7$ Hz, Ar).

2-fluorobenzophenone

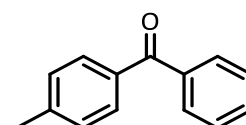
| 1011 |



^1H (400.1 MHz, CDCl_3): δ 7.84 (2H, m, Ar), 7.61-7.44 (5H, m, Ar), 7.25 (1H, td, $J = 7.6, 1.0$ Hz, Ar), 7.15 (1H, t, $J = 9.0$ Hz, Ar); ^{19}F (128.4 MHz, CDCl_3): δ -111.0 (m, ArF).

4-methylbenzophenone

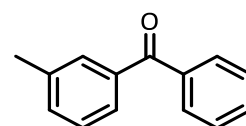
| 1013 |



^1H (400.1 MHz, CDCl_3): δ 7.78 (2H, m, Ar), 7.72 (2H, d, $J = 8.1$ Hz, Ar), 7.56 (1H, t, $J = 7.4$ Hz, Ar), 7.46 (2H, t, $J = 7.5$ Hz, Ar), 7.27 (2H, d, $J = 7.8$ Hz, Ar), 2.43 (3H, s, CH_3).

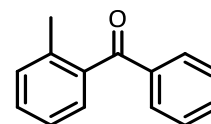
3-methylbenzophenone

| 1015 |



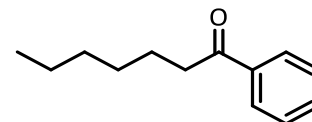
^1H (400.1 MHz, CDCl_3): δ 7.82 (2H, m, Ar), 7.65 (1H, m, Ar), 7.62-7.56 (2H, m, Ar), 7.48 (2H, t, $J = 7.5$ Hz, Ar), 7.43-7.34 (2H, m, Ar), 2.43 (3H, s, CH_3).

2-methylbenzophenone
| 1017 |



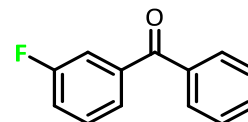
^1H (400.1 MHz, CDCl_3): δ 7.81 (2H, m, Ar), 7.57 (1H, t, $J = 7.3$ Hz, Ar), 7.45 (2H, t, $J = 7.6$ Hz, Ar), 7.39 (1H, t, $J = 7.4$, 1.6 Hz, Ar), 7.33-7.21 (3H, m, Ar), 2.34 (3H, s, CH_3).

1-phenylheptan-1-one
| 1019 |



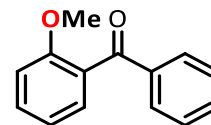
^1H (400.1 MHz, CDCl_3): δ 7.98 (2H, m, Ar), 7.57 (1H, t, $J = 7.3$ Hz, Ar), 7.47 (2H, t, $J = 7.5$ Hz, Ar), 2.98 (2H, t, $J = 7.4$ Hz, COCH_2), 1.77 (2H, m, COCH_2CH_2), 1.39 (2H, m, $\text{COC}_2\text{H}_5\text{CH}_2\text{CH}_2$), 0.94 (3H, m, $\text{COC}_4\text{H}_8\text{CH}_3$).

3-fluorobenzophenone
| 1031 |



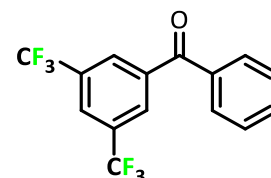
^1H (400.1 MHz, CDCl_3): δ 7.82 (2H, m, Ar), 7.63 (1H, t, $J = 7.5$ Hz, Ar), 7.59 (1H, d, $J = 7.8$ Hz, Ar), 7.55-7.49 (3H, m, Ar), 7.48 (1H, td, $J = 8.0$ Hz, 5.5 Hz, Ar); ^{19}F (126.4 MHz, CDCl_3): δ -111.9 (td, $J = 9.0$, 5.5 Hz, ArF).

2-methoxybenzophenone
| 1033 |



^1H (400.1 MHz, CDCl_3): δ 7.84 (2H, m, Ar), 7.57 (1H, t, $J = 7.4$ Hz, Ar), 7.51-7.46 (1H, m, Ar), 7.44 (2H, t, $J = 7.7$ Hz, Ar), 7.38 (1H, dd, $J = 7.5$, 1.8 Hz, Ar), 7.06 (1H, $J = 7.4$, 1.0 Hz, Ar), 7.02 (1H, d, $J = 8.3$ Hz), 3.73 (3H, s, CH_3).

3,5-bis(trifluoromethyl)benzophenone
| 1035 |



^1H (400.1 MHz, CDCl_3): δ 8.26 (2H, brs, Ar), 8.12 (1H, brs, Ar), 7.82 (2H, m, Ar), 7.70 (1H, t, $J = 7.4$ Hz, Ar), 7.57 (2H, t, $J = 7.7$ Hz, Ar); ^{19}F (126.4 MHz, CDCl_3): δ -63.0 (s, CF_3).

III.II Amidation of esters using lithium amides

n-Butyllithium was commercially obtained as a 1.6 M solution in hexanes. DESs were prepared following literature procedures.^{13, 302} Lithium amides and esters **1053**, **1055**, **1067** were synthesised as outlined below

General procedure the amidation of esters

Additions were performed under air at room temperature in an open Schlenk flask (25 mL) and 1 g of solvent. Lithium amide (1.5 mmol, 1.5 eq.) was added to a stirring solution (960 rpm) of ester/amide (1 mmol). After 20 s the reaction was quenched by the addition of sat. Rochelle's salt sol. (sodium potassium tartrate tetrahydrate, 5 mL) before being extracted into 2-MeTHF (3 x 10 mL). Extractions were combined, dried over MgSO₄ and concentrated under vacuum.

Crude products were purified by silica column chromatography eluted by hexane:EtOAc (10:1 – 2:1 gradient). Products were identified by GCMS and ¹H spectroscopy. Yields were obtained by ¹H NMR spectroscopy by integration against a ferrocene internal standard.

¹H NMR spectra of products matched those previously reported [**1044**,¹⁶⁶ **1046**,³⁰⁸ **1052**,³⁰⁹ **1054**,³¹⁰ (**1056**, **1058**),³¹¹ (**1060**, **1062**),³¹² (**1066**, **1068**),³¹³ **1074**,¹⁶⁶ **1076**,³¹⁰ **1078**,³¹²,³¹⁴ **1080**,³¹⁵ **1082**,^{165, 316} **1084**,^{313, 317} **1086**,³¹⁷ **1088**,³¹⁸ **1099**,¹⁶⁶ **1103**³¹³] or where unreported were characterized by ¹H, ¹³C and ¹⁹F NMR spectroscopy and high-resolution mass spectrometry (**1048**, **1050**, **1064**, **1090**).

General procedure for the synthesis of lithium amides

n-BuLi (19 mL, 30 mmol) was added dropwise to a stirring solution of amine (30 mmol) in hexane (60 mL) and left to stir for 1 h. The resultant suspension was filtered and washed with hexane (3 x 10 mL) before being dried under vacuum. The white solid product obtained was stored in an argon filled glovebox and checked by ¹H and ⁷Li NMR spectroscopy.

*Procedure for the lifetime study of lithium *N*-methylanilide in glycerol and 2-MeTHF*

Additions were performed under air at room temperature in an open Schlenk flask (25 mL). Lithium *N*-methylanilide solution (1.5 mL, 1.5 mmol, 1.5 eq.) was added to a stirring solution (960 rpm) solvent (1 g). After a set time interval ethyl benzoate (144 μL, 1 mmol) was added. After 20 s the reaction was quenched by the addition of sat. Rochelle's salt sol. (sodium

potassium tartrate tetrahydrate, 5 mL) before being extracted into 2-MeTHF (3 x 10 mL). Extractions were combined, dried over MgSO₄ and concentrated under vacuum.

Crude products were purified by silica column chromatography eluted by hexane:EtOAc (10:1 – 2:1 gradient). Products were identified by GCMS and ¹H spectroscopy. Yields were obtained by ¹H NMR spectroscopy by integration against a ferrocene internal standard.

Procedure for the in-situ amidation of ethyl benzoate

Additions were performed under air at room temperature in an open Schlenk flask (25 mL) and 1 g/1.16 mL of 2-MeTHF. *n*-BuLi (0.94 mL, 1.5 mmol, 1.5 eq.) was added to a stirring solution (960 rpm) of ethyl benzoate (144 μL, 1 mmol) and amine (1.5 mmol, 1.5 eq.). After 20 s the reaction was quenched by the addition of sat. Rochelle's salt sol. (sodium potassium tartrate tetrahydrate, 5 mL) before being extracted into 2-MeTHF (3 x 10 mL). Extractions were combined, dried over MgSO₄ and concentrated under vacuum.

Crude products were purified by silica column chromatography eluted by hexane:EtOAc (10:1 – 2:1 gradient). Products were identified by GCMS and ¹H spectroscopy. Yields were obtained by ¹H NMR spectroscopy by integration against a ferrocene internal standard.

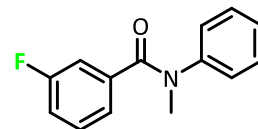
Procedure for the synthesis of esters

Esters **1053**, **1055**, **1067** were prepared from their corresponding acids (*p*-methoxybenzoic acid, *m*-methoxybenzoic acid and *n*-octanoic acid). Typical scale 20 mmol. Acids were dissolved in EtOH, acidified to ≤ pH3 by addition of H₂SO₄ (conc.) and refluxed overnight. The resultant solution was neutralized with sat. NaHCO₃ sol. And extracted into EtOAc (3 x 20 mL). Extracts were combined, dried over MgSO₄ and concentrated under vacuum. The product ester did not require purification, only drying over molecular sieves.

Characterisation of new amidation products

3-fluoro-*N*-methyl-*N*-phenylbenzamide

| 1048 |

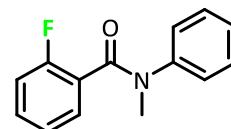


NMR ^1H (400.1 MHz, CDCl_3 , ppm): δ 7.26 (3H, m, Ar), 7.14 (6H, m, Ar), 6.95 (1H, m, Ar), 3.52 (3H, s, CH_3); ^{13}C [^1H] (100.6 MHz, CDCl_3 , ppm): δ 168.6 (CO), 162.7 (Ar), 160.3 (Ar), 144.0 (Ar), 137.6 (d, $J = 7$ Hz, Ar), 128.9 (Ar), 128.8 (Ar), 126.3 (Ar), 123.9 (d, $J = 3.0$ Hz, Ar), 116.1 (d, $J = 21$ Hz, Ar), 115.3 (d, $J = 23$ Hz, Ar), 38 (CH_3); ^{19}F (128.4 MHz, CDCl_3 , ppm): δ -112.8 (s, ArF).

MS: 229.08991 (M^+) - $\text{C}_{14}\text{H}_{12}\text{ONF}$

2-fluoro-*N*-methyl-*N*-phenylbenzamide

| 1050 |

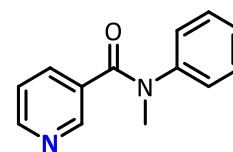


NMR ^1H (400.1 MHz, CDCl_3 , ppm): δ 7.19 (8H, m, Ar), 6.78 (1H, s, Ar), 3.47 (3H, s, CH_3); ^{13}C [^1H] (100.6 MHz, CDCl_3 , ppm): δ 166.6 (CO), 159.2 (Ar), 156.8 (Ar), 143.4 (Ar), 131.1 (d, $J = 8$ Hz, Ar), 129.3 (d, $J = 3$ Hz, Ar), 127.0 (Ar), 126.83 (Ar), 125.3 (d, $J = 17$ Hz, Ar), 123.9 (Ar), 115.5 (d, $J = 22$ Hz, Ar), 37.4 (CH_3); ^{19}F (128.4 MHz, CDCl_3 , ppm): δ 113.1 (s, ArF).

MS: 229.08959 (M^+) - $\text{C}_{14}\text{H}_{12}\text{ONF}$

N-methyl-*N*-phenylnicotinamide

| 1064 |

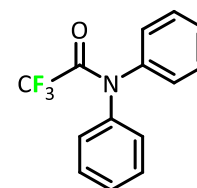


NMR ^1H (400.1 MHz, CDCl_3 , ppm): δ 8.43 (1H, d, $J = 1.7$ Hz, Ar), 8.37 (1H, dd, $J = 4.9, 1.6$ Hz, Ar), 7.53 (1H, $J = 8.0, 2.0$ Hz, Ar), 7.18 (t, $J = 7.5$ Hz, Ar), 7.10 (tt, $J = 7.3, 2.0$ Hz, Ar), 7.03 (1H, dd, $J = 8.0, 4.8$ Hz, Ar), 6.98 (2H, d, $J = 7$ Hz, Ar), 3.43 (3H, s, CH_3); ^{13}C [^1H] (100.6 MHz, CDCl_3 , ppm): δ 168.0 (CO), 150.2 (Ar), 149.5 (Ar), 144.1 (Ar_{ipso}), 136.0 (Ar), 131.7 (Ar_{ipso}), 129.4 (Ar), 127.1 (Ar), 127.0 (Ar), 38.3 (CH_3).

MS: 212.09441 - (M^+) $\text{C}_{13}\text{H}_{12}\text{ON}_2^+$

2,2,2-trifluoro-*N,N*-diphenylacetamide

| 1090 |

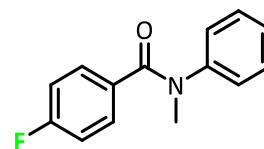


NMR ^1H (400.1 MHz, CDCl_3): δ 7.41 (3H, brs, Ar), 7.39 (2H, brs, Ar), 7.32 (5H, brs, Ar); ^{13}C [^1H] (100.6 MHz, CDCl_3): δ 157.0 (q, $J = 36$ Hz, CO), 141.7 (br, Ar_{ipso}), 129.6 (Ar), 128.8 (br, Ar), 127.8 (br, Ar), 126.2 (br, Ar), 116.7 (q, $J = 289$ Hz, CF_3); ^{19}F (128.4 MHz, CDCl_3): δ -66.9 (s, CF_3).

MS: 265.07090 - (M^+) $\text{C}_{14}\text{H}_{10}\text{ONF}_3^+$

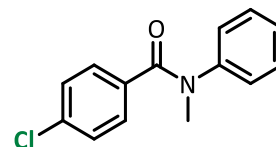
Other amidation products

4-fluoro-*N*-methyl-*N*-phenylbenzamide | 1046 |



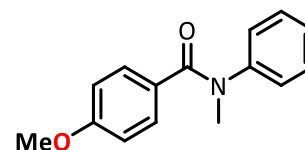
^1H (400.1 MHz, CDCl_3): δ 7.30 (2H, m, Ar), 7.23 (2H, t, $J = 7.5$ Hz, Ar), 7.14 (1H, t, 7.4 Hz, Ar), 7.02 (2H, m, Ar), 6.82 (2H, t, $J = 8.6$ Hz, Ar), 3.48 (3H, s, CH_3); ^{19}F (126.4 MHz, CDCl_3): δ -110.1 (s, ArF).

4-chloro-*N*-methyl-*N*-phenylbenzamide | 1052 |



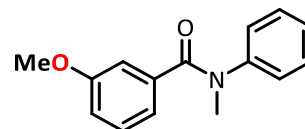
^1H (400.1 MHz, CDCl_3): δ 7.31-7.08 (7H, m, Ar), 7.03 (2H, d, $J = 7.6$ Hz), 3.49 (3H, s, CH_3).

4-methoxy-*N*-methyl-*N*-phenylbenzamide | 1054 |



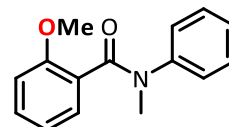
^1H (400.1 MHz, CDCl_3): δ 7.29 (2H, d, $J = 8.5$ Hz, Ar), 7.23 (2H, t, $J = 7.6$ Hz, Ar), 7.13 (1H, t, $J = 7.2$ Hz, Ar), 7.05 (2H, d, $J = 7.6$ Hz, Ar), 3.71 (3H, s, NCH_3), 3.49 (3H, s, OCH_3).

3-methoxy-*N*-methyl-*N*-phenylbenzamide | 1056 |



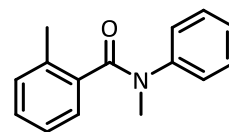
^1H (400.1 MHz, CDCl_3): δ 7.31-6.66 (9H, m, Ar), 3.63 (3H, s, NCH_3), 3.49 (3H, s, OCH_3).

2-methoxy-*N*-methyl-*N*-phenylbenzamide | 1058 |



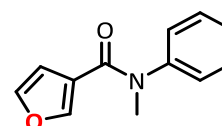
^1H (400.1 MHz, CDCl_3): δ 7.27-6.90 (7H, m, Ar), 6.79 (1H, brs, Ar), 6.62 (1H, brs, Ar), 3.60 (3H, s, NCH_3), 3.48 (3H, s, OCH_3).

N,2-dimethyl-*N*-phenylbenzamide | 1060 |



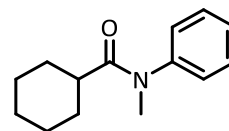
^1H (400.1 MHz, CDCl_3): δ 7.35-6.58 (9H, m, Ar), 3.38 (3H, brs, NCH_3), 2.24 (3H, s, OCH_3).

N-methyl-*N*-phenylfuran-3-carboxamide | 1062 |



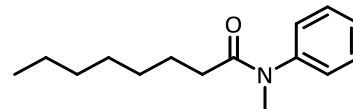
^1H (400.1 MHz, CDCl_3): δ 7.37 (3H, d, $J = 6.6$ Hz, Ar), 7.19 (2H, d, $J = 7.6$ Hz, Ar), 7.11 (1H, brs, Ar), 6.87 (1H, brs, Ar), 6.09 (1H, brs, Ar), 3.39 (1H, brs, NCH_3).

***N*-methyl-*N*-phenylcyclohexane-1-carboxamide**
| 1066 |



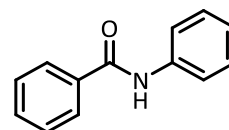
^1H (400.1 MHz, CDCl_3): δ 7.38 (3H, m, Ar), 7.18 (2H, d, $J = 7.2$ Hz, Ar), 3.24 (1H, s, NCH_3), 2.19 (1H, brs, COCH), 1.60 (7H, m, cy), 1.18 (1H, m, cy), 0.96 (1H, m, cy).

***N*-methyl-*N*-phenyloctanamide**
| 1068 |



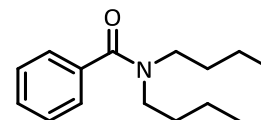
^1H (400.1 MHz, CDCl_3): δ 7.38 (3H, m, Ar), 7.18 (2H, d, $J = 7.6$ Hz, Ar), 3.27 (1H, s, NCH_3), 2.07 (2H, brs, COCH_3), 1.57 (2H, brs, COCH_2CH_3), 1.19 (8H, m, $\text{COC}_2\text{H}_4\text{C}_4\text{H}_8$), 0.85 (3H, t, $J = 6.7$ Hz, $\text{COC}_6\text{H}_{12}\text{CH}_3$).

***N*-phenylbenzamide**
| 1074 |



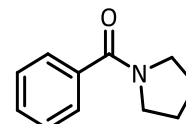
^1H (400.1 MHz, CDCl_3): δ 7.93 (1H, brs, NH), 7.86 (2H, d, $J = 7.8$ Hz, Ar), 7.65 (2H, d, $J = 7.8$ Hz, Ar), 7.54 (1H, t, $J = 7.3$ Hz, Ar), 7.47 (2H, t, $J = 7.6$ Hz, Ar), 7.37 (2H, t, $J = 7.7$ Hz, Ar), 7.15 (1H, t, $J = 7.5$ Hz, Ar).

***N,N*-dibutylbenzamide**
| 1076 |



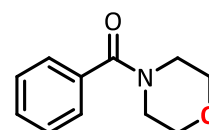
^1H (400.1 MHz, CDCl_3): δ 7.38 (5H, s, Ar), 3.51 (2H, brs, NCH_2), 3.21 (2H, brs, NCH_2), 1.66 (2H, brs, NCH_2CH_2), 1.50 (2H, brs, NCH_2CH_2), 1.42 (2H, brs, $\text{NC}_2\text{H}_4\text{CH}_2$), 1.16 (2H, brs, $\text{NC}_2\text{H}_4\text{CH}_2$), 1.00 (3H, brs, $\text{NC}_3\text{H}_6\text{CH}_3$), 0.80 (3H, brs, $\text{NC}_3\text{H}_6\text{CH}_3$).

***N*-benzoylpyrrolidine**
| 1078 |



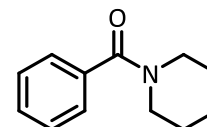
^1H (400.1 MHz, CDCl_3): δ 7.52 (2H, s, Ar), 7.40 (3H, s, Ar), 3.65 (2H, brs, NCH_2), 3.42 (2H, brs, NCH_2), 1.96 (2H, m, NCH_2CH_2), 1.87 (2H, m, NCH_2CH_2).

4-benzoylmorpholine
| 1080 |

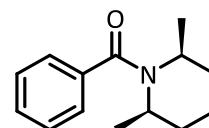


^1H (400.1 MHz, CDCl_3): δ 7.39 (5H, s, Ar), 3.97-3.57 (6H, m, CH_2), 3.57-3.20 (2H, m, CH_2).

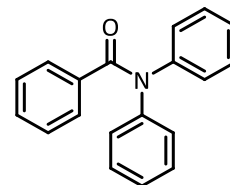
4-benzoylpiperidine
| 1082 |



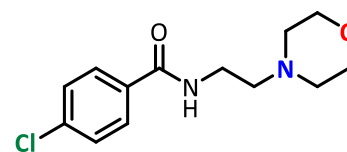
^1H (400.1 MHz, CDCl_3): δ 7.34 (5H, s, Ar), 3.66 (2H, brs, NCH_2), 3.29 (2H, brs, NCH_2), 1.62 (4H, brs, NCH_2CH_2), 1.47 (2H, brs, $\text{NC}_2\text{H}_4\text{CH}_2$).

4-benzoyl(2,6-dimethylpiperidine)**| 1084 |**

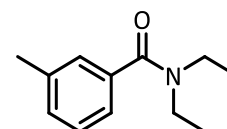
^1H (400.1 MHz, CDCl_3): δ 7.36 (5H, m, Ar), 4.45 (2H, brs, NCH), 1.86 (1H, m, Alk), 1.68 (2H, m, Alk), 1.59 (3H, m, Alk), 1.28 (6H, d, $J = 6.7$ Hz, CH_3).

N,N*-diphenylbenzamide*| 1090 |**

^1H (400.1 MHz, CDCl_3): δ 7.49 (2H, d, $J = 7.0$ Hz, Ar), 7.32 (5H, m, Ar), 7.28-7.10 (8H, m, Ar).

moclobemide**| 1099 |**

^1H (400.1 MHz, CDCl_3): δ 7.73 (2H, d, $J = 7.8$ Hz, Ar), 7.40 (2H, d, $J = 7.8$ Hz, Ar), 7.01 (1H, brs, NH), 3.72 (4H, brs, OCH_2), 3.54 (2H, m, CONHCH_2), 2.60 (2H, m, NCH_2), 3.72 (4H, brs, NCH_2).

N,N*-diethyl-3-methylbenzamide*| 1103 |**

^1H (400.1 MHz, CDCl_3): δ 7.27 (1H, t, $J = 7.3$ Hz, Ar), 7.23-7.06 (3H, m, Ar), 3.54 (2H, brs, NCH_2), 3.26 (2H, brs, NCH_2), 2.37 (3H, s, CH_3), 1.24 (3H, brs, NCH_2CH_3), 1.11 (3H, brs, NCH_2CH_3).

Lithium amide X-ray crystal structures

Compound	lithium 2,2'-bipyridylamide	lithium diphenylamide	Lithium anilide
Empirical formula	Li ₂ O ₂ N ₆ C ₃₀ H ₃₆	Li ₂ O ₄ N ₂ C ₄₄ H ₆₀	Li ₂ O ₄ N ₂ C ₃₂ H ₅₂
Mol. mass	526.53	694.82	542.63
Crystal system	monoclinic	monoclinic	monoclinic
a (Å)	9.7406(4)	10.2268(4)	9.0773(3)
b (Å)	10.9189(4)	19.0435(7)	20.9604(6)
c (Å)	14.1465(7)	10.7658(5)	9.2929(4)
α (°)	90	90	90
β (°)	107.012(5)	102.453(4)	112.088(4)
γ (°)	90	90	90
V (Å³)	1438.74(11)	2047.35(15)	1638.34(11)
Z	2	2	2
λ (Å)	1.54184 (CuKα)	1.54184 (CuKα)	1.54184 (CuKα)
Measured Reflections	10712	23108	7885
Unique reflections	2857	7090	3103
R_{int}	0.0786	0.0775	0.0313
Obs. Reflections [I ≥ 2σ (I)]	2274	6096	2523
Goof [on F²]	1.058	1.225	1.611
R [on F, obs. flns.]	0.0591	0.0987	0.1125
ωR [on F²]	0.1830	0.2948	0.3718
Largest diff. peak/hole e (Å⁻³)	0.29/-0.26	0.72/-0.34	0.83/-0.61

III.III Solvent directed reactivity

Ethyllithium was commercially obtained as a 0.5 M solution in benzene:cyclohexane, ethylmagnesium bromide as a 1M solution in THF , and phenyllithium as a 1.9 M solution in di-*n*-butyl ether. DESs,^{13, 302} TMCDA,³¹⁹ diphenylzinc^{320, 321} and lithium triphenylzincate^{322, 323} were synthesised following literature procedures.

General procedure the addition of organolithium and Grignard reagents to 4-phenylbut-3-ene-2-one in DESs

Additions were performed under air at room temperature in '2D or 4D' (7.4 or 14.8 mL) vials using 0.5 g of solvent (and varied quantity of copper salt additive). EtLi (2 mL, 0.5 M in benzene/cy, 1.0 mmol/2.0 eq.) OR EtMgBr (1 mL, 1 M in THF, 1.0 mmol/2 eq.) was added to a stirring suspension 4-phenylbut-3-ene-2-one (0.073g, 0.5 mmol, 1 eq.). After 20 s the reaction was quenched by the addition of sat. Rochelle's salt sol. (sodium potassium tartrate tetrahydrate) before being extracted into 2-DCM (3 x 10 mL). Extractions were combined, dried over MgSO₄ and concentrated under vacuum.

Crude products were determined by GCMS and yields were obtained by ¹H NMR spectroscopy by integration against a dibromomethane internal standard.

III.IV Hydroalkoxylation/cyclisation of alkynols

(Trimethylsilyl)methyl lithium was commercially obtained as a 1 M solution in pentanes. Pre-catalysts were prepared and isolated prior to being employed in reactions. ME_6TREN ,^{324, 325} $\text{K}(\text{CH}_2\text{SiMe}_3)$,^{326, 327} $[\text{Mg}(\text{CH}_2\text{SiMe}_3)_2, \text{NaMg}(\text{CH}_2\text{SiMe}_3)_3, \text{KMg}(\text{CH}_2\text{SiMe}_3)_3]$,^{218, 328} $[\text{Na}(\text{CH}_2\text{SiMe}_3), \text{Na}_2\text{Mg}(\text{CH}_2\text{SiMe}_3)_4(\text{TMEDA})_2, \text{K}_2\text{Mg}(\text{CH}_2\text{SiMe}_3)_4(\text{TMEDA})_2, \text{K}_2\text{Mg}(\text{CH}_2\text{SiMe}_3)_4(\text{PMDETA})_2]$,²¹⁸ $[\text{LiMg}(\text{CH}_2\text{SiMe}_3)_3, \text{Li}_2\text{Mg}(\text{CH}_2\text{SiMe}_3)_4(\text{TMEDA})_2]$,³²⁹ and alkynols **211**, **213**, **215**, **217**, **219**, **221**, **223** and **225**^{330, 331} were prepared from literature procedures as outlined below.

Synthesis of alkali metal magnesite pre-catalysts

$\text{K}_2\text{Mg}(\text{CH}_2\text{SiMe}_3)_4(\text{PMDETA})_2$ was prepared by suspending $\text{K}(\text{CH}_2\text{SiMe}_3)$ (0.25 g, 2 mmol) and $\text{Mg}(\text{CH}_2\text{SiMe}_3)_2$ (0.20 g, 1 mmol) in hexane (10 mL). The mixture was stirred at ambient temperature for 1 h. PMDETA (0.43 mL, 2 mmol) was added to this white suspension and the mixture gently heated until homogeneity was achieved. After storing at -26°C overnight, the mixture was filtered to yield a pale yellow solid (typical yield; 0.62 g, 78%).

$\text{Li}_2\text{Mg}(\text{CH}_2\text{SiMe}_3)_4(\text{TMEDA})_2$, $\text{Na}_2\text{Mg}(\text{CH}_2\text{SiMe}_3)_4(\text{TMEDA})_2$, $\text{K}_2\text{Mg}(\text{CH}_2\text{SiMe}_3)_4(\text{TMEDA})_2$ were prepared using similar methods to $\text{K}_2\text{Mg}(\text{CH}_2\text{SiMe}_3)_4(\text{PMDETA})_2$ with the following modifications: substitution of TMEDA (0.30 mL, 2 mmol); $\text{Li}(\text{CH}_2\text{SiMe}_3)$ (2 mL, 2 mmol); and/or $\text{Na}(\text{CH}_2\text{SiMe}_3)$ (0.22 g, 2 mmol) where appropriate.

$\text{LiMg}(\text{CH}_2\text{SiMe}_3)_3$, $\text{NaMg}(\text{CH}_2\text{SiMe}_3)_3$, $\text{KMg}(\text{CH}_2\text{SiMe}_3)_3$ were prepared using half the molar quantity of $\text{M}(\text{CH}_2\text{SiMe}_3)_3$ (1 mL, 0.11 g/0.13g respectively), and toluene (5 mL) was added in place of the multidentate amine in order to achieve dissolution upon heating.

Procedure for NMR scale reactions

In the catalytic cyclisation of 4-pentynol **201** with $\text{K}_2\text{Mg}(\text{CH}_2\text{SiMe}_3)_4(\text{PMDETA})_2$ + 18-C-6, 4-pentynol (56 μL , 0.6 mmol, 1.2 eq.) (0.2 eq. / 20 mol% excess required to form the 'active catalyst') was added to a Young's tap NMR tube alongside C_6D_6 (0.54 mL), 1,2,3,4-tetraphenylnaphthalene (0.022 g, 0.05 mmol, 0.1 eq.) and 18-crown-6 (0.013 g, 0.05 mmol, 0.1 eq.). To this $\text{K}_2\text{Mg}(\text{CH}_2\text{SiMe}_3)_4(\text{PMDETA})_2$ (0.020 g, 0.025 mmol, 0.05 eq.) was added and the tube placed in an oil bath at 75°C . The reaction was periodically monitored by ^1H NMR spectroscopy and the yields obtained were calculated using NMR spectroscopic integrals and are relative to the internal standard.

Optimisation and substrate scope reactions were carried out using similar procedures, employing 10 mol% of an appropriate internal standard [1,2,3,4-tetraphenylnaphthalene (0.022 g) or ferrocene (0.009 g)] and with the oil bath temperature being changed where necessary based on observed reaction times. 0.5 mmol of alkynol substrate was used with the monometallic species and lower-order magnesiates, and 0.6 mmol with higher-order magnesiate pre-catalysts. 0.025 mmol precatalyst was employed in all cases.

Procedure for kinetic studies

In the kinetic studies to determine the rate dependence of alkynol in the cyclisation of 4-pentynol **201** with $\text{K}_2\text{Mg}(\text{CH}_2\text{SiMe}_3)_4(\text{PMDETA})_2$ + 18-C-6, 4-pentynol (56 μL , 0.6 mmol) was placed in a Young's tap NMR tube with C_6D_6 (0.6 mL), 1,2,3,4-tetraphenylnaphthalene (0.022 g, 0.05 mmol) and 18-crown-6 (0.010 g, 0.04 mmol). To this $\text{K}_2\text{Mg}(\text{CH}_2\text{SiMe}_3)_4(\text{PMDETA})_2$ (0.016 g, 0.02 mmol) was added. The reaction was maintained at 70°C in the NMR spectrometer and was monitored by ^1H NMR spectroscopy. Yields were calculated using NMR spectroscopic integrals characteristic to **202a** relative to the internal standard, 1,2,3,4-tetraphenylnaphthalene.

This procedure was repeated with 0.90, 1.20 and 1.35 mmol of alkynol **201** and was also applied to the investigation of the dependence on catalyst of the reaction. The same quantity of solvent and standard were used along with a fixed 1.20 mmol quantity of alkynol **201**. In terms of pre-catalyst, 0.025, 0.030 and 0.035 mmol quantities of $\text{K}_2\text{Mg}(\text{CH}_2\text{SiMe}_3)_4(\text{PMDETA})_2$ were employed, necessitating 0.05, 0.06 and 0.07 mmol of 18-crown-6 co-catalyst.

Synthesis and characterisation of new alkynol and cyclic products

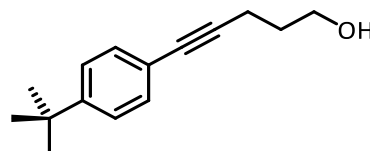
Compounds **211**, **213**, **215**, **217**, **219**, **221**, **223** and **225** were prepared by Sonogashira cross-coupling^{330, 331} from 4-pentynol and the relevant iodoaryl compound. For the example of **211**:

$\text{Pd}(0)(\text{PPh}_3)_4$ (49 mg, 0.04 mmol, 0.01 eq.) and $\text{Cu}(I)I$ (15 mg, 0.08 mmol, 0.02 eq.) were added to a stirring mixture of iodobenzene (0.56 mL, 5 mmol, 1.25 eq.), 4-pentynol (0.37 mL, 4 mmol, 1 eq.) and triethylamine (11 mL, 80 mmol, 20 eq.) in THF (1 mL) and left to stir overnight at rt. The resultant product mixture was filtered and concentrated under reduced pressure yielding the crude product mixture. The crude product mixture was purified by silica column chromatography eluted by hexane:ethyl acetate on a 10:1 to 3:1 gradient.

The appropriate fraction was concentrated under reduced pressure to yield the purified product (typical yield 80%).

Compounds **214a**, **216a**, **218a**, **220a**, **222a** and **224a** were formed by catalytic cyclisation and isolated by silica column chromatography eluted by hexane:ethyl acetate [hexane:diethyl ether for **220a**] on a 10:1 to 3:1 gradient. The appropriate fraction was concentrated under reduced pressure to yield the purified product.

5-[4-(tert-butyl)phenyl]pent-4-yn-1-ol
| 213 |

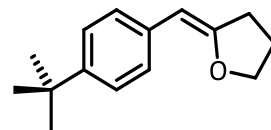


R_f: (Hx:EtOAc 2:1) 0.33, (1:1) 0.55

NMR: ¹H (400.1 MHz, CDCl₃) δ 7.33 (2H, d, J = 8.7 Hz, Ar), 7.30 (2H, d, J = 8.7 Hz, Ar), 3.82 (2H, m, CH₂OH), 2.53 (3H, t, J = 6.9 Hz, CCCH₂), 1.86 (2H, quin, J = 6.5 Hz, CH₂CH₂OH), 1.63 (1H, s, OH), 1.30 (9H, s, tBu). ¹³C[¹H] (100.7 MHz, CDCl₃) δ 150.9 (Ar_{ipso}), 131.4 (Ar), 125.4 (Ar), 120.8 (Ar_{ipso}), 88.6 (ArCC), 81.3 (ArCC), 62.0 (CH₂OH), 34.8 (C[CH₃]₃), 31.6 (CH₂CH₂OH), 31.3 (C[CH₃]₃), 16.2 (CCCH₂).

MS (ASAP/TOF-MS): 217.1592 (M+H) - C₁₅H₂₁O

(Z)-2-(2,2-dimethylpropylidene)tetrahydrofuran
| 214a |

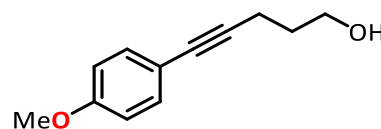


R_f: (Hx:EtOAc 2:1) 0.59, (1:1) 0.68

NMR: ¹H (400.1 MHz, CDCl₃) δ 7.31 (2H, dt, J = 8.4, 2.0 Hz, Ar), 7.13 (2H, dt, J = 8.4, 2.0 Hz, Ar), 5.90 (1H, s, CCH), 4.11 (2H, t, J = 6.8 Hz, CH₂O), 2.82 (2H, dt, J = 7.6, 2.0 Hz, CCH₂), 2.0 (2H, quin, J = 7.0 Hz, OCH₂CH₂), 1.32 (9H, s, tBu). ¹³C[¹H] (100.7 MHz, CDCl₃) δ 158.7 (OCCH), 147.5 (Ar_{ipso}), 134.9 (Ar_{ipso}), 126.7 (Ar), 125.3 (Ar), 98.8 (CCH), 69.5 (OCH₂), 34.5 (C[CH₃]₃), 31.5 (C[CH₃]₃), 28.3 (OCH₂CH₂), 25.5 (CCCH₂).

MS (ASAP/TOF-MS): 216.1514 (M) - C₁₅H₂₀O

5-(4-methoxyphenyl)pent-4-yn-1-ol
| 215 |



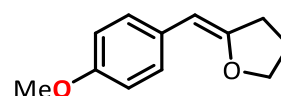
Pale-yellow waxy solid

mp. : 38-40°C / R_f: (Hx:EtOAc 2:1) 0.21, (1:1) 0.38

NMR: ¹H (400.1 MHz, CDCl₃) δ 7.32 (2H, td, J = 9.0, 2.3 Hz, Ar), 6.1 (2H, td, J = 9.0, 2.2 Hz, Ar), 3.81 (2H, t, J = 6.2 Hz, CH₂OH), 3.78 (3H, s, OCH₃), 2.52 (2H, t, J = 6.9 Hz, CCCH₂), 1.85 (2H, quin, J = 6.5 Hz, CH₂CH₂OH), 1.70 (1H, s, OH). ¹³C[¹H] (100.7 MHz, CDCl₃) δ 159.2 (Ar_{ipso}), 134.0 (Ar), 116.0 (Ar_{ipso}), 114.0 (Ar), 87.8 (ArCC), 81.0 (ArCC), 62.0 (CH₂OH), 55.4 (OMe), 31.6 (CH₂CH₂OH), 16.1 (CCCH₂).

MS (NSI-FTMS): 192.1097 (M+H)⁺ - C₁₂H₁₅O₂

(Z)-2-(4-methoxybenzylidene)tetrahydrofuran
| 216a |



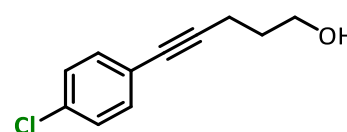
White solid

mp. : 53-55°C / R_f: (Hx:EtOAc 2:1) 0.54, (1:1) 0.61

NMR: ¹H (400.1 MHz, CDCl₃) δ 7.48 (2H, dt, J = 8.9, 2.2 Hz, Ar), 6.83 (2H, dt, J = 8.9, 2.2 Hz, Ar), 5.20 (1H, s, CCH), 4.30 (2H, t, J = 6.7 Hz, CH₂O), 3.79 (3H, s, OMe), 2.70 (2H, dt, J = 7.5, 1.4 Hz, CCH₂), 2.0 (2H, quin, J = 7.0 Hz, OCH₂CH₂). ¹³C[¹H] (100.7 MHz, CDCl₃) δ 156.9 (Ar_{ipso}), 155.9 (OCCH), 130.0 (Ar_{ipso}), 128.3 (Ar), 113.8 (Ar), 96.4 (CCH), 72.1 (OCH₂), 55.4 (OMe), 30.9 (OCH₂CH₂), 24.6 (CCCH₂).

MS (EI/TOF-MS): 190.0994 (M) - C₁₂H₁₄O₂

5-(4-chlorophenyl)pent-4-yn-1-ol
| 217 |



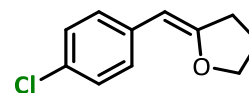
Pale-yellow waxy solid

mp. : 32-34°C / R_f: (Hx:EtOAc 2:1) 0.23, (1:1) 0.39

NMR: ¹H (400.1 MHz, CDCl₃) δ 7.30 (2H, dt, J = 8.6, 2.1 Hz, Ar), 7.24 (2H, dt, J = 8.6, 2.1 Hz, Ar), 3.79 (2H, t, J = 6.1 Hz, CH₂OH), 2.52 (2H, t, J = 7.0 Hz, CCCH₂), 1.93 (1H, s, OH), 1.84 (2H, quin, J = 6.6 Hz, CH₂CH₂OH). ¹³C[¹H] (100.7 MHz, CDCl₃) δ 133.7 (Ar_{ipso}), 132.9 (Ar), 128.6 (Ar), 122.3 (Ar_{ipso}), 90.5 (ArCC), 80.1 (ArCC), 61.7 (CH₂OH), 31.3 (CH₂CH₂OH), 16.0 (CH₂CH₂OH).

MS (ASAP/TOF-MS): 197.0550 (M+H) - C₁₁H₁₂OCl

(Z)-2-(4-chlorobenzylidene)tetrahydrofuran
| 218a |



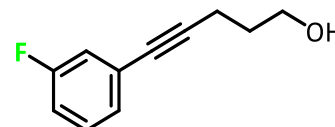
Pale-yellow oil

R_f: (Hx:EtOAc 2:1), (1:1)

NMR: ¹H (400.1 MHz, CDCl₃) δ 7.46 (2H, d, J = 8.6 Hz, Ar), 7.21 (2H, d, J = 8.6 Hz, Ar), 5.20 (1H, s, CCH), 4.33 (2H, t, J = 6.7 Hz, CH₂O), 2.716 (2H, td, J = 6.7, 1.1 Hz, CCH₂), 2.04 (2H, quin, J = 7.2 Hz, OCH₂CH₂). ¹³C[¹H] (100.7 MHz, CDCl₃) δ 156.9 (OCCH), 135.0 (Ar_{ipso}), 129.2 (Ar_{ipso}), 127.7 (Ar), 95.4 (CCH), 71.9 (OCH₂), 30.6 (OCH₂CH₂), 23.8 (CCCH₂).

MS (CI/TOF-MS): 195.0571 (M+H)⁺ - C₁₁H₁₂O₁Cl

5-(3-fluorophenyl)pent-4-yn-1-ol
| 219 |



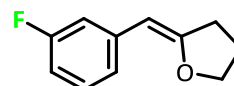
Red oil

R_f : (Hx:EtOAc 2:1) 0.55, (1:1) 0.58

NMR: ¹H (400.1 MHz, CDCl₃) δ 7.23 (1H, td, J = 8.0, 5.9 Hz, Ar), 7.06 (1H, dt, J = 7.7, 1.2 Hz, Ar), 7.08 (1H, ddd, J = 9.6, 2.5, 1.4 Hz, Ar), 6.97 (1H, tdd, J = 8.5, 2.6, 1.1 Hz, Ar), 3.81 (2H, t, J = 6.1 Hz, CH₂OH), 2.53 (2H, t, J = 6.9 Hz, CCH₂), 1.86 (2H, quin, J = 6.6 Hz, CH₂CH₂OH). ¹³C[¹H] (100.7 MHz, CDCl₃) δ 162.5 (d, J = 144.8 Hz, Ar_{ipso}), 129.9 (d, J = 8.8 Hz, Ar), 127.5 (d, J = 3.1 Hz, Ar), 125.7 (d, J = 9.4 Hz, Ar_{ipso}), 177.8 (d, J = 22.4 Hz, Ar), 115.1 (d, J = 21.0 Hz, Ar), 90.6 (ArCC), 80.2 (d, J = 3.3 Hz, ArCC), 61.8 (CH₂OH), 31.4 (CH₂CH₂OH), 16.1 (CH₂CH₂OH). ¹⁹F (128.4 MHz, CDCl₃) δ -113.3 (td, J = 9.3, 6.0 Hz).

MS (ASAP/TOF-MS): 178.0794 (M+H) – C₁₁H₁₁OF

(Z)-2-(3-fluorobenzylidene)tetrahydrofuran
| 220a |



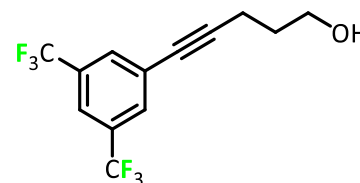
Pale yellow oil

R_f : (Hx:EtOAc 2:1) 0.52, (1:1) 0.60

NMR: ¹H (400.1 MHz, CDCl₃) δ 7.37 (1H, m, Ar), 7.20 (1H, m, Ar), 6.76 (1H, m, Ar), 5.23 (1H, s, CCH), 4.34 (2H, t, J = 6.8 Hz, OCH₂), 2.73 (2H, td, J = 7.6, 1.1 Hz, CCH₂), 2.04 (2H, quin, J = 7.1 Hz, OCH₂CH₂). ¹³C[¹H] (100.7 MHz, CDCl₃) δ 163.0 (d, J = 241.0 Hz, Ar_{ipso}), 158.8 (OCCH), 139.2 (d, J = 8.6 Hz, Ar_{ipso}), 129.3 (d, 8.8 Hz, Ar), 122.7 (Ar), 133.5 (d, J = 22.3 Hz, Ar), 111.2 (d, J = 21.4 Hz, Ar), 96.13 (CCH), 72.4 (OCH₂), 31.1 (OCH₂CH₂), 24.2 (CCCH₂). ¹⁹F (128.4 MHz, CDCl₃) δ -114.3.

MS (EI/TOF-MS): 178.0794 (M) – C₁₁H₁₁OF

5-[3,5-(trifluoromethyl)phenyl]pent-4-yn-1-ol
| 221 |



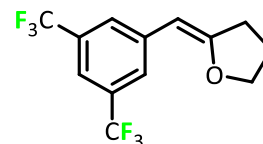
Orange oil

R_f : (Hx:EtOAc 2:1) 0.28, (1:1) 0.46

NMR: ¹H (400.1 MHz, CDCl₃) δ 7.79 (2H, s, Ar), 7.74 (1H, s, Ar), 3.80 (2H, m, CH₂OH), 2.56 (2H, t, J = 7.0 Hz, CCH₂), 1.87 (3H, m, CH₂CH₂OH/OH). ¹³C[¹H] (100.7 MHz, CDCl₃) δ 131.9 (q, J = 33.6 Hz, Ar_{ipso}), 131.6 (m, Ar), 126.3 (Ar_{ipso}), 123.1 (quin, J = 272.5 Hz, CF₃), 121.1 (q, J = 3.7 Hz, Ar), 93.7 (s, ArCC), 78.6 (s, ArCC), 61.5 (CH₂OH), 31.2 (CH₂CH₂OH), 16.0 (CH₂CH₂OH). ¹⁹F (128.4 MHz, CDCl₃) δ -63.3.

MS (ASAP/TOF-MS): 297.0714 (M+H) – C₁₃H₁₁OF₆

(Z)-2-[3,5-(bistrifluoromethyl)benzylidene]tetrahydrofuran
| 222a |



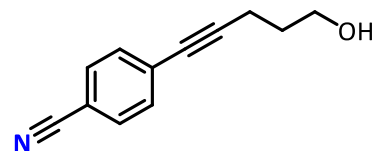
White crystalline solid

mp. : 46-48°C / R_f : (Hx:EtOAc 2:1) 0.64, (1:1) 0.78

NMR: ^1H (400.1 MHz, CDCl_3) δ 7.95 (2H, s, Ar), 7.53 (1H, s, Ar), 5.31 (1H, s, CCH), 4.40 (2H, t, $J = 6.8$ Hz, OCH_2), 2.77 (2H, td, $J = 7.6, 1.2$ Hz, CCH_2), 2.08 (2H, quin, $J = 7.4$ Hz, OCH_2CH_2). ^{13}C [^1H] (100.7 MHz, CDCl_3) δ 161.4 (OCCH), 139.2 (Ar_{ipso}), 131.3 (q, $J = 32.6$ Hz, Ar_{ipso}), 126.7 (m, Ar), 123.9 (q, $J = 272.5$ Hz, CF_3), 117.7 (quin, $J = 3.7$ Hz, Ar), 95.1 (s, ArCC), 73.2 (s, ArCC), 61.5 (CH_2OH), 31.6 ($\text{CH}_2\text{CH}_2\text{OH}$), 24.2 ($\text{CH}_2\text{CH}_2\text{OH}$). ^{19}F (128.4 MHz, CDCl_3) δ -63.0.

MS (ASAP/TOF-MS): 296.0636 (M) – $\text{C}_{13}\text{H}_{11}\text{OF}_6$

4-(5-hydroxypent-1-yn-1-yl)benzonitrile
| 223 |



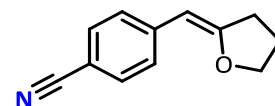
Yellow powdery solid

mp. : 76-79°C / R_f : (Hx:EtOAc 2:1) 0.15, (1:1) 0.30

NMR: ^1H (400.1 MHz, CDCl_3) δ 7.56 (2H, dt, $J = 8.5, 1.9$ Hz, Ar), 7.44 (2H, dt, $J = 8.4, 1.9$ Hz, Ar), 3.80 (2H, t, $J = 6.2$ Hz, CH_2OH), 2.56 (2H, t, $J = 7.0$ Hz, CCCH_2), 1.86 (3H, quin, $J = 6.6$ Hz, $\text{CH}_2\text{CH}_2\text{OH}$), 1.65 (1H, s, OH). ^{13}C [^1H] (100.7 MHz, CDCl_3) δ 132.2 (Ar), 132.1 (Ar), 129.0 (Ar_{ipso}), 118.7 (CN), 111.1 (Ar_{ipso}), 94.7 (ArCC), 79.9 (ArCC), 61.6 (CH_2OH), 31.3 ($\text{CH}_2\text{CH}_2\text{OH}$), 16.2

MS (NSI-FTMS): 209.0766 (M+Na) $^+$ – $\text{C}_{17}\text{H}_{11}\text{ONNa}$

(Z)-4-[(dihydrofuran-2(3H)-ylidene)methyl]benzonitrile
| 224a |



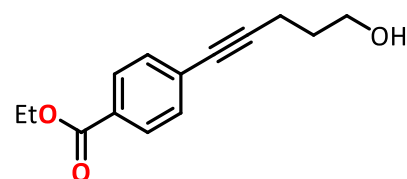
Colourless crystalline solid

mp. : 109-111°C / R_f : (Hx:EtOAc 2:1) 0.50, (1:1) 0.69

NMR: ^1H (400.1 MHz, CDCl_3) δ 7.56 (2H, d, $J = 8.4$ Hz, Ar), 7.48 (2H, d, $J = 8.4$ Hz, Ar), 5.24 (1H, s, CCH), 5.20 (1H, s, CCH), 4.36 (2H, t, $J = 6.8$ Hz, CH_2O), 2.74 (2H, td, $J = 7.6, 0.9$ Hz, CCH_2), 2.04 (2H, quin, $J = 7.2$ Hz, OCH_2CH_2). ^{13}C [^1H] (100.7 MHz, CDCl_3) δ 161.6 (OCCH), 142.0 (Ar_{ipso}), 131.93 (Ar), 127.2 (Ar), 119.9 (CN), 106.8 (Ar_{ipso}), 96.0 (CCH), 73.1 (OCH_2), 31.6 (OCH_2CH_2), 24.0 (CCCH_2).

MS (ASAP/TOF-MS): 186.0919 (M+H) – $\text{C}_{12}\text{H}_{12}\text{NO}$

ethyl 4-(5-hydroxypent-1-yn-1-yl)benzoate
| 225 |



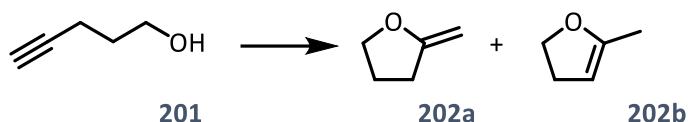
R_f : (Hx:EtOAc 2:1) 0.59, (1:1) 0.68

NMR: ^1H (400.1 MHz, CDCl_3) δ 7.31 (2H, dt, $J = 8.4, 2.0$ Hz, Ar), 7.13 (2H, dt, $J = 8.4, 2.0$ Hz, Ar), 5.90 (1H, s, CCH), 4.11 (2H, t, $J = 6.8$ Hz, CH_2O), 2.82 (2H, dt, $J = 7.6, 2.0$ Hz, CCH_2), 2.0 (2H, quin, $J = 7.0$ Hz, OCH_2CH_2), 1.32 (9H, s, tBu). ^{13}C [^1H] (100.7 MHz, CDCl_3) δ 158.7 (OCCH), 147.5 (Ar_{ipso}), 134.9 (Ar_{ipso}), 126.7 (Ar), 125.3 (Ar), 98.8 (CCH), 69.5 (OCH_2), 34.5 ($\text{C}[\text{CH}_3]_3$), 31.5 ($\text{C}[\text{CH}_3]_3$), 28.3 (OCH_2CH_2), 25.5 (CCCH_2).

MS (ASAP/TOF-MS): 216.1514 (M) – $\text{C}_{15}\text{H}_{20}\text{O}$

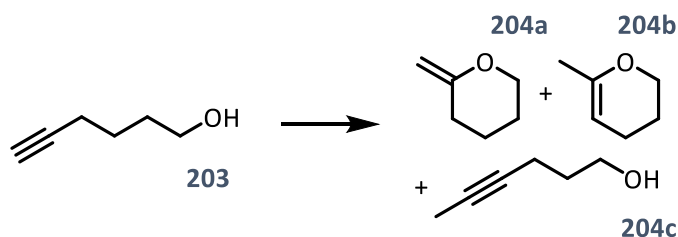
Other cyclisation products

2-methylenetetrahydrofuran, 5-methyl-2,3-dihydrofuran



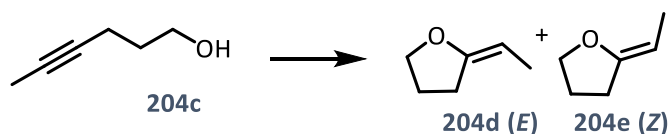
^1H (400 MHz, C_6D_6) | 202a | δ 4.46 (1H, s, CCH_2), 3.87 (1H, s, CCH_2), 3.67 (2H, t, $J = 7$ Hz, CH_2O), 2.14 (2H, tt, $J = 1.7$, 7.5 Hz, CH_2C), 1.38 (2H, quin, $J = 7$ Hz, $\text{CH}_2\text{CH}_2\text{CH}_2$). | 202b | δ 4.27 (1H, m, CH), 4.08 (2H, t, $J = 9.3$ Hz, CH_2O), 2.32 (2H, m, CH_2CH), 1.66 (3H, m, CH_3).

2-methylenetetrahydropyran, 6-methyl-3,4-dihyropyran, hex-4-yn-1-ol



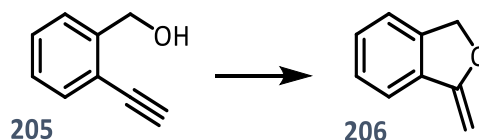
^1H (400 MHz, C_6D_6) | 204a | δ 4.53 (1H, s, CCH_2), 4.04 (1H, s, CCH_2), 3.76 (2H, m, CH_2O), 1.99 (2H, t, $J = 6.3$ Hz, $\text{CH}_2\text{CH}_2\text{CH}_2$), 1.23-1.40 (4H, m, $\text{CH}_2\text{CH}_2\text{CH}_2$). | 204b | δ 4.39 (1H, m, CH), 3.71 (2H, m, CH_2O), 1.78 (2H, m, CH_2CH), 1.71 (2H, m, CH_3), 1.48 (2H, m, $\text{CH}_2\text{CH}_2\text{CH}_2$). | 204c | δ 3.75 (2H, t, $J = 6.3$ Hz, CH_2O), 2.32 (2H, m, CH_2C), 1.82 (2H, m, $\text{CH}_2\text{CH}_2\text{CH}_2$), 1.59 (3H, t, $J = 2.5$ Hz, CH_3).

(E)-2-ethylidenetetrahydrofuran, (Z)-2-ethylidenetetrahydrofuran



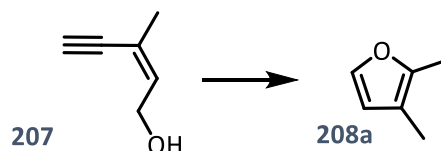
^1H (400 MHz, C_6D_6) | 204d | δ | 204e | δ

1-methylene-1,3-dihydroisobenzofuran



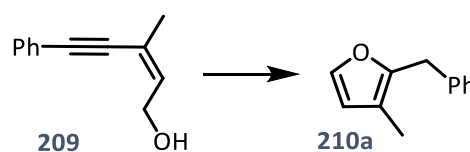
^1H (400 MHz, C_6D_6) | 206 | δ 7.52 (1H, d, $J = 7.6$ Hz, CH), 7.38 (1H, d, $J = 7.6$ Hz, CH), 7.06 (1H, t, $J = 7.5$ Hz, CH), 6.88 (1H, t, $J = 7.5$ Hz, CH), 5.3 (1H, s, CH_2CO), 4.86 (2H, s, CH_2), 3.00 (1H, s, CH_2CO).

2,3-dimethylfuran



^1H (400 MHz, C_6D_6) | 208a | δ 7.08 (1H, s, OCH), 6.00 (1H, s, OCHCH), 1.97 (3H, s, OCCH_3), 1.74 (3H, s, OCCCH_3).

2-benzyl-3-methylfuran



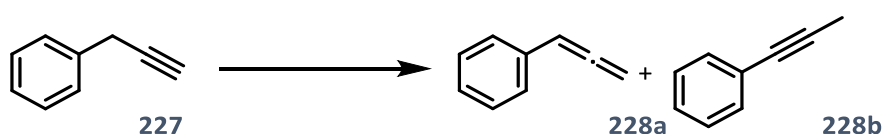
^1H (400 MHz, C_6D_6) | 210a | δ 7.09 (5H, s, Ar), 7.05 (1H, s, OCH), 6.00 (1H, s, OCHCH), 1.77 (3H, s, OCCCH_3).

III.V Isomerisation of terminal alkynes

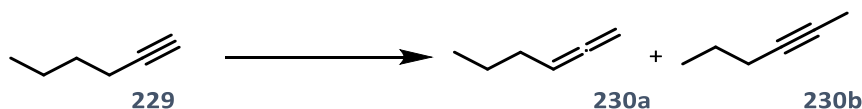
Procedure for NMR scale reactions

Terminal alkyne (0.6 mmol, 1.2 eq.) was added to a Young's tap NMR tube containing C₆D₆ (0.54 mL), ferrocene (0.093 g, 0.05 mmol, 0.0 eq.) and 18-crown-6 (0.013 g, 0.05 mmol, 0.1 eq.). To this K₂Mg(CH₂SiMe₃)₄(PMDETA)₂ (0.020 g, 0.025 mmol, 0.05 eq.) was added and the tube placed in an oil bath. The reaction was periodically monitored by ¹H NMR spectroscopy. Product identity was obtained by GCMS and NMR spectroscopy.²⁹⁹ Yields obtained were calculated using NMR spectroscopic integrals and are relative to the internal standard.

Isomerised products



¹H (400 MHz, C₆D₆) | **228a** | δ 7.21 (2H, d, J = 7.5 Hz, Ar), 7.11 (2H, t, J = 7.6 Hz, Ar), 7.00-7.01 (1H, t, J = 7.3 Hz, Ar), 6.04 (1H, t, J = 6.8 Hz, CHCH₂), 4.86 (2H, d, J = 6.8 Hz, CHCH₂). | **228b** | δ 7.45 (2H, m, Ar), 7.03-6.96 (3H, m, Ar), 1.66 (3H, s, CH₃).



¹H (400 MHz, C₆D₆) | **230a** | δ 5.01 (1H, pent, J = 6.8 Hz, CH₂CCH), 4.60 (2H, dt, J = 6.7, 3.3 Hz, CCH₂), only allene resonances distinguishable peaks at obtained concentration | **230b** | δ 2.00 (2H, tq, J = 7.0, 2.5 Hz, CCCH₂), 1.57 (3H, t, J = 2.5 Hz, CCH₃), 1.40 (2H, sext, J = 7.1 Hz, CH₃CH₂), 0.88 (3H, t, J = 7.4 Hz, CH₂CH₃).

IV – References

1. U. Nations, *2019 Revision of World Population Prospects*.
2. Earth overshoot day 2019, <https://www.overshootday.org/>, (accessed September 2019).
3. R. A. Sheldon, I. Arends and U. Hanefeld, *Green Chemistry and Catalysis*, Wiley, 2007.
4. V. Pace, P. Hoyos, L. Castoldi, P. Domínguez de María and A. R. Alcántara, *ChemSusChem*, 2012, **5**, 1369-1379.
5. C. Capello, U. Fischer and K. Hungerbühler, *Green Chem.*, 2007, **9**, 927-934.
6. P. T. Anastas and J. C. Warner, *Green Chemistry: Theory and Practice*, Oxford University Press, 1998.
7. H. C. Erythropel, J. B. Zimmerman, T. M. de Winter, L. Petitjean, F. Melnikov, C. H. Lam, A. W. Lounsbury, K. E. Mellor, N. Z. Janković, Q. Tu, L. N. Pincus, M. M. Falinski, W. Shi, P. Coish, D. L. Plata and P. T. Anastas, *Green Chem.*, 2018, **20**, 1929-1961.
8. R. A. Sheldon, *Chem. Soc. Rev.*, 2012, **41**, 1437-1451.
9. R. A. Sheldon, *Chem. Commun.*, 2008, 3352-3365.
10. R. A. Sheldon, *Green Chem.*, 2007, **9**, 1273-1283.
11. C. Jimenez-Gonzalez, C. S. Ponder, Q. B. Broxterman and J. B. Manley, *Org. Process Res. Dev.*, 2011, **15**, 912-917.
12. P. G. Jessop, *Green Chem.*, 2011, **13**, 1391-1398.
13. H. Cruz, N. Jordão and L. C. Branco, *Green Chem.*, 2017, **19**, 1653-1658.
14. M. Cvjetko Bubalo, S. Vidović, I. Radojčić Redovniković and S. Jokić, *J. Technol. Biotechnol.*, 2015, **90**, 1631-1639.
15. C. Jiménez-González, A. D. Curzons, D. J. C. Constable and V. L. Cunningham, *Clean Technol. Envir.*, 2004, **7**, 42-50.
16. K. Tanaka and F. Toda, *Chem. Rev.*, 2000, **100**, 1025-1074.
17. in *Alternative Solvents for Green Chemistry*, The Royal Society of Chemistry, 2009, pp. 1-22.
18. S. Santoro, A. Marrocchi, D. Lanari, L. Ackermann and L. Vaccaro, *Chem. – Eur. J.*, 2018, **24**, 13383-13390.
19. C. Ma, A. Laaksonen, C. Liu, X. Lu and X. Ji, *Chem. Soc. Rev.*, 2018, **47**, 8685-8720.
20. F. Curti, M. Tiecco, V. Pirovano, R. Germani, A. Caselli, E. Rossi and G. Abbiati, *Eur. J. Org. Chem.*, 2019, **2019**, 1904-1914.
21. O. S. Hammond, D. T. Bowron and K. J. Edler, *Angew. Chem. Int. Ed.* 2017, **56**, 9782-9785.
22. A. Faraone, D. V. Wagle, G. A. Baker, E. C. Novak, M. Ohl, D. Reuter, P. Lunkenheimer, A. Loidl and E. Mamontov, *J. Phys. Chem. B*, 2018, **122**, 1261-1267.
23. M. Feng, X. Lu, J. Zhang, Y. Li, C. Shi, L. Lu and S. Zhang, *Green Chem.*, 2019, **21**, 87-98.
24. X.-J. Shen, J.-L. Wen, Q.-Q. Mei, X. Chen, D. Sun, T.-Q. Yuan and R.-C. Sun, *Green Chem.*, 2019, **21**, 275-283.
25. T. Palomba, G. Ciancaleoni, T. Del Giacco, R. Germani, F. Ianni and M. Tiecco, *J. Mol. Liq.*, 2018, **262**, 285-294.
26. E. Ünlü Ayşe, A. Arikaya and S. Takaç, *Green Processing and Synthesis*, 2019, **8**, 355.
27. Y. Ma, P. Li, Y. Li, S. J. P. Willot, W. Zhang, D. Ribitsch, Y. H. Choi, R. Verpoorte, T. Zhang, F. Hollmann and Y. Wang, *ChemSusChem*, 2019, **12**, 1310-1315.
28. S. K. Shukla and J.-P. Mikkola, *Chem. Commun.*, 2019, **55**, 3939-3942.

29. W. Zhao, X. Chi, H. Li, J. He, J. Long, Y. Xu and S. Yang, *Green Chem.*, 2019, **21**, 567-577.
30. L. J. B. M. Kollau, M. Vis, A. van den Bruinhorst, A. C. C. Esteves and R. Tuinier, *Chem. Commun.*, 2018, **54**, 13351-13354.
31. G. García, S. Aparicio, R. Ullah and M. Atilhan, *Energy & Fuels*, 2015, **29**, 2616-2644.
32. I. V. Vasilenko, I. A. Bereziianko, D. I. Shiman and S. V. Kostjuk, *Polym. Chem.*, 2016, **7**, 5615-5619.
33. E. L. Smith, A. P. Abbott and K. S. Ryder, *Chem. Rev.*, 2014, **114**, 11060-11082.
34. A. P. Abbott, *Deep Eutectic Solvents, Leuven summer school on Ionic Liquids*, 2010.
35. A. P. Abbott, G. Capper, D. L. Davies and R. K. Rasheed, *Chem. – Eur. J.*, 2004, **10**, 3769-3774.
36. J. Cao, B. Qi, J. Liu, Y. Shang, H. Liu, W. Wang, J. Lv, Z. Chen, H. Zhang and X. Zhou, *RSC Adv.*, 2016, **6**, 21612-21616.
37. M. Karimi, A. Jodaei, A. Sadeghinik, M. R. Ramsheh, T. M. Hafshejani, M. Shamsi, F. Orand and F. Lotfi, *J. Fluorine Chem.*, 2017, **204**, 76-83.
38. A. P. Abbott, J. C. Barron, K. S. Ryder and D. Wilson, *Chem. – Eur. J.*, 2007, **13**, 6495-6501.
39. Y. Dai, J. van Spronsen, G.-J. Witkamp, R. Verpoorte and Y. H. Choi, *Anal. Chim. Acta*, 2013, **766**, 61-68.
40. O. S. Hammond, D. T. Bowron and K. J. Edler, *Green Chem.*, 2016, **18**, 2736-2744.
41. A. H. Turner and J. D. Holbrey, *Phys. Chem. Chem. Phys.*, 2019.
42. S. L. Perkins, P. Painter and C. M. Colina, *J. Chem. Eng. Data*, 2014, **59**, 3652-3662.
43. A. Paiva, R. Craveiro, I. Aroso, M. Martins, R. L. Reis and A. R. C. Duarte, *ACS Sus. Chem. Eng.*, 2014, **2**, 1063-1071.
44. Y. Liu, J. B. Friesen, J. B. McAlpine, D. C. Lankin, S.-N. Chen and G. F. Pauli, *J. Nat. Prod.*, 2018, **81**, 679-690.
45. N. Schaeffer, M. A. R. Martins, C. M. S. S. Neves, S. P. Pinho and J. A. P. Coutinho, *Chem. Commun.*, 2018, **54**, 8104-8107.
46. D. J. G. P. van Osch, C. H. J. T. Dietz, J. van Spronsen, M. C. Kroon, F. Gallucci, M. van Sint Annaland and R. Tuinier, *ACS Sus. Chem. Eng.*, 2019, **7**, 2933-2942.
47. M. A. R. Martins, E. A. Crespo, P. V. A. Pontes, L. P. Silva, M. Bülow, G. J. Maximo, E. A. C. Batista, C. Held, S. P. Pinho and J. A. P. Coutinho, *ACS Sus. Chem. Eng.*, 2018, **6**, 8836-8846.
48. S. H. Zeisel, *Ann. Nutr. Metab.*, 2012, **61**, 254-258.
49. M. Frauenkron, J.-P. Melder, G. Ruider, R. Rossbacher and H. Höke, *Ullmann's Encyclopedia of Industrial Chemistry*, 2001.
50. Choline chloride Process | Johnson Matthey, <https://matthey.com/products-and-services/chemical-processes/licensed-processes/choline-chloride-process>, (accessed 19/09/19).
51. *Ethylene glycol: toxicological overview*, Public Health England, Aug 2015.
52. *Ethylene glycol: general information*, Public Health England, Oct 2016.
53. S. Rebsdats and D. Mayer, *Ullmann's Encyclopedia of Industrial Chemistry*, 2000.
54. Ethylene Oxide/Ethylene Glycol (EO/EG) Process Technology | Shell Catalysts & Technologies | Shell Global, <https://www.shell.com/business-customers/catalysts-technologies/licensed-technologies/petrochemicals/ethylene-oxide-production.html>, (accessed 19/09/19).
55. OMEGA Process | Shell Catalysts & Technologies | Shell Global, <https://www.shell.com/business-customers/catalysts-technologies/licensed->

[technologies/petrochemicals/ethylene-oxide-production/omega-process.html](https://www.elsevier.com/locate/S0926641018300011),
(accessed 19/09/19).

56. D. J. Anneken, S. Both, R. Christoph, G. Fieg, U. Steinberner and A. Westfechtel, *Ullmann's Encyclopedia of Industrial Chemistry*, 2006.
57. R. Christoph, B. Schmidt, U. Steinberner, W. Dilla and R. Karinen, *Ullmann's Encyclopedia of Industrial Chemistry*, 2006.
58. S. Rebsdatt and D. Mayer, *Ullmann's Encyclopedia of Industrial Chemistry*, 2001.
59. P. Roose, *Ullmann's Encyclopedia of Industrial Chemistry*, 2015, 1-10.
60. C. Kurt and J. Bittner, *Ullmann's Encyclopedia of Industrial Chemistry*, 2006.
61. O. Sahu, *An. Agrarian Sci.*, 2018, **16**, 389-395.
62. Y. Tachibana, S. Kimura and K.-i. Kasuya, *Sci. Rep.*, 2015, **5**, 8249.
63. K. Dalvand, J. Rubin, S. Gunukula, M. Clayton Wheeler and G. Hunt, *Biomass. Bioenerg.*, 2018, **115**, 56-63.
64. H. E. Hoydonckx, W. M. Van Rhijn, W. Van Rhijn, D. E. De Vos and P. A. Jacobs, *Ullmann's Encyclopedia of Industrial Chemistry*, 2007.
65. A. Pellis, F. P. Byrne, J. Sherwood, M. Vastano, J. W. Comerford and T. J. Farmer, *Green Chem.*, 2019, **21**, 1686-1694.
66. U. Azzena, M. Carraro, L. Pisano, S. Monticelli, R. Bartolotta and V. Pace, *ChemSusChem*, 2019, **12**, 40-70.
67. F. P. Byrne, B. Forier, G. Bossaert, C. Hoebbers, T. J. Farmer and A. J. Hunt, *Green Chem.*, 2018, **20**, 4003-4011.
68. V. Antonucci, J. Coleman, J. B. Ferry, N. Johnson, M. Mathe, J. P. Scott and J. Xu, *Org. Proc. Res. Dev.*, 2011, **15**, 939-941.
69. D. F. Aycock, *Org. Proc. Res. Dev.*, 2007, **11**, 156-159.
70. J. D. Hayler, D. K. Leahy and E. M. Simmons, *Organometallics*, 2019, **38**, 36-46.
71. H. Gräfe, W. Körnig, H.-M. Weitz, W. Reiß, G. Steffan, H. Diehl, H. Bosche, K. Schneider, H. Kieczka and R. Pinkos, *Ullmann's Encyclopedia of Industrial Chemistry*, 2019, 1-12.
72. H. Müller, *Ullmann's Encyclopedia of Industrial Chemistry*, 2011.
73. ACS, Endangered Elements, www.acs.org/content/acs/en/greenchemistry/research-innovation/endangered-elements.html, (accessed 19/07/2019).
74. *Element Scarcity – EuChemS Periodic Table*, EUChemS 2019, <https://www.euchems.eu/euchems-periodic-table/>, (accessed 20/09/19).
75. *Periodic Table: History*, Royal Society of Chemistry, <http://www.rsc.org/periodic-table/history>, (accessed 20/09/19).
76. *Lithium*, British Geological Survey, 2016.
77. *Mineral Commodities Summery Report 2019*, US Geological Survey, 2019.
78. *Lithium*, British Geological Survey, Mar 2004.
79. *Mineral Commodities Summery Report*, US Geological Survey, 2010 - 2019.
80. W. Schlenk and J. Holtz, *Ber. Dtsch. Chem. Ges.*, 1917, **50**, 262-274.
81. D. B. Collum, *Acc. Chem. Res.*, 1993, **26**, 227-234.
82. R. E. Mulvey and S. D. Robertson, in *Organo-di-Metallic Compounds (or Reagents): Synergistic Effects and Synthetic Applications*, ed. Z. Xi, Springer International Publishing, Cham, 2014, pp. 129-158.
83. R. E. Mulvey and S. D. Robertson, *Angew. Chem. Int. Ed.*, 2013, **52**, 11470-11487.
84. M. Lappert, A. Protchenko, P. Power and A. Seeber, in *Metal Amide Chemistry*, John Wiley & Sons, Ltd, 2008, ch. 2, pp. 7-38.
85. B. Haag, M. Mosrin, H. Ila, V. Malakhov and P. Knochel, *Angew. Chem. Int. Ed.*, 2011, **50**, 9794-9824.

86. R. E. Mulvey and S. D. Robertson, in *Alkaline-Earth Metal Compounds: Oddities and Applications*, ed. S. Harder, Springer Berlin Heidelberg, Berlin, Heidelberg, 2013, pp. 103-139.
87. D. B. Collum, A. J. McNeil and A. Ramirez, *Angew. Chem. Int. Ed.*, 2007, **46**, 3002-3017.
88. A. Bodach, R. Hebestreit, M. Bolte and L. Fink, *Inorg. Chem.*, 2018, **57**, 9079-9085.
89. G. Barozzino-Consiglio, G. Hamdoun, C. Fressigné, A. Harrison-Marchand, J. Maddaluno and H. Oulyadi, *Chem. –Eur. J.*, 2017, **23**, 12475-12479.
90. M. F. Lappert, M. J. Slade, A. Singh, J. L. Atwood, R. D. Rogers and R. Shakir, *J. Am. Chem. Soc.*, 1983, **105**, 302-304.
91. D. R. Armstrong, P. García-Álvarez, A. R. Kennedy, R. E. Mulvey and S. D. Robertson, *Chem. – Eur. J.*, 2011, **17**, 6725-6730.
92. B. L. Lucht and D. B. Collum, *J. Am. Chem. Soc.*, 1994, **116**, 7949-7950.
93. D. Seyferth, *Organometallics*, 2009, **28**, 1598-1605.
94. R. M. Peltzer, O. Eisenstein, A. Nova and M. Cascella, *J. Phys. Chem. B*, 2017, **121**, 4226-4237.
95. J. A. Wanklyn, *Liebigs Ann.*, 1858, **108**, 67-79.
96. J. A. C. F. p. d. Wanklyn, *Proc. R. Soc. Lond.*, 1857, **9**, 341-345.
97. G. Wittig, F. J. Meyer and G. Lange, *Liebigs Ann.*, 1951, **571**, 167-201.
98. T. Klatt, J. T. Markiewicz, C. Sämann and P. Knochel, *J. Org. Chem.*, 2014, **79**, 4253-4269.
99. A. Krasovskiy, V. Krasovskaya and P. Knochel, *Angew. Chem., Int. Ed.*, 2006, **45**, 2958-2961.
100. A. J. Martínez-Martínez, S. Justice, B. J. Fleming, A. R. Kennedy, I. D. H. Oswald and C. T. O'Hara, *Sci. Adv.*, 2017, **3**, e1700832.
101. A. J. Martínez-Martínez, A. R. Kennedy, R. E. Mulvey and C. T. O'Hara, *Science*, 2014, **346**, 834-837.
102. R. L.-Y. Bao, R. Zhao and L. Shi, *Chem. Commun.*, 2015, **51**, 6884-6900.
103. M. B. Smith and J. March, *March's Advanced Organic Chemistry: Reactions, Mechanisms, and Structure*, Wiley, 2007.
104. F. Mongin and A. Harrison-Marchand, *Chem. Rev.*, 2013, **113**, 7563-7727.
105. E. Weiss, *Angew. Chem. Int. Ed. Engl.*, 1993, **32**, 1501-1523.
106. C. T. O'Hara, in *Organometallic Chemistry: Volume 37*, The Royal Society of Chemistry, 2011, vol. 37, pp. 1-26.
107. W. Clegg, E. Crosbie, S. H. Dale-Black, E. Hevia, G. W. Honeyman, A. R. Kennedy, R. E. Mulvey, D. L. Ramsay and S. D. Robertson, *Organometallics*, 2015, **34**, 2580-2589.
108. L. C. H. Maddock, T. Cadenbach, A. R. Kennedy, I. Borilovic, G. Aromí and E. Hevia, *Inorg. Chem.*, 2015, **54**, 9201-9210.
109. D. R. Armstrong, E. Brammer, T. Cadenbach, E. Hevia and A. R. Kennedy, *Organometallics*, 2013, **32**, 480-489.
110. B. M. Wolf, C. Stuhl, C. Maichle-Mössmer and R. Anwender, *Organometallics*, 2019, **38**, 1614-1621.
111. A. R. Kennedy, J. Klett, R. E. Mulvey and D. S. Wright, *Science*, 2009, **326**, 706-708.
112. M. Rouen, P. Chaumont, G. Barozzino-Consiglio, J. Maddaluno and A. Harrison-Marchand, *Chem. – Eur. J.*, 2018, **24**, 9238-9242.
113. F. M. García-Valle, V. Tabernerero, T. Cuenca, J. Cano and M. E. G. Mosquera, *Dalton Trans.*, 2018, **47**, 6499-6506.
114. F. Mongin and A. Harrison-Marchand, *Chem. Rev.*, 2013, **113**, 7563-7727.
115. D. Tilly, F. Chevallier, F. Mongin and P. C. Gros, *Chem. Rev.*, 2014, **114**, 1207-1257.

116. M. Uzelac and R. E. Mulvey, *Chem. – Eur. J.*, 2018, **24**, 7786-7793.
117. S. D. Robertson, M. Uzelac and R. E. Mulvey, *Chem. Rev.*, 2019.
118. S. E. Baillie, T. D. Bluemke, W. Clegg, A. R. Kennedy, J. Klett, L. Russo, M. de Tullio and E. Hevia, *Chem. Commun.*, 2014, **50**, 12859-12862.
119. Y. Yamashita, H. Suzuki, I. Sato, T. Hirata and S. Kobayashi, *Angew. Chem. Int. Ed.*, 2018, **57**, 6896-6900.
120. Z. Peng, Y. Wang, Z. Yu, D. Zhao, L. Song and C. Jiang, *J. Org. Chem.*, 2018, **83**, 7900-7906.
121. D. S. Ziegler, B. Wei and P. Knochel, *Chem. – Eur. J.*, 2019, **25**, 2695-2703.
122. G. Wittig, F. J. Meyer and G. Lange, *Liebigs Ann.*, 1951, **571**, 167-201.
123. W. Tochtermann, *Angew. Chem. Int. Ed. Engl.*, 1966, **5**, 351-371.
124. A. J. Martínez-Martínez and C. T. O'Hara, in *Advances in Organometallic Chemistry*, ed. J. P. Pedro, Academic Press, 2016, vol. Volume 65, pp. 1-46.
125. A. J. Martínez-Martínez, D. R. Armstrong, B. Conway, B. J. Fleming, J. Klett, A. R. Kennedy, R. E. Mulvey, S. D. Robertson and C. T. O'Hara, *Chem. Sci.*, 2014, **5**, 771-781.
126. A. J. Martínez-Martínez, A. R. Kennedy, R. E. Mulvey and C. T. O'Hara, *Science*, 2014, **346**, 834-837.
127. G. Dilauro, A. Francesca Quivelli, P. Vitale, V. Capriati and F. M. Perna, *Angew. Chem. Int. Ed.*, 2019, **58**, 1799-1802.
128. R. E. Mulvey and S. D. Robertson, *Angew. Chem. Int. Ed.*, 2013, **52**, 11470-11487.
129. V. Capriati, F. M. Perna and A. Salomone, *Dalton Trans.*, 2014, **43**, 14204-14210.
130. V. Mallardo, R. Rizzi, F. C. Sassone, R. Mansueto, F. M. Perna, A. Salomone and V. Capriati, *Chem. Commun.*, 2014, **50**, 8655-8658.
131. F. C. Sassone, F. M. Perna, A. Salomone, S. Florio and V. Capriati, *Chem. Commun.*, 2015, **51**, 9459-9462.
132. S. Ghinato, G. Dilauro, F. M. Perna, V. Capriati, M. Blangetti and C. Prandi, *Chem. Commun.*, 2019, **55**, 7741-7744.
133. G. Dilauro, M. Dell'Aera, P. Vitale, V. Capriati and F. M. Perna, *Angew. Chem. Int. Ed.*, 2017, **56**, 10200-10203.
134. C. Vidal, J. García-Álvarez, A. Hernán-Gómez, A. R. Kennedy and E. Hevia, *Angew. Chem. Int. Ed.*, 2016, **55**, 16145-16148.
135. C. Vidal, J. García-Álvarez, A. Hernán-Gómez, A. R. Kennedy and E. Hevia, *Angew. Chem. Int. Ed.*, 2014, **53**, 5969-5973.
136. L. Cicco, S. Sblendorio, R. Mansueto, F. M. Perna, A. Salomone, S. Florio and V. Capriati, *Chem. Sci.*, 2016, **7**, 1192-1199.
137. A. Chanda and V. V. Fokin, *Chem. Rev.*, 2009, **109**, 725-748.
138. R. N. Butler and A. G. Coyne, *J. Org. Chem.*, 2015, **80**, 1809-1817.
139. R. N. Butler and A. G. Coyne, *Org. Biomol. Chem.*, 2016, **14**, 9945-9960.
140. J. A. Padró, L. Saiz and E. Guàrdia, *Hydrogen Bonding - Experimental and Theoretical Studies*, 1997, **416**, 243-248.
141. Y. Jung and R. A. Marcus, *J. Am. Chem. Soc.*, 2007, **129**, 5492-5502.
142. K. D. Beare and C. S. P. McErlean, *Org. Biomol. Chem.*, 2013, **11**, 2452-2459.
143. J. K. Beattie, C. S. P. McErlean and C. B. W. Phippen, *Chem. – Eur. J.*, 2010, **16**, 8972-8974.
144. Z. Huang, W. Hua, D. Verreault and H. C. Allen, *J. Phys. Chem. A*, 2013, **117**, 6346-6353.
145. C. Chen, W. Z. Li, Y. C. Song and J. Yang, *J. Mol. Liq.*, 2009, **146**, 23-28.
146. D. G. Brown and J. Bostrom, *J. Med. Chem.*, 2016, **59**, 4443-4458.

147. J. M. Humphrey and A. R. Chamberlin, *Chem. Rev.*, 1997, **97**, 2243-2266.
148. J. S. Carey, D. Laffan, C. Thomson and M. T. Williams, *Org. Biomol. Chem*, 2006, **4**, 2337-2347.
149. T. J. Deming, *Prog. Polym. Sci.*, 2007, **32**, 858-875.
150. J. R. Dunetz, J. Magano and G. A. Weisenburger, *Org. Proc. Res. Dev.*, 2016, **20**, 140-177.
151. D. J. C. Constable, P. J. Dunn, J. D. Hayler, G. R. Humphrey, J. J. L. Leazer, R. J. Linderman, K. Lorenz, J. Manley, B. A. Pearlman, A. Wells, A. Zaks and T. Y. Zhang, *Green Chem.*, 2007, **9**, 411-420.
152. M. C. Bryan, P. J. Dunn, D. Entwistle, F. Gallou, S. G. Koenig, J. D. Hayler, M. R. Hickey, S. Hughes, M. E. Kopach, G. Moine, P. Richardson, F. Roschangar, A. Steven and F. J. Weiberth, *Green Chem.*, 2018, **20**, 5082-5103.
153. K. Hollanders, B. Maes and S. Ballet, *Synthesis*, 2019, **51**, 2261-2277.
154. R. M. de Figueiredo, J. S. Suppo and J. M. Campagne, *Chem. Rev.*, 2016, **116**, 12029-12122.
155. V. R. Pattabiraman and J. W. Bode, *Nature*, 2011, **480**, 471-479.
156. A. Ojeda-Porras and D. Gamba-Sanchez, *J. Org. Chem.*, 2016, **81**, 11548-11555.
157. J. D. Munoz, J. Alcazar, A. de la Hoz, A. Diaz-Ortiz and S. A. A. de Diego, *Green Chem.*, 2012, **14**, 1335-1341.
158. L. Zhu, L. Le, M. Yan, C. T. Au, R. Qiu and N. Kambe, *J. Org. Chem.*, 2019, **84**, 5635-5644.
159. Y. L. Zheng and S. G. Newman, *ACS Catal.*, 2019, **9**, 4426-4433.
160. C. L. Allen and J. M. Williams, *Chem. Soc. Rev.*, 2011, **40**, 3405-3415.
161. X. Wang, *Nat. Catal.*, 2019, **2**, 98-102.
162. G. Li and M. Szostak, *Nat. Commun.*, 2018, **9**, 4165.
163. F. Messa, S. Perrone, M. Capua, F. Tolomeo, L. Troisi, V. Capriati and A. Salomone, *Chem. Commun.*, 2018, **54**, 8100-8103.
164. D. S. MacMillan, J. Murray, H. F. Sneddon, C. Jamieson and A. J. B. Watson, *Green Chem.*, 2013, **15**, 596-600.
165. B. R. Kim, H.-G. Lee, S.-B. Kang, G. H. Sung, J.-J. Kim, J. K. Park, S.-G. Lee and Y.-J. Yoon, *Synthesis*, 2012, **44**, 42-50.
166. G. Li and M. Szostak, *Nature Commun.*, 2018, **9**, 4165.
167. C. Su, J. Guang and P. G. Williard, *J. Org. Chem.*, 2014, **79**, 1032-1039.
168. R. Stefanovic, M. Ludwig, G. B. Webber, R. Atkin and A. J. Page, *Phys. Chem. Chem. Phys.*, 2017, **19**, 3297-3306.
169. C. Vidal, L. Merz and J. García-Álvarez, *Green Chem.*, 2015, **17**, 3870-3878.
170. M. J. Rodríguez-Álvarez, J. García-Álvarez, M. Uzelac, M. Fairley, C. T. O'Hara and E. Hevia, *Chem.–Eur. J.* 2018, **24**, 1720-1725.
171. R. von Bülow, H. Gornitzka, T. Kottke and D. Stalke, *Chem. Commun.*, 1996, 1639-1640.
172. W. Clegg, S. T. Liddle, R. E. Mulvey and A. Robertson, *Chem. Commun.*, 1999, 511-512.
173. C. Su, J. Guang and P. G. Williard, *J. Org. Chem.*, 2014, **79**, 1032-1039.
174. F. Lotufo-Neto, M. Trivedi and M. E. Thase, *Neuropsychopharmacology*, 1999, **20**, 226-247.
175. A. Fitton, D. Faulds and K. L. Goa, *Drugs*, 1992, **43**, 561-596.
176. B. Fulton and P. Benfield, *Drugs*, 1996, **52**, 450-474.
177. T. M. Katz, J. H. Miller and A. A. Hebert, *J. Am. Ac. Dermatol.*, 2008, **58**, 865-871.

178. J. Clayden, N. Greeves and S. Warren, OUP Oxford, 2012, ch. 10 - Conjugate addition, pp. 227-243.
179. P. Ortiz, F. Lanza and S. R. Harutyunyan, Springer International Publishing, Cham, 2016, pp. 99-134.
180. A. V. R. Madduri, A. J. Minnaard and S. R. Harutyunyan, *Chem. Commun.*, 2012, **48**, 1478-1480.
181. A. V. R. Madduri, S. R. Harutyunyan and A. J. Minnaard, *2013 Spring Issue*, 2013, **10**, e21-e27.
182. R. Naasz, L. A. Arnold, M. Pineschi, E. Keller and B. L. Feringa, *J. Am. Chem. Soc.*, 1999, **121**, 1104-1105.
183. S. R. Harutyunyan, T. den Hartog, K. Geurts, A. J. Minnaard and B. L. Feringa, *Chem. Rev.*, 2008, **108**, 2824-2852.
184. F. López, S. R. Harutyunyan, A. Meetsma, A. J. Minnaard and B. L. Feringa, *Angew. Chem. Int. Ed.*, 2005, **44**, 2752-2756.
185. D. Peña, F. López, S. R. Harutyunyan, A. J. Minnaard and B. L. Feringa, *Chem. Commun.*, 2004, 1836-1837.
186. P. De Vreese, N. R. Brooks, K. Van Hecke, L. Van Meervelt, E. Matthijs, K. Binnemans and R. Van Deun, *Inorg. Chem.*, 2012, **51**, 4972-4981.
187. M. Hatano, S. Suzuki and K. Ishihara, *J. Am. Chem. Soc.*, 2006, **128**, 9998-9999.
188. S. R. Harutyunyan, F. López, W. R. Browne, A. Correa, D. Peña, R. Badorrey, A. Meetsma, A. J. Minnaard and B. L. Feringa, *J. Am. Chem. Soc.*, 2006, **128**, 9103-9118.
189. C. C. C. Johansson Seechurn, M. O. Kitching, T. J. Colacot and V. Snieckus, *Angew. Chem. Int. Ed.*, 2012, **51**, 5062-5085.
190. J. A. Gladysz, M. Bochmann, D. L. Lichtenberger, L. S. Liebeskind, T. J. Marks and D. A. Sweigart, *Organometallics*, 2010, **29**, 5737-5737.
191. K. C. Nicolaou, P. G. Bulger and D. Sarlah, *Angew. Chem. Int. Ed.*, 2005, **44**, 4442-4489.
192. P. Ruiz-Castillo and S. L. Buchwald, *Chem. Rev.*, 2016, **116**, 12564-12649.
193. N. Miyaoura, K. Yamada and A. Suzuki, *Tet. Lett.*, 1979, **20**, 3437-3440.
194. J. Li, S. Yang, W. Wu and H. Jiang, *Eur. J. Org. Chem.*, 2018, **2018**, 1284-1306.
195. I. Kalvet, G. Magnin and F. Schoenebeck, *Angew. Chem. Int. Ed. Engl.* 2017, **56**, 1581-1585.
196. D. Heijnen, F. Tosi, C. Vila, M. C. A. Stuart, P. H. Elsinga, W. Szymanski and B. L. Feringa, *Angew. Chem. Int. Ed.*, 2017, **56**, 3354-3359.
197. G. Dilauro, S. M. García, D. Tagarelli, P. Vitale, F. M. Perna and V. Capriati, *ChemSusChem*, 2018, **11**, 3495-3501.
198. K. Tamao, K. Sumitani and M. Kumada, *J. Am. Chem. Soc.*, 1972, **94**, 4374-4376.
199. R. J. P. Corriu and J. P. Masse, *J. Chem. Soc., Chem. Commun.*, 1972, 144a-144a.
200. A. O. King, N. Okukado and E.-i. Negishi, *J. Chem. Soc., Chem. Commun.*, 1977, 683-684.
201. A. Fürstner and A. Leitner, *Angew. Chem. Int. Ed.*, 2002, **41**, 609-612.
202. J. Quintin, X. Franck, R. Hocquemiller and B. Figadère, *Tet. Lett.*, 2002, **43**, 3547-3549.
203. Q. Shen and J. F. Hartwig, *J. Am. Chem. Soc.*, 2006, **128**, 10028-10029.
204. N. Marion, E. C. Ecarnot, O. Navarro, D. Amoroso, A. Bell and S. P. Nolan, *J. Org. Chem.*, 2006, **71**, 3816-3821.
205. R. E. Tundel, K. W. Anderson and S. L. Buchwald, *J. Org. Chem.*, 2006, **71**, 430-433.
206. A. S. S. Wilson, M. S. Hill, M. F. Mahon, C. Dinoi and L. Maron, *Science*, 2017, **358**, 1168.
207. S. Brand, H. Elsen, J. Langer, W. A. Donaubaue, F. Hampel and S. Harder, *Angew. Chem. Int. Ed.*, 2018, **57**, 14169-14173.

208. S. Brand, H. Elsen, J. Langer, S. Grams and S. Harder, *Angew. Chem. Int. Ed.*, 2019, **0**.
209. A. S. S. Wilson, C. Dinoi, M. S. Hill, M. F. Mahon and L. Maron, *Angew. Chem. Int. Ed.*, 2018, **57**, 15500-15504.
210. H. Bauer, M. Alonso, C. Färber, H. Elsen, J. Pahl, A. Causero, G. Ballmann, F. De Proft and S. Harder, *Nature Catal.*, 2018, **1**, 40-47.
211. D. Schuhknecht, C. Lhotzky, T. P. Spaniol, L. Maron and J. Okuda, *Angew. Chem. Int. Ed.*, 2017, **56**, 12367-12371.
212. N. P. Mankad, *Chem. – Eur. J.*, 2016, **22**, 5822-5829.
213. J. Park and S. Hong, *Chem. Soc. Rev.*, 2012, **41**, 6931-6943.
214. Y. Hua, Z. Guo, H. Han and X. Wei, *Organometallics*, 2017, **36**, 877-883.
215. M. Ma, X. Shen, W. Wang, J. Li, W. Yao and L. Zhu, *Eur. J. Inorg. Chem.*, 2016, **2016**, 5057-5062.
216. C. Glock, F. M. Younis, S. Ziemann, H. Görls, W. Imhof, S. Krieck and M. Westerhausen, *Organometallics*, 2013, **32**, 2649-2660.
217. C. Glock, H. Görls and M. Westerhausen, *Chem. Commun.*, 2012, **48**, 7094-7096.
218. W. Clegg, B. Conway, A. R. Kennedy, J. Klett, R. E. Mulvey and L. Russo, *Eur. J. Inorg. Chem.*, 2011, **2011**, 721-726.
219. A. Hernan-Gomez, T. D. Bradley, A. R. Kennedy, Z. Livingstone, S. D. Robertson and E. Hevia, *Chem. Commun.*, 2013, **49**, 8659-8661.
220. M. De Tullio, A. Hernán-Gómez, Z. Livingstone, W. Clegg, A. R. Kennedy, R. W. Harrington, A. Antiñolo, A. Martínez, F. Carrillo-Hermosilla and E. Hevia, *Chem. - Eur. J.*, 2016, **22**, 17646.
221. L. Davin, A. Hernán-Gómez, C. McLaughlin, A. R. Kennedy, R. McLellan and E. Hevia, *Dalton Trans.*, 2019.
222. M. De Tullio, A. Hernán-Gómez, Z. Livingstone, W. Clegg, A. R. Kennedy, R. W. Harrington, A. Antiñolo, A. Martínez, F. Carrillo-Hermosilla and E. Hevia, *Chem. Eur. J.*, 2016, **22**, 17646-176456.
223. S. D. Wobser and T. J. Marks, *Organometallics*, 2013, **32**, 2517-2528.
224. B. M. Trost, *Science*, 1991, **254**, 1471-1477.
225. D. J. Faulkner, *Nat. Prod. Rep.*, 1984, **1**, 251-280.
226. T. L. B. Boivin, *Tetrahedron*, 1987, **43**, 3309-3362.
227. S. Y. Seo, X. H. Yu and T. J. Marks, *J. Am. Chem. Soc.*, 2009, **131**, 263-276.
228. T. M. Ha, Q. Wang and J. Zhu, *Chem. Commun.*, 2016.
229. T. Huld, N. Lassen, J. Norgaard and P. V. Petersen, *Journal*, 1969.
230. Y.-H. Dou, H.-X. Ding, R.-C. Yang, W. Li and Q. Xiao, *Chin. Chem. Lett.*, 2013, **24**, 379-382.
231. Y. Kato, N. Fusetani, S. Matsunaga and K. Hashimoto, *Tet. Lett.*, 1985, **26**, 3483-3486.
232. B. B. Weksler, A. J. Marcus and E. A. Jaffe, *Proc. Natl. Acad. Sci. USA*, 1977, **74**, 3922-3926.
233. A. H. Gray, J. Wright, V. Goodey and L. Bruce, *Injectable Drugs Guide*, Pharmaceutical Press, 2010.
234. D. Villemin and D. Goussu, *Heterocycles*, 1989, **29**, 1255-1261.
235. B. Seiller, C. Bruneau and P. H. Dixneuf, *J. Chem. Soc., Chem. Commun.*, 1994, 493-494.
236. P. N. Liu, T. B. Wen, K. D. Ju, H. H. Y. Sung, I. D. Williams and G. Jia, *Organometallics*, 2011, **30**, 2571-2580.
237. P. N. Liu, F. H. Su, T. B. Wen, H. H. Y. Sung, I. D. Williams and G. Jia, *Chem. Eur. J.*, 2010, **16**, 7889-7897.

238. V. Cadierno, J. Diez, J. Garcia-Alvarez, J. Gimeno, N. Nebra and J. Rubio-Garcia, *Dalton Trans.*, 2006, 5593-5604.
239. B. Gabriele, G. Salerno and E. Lauria, *J. Org. Chem.*, 1999, **64**, 7687-7692.
240. W. Huang, J. H.-C. Liu, P. Alayoglu, Y. Li, C. A. Witham, C.-K. Tsung, F. D. Toste and G. A. Somorjai, *J. Am. Chem. Soc.*, 2010, **132**, 16771-16773.
241. G. Zeni and R. C. Larock, *Chem. Rev.*, 2004, **104**, 2285-2310.
242. R. Mancuso, A. Maner, L. Cicco, F. M. Perna, V. Capriati and B. Gabriele, *Tetrahedron*, 2016, **72**, 4239-4244.
243. H. Harkat, J.-M. Weibel and P. Pale, *Tet. Lett.*, 2007, **48**, 1439-1442.
244. C. Vidal, L. Merz and J. Garcia-Alvarez, *Green Chem.*, 2015, **17**, 3870-3878.
245. B. Alcaide, P. Almendros and J. M. Alonso, *Org. Biomol. Chem.*, 2011, **9**, 4405-4416.
246. X. Du, F. Song, Y. Lu, H. Chen and Y. Liu, *Tetrahedron*, 2009, **65**, 1839-1845.
247. A. G. Nair, R. T. McBurney, M. R. D. Gatus, S. C. Binding and B. A. Messerle, *Inorg. Chem.*, 2017, **56**, 12067-12075.
248. R. J. Harris, R. G. Carden, A. N. Duncan and R. A. Widenhoefer, *ACS Catal.*, 2018, **8**, 8941-8952.
249. B. Seiller, C. Bruneau and P. H. Dixneuf, *J. Chem. Soc., Chem. Commun.*, 1994, 493-494.
250. P. Pale and J. Chucho, *Eur. J. Org. Chem.*, 2000, 1019-1025.
251. A. Varela-Fernández, C. García-Yebra, J. A. Varela, M. A. Esteruelas and C. Saá, *Angew. Chem. Int. Ed.*, 2010, **49**, 4278-4281.
252. E. Benedetti, A. Simonneau, A. Hours, H. Amouri, A. Penoni, G. Palmisano, M. Malacria, J.-P. Goddard and L. Fensterbank, *Adv. Synth. Cat.*, 2011, **353**, 1908-1912.
253. V. Diachenko, M. J. Page, M. R. D. Gatus, M. Bhadbhade and B. A. Messerle, *Organometallics*, 2015, **34**, 4543-4552.
254. J. L. Arbour, H. S. Rzepa, A. J. P. White and K. K. Hii, *Chem. Commun.*, 2009, **46**, 7125-7127.
255. M. J. Pouy, S. A. Delp, J. Uddin, V. M. Ramdeen, N. A. Cochrane, G. C. Fortman, T. B. Gunnoe, T. R. Cundari, M. Sabat and W. H. Myers, *ACS Catal.*, 2012, **2**, 2182-2193.
256. X. Xu, J. Liu, L. Liang, H. Li and Y. Li, *Adv. Synth. Cat.*, 2009, **351**, 2599-2604.
257. Y. Sheng, D. G. Musaev, K. S. Reddy, F. E. McDonald and K. Morokuma, *J. Am. Chem. Soc.*, 2002, **124**, 4149-4157.
258. S. B. Moilanen and D. S. Tan, *Org. Biomol. Chem.*, 2005, **3**, 798-803.
259. M. J. Pouy, S. A. Delp, J. Uddin, V. M. Ramdeen, N. A. Cochrane, G. C. Fortman, T. B. Gunnoe, T. R. Cundari, M. Sabat and W. H. Myers, *ACS Catal.*, 2012, **2**, 2182-2193.
260. X. Xu, J. Liu, L. Liang, H. Li and Y. Li, *Adv. Synth. Catal.*, 2009, **351**, 2599-2604.
261. J. E. Baldwin, *J. Chem. Soc., Chem. Commun.*, 1976, 734-736.
262. F. E. McDonald and C. C. Schultz, *J. Am. Chem. Soc.*, 1994, **116**, 9363-9364.
263. F. E. McDonald, K. S. Reddy and Y. Díaz, *J. Am. Chem. Soc.*, 2000, **122**, 4304-4309.
264. J. A. Varela and C. Saá, *Synthesis*, 2016, **48**, 3470-3478.
265. T. Cai, W.-W. Li, W.-B. Qin and T.-B. Wen, *Chem. - Eur. J.*, 2017, **24**, 1606-1618.
266. M. Mellor, A. Santos, E. G. Scovell and J. K. Sutherland, *J. Chem. Soc., Chem. Commun.*, 1978, 528-529.
267. M. D. Weingarten and A. Padwa, *Tetrahedron Lett.*, 1995, **36**, 4717-4720.
268. X. H. Yu, S. Seo and T. J. Marks, *J. Am. Chem. Soc.*, 2007, **129**, 7244-7245.
269. J. Martínez, A. Otero, A. Lara-Sánchez, J. A. Castro-Osma, J. Fernández-Baeza, L. Sánchez-Barba and A. M. Rodríguez, *Organometallics*, 2016, **35**, 1802-1812.
270. C. Brinkmann, A. G. M. Barrett, M. S. Hill, P. A. Procopiou and S. Reidt, *Organometallics*, 2012, **31**, 7287-7297.

271. X. H. Yu, S. Seo and T. J. Marks, *J. Am. Chem. Soc.*, 2007, **129**, 7244.
272. J. Martínez, A. Otero, A. Lara-Sánchez, J. A. Castro-Osma, J. Fernández-Baeza, L. F. Sánchez-Barba and A. M. Rodríguez, *Organometallics*, 2016, **35**, 1802-1812.
273. Y. Sun, G. Wu, D. Cen, Y. Chen and L. Wang, *Dalton Trans.*, 2012, **41**, 9682-9688.
274. D. Y. Li, K. J. Shi, X. F. Mao, Z. L. Zhao, X. Y. Wu and P. N. Liu, *Tetrahedron*, 2014, **70**, 7022-7031.
275. J. K. Vandavasi, W.-P. Hu, G. C. Senadi, S. S. K. Boominathan, H.-Y. Chen and J.-J. Wang, *Eur. J. Org. Chem.*, 2014, 6219-6226.
276. S. Gandhi and B. Baire, *ChemistrySelect*, 2018, **3**, 4490-4494.
277. L. Garcia, M. D. Anker, M. F. Mahon, L. Maron and M. S. Hill, *Dalton Trans.*, 2018, **47**, 12684-12693.
278. A. Motta, I. L. Fragalà and T. J. Marks, *Organometallics*, 2010, **29**, 2004-2012.
279. P. B. Hitchcock, M. F. Lappert and A. V. Protchenko, *J. Am. Chem. Soc.*, 2001, **123**, 189-190.
280. I. Koehne, S. Bachmann, R. Herbst-Irmer and D. Stalke, *Angew. Chem., Int. Ed.*, 2017, **56**, 15141-15145.
281. J. Kretsch, A. Kreyenschmidt, R. Herbst-Irmer and D. Stalke, *Dalton Trans.*, 2018, **47**, 12606-12612.
282. S. Neander, F. E. Tio, R. Buschmann, U. Behrens and F. Olbrich, *J. Organomet. Chem.*, 1999, **582**, 58-65.
283. A. Imberdis, G. Lefèvre, P. Thuéry and T. Cantat, *Angew. Chem., Int. Ed.*, 2018, **57**, 3084-3088.
284. S. M. Härling, S. Kriek, H. Görls and M. Westerhausen, *Inorg. Chem.*, 2017, **56**, 9255-9263.
285. H. Abas, J. Mas-Roselló, M. M. Amer, D. J. Durand, R. R. Groleau, N. Fey and J. Clayden, *Angew. Chem., Int. Ed.*, 2019, **58**, 2418-2422.
286. C. Lichtenberg, T. P. Spaniol, L. Perrin, L. Maron and J. Okuda, *Chem. - Eur. J.*, 2012, **18**, 6448-6452.
287. M. Weller, T. Overton, J. Rourke and F. Armstrong, *Inorganic Chemistry*, OUP Oxford, 2014.
288. M. D. Weingarten and A. Padwa, *Tet. Lett.*, 1995, **36**, 4717-4720.
289. P. Vollhardt and N. Schore, W. H. Freeman and company, New York, Sixth Ed. edn., 2011, ch. Ch.13 - Alkynes.
290. S. Seo and T. J. Marks, *Chem. - Eur. J.*, 2010, **16**, 5148-5162.
291. J. Burés, *Angew. Chem. Int. Ed.*, 2016, **55**, 2028-2031.
292. J. Burés, *Angew. Chem. Int. Ed.*, 2016, **55**, 16084-16087.
293. C. D. T. Nielsen and J. Burés, *Chem. Sci.*, 2019, **10**, 348-353.
294. M. Shigeno, K. Hanasaka, K. Sasaki, K. Nozawa-Kumada and Y. Kondo, *Chem - Eur. J.*, 2019, **25**, 3235-3239.
295. C. Vallance, *An Introduction to Chemical Kinetics*, Morgan & Claypool Publishers, 2017.
296. S. Bachmann, R. Neufeld, M. Dzemski and D. Stalke, *Chem. - Eur. J.*, 2016, **22**, 8462-8465.
297. S. Bachmann, B. Gernert and D. Stalke, *Chem. Commun.*, 2016, **52**, 12861-12864.
298. R. Neufeld and D. Stalke, *Chem. Sci.*, 2015, **6**, 3354-3364.
299. R. Rochat, K. Yamamoto, M. J. Lopez, H. Nagae, H. Tsurugi and K. Mashima, *Chem. - Eur. J.*, 2015, **21**, 8112-8120.
300. A. Koch, M. Wirgenings, S. Kriek, H. Görls, G. Pohnert and M. Westerhausen, *Organometallics*, 2017, **36**, 3981-3986.

301. D. F. Shriver and M. A. Drezdson, *The Manipulation of Air-Sensitive Compounds*, Wiley, 1986.
302. A. P. Abbott, G. Capper, D. L. Davies, R. K. Rasheed and V. Tambyrajah, *Chem. Commun.*, 2003, 70-71.
303. M. Li, C. Wang and H. Ge, *Org. Lett.*, 2011, **13**, 2062-2064.
304. J. A. Murphy, A. G. J. Commeureuc, T. N. Snaddon, T. M. McGuire, T. A. Khan, K. Hisler, M. L. Dewis and R. Carling, *Org. Lett.*, 2005, **7**, 1427-1429.
305. J. Ruan, O. Saidi, J. A. Iggo and J. Xiao, *J. Am. Chem. Soc.*, 2008, **130**, 10510-10511.
306. A. T. Biju and F. Glorius, *Angew. Chem.*, 2010, **122**, 9955-9958.
307. C. J. Rohbogner, C. R. Diène, T. J. Korn and P. Knochel, *Angew. Chem. Int. Ed.*, 2010, **49**, 1874-1877.
308. L. Ran, Z.H. Ren, Y.Y. Wang and Z.H. Guan, *Chem. – Asian J.*, 2014, **9**, 577-583.
309. Z. Yin, Z. Wang and X.-F. Wu, *Eur. J. Org. Chem.*, 2017, 3992-3995.
310. S. Wang, J. Wang, R. Guo, G. Wang, S.-Y. Chen and X.-Q. Yu, *Tet. Lett.*, 2013, **54**, 6233-6236.
311. F. Bruyneel and J. Marchand-Brynaert, *Synlett*, 2010, 1974-1978.
312. L. Hie, N. F. Fine Nathel, T. K. Shah, E. L. Baker, X. Hong, Y.-F. Yang, P. Liu, K. N. Houk and N. K. Garg, *Nature*, 2015, **524**, 79-83.
313. J. M. Gaudin, T. Lander and O. Nikolaenko, *Chem. Biodiversity*, 2008, **5**, 617-635.
314. Y. Rao, X. Li and S. J. Danishefsky, *J. Am. Chem. Soc.*, 2009, **131**, 12924-12926.
315. Y.L. Zheng and S. G. Newman, *ACS catal.*, 2019, **9**, 4426-4433.
316. T. Ohshima, T. Iwasaki, Y. Maegawa, A. Yoshiyama and K. Mashima, *J. Am. Chem. Soc.*, 2008, **130**, 2944-2945.
317. L. Lunazzi, D. Macciantelli, D. Tassi and A. Dondoni, *J. Chem. Soc., Perkin Trans. 2*, 1980, 717-723.
318. S. Zhou, K. Junge, D. Addis, S. Das and M. Beller, *Angew. Chem. Int. Ed.*, 2009, **48**, 9507-9510.
319. J.C. Kizirian, N. Cabello, L. Pinchard, J.C. Caille and A. Alexakis, 2005, **61**, 8939-8946.
320. J. E. Fleckenstein and K. Koszinowski, *Organometallics*, 2011, **30**, 5018-5026.
321. P. R. Markies, G. Schat, O. S. Akkerman, F. Bickelhaupt and A. L. Spek, *J. Organomet. Chem.*, 1992, **430**, 1-13.
322. E. Erdik and T. Daşkapan, *J. Chem. Soc., Perkin Trans. 1*, 1999, 3139-3142.
323. A. Hernán-Gómez, E. Herd, M. Uzelac, T. Cadenbach, A. R. Kennedy, I. Borilovic, G. Aromí and E. Hevia, *Organometallics*, 2015, **34**, 2614-2623.
324. G. J. P. Britovsek, J. England and A. J. P. White, *Inorg. Chem.*, 2005, **44**, 8125-8134.
325. M. Ciampolini and N. Nardi, *Inorg. Chem.*, 1966, **5**, 41-44.
326. B. Conway, D. V. Graham, E. Hevia, A. R. Kennedy, J. Klett and R. E. Mulvey, *Chem. Commun.*, 2008, 2638-2640.
327. W. Clegg, B. Conway, D. V. Graham, E. Hevia, A. R. Kennedy, R. E. Mulvey, L. Russo and D. S. Wright, *Chem. – Eur. J.*, 2009, **15**, 7074-7082.
328. S. E. Baillie, W. Clegg, P. García-Álvarez, E. Hevia, A. R. Kennedy, J. Klett and L. Russo, *Organometallics*, 2012, **31**, 5131-5142.
329. S. E. Baillie, W. Clegg, P. García-Álvarez, E. Hevia, A. R. Kennedy, J. Klett and L. Russo, *Organometallics*, 2012, **31**, 5131-5142.
330. G. Liu and S. S. Stahl, *J. Am. Chem. Soc.*, 2007, **129**, 6328-6335.
331. H. Lu, C. Li, H. Jiang, C. L. Lizardi and X. P. Zhang, *Angew. Chem. Int. Ed.*, 2014, **53**, 7028-7032.